



**HAL**  
open science

# Identification de composés immuno-stimulateurs anti-microbiens de nouvelle génération

Alissa Majoor

► **To cite this version:**

Alissa Majoor. Identification de composés immuno-stimulateurs anti-microbiens de nouvelle génération. Microbiologie et Parasitologie. Université Côte d'Azur, 2021. Français. NNT : 2021COAZ6027 . tel-04416329

**HAL Id: tel-04416329**

**<https://theses.hal.science/tel-04416329>**

Submitted on 25 Jan 2024

**HAL** is a multi-disciplinary open access archive for the deposit and dissemination of scientific research documents, whether they are published or not. The documents may come from teaching and research institutions in France or abroad, or from public or private research centers.

L'archive ouverte pluridisciplinaire **HAL**, est destinée au dépôt et à la diffusion de documents scientifiques de niveau recherche, publiés ou non, émanant des établissements d'enseignement et de recherche français ou étrangers, des laboratoires publics ou privés.

# THÈSE DE DOCTORAT

## Identification de composés immuno- stimulateurs anti-microbiens de nouvelle génération

**Alissa MAJOOR**

Centre Méditerranéen de Médecine Moléculaire – INSERM U1065

**Présentée en vue de l'obtention  
du grade de docteur en Immunologie et  
Microbiologie  
d'Université Côte d'Azur**

**Dirigée par :** Laurent BOYER  
**Co-encadrée par :** Grégory MICHEL  
**Soutenue le :** 15 décembre 2021

**Devant le jury, composé de :**  
Laurent BOYER, DR2 INSERM, C3M  
Rachel BRAS-GONCALVES, DR, IRD  
Anne-Marie CUISINIER, Clinical  
Development Manager, VIRBAC  
Pierre MARTY, PU-PH, CHU Nice  
Grégory MICHEL, IR UCA, C3M  
Thomas MICHEL, Maître de Conférence  
UCA, ICN  
Florence ROBERT-GANGNEUX, PU-PH,  
Université de Rennes 1



# Identification de composés immuno- stimulateurs anti-microbiens de nouvelle génération

## **Composition du Jury :**

### **Président :**

Pierre MARTY, PU-PH, Université Côte d'Azur

### **Rapportrices :**

Rachel BRAS-GONCALVES, DR IRD, Institut de Recherche pour le Développement.

Florence ROBERT-GANGNEUX, PU-PH, Université de Rennes 1

### **Examineurs :**

Anne-Marie CUISINIER, Clinical Development Manager, VIRBAC

Thomas MICHEL, Maître de Conférence UCA, Université Côte d'Azur

### **Co-directeurs de la thèse :**

Laurent BOYER, DR2 INSERM, Université Côte d'Azur

Grégory MICHEL, IR UCA, Université Côte d'Azur

## Identification de composés immuno-stimulateurs anti-microbiens de nouvelle génération

La Leishmaniose est une maladie tropicale négligée que l'on retrouve dans plus de 98 pays à travers le monde. On compte par an jusqu'à 1 000 000 de nouveaux cas, menant à près de 30 000 morts. Chez l'homme, il existe plusieurs formes de la maladie, allant d'une forme cutanée pouvant guérir spontanément, à la forme viscérale la plus grave.

La leishmaniose viscérale est conférée par plusieurs espèces de leishmanies, dont *L. infantum* dans le pourtour du bassin Méditerranéen. Ce parasite dimorphique envahit les macrophages de ses hôtes notamment l'humain et le chien où il est responsable de la maladie. En l'absence de traitement, la leishmaniose viscérale est mortelle et les traitements existants aujourd'hui sont toxiques, coûteux, et font face à l'apparition croissante de résistances.

Trouver de nouveaux traitements est donc aujourd'hui une priorité, et ce projet de thèse vise à identifier des alternatives naturelles aux molécules anti-*Leishmania*. En prenant une approche écologique, nous récupérons des déchets de la parfumerie et des plantes issues de la biodiversité locale et nous en testons les extraits sur les parasites afin d'identifier des composés immunostimulateurs, qui permettraient de favoriser une élimination du parasite par l'hôte. Afin de pouvoir suivre l'évolution au cours du temps d'une infection *in vitro* et/ou *in vivo*, nous avons également cherché à créer de nouveaux outils pour visualiser la présence du parasite *Leishmania* en développant de nouvelles souches rapportrices fluorescentes et bioluminescentes.

Au cours de ma thèse, nous avons identifié une plante dont l'extrait favorise l'élimination de la forme amastigote intracellulaire retrouvée dans les macrophages hôtes. A l'aide de nos collaborateurs à l'Institut de Chimie de Nice (ICN), nous avons réalisé un fractionnement bioguidé et obtenu des sous-fractions de cette plante ainsi que des molécules pures capables d'éliminer le parasite *Leishmania infantum*.

Une seule molécule, dont le nom est soumis à confidentialité pour des raisons de dépôt de brevet, a montré un effet sur le parasite intracellulaire, sans montrer de toxicité. Cette dernière module la sécrétion de cytokines de la cellule hôte. Actuellement, l'étude de 20 dérivés structuraux de cette molécule est en cours. Des études préliminaires chez la souris ont permis de montrer que la prise de cette molécule par voie orale, de façon préventive, pouvait diminuer la charge parasitaire dans l'animal.

Nous avons en parallèle développé la construction de nouvelles souches rapportrices de *Leishmania* exprimant la luciférase teLuc, le fluorophore rouge mRuby ou rouge lointain mMaroon1, et des souches exprimant fluorescence et bioluminescence, eFFly-mCherry. Cette dernière construction a été intégrée dans 3 espèces différentes de leishmanies : *L. infantum*, responsable de leishmaniose viscérale, *L. major* responsable de leishmaniose cutanée, et *L. tarentolae* qui est une souche non pathogène pour l'homme.

**Mots clef : *Leishmania*, immunostimulation, souche rapportrice**

## Identification of new immune-stimulators and anti-microbial compounds

Leishmaniasis is a neglected tropical disease found in more than 98 countries around the world. There are up to 1,000,000 new cases per year, leading to nearly 30,000 deaths. In humans, there are several forms of the disease, ranging from a cutaneous form that can heal spontaneously, to the most severe visceral form.

Visceral leishmaniasis is conferred by several species of *Leishmania*, including *L. infantum* around the Mediterranean basin. This dimorphic parasite invades the macrophages of its hosts, particularly humans and dogs, in which it is responsible for the disease. Left untreated, visceral leishmaniasis is fatal, and treatments available today are toxic, expensive, and face growing resistance.

Finding new treatments is therefore a priority, and this thesis project aims to identify natural alternatives to anti-leishmanial molecules. By taking an ecological approach, we recover waste from the perfumery industry and plants from the local biodiversity. We then test the extracts on the parasites in order to identify immunostimulatory compounds, which would favor promotion of elimination of the parasite by the host's own immune system. In order to follow the evolution over time of the infection *in vitro* and/or *in vivo*, we have also sought to create new tools to visualize the presence of *Leishmania* parasites by developing new fluorescent and bioluminescent reporter strains.

We have identified a plant whose extract promotes the elimination of the intracellular amastigote form found in host macrophages. With the help of our collaborators at the Institut de Chimie de Nice (ICN), we performed a bioguided fractioning. We obtained sub-fractions of this plant as well as pure molecules capable of eliminating the parasite *Leishmania infantum*. One single molecule, whose name is confidential because of a pending patent registration, showed an effect on the intracellular parasite, without showing toxicity. It is capable of modulating the secretion of cytokines from the host cell. We are currently studying 20 structural derivatives of this molecule. Preliminary studies in mice have shown that taking this molecule orally, as a preventive measure, can reduce the parasite load in animals.

In the meantime, we have developed the construction of new reporter strains of *Leishmania* expressing the luciferase teLuc, the red mRuby or far red mMaroon1 fluorophore, and strains expressing fluorescence and bioluminescence, eFFly-mCherry. This last construction has been integrated into 3 different species of *Leishmania*: *L. infantum*, responsible for visceral leishmaniasis, *L. major* responsible for cutaneous leishmaniasis, and *L. tarentolae*, which is a non-pathogenic strain for humans.

**Mots clef : *Leishmania*, immuno-stimulation, reporter strain**

*Je dédie cette thèse à ma famille :*

*Mes parents, qui m'ont toujours soutenue,  
Mes frères, sur qui j'ai toujours pu compter,  
Ma moitié, qui est toujours restée à mes côtés.*

# Remerciements

Je tiens en premier lieu à remercier les personnes qui font partie de mon jury de thèse.

Un grand merci au Dr Rachel Bras-Goncalves et au Pr Florence Robert-Gangneux pour avoir accepté d'être mes rapportrices. J'espère que vous apprécierez lire les travaux qui m'ont gardé occupée pendant ces trois dernières années.

Un grand merci également aux examinateurs, le Dr Anne-Marie Cuisinier, le Pr Pierre Marty, et le Dr Thomas Michel.

Merci à mes encadrants de thèse qui ont rendu ce travail possible, Laurent Boyer et Grégory Michel. Je me rappellerai toujours la première fois que nous nous sommes vus, au C3M pour un stage de Master 2 sur la leishmaniose. Vous étiez mon seul choix de stage, et je suis très reconnaissante que vous ayez retenu ma candidature et que vous m'ayez ouvert la porte à la thèse, que je n'étais pas sûre de vouloir réaliser en premier lieu ! Ça a été difficile par moments, mais je ne changerais ça pour rien au monde.

Merci Laurent pour tes conseils, ta bonne humeur et ton accessibilité. Tu m'as fait savoir que tu étais toujours là en cas de besoin et que je pouvais compter sur toi. Tu as été d'un très grand soutien sur le plan scientifique, toujours disponible lorsque j'ai eu besoin d'un avis ou d'un conseil et je te remercie pour ça. J'ai eu beaucoup de chance d'avoir un directeur de thèse comme toi.

Un énorme merci à Greg. Par où commencer ? Tu as été un encadrant fabuleux qui m'a apporté énormément tant sur le plan professionnel que personnel. Merci de m'avoir tout appris, d'avoir eu la patience de former la Master 2 incertaine que j'étais au début. J'ai énormément progressé grâce à toi et je ne t'en remercierai jamais assez. Toi aussi tu as toujours été disponible pour moi. Peu importe combien tes journées étaient pleines (et Oh ! elles l'étaient !) tu as toujours pris du temps quand j'en avais besoin. Ta bienveillance m'a énormément aidé et m'a permis de me faire plus confiance, que ce soit en manips ou en



présentations orales. Tu as toujours été là pour m'aider à progresser, et parfois à réparer mes bêtises (parce que ça arrive...). Ne reculant devant rien, tu as même fouillé les poubelles pour moi... haha tu pouvais t'y attendre à ce qu'elle sorte celle-là ! J'ai adoré chanter et danser sur des chansons des Maroon5 avec toi dans le labo, même si c'était généralement pendant les manip souris. Ta bonne humeur les a rendues moins longues. Merci pour les discussions des pauses midi sur les dernières séries et films Marvel, j'ai adoré pouvoir partager avec toi sur Harry Potter, The 100 et tous nos autres visionnages ! Merci de m'avoir encouragé même les jours où c'était plus dur de garder le moral, de m'avoir rassuré lorsque j'étais stressée, merci pour les chocolats chauds, en somme, merci pour tout. Je n'aurais pas pu rêver meilleur encadrant.

Merci aux membres de l'Équipe 6. Tout d'abord à mes collègues de notre petite équipe de parasitologie. Loïc (note que tu as ton tréma ;) ) ça a été un plaisir de travailler avec toi. Ça a été tellement bien que je te pardonnerai même d'avoir craché dans mes flasques... Tu as toujours été d'une bonne humeur contagieuse, et je suis ravie d'avoir pu passer du temps avec toi comme mon voisin de bureau. Tu resteras longtemps gravé dans ma mémoire ; en même temps, à chaque fois que je vois Cuichette je pense à toi ! J'ai adoré partager les aspects de la recherche scientifique avec toi. Et aussi le reste. Je ne dirais qu'une dernière chose : le « Ha-PEE Birthday » est un de mes meilleurs souvenirs !

Merci à Alexandre Perrone (Damoiseau). Même si tu n'es resté que 6 mois pendant ton master, on s'est tout de suite bien entendu. J'ai beaucoup aimé participer à ton encadrement, tu es quelqu'un de très appliqué et assidu. Je croise les doigts pour que tu puisses revenir au laboratoire pour faire ta thèse, comme tu le voulais. Merci pour tout.

Un grand merci à Chaïma, Abigail et Nina, nos techs préférées du PHRC qui ne sont plus toutes avec nous maintenant. Faire des soirées jusqu'à 20h n'a jamais été aussi plaisant qu'avec vous les filles. J'ai une série de selfies conséquente montrant nos exploits d'horaires. Il me semble que le record avait été atteint pour 18h et quelques, mais je ne me souviens plus avec qui. Un

grand merci à vous trois, vous resterez un de mes meilleurs souvenirs, votre bonne humeur a toujours rendu les journées plaisantes.

Merci également à l'équipe de parasito du CHU. Un grand merci à Christelle, ton aide sur le plan scientifique a été extrêmement appréciée. Les idées que nous avons pu discuter pendant les réunions du jeudi matin ont été extrêmement bénéfiques à l'avancée des projets, et j'ai beaucoup aimé échanger avec toi. Sans en avoir fait beaucoup, les repas sur le toit du CHU restent parmi mes souvenirs préférés. Merci également au Pr Pierre Marty. Vous avez toujours été extrêmement bienveillant avec moi, toujours disponible et souriant. Grégory m'en a beaucoup parlé, mais je regrette de ne jamais avoir vécu un Congrès avec vous ! Merci pour votre présence et vos anecdotes pendant les repas de midi !

Merci également au reste de l'équipe 6, merci à Orane et à Céline, d'avoir pris le temps de m'aider lorsque j'étais en difficulté sur les constructions de mes plasmides. Vous m'avez évité de belles bourdes, et m'avez toujours donné un coup de main avec le sourire. Merci également Céline pour toutes les fermetures éclair. Je vais penser à toi pendant de nombreuses années à venir pendant mes projets couture !! Merci à Anne et à Patrick, vous avez tous les deux été tellement gentils. Merci d'avoir partagé votre savoir avec moi, et merci aussi de m'avoir très fréquemment indiqué où se trouvaient nos réactifs et produits chimiques !

Merci à Océane et Juan. Nous avons commencé nos thèses à peu près en même temps, et je pense très fort à vous en étant la première à la passer !! Courage à vous. Vous avez tous les deux des qualités extraordinaires et j'ai adoré partager le labo avec vous. Merci également à Cédric, ton calme a été le bienvenu dans un bureau parfois turbulent !

Je n'oublie pas Johan, Romain et Alicia, même si nous n'avons pas beaucoup échangé car nous n'étions pas dans le même bureau !

Merci aux anciens masters de cette dernière année, Zak, Eva, Lina. Vous avez contribué à rendre les pauses café très agréables, dehors dans l'herbe, au milieu des fourmis.

Je souhaite également remercier les personnes ayant pris de leur temps pour faire partie de mon comité de Suivi de thèse. Merci au Dr Anne-Marie Cuisinier, que je retrouverai avec plaisir à mon jury de thèse, et merci au Dr Jean-Loup Lemesre. Vous avez été un fabuleux comité de suivi de thèse, avec qui il a été extrêmement agréable d'échanger.

Merci à toutes les autres équipes du C3M également. Travailler dans ce centre a été très agréable, tout le monde a toujours été si gentil et toujours prêt à aider ou à dépanner. Je ne suis pas la personne la plus extravertie mais votre gentillesse m'a toujours fait me sentir à ma place ici. Une petite mention spéciale à Marina, qui a été là pour parler avec moi honnêtement des difficultés que nous pouvions partager, et de nos incertitudes sur l'après thèse. Tu m'as aidé plus que tu ne le penses !

Merci aux plateformes du C3M et aux personnes qui s'en occupent. Merci à Marie Ironnelle pour ses conseils de Microscopie. Merci à Marielle Nebout, toujours disponible pour m'aider sur les cytomètres. Merci à tout le personnel de l'animalerie qui se sont toujours arrangé pour que nous puissions réaliser nos expérimentations *in vivo* en toute sérénité. Merci aussi au personnel de la laverie, sans qui le fonctionnement du centre serait très compliqué.

Un grand merci aux chimistes de l'ICN avec qui j'ai eu l'honneur de collaborer pendant ces trois années de thèse. Merci au Dr Thomas Michel, qui a été mon interlocuteur premier. Merci pour tes explications sur les techniques, la collaboration avec toi a toujours été très agréable. Merci aussi à Mariam, qui a été ma binôme Chimie du Master 2. Je te remercie d'avoir pris de ton temps pour me montrer les méthodes d'extractions : le fait d'avoir pu participer m'a fait vraiment mieux comprendre votre travail et toutes les étapes nécessaires avant d'obtenir les molécules que j'ai pu tester !

Merci également à l'Équipe "Immunology, Vaccine & Diagnosis of leishmaniasis" de l'IRD Montpellier, et au Dr Rachel Bras-Goncalves de nous avoir fourni la souche de *L. tarentolae*.

Je remercie la Fondation de la Recherche Médicale, qui a financé ma thèse sur les premières 3 années et sans qui je n'aurais pu vivre cette aventure fabuleuse. Je remercie l'association Recherche et Développement en Pathologie Infectieuse et Tropicale pour m'avoir financé 3 mois complémentaires afin que je puisse terminer ma thèse dans les meilleures conditions. Merci également à l'École Doctorale 85 et toutes les personnes qui en font partie. Un grand merci à Nadine Loudig qui a toujours répondu à mes questions à une vitesse éclair !

Spéciale dédicace et un grand merci à Columbus Café et leur personnel adorable. Vous m'avez fourni en thé glacé et en muffins pendant mes longues après-midis de rédaction sur ce mémoire, donc il ne paraît que juste de vous créditer un peu pour sa finalisation. Mention spéciale pour Aline avec qui je partage mon amour pour les Muffins au Spéculoos.

Au paragraphe pour les amis et la famille maintenant !

Merci à mes amies d'avoir été d'une patience à toute épreuve avec moi et de m'avoir apporté du bonheur et du soutien. Merci à Anaïs et à Laury, et désolée d'avoir annulé nos séances de JDR à répétition !

Un énorme merci à Galou et Adelyne. Vous avez été des amies en or, toujours présentes quand j'en ai eu besoin, que ce soit pour aider ou me changer les idées. Je serai toujours reconnaissante d'avoir fait votre connaissance, et même si vous êtes entrées dans ma vie « tard » ou il n'y a pas si longtemps que ça, je vous fais une confiance aveugle et je ne vous remercierai jamais assez pour toute la patience dont vous avez fait preuve. Vous avez été d'un soutien inconditionnel et je vous en remercie du fond du cœur.

Merci à ma famille, à mes parents : vous m'avez toujours encouragé à faire ce que j'aimais. Ik heb jullie nooit horen zeggen « dat kan je niet » of « dat gaat je niet lukken ». Jullie hebben mij altijd geholpen in alles wat ik wilde doen, en jullie hebben altijd in mij geloofd. Ik heb zo veel geluk met jullie als ouders, want alles wat ik hierin heb geschreven is door jullie mogelijk

gemaakt. Allen uren dat jullie hebben geholpen met school, ook al was het lastig in een anderen taal, alle hulp om mij te helpen naar Nice te verhuizen, allen uren dat jullie in de auto hebben gezeten zo dat ik jullie kan zien in de weekends. Ik hou enorm veel van jullie en ik ben trots dat ik jullie dochter ben.

Merci à mes petits frères (plus si petits que ça maintenant, vous me dépassez peut-être de loin en taille, mais jamais en âge...). Je suis super fière de vous mes futurs ingénieurs. Vous ne m'avez jamais apporté la paix pendant que je faisais mes devoirs ou que je révisais mes cours de master, mais je vous aime plus que tout et je suis chanceuse d'être votre grande sœur.

Finalement, merci à Manon. Tu as été là chaque seconde pour me soutenir, me féliciter, m'encourager, m'aider, m'écouter, me consoler, me motiver et m'aimer. Je n'aurais pas pu souhaiter meilleure partenaire dans la vie. Merci de m'avoir nourri pendant mes longues soirées de rédaction de ce manuscrit. Merci de n'avoir jamais perdu patience avec moi, et merci pour le soutien inconditionnel que tu m'as toujours apporté, et que j'espère nous nous apporterons pendant les années à venir. Je n'ai pas mis de citation intelligente en début de ce rapport, parce que ça ne m'a honnêtement jamais inspiré. Mais pour toi j'en mets une, qui je pense nous représente assez bien :

"I'm so glad you're my partner in crime."

"As long as you're my partner in time."

*-Life is Strange-*

# Table des matières

<b>Introduction</b> .....	<b>16</b>
<i>I. Épidémiologie</i> .....	<i>17</i>
a. Chez l'humain .....	17
b. Chez l'animal .....	19
<i>II. Parasites</i> .....	<i>20</i>
a. Morphologie .....	20
b. Cycle de Vie .....	21
<i>III. Vecteurs et Réservoirs</i> .....	<i>23</i>
a. Le Phlébotome femelle .....	23
b. Les Réservoirs .....	24
<i>IV. Formes Cliniques</i> .....	<i>25</i>
a. Leishmanioses Cutanées .....	25
b. Leishmanioses Muco-cutanées .....	26
c. Leishmanioses Viscérales .....	26
<i>V. La relation hôte-pathogène</i> .....	<i>28</i>
<i>VI. Les traitements</i> .....	<i>29</i>
a. Antimoniés pentavalents.....	29
b. Pentamidine .....	29
c. Amphotéricine B.....	30
d. Miltefosine.....	30
e. Paromomycine.....	30
f. L'allopurinol pour la leishmaniose canine.....	31
g. Autres traitements .....	31
<b>Objectifs de la Thèse</b> .....	<b>65</b>
<b>Résultats</b> .....	<b>66</b>
<i>Partie I : Création de nouvelles souches rapportrices de Leishmania</i> .....	<i>67</i>
I. Introduction.....	67
II. Matériel et Méthodes .....	68
III. Résultats .....	69
	11

IV. Discussion .....	107
V. Conclusion et Perspectives .....	108
<i>Partie II : Recherche de nouveaux composés immuno-stimulateurs contre Leishmania .....</i>	<i>110</i>
I. Introduction .....	112
II. Matériel et Méthodes .....	118
III. Résultats .....	122
IV. Discussion .....	143
<b>Conclusion et perspectives.....</b>	<b>147</b>
<b>Bibliographie.....</b>	<b>152</b>
<b>Annexes.....</b>	<b>156</b>

## Liste des Abréviations

AmB : Amphotericin B  
BMDM : Bone Marrow Derived Macrophages  
C3M : Centre Méditerranéen de Médecine Moléculaire  
CC50 : valeur 50% de la concentration Cytotoxique  
CHU : Centre Hospitalier Universitaire  
dSVF : Sérum de Veau Fœtal décomplémenté  
EDTA : Ethylene-Diamine-Tetraacetic Acid  
ELSD : Evaporative Light Scattering Detector (DéTECTEUR Evaporatif à Diffusion de Lumière)  
G418 : Généticine  
GFP : Green Fluorescent Protein  
HPLC : High Performance Liquid Chromatography (Chromatographie en phase Liquide Haute Performance)  
Hyg : Hygromycine B  
IC50 : valeur 50% de la concentration Inhibitrice  
ICN : Institut de Chimie de Nice  
iNOS : inducible Nitric Oxide Synthase (Oxide Nitrique Synthase inductible)  
*L. infantum* : *Leishmania infantum*  
*L. major* : *Leishmania major*  
*L. tarentolae* : *Leishmania tarentolae*  
LPG : Lipophosphoglycan  
M-CSF : Macrophage-Colony Stimulating Factor  
MGG : May-Grünwald Giemsa  
MOI : Multiplicity Of Infection (Multiplicité d'infection)  
NO : Nitric Oxide (Oxide Nitrique)  
OMS : Organisation Mondiale de la Santé  
PBMC : Peripheral Blood Monocytes (Cellules mononuclées de sang périphérique)  
PBS : Phosphate Buffered Saline (Tampon Phosphate Salin)  
PCR : Polymerase Chain Reaction (Amplification en chaine par polymérase)  
ROS : Reactive Oxygen Species (Espèces réactives de l'Oxygène)  
SATT Sud-Est : Société d'accélération du Transfert des Technologies Sud-Est  
UCA : Université Côte d'Azur  
WT : Wild Type (Sauvage)



# Liste des Figures

Figure 1 : Cartes du monde indiquant les pays d'endémicité de la Leishmaniose cutanée et viscérale .....	18
Figure 2 : Deux formes du parasite <i>Leishmania</i> .....	20
Figure 3 : Cycle biologique du parasite <i>Leishmania</i> .....	22
Figure 5 : Schéma des trois formes de la Leishmaniose.....	25
Figure 6 : Test d'infectivité de 4 souches sauvages isolées au CHU de Nice .....	70
Figure 7 : Croissance, mortalité et émission de bioluminescence de <i>L. tarentolae</i> WT et eFFly-mCherry. ....	102
Figure 8 : Promastigotes <i>L. tarentolae</i> -eFFly-mCherry en microscopie confocale. ....	103
Figure 9 : Quantification par qPCR de la charge parasitaire dans le foie et la rate de souris infectées .....	104
Figure 10 : Infection de souris Balb/c avec des <i>L. infantum</i> Luc et eFFly-mCherry.....	105
Figure 11 : Quantification de l'émission de bioluminescence au niveau du foie et de la rate de souris infectées par <i>L. infantum</i> Luc et eFFly-mCherry .....	105
Figure 12 : Évolution de l'infection de souris Balb/c par <i>L. infantum</i> eFFly-mCherry sur des temps courts... ..	106
Figure 13 : Quantification de l'émission de bioluminescence dans le foie de souris infectées par <i>L. infantum</i> eFFly-mCherry. ....	106
Figure 14 : Tableau des correspondances entre les numéros des molécules et leur nom. ....	111
Figure 15 : Résumé du projet de thèse à l'origine des travaux présentés ici.....	114
Figure 16 : Schéma du procédé d'obtention des chromatogrammes HPLC.....	115
Figure 17 : Chromatogramme HPLC de l'extrait CA-TM-0015. ....	115
Figure 18 : Chromatogramme HPLC des fractions C et E.....	116
Figure 19 : Résultat de la chromatographie de partage centrifuge sur la séparation de la fraction E .....	117
Figure 20 : Structure chimique des molécules 1 à 8 .....	122

Figure 21 : Cytotoxicité des molécules pures sur des cellules primaires BMDM murines. ....	123
Figure 22 : Cytotoxicité des molécules pures sur une lignée de cellules THP-1 humaines.....	124
Figure 23 : Cytotoxicité des molécules pures sur des PBMC primaires humains. ....	124
Figure 24 : Effet sur la forme promastigote de <i>L. infantum</i> des molécules pures.....	125
Figure 25 : Effet sur la forme amastigote de <i>L. infantum</i> dans des BMDM des molécules pures.....	126
Figure 26 : Modifications induites par la molécule 8 sur la sécrétion de cytokines par des BMDM.....	127
Figure 27 : Quantification par ELISA sandwich de l'IL-1ra dans les surnageants de cellules BMDM. ....	128
Figure 28 : Schéma de la technique de chromatographie sur colonne HPLC. ....	129
Figure 29 : Spectre HPLC classique de la Molécule 8. ....	130
Figure 30 : Spectre HPLC de la Molécule 8 après 7 jours à 100°C. ....	131
Figure 31 : Quantification de la stabilité de la molécule 8 en suivi HPLC. ....	131
Figure 32 : Intégrité de la molécule 8 au cours du temps. ....	132
Figure 33 : Structure des dérivés de la molécule 8.....	133
Figure 34 : Cytotoxicité des dérivés sur cellules BMDM .....	135
Figure 35 : Effet des molécules pures sur la forme promastigote de <i>L. infantum</i> .....	136
Figure 36 : Tableau récapitulatif des valeurs de CC <sub>50</sub> , IC <sub>50</sub> et SI .....	137
Figure 37 : Schéma expérimental du protocole de prévention à l'aide de la molécule 8 .....	140
Figure 38 : Souris représentatives des groupes traités ou non avec la molécule 8 après infection à <i>L. infantum</i> .....	140
Figure 39 : Effet du pré-traitement avec la Molécule 8 sur l'infection de souris à <i>L. infantum</i> .....	141
Figure 40 : Schéma expérimental du protocole de traitement de souris avec la molécule 8.....	142
Figure 41 : Effet du traitement avec la Molécule 8 sur l'infection de souris à <i>L. infantum</i> .....	142



# Introduction



# I. Épidémiologie

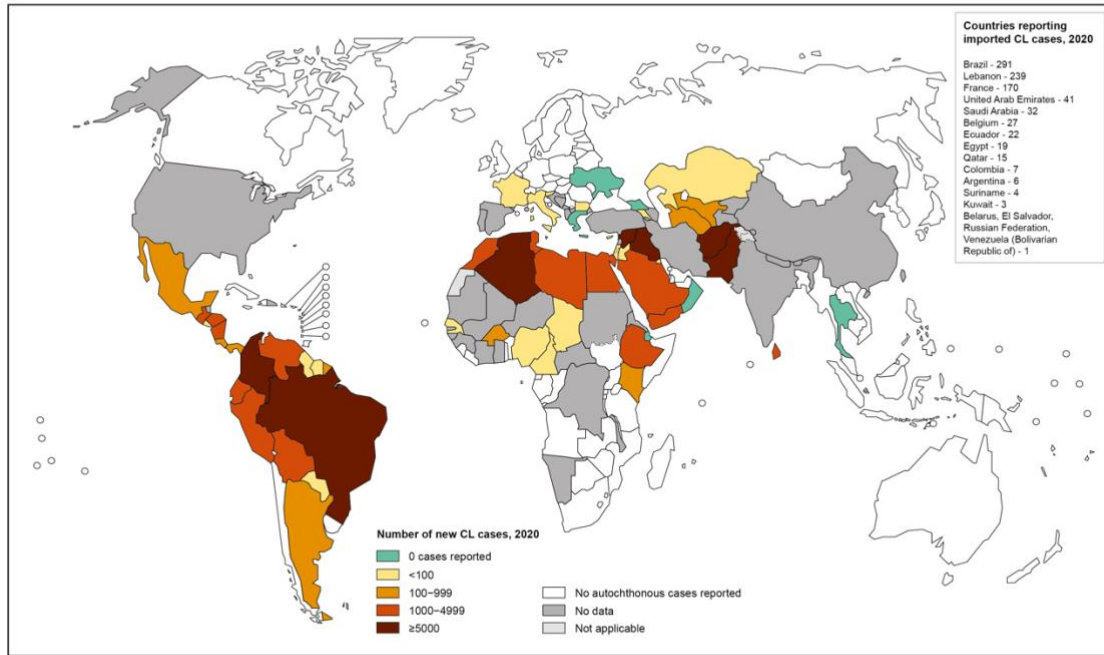
## a. Chez l'humain

Les leishmanioses sont un groupe de maladies tropicales négligées. Selon l'Organisation Mondiale de la Santé (OMS), il s'agit de la seconde cause de mortalité parmi les maladies tropicales négligées, et de la quatrième cause de morbidité des maladies tropicales.

Chaque année, on estime qu'il y a entre 700 000 – 1 000 000 de nouveaux cas de leishmaniose dans le monde, avec 1 milliard de personnes à risque d'une infection dans les zones endémiques de la maladie. Les personnes les plus à risque vivent dans des pays en voie de développement, où le risque de transmission et de développement de la maladie sont largement favorisés par la pauvreté et la malnutrition (WHO, 2021).

Des cas de leishmaniose ont été reportés sur tous les continents à l'exception de l'Antarctique, et on estime qu'elles sont endémiques dans plus de 98 pays pour la forme cutanée et 84 pays pour la forme viscérale à travers le monde (Fig 1).

Status of endemicity of cutaneous leishmaniasis worldwide, 2020

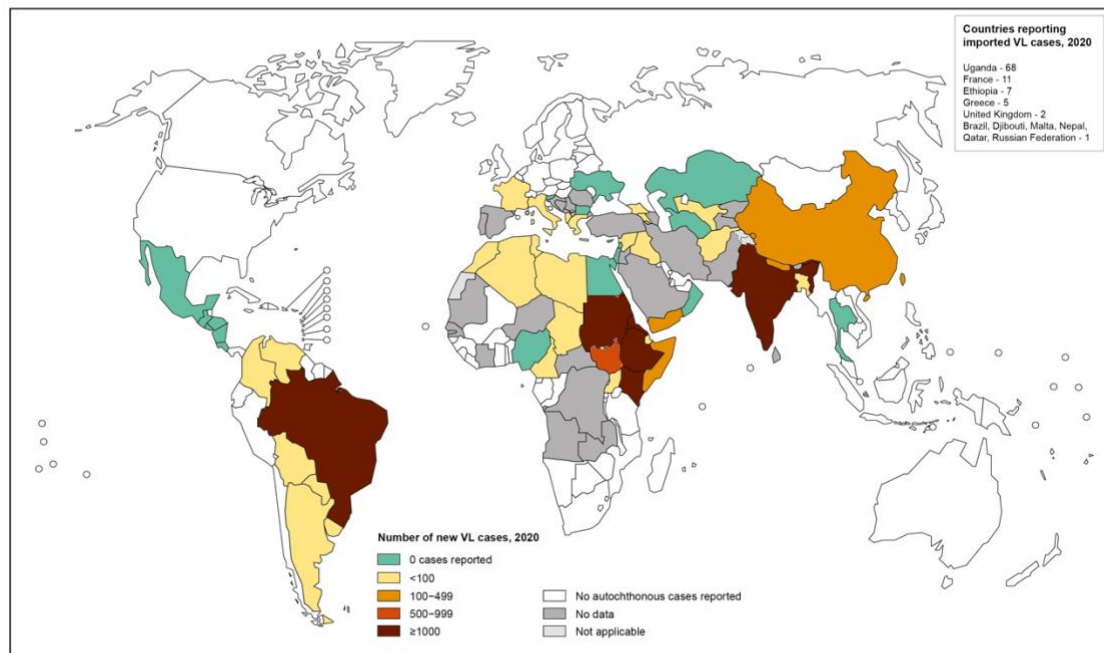


The boundaries and names shown and the designations used on this map do not imply the expression of any opinion whatsoever on the part of the World Health Organization concerning the legal status of any country, territory, city or area or of its authorities, or concerning the delimitation of its frontiers or boundaries. Dotted lines on maps represent approximate border lines for which there may not yet be full agreement. © WHO 2021. All rights reserved

Data Source: World Health Organization  
Map Production: Control of Neglected Tropical Diseases (NTD)  
World Health Organization



Status of endemicity of visceral leishmaniasis worldwide, 2020



The boundaries and names shown and the designations used on this map do not imply the expression of any opinion whatsoever on the part of the World Health Organization concerning the legal status of any country, territory, city or area or of its authorities, or concerning the delimitation of its frontiers or boundaries. Dotted lines on maps represent approximate border lines for which there may not yet be full agreement. © WHO 2021. All rights reserved

Data Source: World Health Organization  
Map Production: Control of Neglected Tropical Diseases (NTD)  
World Health Organization



Figure 1 : Cartes du monde indiquant les pays d'endémicité de la Leishmaniose cutanée et viscérale

Source : [https://apps.who.int/neglected\\_diseases/ntddata/leishmaniasis/leishmaniasis.html](https://apps.who.int/neglected_diseases/ntddata/leishmaniasis/leishmaniasis.html)

L'infection à *Leishmania* peut être asymptomatique, mais lorsque la maladie est déclarée, différentes formes cliniques se présentent. Elles sont conférées par différentes espèces de leishmanies et peuvent aller de sévérité croissante d'une leishmaniose cutanée localisée à une leishmaniose viscérale mortelle en l'absence de traitement.

## b. Chez l'animal

En Europe, et précisément sur le pourtour du bassin méditerranéen, *L. infantum* est souvent retrouvée chez le chien qui est considéré comme étant le réservoir majoritaire. Il est estimé que 2,5 millions de chiens sont atteints de la leishmaniose en Europe, dont 1 million en France (Virbac, 2018) et que la prévalence varie entre 40% à 80% de chiens infectés, en dépit de l'existence d'un vaccin préventif (Bourdoiseau, 2015). Cependant depuis quelques années, on sait que le parasite *Leishmania* peut aussi être retrouvé chez le chat (Pennisi *et al.*, 2013), les rongeurs comme les souris, rats et lapins (Alcover, Riera, & Fisa, 2021), les renards (Dipineto *et al.*, 2007) et même chez les kangourous (Rose *et al.*, 2004), même si les prévalences sont bien inférieures à celles retrouvées chez le chien.



## II. Parasites

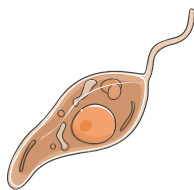
### a. Morphologie

Les leishmanies sont des parasites dimorphiques capables d'alterner entre deux formes.

La première est une forme extracellulaire « promastigote » flagellée, d'une longueur de 10 – 25  $\mu\text{m}$  de long sur 1 – 4  $\mu\text{m}$  de large. Elle est retrouvée dans le tube digestif et au niveau du rostre du vecteur, le phlébotome. Les promastigotes vivent et se multiplient dans le phlébotome à température ambiante, et se cultivent au laboratoire à une température d'environ 26°C.

La seconde est une forme intracellulaire appelée forme « amastigote » ne présentant pas de flagelle externe, mesurant entre 2 – 4  $\mu\text{m}$  de diamètre. Cette forme est retrouvée dans les hôtes et réservoirs de la maladie. La transformation en cette forme se fait sous l'effet d'une augmentation de la température et la diminution du pH de la vacuole parasitophore, dans laquelle le parasite est contenu. Ainsi la forme amastigote est trouvée à une température de 37°C dans les macrophages des espèces hôtes, ou dans des macrophages en culture (Fig 2).

#### Forme Promastigote



Retrouvée chez le phlébotome femelle  
Flagelle externe  
Taille : 10 – 25  $\mu\text{m}$  de long sur 1 – 4  $\mu\text{m}$  de large  
Conditions de vie : pH neutre et T° ambiante

#### Forme Amastigote



Retrouvée dans les cellules du système  
Réticulo-Histiocytaire de l'hôte  
Flagelle internalisé  
Taille : 2– 4  $\mu\text{m}$  de diamètre  
Conditions de vie : pH acide et T°= 37°C

**Figure 2** : Deux formes du parasite *Leishmania*

## b. Cycle de Vie

Les parasites du genre *Leishmania* possèdent un cycle de vie particulier qui nécessite leur passage entre deux formes.

Dans le phlébotome femelle, les parasites sont présents sous leur forme promastigote. Lors du repas sanguin d'un phlébotome, et contrairement aux moustiques qui piquent afin de se nourrir de sang, le phlébotome déchiquète les tissus afin de créer un lac sanguin dans lequel il se nourrit.

Lors du repas sanguin, le phlébotome va régurgiter les promastigotes contenus au niveau de son rostre dans le lac sanguin. Ils vont ensuite pouvoir être phagocytés et entrer par un mécanisme d'invasion active dans les macrophages hôtes, où ils seront contenus dans une vacuole parasitophore. Les vacuoles parasitophores fusionnent avec les lysosomes qui mènent à une acidification forte jusqu'à un pH d'environ 5,5 dans le phagolysosome. Afin de s'adapter aux nouvelles conditions de vie dans l'hôte (pH acide et température de 37°C), les promastigotes se transforment en amastigotes. Les cellules s'arrondissent, internalisent leur flagelle et en ralentissent tout métabolisme non essentiel à la croissance. Ils vont ensuite se multiplier par scissiparité jusqu'à lyser la cellule hôte pour se disséminer, infecter de nouveaux macrophages et ainsi amplifier l'infection aboutissant au développement des symptômes.

Lorsqu'un phlébotome sain vient prendre son repas sanguin sur un hôte infecté, il ingère des macrophages et monocytes sanguins contenant des leishmanies, qui sont rapidement lysés mécaniquement dans le tractus digestif, libérant ainsi les amastigotes. Ils vont alors se transformer en promastigotes procycliques sous l'effet de la diminution de température et du retour à un pH moins acide. Dans le tractus intestinal du phlébotome, les promastigotes procycliques vont se multiplier, puis migrer le long du tractus digestif vers le rostre du phlébotome, où une seconde transformation s'opère en promastigotes métacycliques, qui correspondent à la forme la plus infectante du parasite.

Finalement le cycle se complète lorsque le phlébotome infecté vient prendre son repas sanguin sur un hôte sain, et ainsi de suite (Fig 3).

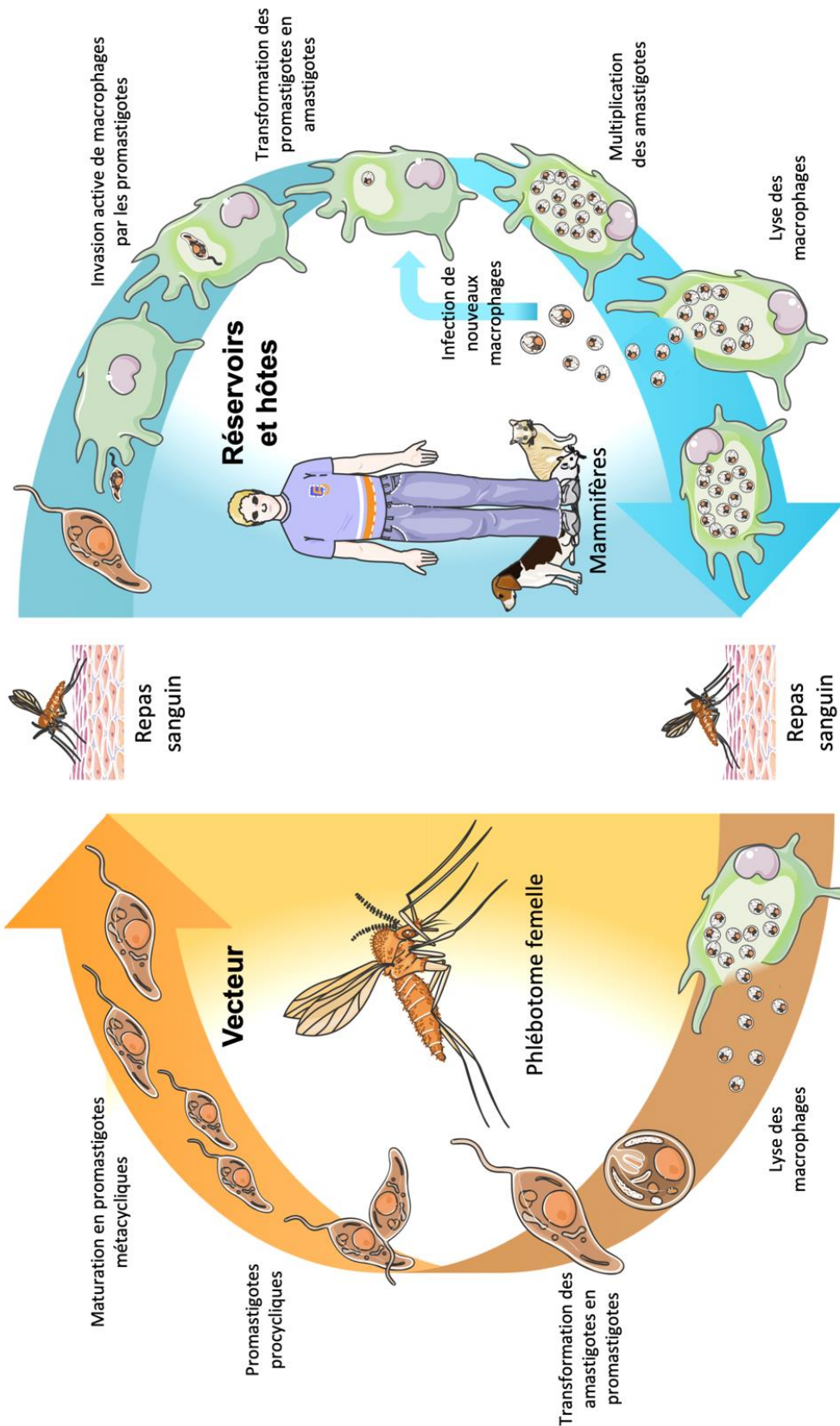


Figure 3 : Cycle biologique du parasite *Leishmania*

Source : Le cycle a été adapté depuis la thèse de Grégory Michel (Michel, 2011)

### III. Vecteurs et Réservoirs

#### a. Le Phlébotome femelle

Il existe une vingtaine d'espèces de leishmanies pathogènes pour l'Homme dans le monde, transmises par environ trente espèces de phlébotomes différents. Ces insectes diptères de la famille des *Psychodidae* mesurent 2 à 3 mm de long, et seules les femelles ont besoin d'un repas sanguin afin de stimuler leur oogenèse. Les phlébotomes femelles constituent donc le vecteur des leishmanioses. Lors du repas sanguin les phlébotomes régurgitent une grande quantité d'agents anticoagulants et anesthésiants, en même temps que les parasites accumulés dans la zone buccale. Chaque espèce de phlébotome sera souvent porteuse spécifiquement d'une seule espèce de leishmanie, qui possède souvent un hôte préférentiel ce qui rend les répartitions des maladies très spécifiques d'un point de vue géographique (Alemayehu & Alemayehu, 2017) (Fig 4).

Sand fly species	Geographical distribution
<i>Phlebotomus papatasi</i> , <i>Phlebotomus dubosqi</i> , <i>Phlebotomus salehi</i>	Central and West Asia, North Africa, Sahel of Africa, Central and West Africa
<i>Phlebotomus sergenti</i>	Central and West Asia, North Africa
<i>Phlebotomus longipes</i> , <i>Phlebotomus pedifer</i>	Ethiopia, Kenya
<i>Phlebotomus argentipes</i> , <i>Phlebotomus orientalis</i> , <i>Phlebotomus martini</i>	Indian subcontinent, East Africa
<i>Phlebotomus ariasi</i> , <i>Phlebotomus perniciosus</i>	Mediterranean basin, Central and West Asia
<i>Lutzomyia longipalpis</i>	Central and South America
<i>Lutzomyia olmecaolmeca</i>	Central America
<i>Lutzomyia flaviscutellata</i>	South America
<i>Lutzomyia wellcomei</i> , <i>Lutzomyia complexus</i> , <i>Lutzomyia carrerai</i>	Central and South America
<i>Lutzomyia peruensis</i> , <i>Lutzomyia verrucarum</i>	Peru
<i>Lutzomyia umbratilis</i>	South America
<i>Lutzomyia trapidoi</i>	Central America

Figure 4 : Principales espèces de phlébotome transmettant des leishmanies capables d'infecter l'homme

## b. Les Réservoirs

Selon l'OMS, il existe environ 70 espèces hôtes pour *Leishmania* (WHO, 2021).

Deux grandes classes de leishmanioses sont connues : les leishmanioses zoonotiques, caractérisées par un réservoir animal, et les leishmanioses anthroponotiques, caractérisées par un réservoir humain.

Un exemple de leishmaniose zoonotique est la transmission méditerranéenne de *L. infantum* par le phlébotome *P. perniciosus*, avec pour réservoir principal le chien. Les infections à *L. infantum* chez le chien peuvent rester indétectées pendant une longue durée. La période d'incubation varie de quelques mois à quelques années, puis les chiens développent une forme viscérale de la maladie. Les principaux symptômes sont la perte de poils autour des yeux, la pousse incontrôlée des griffes (onychogryphose) et des affections cutanées. Dans les cas les plus sévères, on observe une perte de poids importante de l'animal, qui précède généralement le décès.

Si pendant longtemps le chien a été considéré comme le réservoir principal de *L. infantum* sur le pourtour du bassin méditerranéen, aujourd'hui le chat apparaît de plus en plus comme un réservoir potentiel. En Italie, des études ont montré une prévalence de 3,9% chez les chats, (Iatta *et al.*, 2019) et dans des foyers de leishmaniose canine dans les Alpes-Maritimes, 12,5% des chats présentaient des anticorps contre des antigènes de *L. infantum* (Mancianti, 2004).

La leishmaniose anthroponotique est caractérisée par le fait que le réservoir est l'humain. Un exemple est la transmission de la leishmaniose anthroponotique viscérale sur le continent Indien de *L. donovani* par le phlébotome *P. argentipes*. Le second exemple est la transmission de *L. tropica* par *P. sergenti* au Moyen-Orient, caractérisé comme une leishmaniose anthroponotique cutanée (Reithinger *et al.*, 2003).

## IV. Formes Cliniques

Les symptômes de la maladie chez l'humain sont extrêmement variables, et on considère qu'il y a largement plus de cas asymptomatiques que de cas symptomatiques des suites d'une infection à *Leishmania* (Michel, Pomares, Ferrua, & Marty, 2011). Dans les cas symptomatiques, les manifestations cliniques dépendent principalement de deux choses : le statut immunitaire du patient, et l'espèce de leishmanie. On retrouve principalement 3 formes de la maladie d'une sévérité croissante : la forme cutanée, la forme muco-cutanée et la forme viscérale (Fig 5).



**Figure 5** : Schéma des trois formes de la Leishmaniose.

D'une intensité et gravité croissante, on distingue la forme cutanée, muco-cutanée et viscérale parmi les manifestations cliniques de la leishmaniose.

### a. Leishmanioses Cutanées

La leishmaniose cutanée est la forme la plus fréquente de la maladie. Elle cause des lésions cutanées au site d'infection, qui peuvent guérir spontanément mais laissent d'importantes cicatrices, responsables de problèmes sociaux d'exclusion et de stigmatisation. On estime entre 600 000 à 1 000 000 de nouveaux cas par an de leishmaniose cutanée, et 95% de ces cas sont retrouvés sur le continent Américain, sur le pourtour du Bassin Méditerranéen, au

Moyen-Orient et en Asie centrale, avec 87% de ces cas observés dans les 10 pays les plus touchés par la leishmaniose cutanée (Afghanistan, Algérie, Brésil, Colombie, Iran, Iraq, Libye, Pakistan, Syrie et Tunisie) (WHO, 2017; WHO, 2021). La leishmaniose cutanée peut être conférée par *L. major*, *L. tropica*, *L. aethiopica*, le complexe *L. mexicana* (*L. mexicana*, *L. amazonensis*, *L. venezuelensis*) ou le complexe *Vianna* (*L. braziliensis*, *L. guyanensis*, *L. panamensis*, *L. peruviana*) (CDC, 2020).

## b. Leishmanioses Muco-cutanées

La leishmaniose muco-cutanée provoque d'importantes lésions au niveau des muqueuses du nez et de la bouche. En l'absence de traitement, ces lésions peuvent évoluer et mener à la destruction des muqueuses, de la cloison nasale et présenter des cas de défiguration sévère. Dans la majorité des cas, les lésions muqueuses surviennent quelques années voire dizaines d'années après une leishmaniose cutanée, et sont le résultat de la dissémination métastatique des parasites après une absence de traitement ou un traitement incomplet ou sub-optimal. La leishmaniose muco-cutanée est le plus souvent conférée par les espèces du complexe *Vianna*, majoritairement par *L. braziliensis*, mais aussi par *L. guyanensis* et *L. panamensis*. *L. amazonensis* peut aussi conférer la leishmaniose muco-cutanée. Les risques de développement de leishmaniose muco-cutanée sont encore largement méconnus, tant en matière de réponse de l'hôte que des parasites (CDC, 2020).

## c. Leishmanioses Viscérales

La leishmaniose viscérale est la forme la plus sévère de la maladie, car elle est fatale en l'absence de traitement, contrairement aux formes cutanées qui n'entraînent pas directement la mort, même si elles présentent un risque de morbidité associée. Elle peut être conférée par *L. donovani* et *L. infantum* (aussi appelé *L. chagasi*) et provoque de la fièvre

irrégulière, une importante perte de poids, une pancytopénie (anémie, leucopénie et thrombocytopénie), avec une hypergammaglobulinémie et une hépatosplénomégalie. En effet, ces espèces ont un tropisme particulier pour le foie et la rate, où la multiplication des leishmanies s'opère. En Inde, cette forme est appelée Kala-azar (traduit par « fièvre noire ») et elle donne également son nom à la leishmaniose Post Kala-Azar, un syndrome caractérisé par des lésions cutanées disséminées arrivant des suites d'une infection à *L. donovani*.



## V. La relation hôte-pathogène

Lors du repas sanguin sur les hôtes, le phlébotome régurgite dans sa salive les promastigotes et de nombreux autres composés. Si plus de 90% des parasites seront détruits par la lyse de la cascade du complément, une partie est capable d'utiliser le dépôt des fragments C3b liés à l'opsonisation pour faciliter l'entrée dans les macrophages par le récepteur au complément CR2 (Elmahallawy, Alkhalidi, & Saleh, 2021). Parmi les composés sécrétés par le phlébotome, on trouve des facteurs pro-inflammatoires qui vont permettre le recrutement de cellules immunitaires au site de l'infection et favoriser la phagocytose des promastigotes, qui se retrouvent alors dans leur cellule hôte directement (Chagas et al., 2014). Afin de réussir à échapper à la réponse du système immunitaire, le parasite se transforme en forme amastigote pour résister au pH acide de la vacuole parasitophore, suite à la fusion des lysosomes à la vacuole parasitophore. Le promastigote, par ses protéines de surface comme le Lipophosphoglycan (LPG), est capable de retarder la maturation du phagosome et d'atténuer les fonctions microbicides du macrophage (Vinet, Fukuda, Turco, & Descoteaux, 2009). La métalloprotéase GP63 est un autre facteur de virulence important, permettant la survie intracellulaire de *Leishmania* même si les mécanismes spécifiques n'ont pas encore été mis en lumière (Olivier, Atayde, Isnard, Hassani, & Shio, 2012). Une fois le parasite contenu dans les macrophages de l'hôte, la réponse immunitaire est très dépendante de l'espèce de leishmanie étudiée, mais aussi de l'hôte. Il a été admis longtemps qu'une réponse de type Th1 serait plus favorable pour une élimination du parasite. Les cellules T Th1, en sécrétant de l'IFN- $\gamma$  et TNF- $\alpha$ , sont capables d'activer les mécanismes microbicides des macrophages, tel que la sécrétion d'espèces réactives de l'oxygène (ROS) et d'Oxide nitrique (NO) par induction de l'Oxide nitrique synthase inductible (iNOS). Au contraire, une réponse Th2 caractérisée par la sécrétion d'IL-4 et IL-13 serait bénéfique à la réplication du parasite. Aujourd'hui, il est admis qu'il faut une balance entre les deux réponses, et qu'une réponse trop forte Th1 et TNF-  $\alpha$  pourrait même favoriser la dissémination de lésions cutanées (Rossi & Fasel, 2018).

## VI. Les traitements

Actuellement il n'existe aucun vaccin pour l'homme, et les mesures préventives se limitent à l'application de produits répulsifs pour moustiques sur la peau et les vêtements dans les zones endémiques de la maladie. Il existe des traitements curatifs pour la leishmaniose humaine, qui totalisent 7 molécules autorisées. Les indications des traitements de référence sont différentes en fonction des pays et des régions, cependant aujourd'hui en Europe le traitement préconisé contre la leishmaniose est l'Amphotéricine B sous sa forme Liposomale (WHO, 2010).

### a. Antimoniés pentavalents

Historiquement, les antimoniés Pentavalents sont les premiers traitements approuvés contre la leishmaniose et sont encore utilisés aujourd'hui. Ils ont remplacé en 1922 les antimoniés trivalents, plus dangereux pour la santé. Il existe aujourd'hui sur le marché deux antimoniés pentavalents préconisés dans le traitement de la leishmaniose, le Sodium Stibogluconate et la Meglumine antimoniate. Ces composés ont été largement utilisés jusque dans les années 1980, mais présentent aujourd'hui un grand risque d'échec thérapeutique dû au nombre important de souches résistantes présentes.

### b. Pentamidine

La pentamidine, même si elle figure toujours sur la liste des traitements autorisés pour traiter la leishmaniose, a vu son utilisation limitée par l'OMS à la suite d'occurrences d'effets secondaires sévères tel que le diabète et la myocardite.

### c. Amphotéricine B

L'Amphotéricine B est disponible depuis 1996 et avait au départ été approuvé comme un antifongique pour traiter la candidose invasive. L'injection par voie intraveineuse de ce composé, bien qu'efficace et avec peu de résistances connues à ce moment-là, possède une néphrotoxicité importante. C'est pour cela que quelques années plus tard, sa forme encapsulée liposomale a été mise sur le marché et a permis de réduire drastiquement sa toxicité. L'Amphotéricine B interagit avec l'ergostérol de la membrane, retrouvé seulement chez les pathogènes et non chez l'humain, et y crée des pores responsables de la mort des parasites. Bien que très efficace sous sa forme liposomale, la réduction de la toxicité a drastiquement augmenté le coût de production de l'Amphotéricine B, ce qui fait qu'il n'est pas accessible à des personnes vivant dans des pays à faible revenu. De plus, afin de limiter la néphrotoxicité, le traitement est administré par perfusion, et les patients doivent rester hospitalisés quelques jours afin de surveiller la fonction rénale.

### d. Miltefosine

La miltefosine est le seul traitement anti-*Leishmania* à pouvoir être pris sous forme orale. Repositionné depuis une drogue anti-cancéreuse, la miltefosine a la particularité de moduler la réponse de l'hôte vers une immunité de type « Th1 », bénéfique pour la résolution de l'infection, en même temps que d'inhiber la synthèse de lipides essentiels pour les membranes parasitaires.

### e. Paromomycine

La paromomycine est la drogue la plus récemment approuvée. Elle est capable d'inhiber la synthèse protéique de *Leishmania* mais présente une importante toxicité rénale et hépatique.

Elle est administrée par voie intramusculaire ou par voie topique dans le cas de traitement de leishmaniose cutanée. La paromomycine est à l'origine un antibiotique.

#### f. L'allopurinol pour la leishmaniose canine

Utilisée seule ou en combinaison avec le Meglumine antimoniate, l'allopurinol est le traitement de choix pour les chiens atteints de leishmaniose. Ce composé est un leishmaniostatique inhibant la multiplication des parasites qui, utilisé en combinaison avec une autre drogue comme par exemple la miltefosine, permet de diminuer le nombre de cas de rechute après traitement (Dias *et al.*, 2020).

#### g. Autres traitements

La recherche de nouveaux traitements contre la leishmaniose est aujourd'hui une priorité. Ainsi, les stratégies actuelles de développement de nouveaux traitements visent à contourner les problèmes des anciens traitements : les effets secondaires, la toxicité, l'administration invasive qui rend la continuité des traitements problématique dans des zones où l'accès à l'hôpital n'est pas toujours facile. Le coût des traitements et la nécessité d'hospitalisation prolongée.

Afin de comprendre comment les stratégies actuelles de recherche de nouveaux traitements permettent de contourner ces problèmes, j'ai réalisé un travail de synthèse sous la forme d'une revue de la littérature.

Brièvement, nous avons regardé entre 2015 et aujourd'hui les traitements approuvés et les avancées récentes dans la recherche de nouveaux traitements. Sur les 598 articles recueillis sur le sujet, nous avons réalisé un premier tri afin de ne garder que des articles traitant d'expérimentations *in vivo* ou *in vitro* sur des amastigotes.

Dans un premier temps, nous avons documenté les traitements actuellement approuvés, avec leur mécanisme d'action et leur limite, puis nous avons regardé comment les traitements actuellement développés cherchaient à améliorer la prise en charge des patients. Nous avons fini par trier 89 articles restants dans 6 grands groupes. En regardant les 7 traitements approuvés contre la leishmaniose, nous avons pu identifier 2 stratégies principales de contournement des problèmes liés aux traitements. Dans un premier temps, près de la moitié des traitements approuvés sont issus du repositionnement de composés utilisés à l'origine pour traiter d'autres maladies. On peut ainsi citer l'Amphotéricine B, la miltefosine et la paromomycine. Ensuite, la formulation sous forme de nanoparticules a montré d'importants effets de réduction de la toxicité de l'amphotéricine B, car elle peut améliorer la biodisponibilité et permettre un changement de formulation de nombreux composés.

Ensuite, la dose nécessaire pour traiter efficacement la leishmaniose est souvent problématique. C'est pour cela que l'une des stratégies les plus explorées est la combinaison de traitements approuvés afin de réduire la dose nécessaire de chaque traitement et ainsi limiter les effets toxiques de chaque drogue. Dans la même idée, la combinaison de traitements approuvés et de cytokines ou d'agents immuno-modulateurs permettrait la réduction de la dose nécessaire de chémo-thérapie, étant donné que la leishmaniose et la progression de cette maladie est liée à la réponse Th1/Th2 des cellules. Finalement, nous avons consacré une partie de cette revue à la recherche de traitements sur la base de l'ethnobotanique, qui vise à découvrir de nouvelles molécules en s'appuyant sur l'expérience de groupes ethniques et de leur connaissance des plantes médicinales. Ceci permet de cribler des plantes, qui sont connues pour être un grand réservoir de molécules actives, tout en limitant le coût d'un crible à grande échelle en le resserrant d'emblée sur des plantes connues pour leur vertus médicinales.

Ainsi, cette revue met en perspective comment la recherche aborde actuellement la problématique de la leishmaniose en ayant recours à diverses stratégies pour réduire la toxicité, le coût ou modifier la voie d'administration de traitements actuellement approuvés, et quelles sont les méthodes pour la découverte de nouveaux traitements dans le contexte d'une maladie tropicale négligée.

## Leishmaniasis : Strategies in treatment development

Alissa MAJOOR<sup>1</sup>, Grégory MICHEL<sup>1,\*</sup>, Pierre MARTY<sup>1,2</sup>, Laurent BOYER<sup>1</sup>, Christelle POMARES<sup>1,2</sup>

<sup>1</sup> Université Côte d'Azur, INSERM U1065, Centre Méditerranéen de Médecine Moléculaire (C3M), Nice, France. <sup>2</sup> Service de Parasitologie-Mycologie, Centre Hospitalier Universitaire de Nice, Hôpital de l'Archet, Nice, France. \* Corresponding author. Electronic address: gregory.michel@univ-cotedazur.fr

### Abstract

Leishmaniasis is a vector-borne disease that threatens over 1 billion people worldwide. This dimorphic parasite targets cells of the reticulo-histiocitary system like macrophages where they multiply until macrophage burst and propagate infection. Several forms of this disease exist, ranging from localized cutaneous afflictions to life-threatening visceral forms leading to death in 95% of cases in the absence of treatment. Actual treatments rely on the invasive administration of toxic, expensive treatments facing more and more frequent apparition of resistance. Thus, it is important to find alternative treatments for this disease. This review of literature bases itself on recent development of alternative treatments in the last 5 years, and aims to show the different strategies used to bypass actual limitations such as cost, toxicity, off-target effects, administration route and the emergence of resistance. Starting with the review of actual authorized treatments and their specific limitations, we have divided the strategies of treatment development in 5 classes. The use of a combination of approved treatments allowed for the bypassing of resistance, dosage-decrease, thus limiting adverse effects and toxicity. Formulation in nanoparticle carriers allowed for specific targeting in infected organs, as well as efficiency increase, coming with a higher cost due to formulation. Drug repositioning, a technique already used for more than half of the actual approved compounds, showed promising results for the identification of molecules with an anti-leishmanial effect. Immunomodulation in combination with current chemotherapies allowed for efficiency increase of reference treatments and reduced risks of relapse by stimulating the immune system, but did not always skew the host response in a favorable way. Last the use of ethnobotanics gave rise to some promising *in vitro* results, that combined molecules with low toxicity, immunomodulatory properties, and a good anti-parasitic effect. In summary, this review has listed some classes of current strategies of treatment development with their benefits over reference treatments and their limitations.

## Author Summary

Leishmaniasis is a disease conferred by a flagellated parasite called *Leishmania* that is transmitted through the bite of sandflies. Whereas the cutaneous form of this disease leads to localized self-healing infections on the skin, the visceral form leads to death in 95% of cases when left untreated. There is no human vaccine against this disease, and current treatments present import limitations, with a high cost, toxicity, relapses after treatment and increase of therapeutic failures due to the apparition of resistances against approved molecules. It is thus important to develop new treatments against this disease. Among actual strategies to reduce adverse effects and limitations of current treatments, this review investigates the advantages of combination of approved molecules, their formulation in nanocarriers and combination with immunomodulators in order to limit actual treatment issues. Novel treatments are being investigated by using a time and money-saving strategy of drug repurposing by using approved drugs against other diseases in the treatment of leishmaniasis. Last, in an attempt to obtain cheaper, more sustainable products with low toxicity and available in great numbers, the strategy of ethnobotany relies on the knowledge of indigenous populations in order to tests plants for anti-parasitic compounds. In summary, numerous strategies exist to try and find alternative treatments against leishmaniasis.

## **Introduction**

Leishmaniasis is a vector-borne disease transmitted by the bite of phlebotomine sandflies, that can be found in over 98 countries in the world, thus putting over 1 billion people at risk of exposure [1]. It is responsible for 20 000 to 30 000 deaths a year and figures since 2011 on the list of uncontrolled neglected tropical diseases [2].

*Leishmania* parasites target the reticulo-histiocitary system of mammals, targeting macrophages as their main host cell, where they replicate until macrophage burst and propagate infection. There are over 20 causative species of *Leishmania*, with different tropisms leading to either asymptomatic carriage or to various clinical manifestations, ranging from self-healing skin ulcers to systemic infection, with severe hepatosplenomegaly, which is fatal without treatment [3].

In the case of human leishmaniasis, there are four main forms with increasing severity. Cutaneous leishmaniasis, giving rise to ulcerating skin lesions, is the most common form and is generally due to infection with *Leishmania (L.) major*, *L. tropica* or *L. mexicana*. Muco-cutaneous leishmaniasis conferred by *L. braziliensis*, *L. panamensis* and *L. amazonensis* targets the mucosa of the nose and mouth, leading to severe disfiguration with the progression of the disease. Visceral leishmaniasis is the most severe form of the disease, targeting the liver and spleen, leading to irregular fever, severe hepatosplenomegaly, with a mortality of 95% in the absence of treatment. It can be conferred by *L. donovani*, which can give rise to Post Kala-Azar Dermal Leishmaniasis (PKDL) manifesting as a disseminated skin affection after initial successful cure from VL [3]. It can also be conferred by *L. infantum*.

In the case of *L. infantum*, dogs are the main reservoir of the parasite, since the circulating burden in the bloodstream is high enough that a non-infected sandfly can become infected during a bloodmeal. Transmission can then occur to other mammals including foxes, rodents, and humans. In symptomatic dogs, clinical symptoms often start by showing cutaneous affections such as alopecia, onychogryphosis, keratoconjunctivitis and eye lesions such as uveitis. These symptoms can gradually evolve to a visceral form with splenomegaly and renal failure in later stages, leading to weight loss, muscular atrophy, and lethargy [4].

Up to date, there are three commercialized vaccines with proven efficacy against canine leishmaniasis due to *L. infantum* : CaniLeish® and LetiFend® in Europe, and Leish-Tec® in Brazil, but there is no human vaccine efficient against any form the disease [5]. Prevention of the disease in humans relies solely on repulsive methods, such as sprays or mosquito nets, to avoid initial infection by the parasite after contact with sandflies. Once the infection took place, the only option is to rely on curative treatments. WHO has recommended the use of Pentavalent antimonials as first line treatment in most parts of the world, but today Liposomal Amphotericin B (L-AMB) is considered first line treatment in high-income



countries [6]. Overall, approved molecules for the treatment of leishmaniasis present problems including high cost, toxicity, the need for invasive administration, important duration of treatment and the emergence of resistance towards all approved treatment regimens [7]. Thus, it is a priority today to develop alternative treatments to cure leishmaniasis.

This review aims to focus on the strategies used to avert and bypass these limitations regarding current treatments against leishmaniasis. We will focus on the development of alternative treatments or administration seeking to reduce toxicity, cost, and resistance, as well as administration routes and reduction of treatment duration.

## **Methods**

This review sheds light on strategies of drug development to treat leishmaniasis and focuses on recent developments from the last five years, between 2015 and 2020. Briefly, we conducted bibliography research on PubMed with different keywords including: leishmaniasis, treatment, cutaneous or mucocutaneous or visceral, mechanism, combination. All 598 articles matching our keywords *criteria* were divided into sub-categories depending on the selected strategy for drug development. First, we have reviewed current therapies used and validated for *Leishmania* treatment, with their mechanism of action and limitations. Combination therapies focused on the simultaneous use of several approved compounds against leishmaniasis. Next, we focused on the two strategies that gave rise to more than half of the major approved molecules: Nanoparticle carriers like in the case of Liposomal Amphotericin B, and drug repositioning, like but not limited to miltefosine and paromomycin. Next, we looked at articles combining Immuno-therapy with current treatment and last, ethnobotanics as a strategy of novel drug discovery. We included all articles from *in vivo* studies, plus articles from *in vitro* studies on intracellular amastigotes only because this is the form found inside hosts that is responsible for the disease. All articles focusing exclusively on the promastigote form were not included.

## **Results**

### **Current treatment options and limitations**

Currently, there are 7 approved and frequently used treatments against different forms of leishmaniasis throughout the world (Table 1). Historically, the first approved treatment for leishmaniasis was based upon the administration of trivalent antimonials starting 1912, soon to be replaced by a safer alternative in 1922 consisting of pentavalent antimonials, giving rise to today's two approved molecules: Sodium stibogluconate and Meglumine antimoniate. Their mechanism of action remains unclear, although it is known they induce DNA damage and Oxidative stress in parasites [8,9]. Pentamidine, a drug approved around 1940 is still on the list of approved molecules to treat leishmaniasis, but WHO has limited its use following the observation of severe side effects including diabetes mellitus, severe hypoglycemia, shock, and myocarditis. Sodium stibogluconate and Meglumine antimoniate, although showing important side effects such as gastrointestinal troubles including vomiting, anorexia and cardiotoxicity, have shown a high efficacy rate until the 1970's and 80's, when important treatment failures were observed and the first resistant strains appeared [6]. The problematic of emerging resistance strains was partially solved in 1996 with the approval of Amphotericin B (AMB) as a therapeutic molecule. Developed initially as an antifungal drug treating invasive candidiasis, AMB interacts with membrane ergosterol, specific to pathogen cell walls, and form pores leading to cytosol leakage. Further studies have also shown it could induce gene overexpression and immunomodulation as described in Table 1. The most observed side effects are fever, rigor, chills, and an important nephrotoxicity, which could be partially solved with the development of an encapsulated form in 1999: Liposomal Amphotericin B (L-AMB). Although reducing toxicity of the compound, liposomal encapsulation dramatically increased the cost of this treatment, making it difficult to implement in developing countries [10]. All the previous treatments were based upon invasive administration via intravenous or intramuscular route, making treatments difficult to observe in some parts of the world because of the need to return to a hospital several times for injections. Thus in 2004, Miltefosine, the first oral drug for the treatment of leishmaniasis was approved. Miltefosine induces a bias in host immune response, skewing it towards a Th1 profile which is beneficial in the course of remission. Moreover, this drug targets  $Ca^{2+}$  homeostasis in parasites and

inhibits the synthesis of lipids essential for parasite membrane integrity and biological functions, namely sphingomyelin and phosphatidylcholine, forcing parasites to enter an apoptotic state. Although the oral administration of this drug is an improvement over other therapies, it is nonetheless teratogenic, making its use impossible in pregnant women, and it leads to gastrointestinal side effects [10]. The last drug to be approved for anti-leishmanial treatment dates back to 2006, and is the aminoside antibiotic Paromomycin, which inhibits protein synthesis through RNA translation in *leishmania* by targeting the decoding center of ribosomes [11,12]. Limitations of this drug include its side effects including ototoxicity, renal toxicity, and hepatotoxicity.

Today, these drugs are used as first line treatment regimens and are recommended in WHO guidelines for all forms of leishmaniasis. In addition to showing important limitations, including invasive administration of most treatments, long duration of treatment regimens, and a high cost and toxicity, we observe today an increasing number of patients that fail to respond to treatment, and resistant *Leishmania* isolates become more frequent for all approved treatment regimens [7].

Compound	Commercial form	Administration	Mechanism of action	References
Sodium stibogluconate (SSG)	Pentostam®	IM / IV	Unclear, but can lead to inhibition of DNA topoisomerase I and increased ROS production. Up to date it remains unknown if it is the pentavalent form or the reduced trivalent form exerting leishmanicidal activity.	[7]
Meglumine antimoniato	GLUCANTIME®	IM / IV / IL	Unclear, but induces DNA damage mediated by oxidative stress and glutathione (GSH) depletion.	[8]
Amphotericin B deoxycholate	Amphotericin B	IV	Interaction with membrane ergosterol, pore formation and leakage of cytosolic content. Sequestration of cholesterol abrogating parasite/macrophage interaction. Functional gene overexpression leading to ROS and Ca <sup>2+</sup> increase, cytochrome-c liberation and metacaspase activation, inducing DNA fragmentation and cell death. Immunomodulation of chemokines and cytokines, including IL-1B leading to increasing NO levels.	[9]
Liposomal Amphotericin B	AmBisome®	IV	Disruption of Ca <sup>2+</sup> homeostasis, alkalization of acidocalcisomes. Induction of IFN-g leading to a Th1 inflammatory profile. Respiratory chain disruption by cytochrome-c inhibition. Inhibition of phosphatidylcholine and sphingomyelin biosynthesis leading to apoptosis.	
Miltefosine	IMPAVIDO®	O	Affects leishmania cytosolic RNA translation and intracellular trafficking by inhibition of protein synthesis and targeting the decoding center of ribosomes.	[10]
Paromomycine	Aminosidine	IM	Unclear, but other diamine compounds exert their activity by accumulation and blocking replication of <i>leishmania</i> kinetoplast DNA	[11]
Pentamidine	PENTACARINAT®	IM / IV		

IM : intramuscular ; IV : intravenous ; IL : intralesional , O : oral

**Table 1:** Classical monotherapies

## Combination therapies

One option to overcome current limitations of approved drugs is the use of combination therapy based on the hypothesis that combining two functional treatments should add the leishmanicidal effects of both treatments and reduce their doses, possibly bringing them down to a less toxic quantity, as well as reducing the cost of some expensive therapies such as L-AMB, rendering them much easier to access.

Based on these assumptions, several drug combinations have been tested and managed to successfully reduce treatment duration (Table 2). In humans, the combination of 20mg/kg of Sodium Stibogluconate (SSG) and 15mg/kg of Paromomycin led to a reduction of treatment time from 30 days to 17 days all the while retaining the same efficiency, while the combination of L-AMB with 50-100mg/kg of Miltefosine or 11mg/kg of Paromomycin in India reduced treatment duration from 31 to 15 days and reduced the needed L-AMB dose from 15mg/kg over 30 days to a single injection of 5mg/kg, thus reducing duration of treatment, cost and toxicity [14]. These two combination therapies are now first line recommended treatment by WHO in Eastern Africa and Yemen for SSG + Paromomycin, and second intention treatments in Bangladesh, Bhutan, India, and Nepal for L-AMB combination treatments.

In HIV positive patients, combination therapy of 30mg/kg L-AMB and 100mg/day miltefosine during 28 days led to increased efficiency from 50% cure rate for 40mg/kg L-AMB monotherapy at 29 days to 81% cure rate in combination therapy [15].

Other articles sought not to reduce time, cost or toxicity, but to increase efficiency and to overcome resistance to treatment, as seen in the article of Chung *et al.*, where patients unresponsive to SSG or relapsed after treatment were given a combination of 20mg/kg of SSG and 20mg/kg Allopurinol leading to remission with no observed relapses over the course of 12 months [16].

In dogs, reference treatment for leishmaniasis is a combination therapy of 100mg/kg/day Meglumine Antimoniate (MA) and Allopurinol. Efforts have been made to improve these treatments, seeking to combine Miltefosine or Paromomycin with Allopurinol. Miltefosine seems to lead to a favorable remission of sick dogs, with sustained inflammatory environment deleterious for the parasite [17], although Manna *et al.*, showed that less relapses were observed in the reference treatment group MA + Allopurinol as compared to the Miltefosine group [18]. Treatment with Paromomycin appeared safe in dogs although it did not significantly improve cure rates in comparison with reference treatment [19].

Some experimental treatments in hamsters try using topical applications namely of Paromomycin for cutaneous leishmaniasis in combination with classical treatments of Glucantime or Miltefosine, and

showed that each combination therapy at suboptimal doses proved more effective than monotherapy, suggesting combination with topical Paromomycin as an alternative strategy for parasite load reduction [20]. The efficiency of Miltefosine and Paromomycin has also been assessed, showing an increased efficiency upon combination treatment, without cross resistance observed between parasites and no notable resistance appearance upon repeated exposition, meaning combination treatment can be an efficient way of avoiding treatment failures due to resistant strains [21].

Although it is possible to increase treatment efficiency or reduce duration, toxicity and cost, this method of combination is not always successful [22–24]. Another strategy that has already proven its use in overcoming limitations of current anti-leishmanial treatments is their encapsulation by nanoparticles, as in the case of Amphotericin B.

	Combination treatment		Inclusion and health status	Region	Administration	Leishmania species	Advantages	References		
Humans	(IV/IM, 20mg/kg, 17 days)	SSG (IM, 15mg/kg, 17 days)	Primary VL, age 4-60, all immune status	Eastern Africa	Concomitant	Visceral leishmaniasis	Maintained/increased efficiency with treatment reduction time from 30 to 17 days. Reduced hospitalization. 1st line recommended treatment by WHO in Eastern Africa and Yemen.	[12]		
	(IV, 5mg/kg, single dose)	Miltefosine (O, 50-100mg/day, 7 days)	Primary VL, age 5-60, non pregnant, HIV-, Hepatitis B and C-, no anti lungal/malaria drug for 45 days prior to treatment	India	Sequential combination		Reduction of L-AMB dose from 15mg/kg total over 30 days to a single injection of 5mg/kg. Less adverse events in each combination therapy condition and reduction of treatment time from 31 to 15 days. 2nd line recommended VL treatment by WHO in Bangladesh, Bhutan, India and Nepal			
	(IV, 5mg/kg, single dose)	Paromomycin (IM, 1.1mg/kg/day, 10 days)	Primary VL, age 7-60, not of child-bearing age HIV-, 151 patients in the study	Eastern Africa	Concomitant		Efficacy >90% cure in phase II trial		[12]	
	(O, 50-100mg/day, 10 days)	Miltefosine (IM, 1.1mg/kg/day, 10 days)								
	(IV, 10mg/kg, single dose)	L-AMB (IM, 20mg/kg/day, 10 days)	5 patients: unresponsive/relapsed after SSG; 19 patients: relapsed after SSG; 30 patients: relapsed after SSG + miltefosine	Kenya	Concomitant		Cured visceral leishmaniasis in patients unresponsive to SSG. Recommended by WHO for leishmaniasis recidivans.		[14]	
	(IV/IM, 20mg/kg/day, 14-54 days)	SSG (O, 2.5mg/kg/day, 10 days)								
	(IV, 30mg/kg total 5mg/kg/day on alternate days)	AMB (O, 20mg/kg/day, 14-54 days)	HIV-, 30 patients: relapsed after SSG + miltefosine + 19 for monotherapy. No exclusion for relapses	Ethiopia, Eastern Africa	Concomitant		Increased efficiency compared to L-AMB monotherapy at 4.0mg/kg as recommended by WHO. Highest documented efficiency in HIV+/VL patients.		[13]	
	(O, 150mg/day, 28 days)	Miltefosine (O, 100mg/day, 28 days)	52 patients: age >12, no immunosuppression, no antileishmanial therapy for 3 months prior to treatment	Bolivia						
	(IL, 1ml/cm <sup>2</sup> of lesion, 1x/week, 6 weeks)	Glicantime (O, 150mg/day, 28 days)	35 patients: age 16-60, no pregnancy, no antileishmanial treatment 2-3 months prior to treatment	Pakistan	Concomitant		Cutaneous leishmaniasis		Additive effect of combination therapy, but also of adverse effects and cost. Can be an alternative for local treatment and dissemination prevention or when parenteral administration is to be avoided.	[21]
	(SC, 100mg/kg/day, 28 days)	Miltefosine (O, 100mg/day, 28 days)	40 dogs, no CanL vaccination, no leishmanicidal or leishmanostatic drugs for 12 or 3 months prior to treatment respectively	Greece						
	(SC, 15mg/kg/day, 28 days)	Paromomycin (O, 200mg/day, 6 weeks)	19 dogs, no leishmanicidal or leishmanostatic use prior to treatment	Southern Italy	Concomitant, then maintained for 6 years		Visceral leishmaniasis (L. infantum)		Itraconazole offered no benefit in terms of efficiency or in terms of treatment duration as compared to Glucantime only.	[22]
	(SC, 100mg/kg/day, 30 days)	Miltefosine (O, 2mg/kg/day, 30 days)	Normal BUN, Creatinine, ALT/AST	Liboa, Portugal						
	(SC, 100mg/kg/day, 4 weeks)	Miltefosine (O, 10mg/kg 2x/day, 6 months)	Increased BUN, ALT/AST		Concomitant				Both therapies show a similar efficiency in parasite burden reduction. Less relapses were observed in combination with Miltefosine as compared to Miltefosine.	[16]
(O, 2mg/kg/day, 4 weeks)	Miltefosine (O, 2mg/kg/day, 4 weeks)			Concomitant		Both treatment protocols favor remission. Both combination treatments lead to sustained inflammatory environment deleterious for the parasite, directly affecting cytokine generation.	[15]			

IV : intravenous ; IP : intraperitoneal ; IM : intramuscular ; IL : intralosomal ; SC : subcutaneous ; O : oral ; T : topical  
SSG : Sodium Stibogluconate

Table 2: Combination therapies

## Nanoparticle carriers

Nanoparticles are defined as small assemblies of organic or inorganic matter that are sized between 1 and 100 nm. The organic class can be divided into two sub-groups: Polymeric nanoparticles, like dendrimers, and Lipid-based nanoparticles. Lipid based nanoparticles like liposomes are structures comprised mainly of phospholipids that are very biocompatible. They assemble into a bilayered structure due to their amphipathic properties, with a hydrophobic layer and a hydrophilic interior, allowing solubilization and delivery of both hydrophilic and hydrophobic drugs. This class of nano-carriers is the most commonly FDA-approved. Polymeric nanoparticles have a wide variety of structures because of the ability to modify the composition and allow insertion of compounds allowing for intracellular targeting [25].

Although Nanoparticles have been largely studied to increase efficiency of anti-cancer drugs [26], liposomes have already proven to be effective in the case of anti-leishmanial treatment, as Amphotericin B is administered in its liposomal form in humans. Here we review the experimentation in mice and hamsters of other approved anti-leishmanial treatments that have been encapsulated in a variety of nanoparticles, seeking for improvements in efficiency of current treatments (Table 3).

Encapsulation of approved treatments in Lipid-based structures like liposomes has led to a range of improvements, starting with increased stability allowing oral route administration, because it is not directly in contact with a harsh environment like gastrointestinal fluids [27].

Encapsulation in nanoparticles allowed for different formulations of treatments. Except for miltefosine that can be administered orally, all other approved anti-leishmanial treatments need an invasive gesture for administration, limiting its use in developing countries and severely affecting treatment follow-up because of the need to return several times for injections. Formulation in nanoparticles allowed for oral administration of AmB [28], Paromomycin [29] and pentamidine [30]. It also allowed topical administration of AmB, Meglumine antimoniate, Miltefosine [31] and SSG [32].

Increased efficiency has also been observed. This could partly be attributed to the capacity of liposomes to increase half-life of compounds by allowing for slower delivery. In a second time, slower delivery also led to decreased toxicity on renal functions because of the lower concentration available at one time. Last, liposomes being lipid-based structures, their interaction with target organs liver and spleen was increased, thus increasing bioavailability while reducing toxicity [33].

Following-up on increased bioavailability, the use of nanoparticles allowed for the addition of functional groups capable of targeting whole organs or even specific types of cells, allowing for better



tissue-permeation. Phosphatidylserine [33] acts as a target signal to macrophages, that then migrate towards macrophage-rich organs such as the liver and the spleen. Similarly, lactoferrin is recognized by a group of C-type lectin receptors which are present on the surface of Antigen Presenting Cells, allowing for specific targeting to macrophages [34], and the natural polysaccharide Guar gum targets mannose-like receptors on macrophages [28]. Chitosan presence induces preferential phagocytosis, also targeting compounds directly to spleen and liver [35]. Other than relying on additional targeting signals, it is known that polymeric structures are preferentially recognized by the Mononuclear Phagocyte System, and thus structure only can favor targeting of nanoparticles toward target organs liver and spleen of dendrimers [36] and liposomes [31], or globally negatively charged structures [37]. Addition of compounds on nanoparticle surface not only allowed for targeting, but also for stabilization like PEG inclusion provided steric hindrance which reduced opsonization by plasma proteins and thus allowed for longer persistence in the blood and accumulation in target organs [37].

The use of dendrimers that present a very specific 3D structure allowed for great increase in compound solubilization. As such, solubility of Amphotericin B could be increased 478-fold by using an Anionic Linear Globular Dendrimer (ALDGD) carrier [38].

The addition of functional groups also allowed for immunomodulation. Stearylamine based Lipid nanoparticles devoid of any anti-leishmanial drug were found to increase antiparasitic effect by potentializing a Th1 response mediated by upregulation of IL-12, IFN- $\gamma$  and TNF- $\alpha$  in splenocytes, while inducing iNOS pathways, important in intracellular pathogen destruction [39]. This showed a synergistic anti-leishmanial effect between the nanoparticle carrier and the drug, that could be exploited in order to decrease drug concentration and so reduce cost and toxicity. Lactoferrin presence is capable of inducing cell signaling through the modulation of cytokines, chemokines and interleukins [34], as is Sodium alginate, also shown to activate macrophages and thus activating the innate immune system [36]. Similarly, guar gum could activate macrophages by induction of pro-inflammatory polarization [28].

Another strategy to overcome current treatment limitations is through the use of drug repositioning. This strategy has already proven its efficacy in the fight against this neglected tropical disease with the repositioning of the antifungal Amphotericin B, the anti-cancer drug miltefosine and the antibiotic paromomycin, used as first intention treatment against *Leishmaniasis* in several countries.

Treatment	Type of Nanoparticle	Main Components	Host species	Leishmania species	Administration	Effect compared to drug's free form	References	
<b>Amphotericin B</b>	Polymeric nanoparticle	PLGA	Mouse	<i>L. major</i>	IL	Efficiency increase in IL injection, no systemic toxicity	[92]	
		PLGA - PS			IV	Increased efficiency by specific distribution to target organs (liver, spleen).	[26]	
		PLGA - Lactoferrin	Hamster	<i>L. donovani</i>	IP	Efficiency increase by accumulation in target organs (liver, spleen) and reduced toxicity. Decrease of disease promoting cytokines and increase in protective pro-inflammatory mediators	[27]	
		PLGA - PEG			IV	Increased efficiency compared to free form	[93]	
		PLGA - stearylamine				Toxicity decrease and immunomodulatory effect in favor of Th1 response. Synergistic effect of drug with stearylamine	[37]	
		BSA	Mouse	<i>L. amazonensis</i>		Toxicity decrease (heart, lungs, liver, spleen, kidneys). Superior efficiency towards amastigotes	[94]	
	Polymeric nanoparticle or dendrimer	Glycol chitosan stearate	Hamster	<i>L. donovani</i>	IP	Toxicity decrease and efficiency increase. Specific distribution in target organs (liver, spleen) and less in kidneys	[30]	
		Chitosan anchor and millerfosine stabilization				Toxicity decrease and specific distribution to target organs (liver, spleen)	[29]	
		TGNP	Mouse	<i>L. amazonensis</i>		Increased efficiency accompanied by reduced overall toxicity even at high doses.	[95]	
		Guar Gum- Eudragit - Pipeime	Hamster	<i>L. donovani</i>	O / IP	Enhanced drug bioavailability and delivery to target organs (liver, spleen) limiting nephrotoxicity. Increased activity upon oral delivery	[28]	
		Chitosan nanoparticles or LGD			IP	Toxicity decrease and efficiency increase for Chitosan nanoparticle formulations, to a lesser extent for LGD formulations	[96]	
		ALGD				Increased efficiency and solubility. Toxicity decrease by limitations of the appearance of adverse effects	[33]	
<b>Meglumine antimoniate</b>	Liposome - polymer	DSHemsPC		<i>L. major</i>	IV	Maintained efficiency as compared to L-AMB with cost decrease due to stigma sterol use	[80]	
		PC - Cholesterol	Mouse		T	Increased efficiency due to higher penetration properties	[31]	
	Solid lipid nanoparticle	Complitol® 888 ATO				Increased efficiency, reduction in lesion size and amastigote count.	[97]	
	Polymeric nanoparticle	Polycaprolactone		<i>L. amazonensis or L. infantum</i>	RO	Increased specificity in targeting to liver, spleen and lungs.	[98]	
	Liposome - polymer	Stearylamine		<i>L. major</i>	T	Stearylamine shows an anti-parasitic activity by itself and increases efficiency. Liposomal formulation increased permeation of the cream.	[31]	
	Liposome	Cholesterol - DP - DSPC and DSPE - PEG2000		<i>L. infantum</i>	IV	Immunomodulatory effect in favor of Th1 response with reduction of inflammation.	[99]	
	Polymeric nanoparticle	PLGA-PEG-CD14	Hamster				Efficiency increase with a decreased EG50 due to specific macrophage targeting.	[100]
		PC - Cholesterol			O	Toxicity decrease (macrophages, gastrointestinal irritability) due to oral administration, and increased stability.	[25]	
	<b>Miltefosine</b>	Liposome	PC - Cholesterol - PG		<i>L. major</i>	T	Limitation of systemic toxicity by topical application.	[31]
		Polymeric nanoparticle	PLGA - Mannosylated thiolated chitosan		<i>L. donovani</i>	O	Efficiency increase (decreased IC50) due to high tissue permeation, with toxicity decrease.	[34]
		Liposome	PC - PEG	Mouse	<i>L. infantum</i>	IV	Increased efficiency by targeting to spleen, liver and lungs. Increased persistence in blood by stabilization.	[32]
		Solid lipid nanoparticle	Stearic acid		<i>L. major</i>	IM	Efficiency increase with immunomodulatory effects towards a Th1 response.	[101]
<b>Pentamidine</b>	Polymeric nanoparticle	PLGA		<i>L. infantum</i>	O	Facilitated administration by oral use	[35]	
	Liposome	Phospholipon®		<i>L. tropica</i>	T	Increased efficiency (decreased IC50 and increased selectivity index). Better retention to deep skin layers without permeation enhancers	[36]	

IV : intravenous ; IP : intraperitoneal ; IM : intramuscular ; IL : intralésional ; O : oral ; T : topical ; RO : retro-orbital  
DSPE : distearoylphosphatidylethanolamine ; DP : dicytylphosphate ; DSHemsPC : 1,2 distigmasterylthiomiscinyl-sn-glycero-3-phosphocholine ; TGNP : Triglycérine-rich nanoparticles  
\*Mouse model used in articles are BALB/c mice. \*\*Hamster model used in articles are Syrian Golden Hamsters

Table 3: Nanoparticle carriers

## Drug repositioning

As addressed in a previous review, 60% of current approved anti-leishmanial drugs are repositioned [10]. Repositioning strategies have thus already proven useful in anti-leishmanial treatment research. Here we reported some of the more recent advances in repositioning testing by selecting previously approved compounds against a disease other than leishmaniasis, used as monotherapies against any *Leishmania* species.

The most represented class of repositioned drugs against leishmaniasis are anti-microbial compounds (Table 4). As mentioned above, Amphotericin B is an anti-fungal that has successfully been repositioned. Several other anti-fungals have been approved and are recommended by WHO against cutaneous leishmaniasis, like Ketoconazole, Fluconazole and Itraconazole [6]. Multiple *in vitro* studies have shown efficiency of other anti-fungal compounds as anti-leishmanial treatments. Anti-fungal compounds mainly target the sterol synthesis pathway, which is essential for fungal and *Leishmania* cell membrane integrity. The membrane composition between mammal cells and microbes is very different, thus targeting the ergosterol pathway allows for great selectivity indexes and specificity as it does not perturb mammal cells. The use of butenafine was shown to inhibit ergosterol synthesis in *L. infantum*, and showed activity against *L. amazonensis* and *L. braziliensis* in other studies [51]. Ravuconazole and Miconazole both inhibited the sterol pathway by inhibiting C14-demethylases, blocking conversion of sterols, and leading to the accumulation of intermediate forms [52,53].

Anti-bacterial compounds have also been repositioned, as in the case of Paromomycin. In a similar fashion to anti-fungals disrupting cellular membranes, the anti-bacterial Delamanid, an anti-tuberculosis treatment approved for multi-resistant strains was shown to inhibit cell wall component synthesis [54].

Most anti-bacterial compounds targeted intracellular pathways and homeostasis *in vivo* studies. SQ109, a small 1,2-ethylene diamine molecule, is another compound repositioned from tuberculosis, that can collapse mitochondrial potential, and disrupt intracellular  $Ca^{2+}$  homeostasis which is essential for parasite motion and macrophage invasion [55].

Among antimicrobial compounds, two repositioned anti-trypanosomatids targeted metabolic pathways in *Leishmania* parasites. The first one, fexinidazole targets nitroreductase in trypanosomatids, which possess a homolog in *Leishmania* parasites. At a dose of 200mg/kg, fexinidazole showed activity similar to approved drugs miltefosine and Pentostam, and overexpression of NADPH-dependent nitroreductase increased sensitivity to the compound, validating the target [54]. The second one, suramin targets enzymes of Trypanosomes and appeared to have a strong immunomodulatory profile when administered *in vivo*, showing elevated pro-inflammatory Th1 cytokine secretion and decreased Th2 biased response [56].

Another class of repositioned compounds are Anti-cancer drugs. Validated and successful application has already been seen in the case of miltefosine. Anti-cancer drugs mostly increased host-mediated response in terms of pro-inflammatory cytokines, as seen with Ibrutinib *in vivo* and Imiquimod TLR 7 agonist *in vitro* [57,58]. Other compounds, as Miransterib and AR-12 acted through inhibition of specific host pathways, like the Akt kinase pathway, capable of phosphorylating a series of downstream targets ultimately regulating cell growth, survival, and metabolism. Akt has been shown to be important in *Leishmania* survival, thus the use of an oral inhibitor of Akt was a good molecular target for treatment and led to reduction of parasite burdens *in vivo* [59,60].

A surprising class of repositioned drugs can be found in the anti-depressants. All molecules acted as selective inhibitors of serotonin uptake to treat depression, anxiety or Obsessive Compulsive Disorders (OCD) as first intention. Use *in vivo* or *in vitro* showed activity on parasite metabolic pathways. Sertraline and Clomipramine led to energetic stress in parasites, as oxidative stress, intracellular ATP reduction and mitochondrial targeting with disruption of mitochondrial potential [61] or respiration uncoupling [62]. Sertraline led to shortage of intracellular amino acids and variation of thiol-redox intermediates, and clomipramine led to trypanothione reductase inhibition, with hallmarks of apoptosis visible [61,62]. Imipramine interacted with lipid bilayers and inhibited methyl transferase leading to membrane destruction [53].

Various other classes of molecules have been repositioned against leishmaniasis. Cholesterol reducer Simvastatin enhanced host protection by increasing production of hydrogen peroxide and enhancing phagosome maturation [63]. Rapamycin, an immunosuppressor given to avoid graft rejects, biased immune responses towards protective Th1 cytokine secretion [64]. The anti-arrhythmic drug amiodarone disrupted Ca<sup>2+</sup> homeostasis and was shown to block sterol biosynthesis in *Leishmania* parasites [65]. Various repositioned compounds have shown a bias in cytokine response. Knowing that leishmaniasis cure is dependent on Th1/Th2 balance, another strategy of treatment development involves the use of a combination of immunomodulators and classical compounds.

Class of compounds	Compound	Repositioned from	Function	Mechanism of action	Administration	Leishmania species	Host species	Reference
Anti-Fungal	Miconazole	Anti-fungal	Disruption of sterol synthesis.	IC50 of Miconazole on promastigote and amastigote forms was 1.71, 1.03 μM and 2.2, 0.2 μM, respectively. Sterol synthesis was inhibited by inhibition of C14 demethylase, leading to accumulation of C14 methyl sterols (14α-methylglucosyl-8,24-(24'1)-dialco-3β-ol and 14α-methylglucosyl-8,24-(24'1)-dialco-3β-ol and other sterol intermediates.	Miconazole (0 - 16 μM, 72h)	L. amazonensis	Peritoneal macrophages from Balb/c mice	[40]
	Ravacizole	Invasive fungal infections (trigonocephalus, jock itch, athlete's foot)	Acidic inhibit the lipid biosynthesis pathway by inhibiting the conversion of lanosterol to ergosterol by the monooxygenase lanosterol C14α-demethylase.	IC50=0.5, 1.1 μM at 24h and IC50=1.6 μM at 72h treatment, with a good selectivity index. Visualisation showed mitochondrial alteration, accumulation of lipid bodies.	0.01-70 μM, 24-72h		Peritoneal macrophages from C57 mice	[39]
	Bulethine	Anti-tuberculosis (approved for multidrug resistant strains)	Ergosterol biosynthesis disruption via inhibition of Squalene epoxidase.	In vitro promastigotes show programmed cell death attributed to blockage of biosynthesis of ergosterol (B-SNEDDS) decreased survival index for the drug.	Bulethine (25-100 μM) encapsulated in B-SNEDDS liposomes, 48h.	L. infantum	Peritoneal macrophages from Balb/c mice	[38]
	Delamanid	Resistant mycobacterium tuberculosis (phase I/II)	Inhibition of mycobacterial cell wall components synthesis, methoxy mycolic acid and ketomycolic acid. Activation by the enzyme desaturase in the cell wall, which converts the methoxy mycolic acid to mycolic acid production.	Low toxicity towards host cells. In vitro amastigote EC50 inferior to miltefosine. Reduction of parasite burden in the liver. Most of actions needs further investigation, other classical microtubule inhibitors.	O, 1 - 50 mg/kg, 2x/day, 5-10 days	L. dobovani	Balbc mice	[41]
Anti-Bacterial	SO109	Disruption of intracellular Ca <sup>2+</sup> homeostasis, causing cell death and affecting nucleocapsid assembly.	IC50=7.17 nM ± 0.08. SB-800. Treatment decreased the number of infected macrophages. IC50 on promastigotes is 6 times lower than miltefosine and equal to amphotericin B, while on amastigotes it is 614 times and 57 times lower than miltefosine and amphotericin B respectively.	O, 25-200 mg/kg/day, 5 days	L. dobovani	J774 murine macrophages		[42]
	Fexidazole	Targets nitroreductase in trypanosomatids, which possesses an homolog in Leishmania parasites	200 mg/kg doses showed similar efficacy to miltefosine and Pentam. Over expression of an NADPH-dependent nitroreductase in parasites increases sensitivity to fexidazole, suggesting it as a potential target.	O, 25-200 mg/kg/day, 5 days	L. dobovani			[41]
	Suramin	Neurodegenerative stage of African trypanosomiasis (T. brucei rhodesiense)	Inhibition of glycolytic enzymes of the parasite.	Elevated NO and TNF-α levels. Enhanced T-cell proliferation with an elevated CD4 <sup>+</sup> CD8 <sup>+</sup> ratio. Decrease in TH1 cytokine secretion (IL-10 and TGF-β) and increase in pro-inflammatory TH1 cytokine secretion (IFN-γ, TNF-α and IL-12).	IP, 20 mg/kg/day, 2x/week, 2 weeks			[43]
	Mianserin (ARQ 052)	PKA/MK-driven tumors or Prionus Syndrome	AKT inhibitor, which is activated by leishmania and regulates cell growth, survival and metabolism by phosphorylating downstream targets	Active towards both promastigotes and amastigotes <i>in vitro</i> . Enhanced mTOR dependent autophagy in infected macrophages. <i>In vivo</i> , reduction of lesions by 40% as compared to control. Reduction of parasite load in the spleen similar to miltefosine, moderate suppression of miltefosine in the liver.	Cutaneous model O, 50 - 100 mg/kg, 5 days Vesicular model O, 50 - 75 mg/kg/day, 5 days/week, 4 weeks	L. amazonensis L. dobovani	Balbc mice	[46]
Anti-Cancer	AR-12 (OSU-03012)	Anti-cancer (FDA IND-approved)	Host-mediated compound promoting other intracellular pathogen eradication, mediated by regulation of autophagy and Akt kinase pathway inhibition	Encapsulation increased activity of AR-12, and reduced liver, spleen, and bone marrow parasite load. Combination therapy with Amphotericin B and miltefosine showed synergistic activity. In vivo, clearance of amastigotes suggests host-mediated activity.	Foundation in acetylated dextran microparticles IP, 31.5 mg AR-12/injection, injections on day 14 and 21 <i>p.p.</i>	L. dobovani		[47]
	Ibrutinib	Anti-cancer (for B cell malignancy)	ITK/BTK inhibitor, blocking B-cell receptor signaling and proliferation (activated by leishmania). Modulation of T-helper response.	Promotes host immunity, with no direct activity against Leishmania. Increased number of IL-4 and IFN-γ-producing NK T cells in the liver and spleen, enhanced granuloma formation in the liver. Reduction of susceptibility to invading Lybchi inflammatory monocytes influx. Increased production of proinflammatory IFN-γ, TNF-α, IL-4, and IL-17 in the liver and spleen.	O, 6 mg/kg/day, 14 days			[44]
	EAP9503 (Iniquimod analog) and Iniquimod	Skin cancer and Condyloma	TLR7 agonist leading to NF-κB pathway activation	Reduction of amastigote replication. EAP9503 proved more potent, whereas iniquimod showed similar activity. Both compounds led to IL-12, IL-6 and IL-10 up regulation, and activation of the NF-κB canonical pathway with increase of pro-inflammatory cytokines (IL-12, IL-15, TNF-α and IL-6).	0.01 - 1 μM, 24h	L. major and L. tropica	Human THP-1 macrophage cell line	[45]
	Sertitraline	Anti-depressant	Serotonin reuptake inhibitor	Multi target mechanism of action on essential metabolic pathways, targeting the mitochondrion (respiration uncoupling, decrease of intracellular ATP, oxidative stress), and the nucleus (DNA fragmentation, PS exposure and cell shrinkage), and mitochondrial potential disruption. In amastigotes energetic storage of intracellular amino acids used as metabolic fuel. <i>In vivo</i> , sertitraline reduced splenic and liver parasite loads by 72% and 70%, respectively when compared to controls.	O, 10 mg/kg, 2x/week, 1 month	L. infantum L. dobovani	Balbc mice	[49]
Anti-Depressants	Comrigramine	Anti-depressant and anxiolytic treatment of post-traumatic stress disorder and OCD	Selective inhibition of Serotonin reuptake. Previous neuroprotection studies showed effect on parasites through tyrosinohormone reductase	Selective inhibition of amastigote growth (IC50=15.45 ± 4.92 μM, SH1172). Parasites showed signs of oxidative stress with tyrosinohormone reductase inhibition; hallmarks of apoptosis (DNA fragmentation, PS exposure and cell shrinkage), and mitochondrial potential disruption. In amastigotes energetic storage of intracellular amino acids used as metabolic fuel. <i>In vivo</i> , sertitraline reduced splenic and liver parasite loads by 72% and 70%, respectively when compared to controls.	Comrigramine (15-30 μM, 48h)	L. amazonensis	J774A.1 murine macrophage cell line	[48]
	Imipramine	Severe chronic depression	Inhibition of serotonin and norepinephrine reuptake. Known interaction with lipid bilayers and inhibition of methyltransferase leading to membrane disruption.	Imipramine has an antishistaminic activity on both promastigotes and amastigotes (IC50=13.32 ± 1.1 μM). It was shown to decrease parasite load and ergosterol-derived steroids, with accumulation of steroid precursors.	Imipramine (0 to 50 μM, 72h)		Peritoneal macrophages from Balb/c mice	[40]
	Shvaxistatin	Cholesterol reductor	Increase in LDL-Cholesterol degradation and HMG CoA reductase inhibitor.	As treatment, application on ear lesions reduced size, ulceration and parasite burden. In combination with miltefosine, shvaxistatin reduced parasite burden and ulceration/necrosis. <i>In vivo</i> , primary macrophages treated with simvastatin showed reduced cholesterol levels, increased production of hydrogen peroxide and enhanced phagosome maturation, thus enhancing host response.	Treatment T, 20 μg/100 μl/day, 5-8 weeks Propylhexy T, 20 mg/kg/galactate day, 2 weeks	L. major	Balbc and C57B/6 mice	[50]
Other	Rapamycin, GSK-2126498	Graft rejection prevention (Immunosuppressant)	mTOR inhibitors. TOR from leishmania is important in autophagy, and TOR1 and 2 are essential to parasite growth and viability.	Reduction of hepatic swelling and parasite load in draining lymph nodes. Rapamycin performing best. Harvested splenocytes showed a Th1 biased response, with decreased secretion of IL-4.	IP, 10.2 μg/galactose/day, 10 days	L. major L. tropica		[51]
	Amiodolone	Anti-arthritis	Disruption of intracellular Ca <sup>2+</sup> homeostasis by direct action on mitochondrion and inhibition of the sarcoplasmic reticulum pathway through inhibition of sarcoplasmic endoplasmic reticulum activity.	Oral treatment reduces lesion size as compared to vehicle treatment. Used in combination with 200 mg/kg miltefosine, oral treatment leads to 50% cure rate for murine leishmaniasis.	O, 50 mg/kg/day, 21 days	L. mexicana	Balbc mice	[52]

BTX: Biotin; Tyrosine Kinase; NK: Natural Killer; B-SNEDDS: Bioactive Self-Nano-Emulsifying Drug Delivery Systems; OCD: Obsessive-Compulsive Disorder; TLR: Toll-Like Receptor; PRM8: polyphosphoinositide 3-kinase; IFN: Interferon; IP: Intraperitoneal; O: Oral; T: Topical

Table 4: Repositioned drugs

## Immunotherapies

In the last 20 years, immunotherapy has been developed either as monotherapy or in combination with classically used treatment against leishmaniasis. Immunity is extremely important in the progression and outcome of leishmaniasis. In a general manner, it has been stipulated that Th1 responses with IL-12, IL-18, IFN- $\gamma$  and TNF- $\alpha$  act as protective cytokines in the case of *Leishmania* infections. On the other hand, Th2 responses with predominant IL-4, IL-10, IL-13 and TGF- $\beta$  cytokines favored parasite survival and infection progression [66]. Research on leishmaniasis has revolved around this dogma for a long time, although today it is accepted that to efficiently eliminate *Leishmania*, there must be a balance between these two pathways, and it is known that susceptibility highly depends on host immunity and parasite species [67].

Thus, by combining current treatments with immunotherapy, it could be possible to reduce concentration and duration of chemotherapy while skewing host immunity to favor *Leishmania* elimination (Table 5).

Unsurprisingly, as Th1 responses induce protection against *Leishmania* infections, the first strategy used to enhance approved treatments has been to stimulate associated cytokines in order to favor remission. As such, combination of Glucantime with IFN- $\gamma$  was shown to both enhance cure rate and decrease treatment time in humans. Interestingly, it also allowed patients previously unresponsive to antimony to cure [68] and combination of IFN- $\gamma$  with L-AMB even allowed to bypass a multi-resistant strain conferring visceral leishmaniasis found in a 2-year-old boy [69]. Administration of IL-12 in combination with amphotericin B in mice increased efficiency of 2mg/kg to the same efficiency as a dose of 15mg/kg [70].

The use of upstream agonists of Toll Like Receptors (TLR) has already been proposed, as release of cytokines is often associated with upstream recognition of pathogens mediated by Pathogen Associated Molecular Patterns (PAMP) recognition by TLRs [71]. Agonists of these TLR were shown to enhance effects by downstream transcription of NF- $\kappa$ B leading to pro-inflammatory responses. As such, TLR-7 agonist Imiquimod was able to increase efficiency of Glucantime against *L. major* [72] and TLR-2 agonist Pam3Cys enhanced efficiency of sub-optimal treatment dosage of oral miltefosine against *L. donovani* in mice [68].

The use of Thalidomide as an immunomodulator decreased TNF- $\alpha$  secretion while increasing IFN- $\gamma$ , thus modulating Th1 responses towards a multiresistant strain of mucosal leishmaniasis [73]. In dogs, supplementation of Glucantime with Active Hexose Correlated Compound (AHCC) known to increase Th1 response, reduced the apparition of adverse effects due to Allopurinol [68]. Another strategy would also be to inhibit Th2 responses by modulating cytokines. The administration of Anti IL-10R

accelerated *L. donovani* elimination in mice and increased efficiency in combination with either Pentostam or Amphotericin B [70,74]. The use of immuno-therapies is still quite recent and calls for a lot of complex experimentation and development as it depends entirely on parasite species and host immunity. Knowing that, rather than spending time developing complex therapies to combine with toxic treatments that should be replaced with safer alternatives, one other way of approach is to find novel immunostimulators. Research on plant extracts has shown to be another way to skew host immune response in a favorable way to eliminate *Leishmania*.

	Treatment	Immunomodulator	Inclusion & Health status	Region	Leishmania species	Effect and advantages	References
Human	Antimony (Glucantime) (IV, 20mg/kg/day, 10-40 days)	IFN-g (IM, 100-400 ug/m <sup>2</sup> body area)	Primary VL or patients refractory to treatment, +/- 15 patients/group	India / Brazil	Visceral leishmaniasis	Increase in cure rates and decrease in treatment time for responsive patients. Induction of cure in previously antimony unresponsive patients	[55]
	SSG (IV, 20mg/kg/day, 20 days)	Imiquimod (T, 125-250mg of 5% cream 3x/week, 20 days)	Primary VL, 80 patients (40/group), age 5-65, non pregnant	Peru	<i>L. braziliensis</i>	Combination treatment performed better but no statistically significant differences were observed	[85]
	L-AMB (IV, 5mg/kg/day, 5 days then 2x over 2 weeks) + Allopurinol (O, 25mg/day, 5 days then 2x over 2w)	IFN-g (SC, 50ug/m <sup>2</sup> , 3x/week)	Case report: 2 yo boy with resistance to SbV, AMB and L-AMB	Iran	Visceral leishmaniasis	Patient remission observed rapidly after combination treatment	[56]
	Glucantime (IV, 20mg/kg/day, 20 days)	Pentoxifylline (TNF- $\alpha$ inhibitor) (O 400mg 3x/day, 20 days)	82 patients/group, age 18-50, HIV-, no pregnancy, no serious underlying disease or infection	Bahia, Brazil	<i>L. braziliensis</i>	No increased cure rate or reduced healing time observed in patients, but increased incidence of adverse events under pentoxifylline treatment.	[84]
	Meglumine antimoniate (IV, 20mg/kg/day, 30 days)	Pentoxifylline (O, 400mg, 3x/day, 30 days)				Reduction of healing time with increased adverse effects in combination treatment	[102]
	Glucantime (IM, 850mg/day, 28 days)	Thalidomide (O, 100mg/day, 2 months)	Case report, 20 yo man release after MA treatment, resistant to Glucantime, AMB, L-AMB and Miltefosine	Iran	<i>L. tropica</i> mucosal leishmaniasis	Thalidomide is used as an immunomodulator (TNF- $\alpha$ inhibition and IFN-g increasing).	[60]
	SSG (Pentostam) (IP, 1-50mg/kg/day, 5 days)	anti IL-10 R (IP, 0.1 mg single dose)				Accelerated parasite killing and over 10 fold reduction in antimony effective dose	[61]
	Amphotericin B (IP, 1mg/kg/day, 2mg/kg total)	anti CD40 (IP, 0.1mg single dose) anti IL-10R (IP, 0.1mg single dose) IL-12 (Osmotic pump, 0.1ug/day, 7 days) anti IL-4 (IP, 5mg single dose) IL-13 (IP, 0.2 mg/2days, 9 days) TGF- $\beta$ (IP, 4mg/kg (~100ug) single injection) anti IL-4 (IP, 5mg single injection)				3.4 fold increased efficiency in treatment over aCD40 alone, as efficient as 15mg/kg total dose of Amphotericin B 6.3 fold increased efficiency in treatment over all-10 R alone, as efficient as 15mg/kg total dose of Amphotericin B 9 fold increased efficiency in treatment over IL-12 alone, as efficient as 15mg/kg total dose of Amphotericin B. No effect alone or in combination therapy.	[57]
	SSG (Pentostam) (IP, 50mg/kg, single dose)		NR		<i>L. donovani</i>	Immunomodulation alone inhibits parasite replication but does not favor parasite killing. Combination therapy does not increase parasite killing in sub-optimal SSG conditions.	[83]
	Mice	Miltefosine (O, 2.5mg/kg, 5 days)	Pam3Cys (TLR2 agonist) (IP, 100ug 2x spaced 2 weeks)			<i>L. donovani</i>	Reduction of infection, increase in IFN-g production. Enhanced efficacy of sub-curative doses of miltefosine.
	Glucantime (IP, 100mg/kg/day, 5 days)	QNZ (NF- $\kappa$ B inhibitor) (IP, 1mg/kg/day, 5 days)			<i>L. amazonensis</i>	NF- $\kappa$ B inhibitor: TNF- $\alpha$ inhibition, IL-1 $\beta$ and NO increase. Reduction in macrophage count and in size of footpad lesion.	[86]
	Paromomycin (T, 15% cream, 50mg/cm <sup>2</sup> )	anti TNF- $\alpha$ (T, 0.4% cream, 50mg/cm <sup>2</sup> ) anti-TNF- $\alpha$ (20 mg/mL)			<i>L. major</i>	Enhanced effect as compared to monotherapy. Similar reduction of parasite load, better control of local inflammation, enhancement of leishmanicidal and anti-inflammatory effect.	[87]
	Glucantime (IP, 100 mg/kg/day, 12 days)	Imiquimod (TLR7 agonist) (T, 5% cream, 1x/3 days, 2 weeks)			<i>L. major</i>	Increased efficiency as compared to each drug alone	[59]
Dogs	Glucantime (SC, 50mg/kg 2x/day, 28 days)	Impromune®: AHCC (17mg/kg/day) + nucleotides Nucleoforce® (32mg/kg/day) (O, 180 days)	69 dogs, non CanL vaccinated, no allopurinol 3 weeks prior, no antileishmanial treatment, domperidone, cyclosporin or glucocorticoids 3 months prior.	Spain	Visceral leishmaniasis	AHCC is known to improve Th1 immune response. Absence of adverse effects due to allopurinol combination (Xanthinuria) in Impromune group. Increased CD4+/CD8+ ratio.	[55]

IV : Intravenous ; IP : Intra-peritoneal ; IM : Intramuscular ; IL : Intralésional ; SC : subcutaneous ; O : oral ; T : topical  
 AMB : Amphotericin B ; L-AMB : Liposomal Amphotericin B ; SSG : Sodium stibogluconate ; SbV : Pentavalent Antimony ; AHCC : Active Hexose Correlated Compounds  
 NR : Non Relevant

Table 5: Immuno-chemotherapy



## Ethnopharmacology

Ethnopharmacology is defined as a fast-growing branch of science mixing botany, chemistry, and pharmacology, that aims to assess biological activity and scientific relevance in traditionally used plants. By using the knowledge of indigenous populations, ethnopharmacology can help identifying plants for drug development through empirical evidence, and lead to valuable time and resource savings. It can thus be considered as a shortcut for the discovery of new active compounds.

It is interesting to note that all the articles presented in the *in vivo* section of the table showed an increase in Th1 response and a decrease in Th2 cytokine secretion, thus modeling immunity to favor host over parasite survival. It is also interesting to see that most of the compounds were used in a vast array of applications by indigenous people, often treating various microbial infections without important specificity towards *Leishmania*. Most articles described an effect in parasitic burden reduction without unraveling the mechanisms behind this elimination *in vivo*. *In vitro*, however, three compounds, Lupeol, Mahanine and *Croton caudatus Geisel* extract, were shown to upregulate classical pathways for intracellular pathogen destruction, the Reactive Oxygen Species (ROS) and Nitric Oxide (NO) pathways [81–83]. For two of these compounds, molecular docking helped identifying potential targets for the compounds, such as parasite antioxidants like ascorbate peroxidase [82] or in the case of Lupeol, binding to several potential drug targets in *Leishmania* parasites (PTR1, APRT, LPG and GP63) [81]. This allowed identification of potential targets for these compounds and allowed to identify a multicomponent mechanism by potential direct parasite targeting on top of host immunomodulation. In the case of Mahanine and JdHex, oral formulation was used, making administration easier than that of most anti-leishmanial drugs for visceral leishmaniasis [82,83].

As concerning the *in vitro* testing of novel molecules, most isolated compounds showed very low cytotoxicity. Studies assessing activity without further investigation on molecular mechanisms by which extracts exerted their activity were common [84–87]. Among studies that did assess mechanisms of activity, the majority of studies highlighted compounds that could inhibit pathways specific to the parasites, like parasite arginase [88,89], trypanothione reductase [90], or both these pathways at the same time [91]. Other plant extracts exerted their effect by stimulation of cytokine secretion or inhibition of cytokines involved in parasite progression, like *T. riparia* essential oil, stimulating IFN- $\gamma$  secretion that is critical for resolution of the disease [92]. Increase of NO secretion and phagocytic activity [93] as well as phagocytic capacity [94] or macrophage activation state [95] was also observed. Finally, ROS are known to be important in intracellular parasite clearance, and number of studies evidenced an increase in ROS levels leading to parasite death [95–97].

**Table 6: Ethnopharmacology**

Plant	Famille	Region	Compounds (major/active)	Leishmania species	Concentration	Effect	Reference
<i>Sterculia villosa</i> Robx.	Malvaceae		Lupeol	<i>L. donovani</i>	Lupul (IP, 5-100 mg/kg/day, 5 times on alternate days)	<i>In vivo</i> , activity against promastigote and amastigote forms with increase of NO. <i>In vivo</i> , 75mg/kg/day treatment reduced splenic and hepatic burden and up regulated the release pro inflammatory Th1 cytokines IL-12 and IFN-γ while down regulating release of anti-inflammatory IL-10 and TGF-β. Molecular docking revealed binding to 4 major potential drug targets (PTR1, APRT, biosynthetic LPS and GP83)	[62]
<i>Croton caudatus</i> Geisel (var. <i>lonchocarpus</i> Hook)	Euphorbiaceae	India	Terpenoids	<i>L. donovani</i>	JDHex (O, 1.25-5 mg/kg/day, 5 days)	<i>In vitro</i> , alteration of promastigote metabolism (lipids, proteins, carbohydrates) and flagellin (DNA condensation, PS externalization, apoptosis). Reduced replication of amastigotes, increased release of NO, pro-inflammatory IL-12 and TNF-α, reduction of TGF-β and IL-10. <i>In vivo</i> , reduction of parasite burden in liver and spleen, induction of Th1 response by IFN-γ secretion and degradation of IL-10 secretion.	[64]
<i>Murraya koenigii</i>	Rutaceae		Mahanine	<i>L. donovani</i>	Mahanine (O, 20-40 mg/kg/day, 5 days)	<i>In vitro</i> , apoptosis through PS externalization, increased ROS and NO generation, suppression of UCP2, and Th1 cytokines through modulation of the STAT pathway. Molecular modeling revealed interaction with leishmanin antibody and enzyme like ascorbate peroxidase. <i>In vivo</i> , reduction of parasite burden, upregulation of NO, iNOS, ROS, IL-12 and T cell proliferation.	[63]
<i>Pentlanon andreauxii</i> .	Apocynaceae	Mexico	Pentalinosterol (PEN)	<i>L. amazonensis</i>	Liposome encapsulated PEN (IV, 2.5mg/kg, single shot)	<i>In vivo</i> , targeted towards infected organs and reduction of parasite load in liver, spleen and bone marrow. Enhanced T cell proliferation. Strong Th1 protective response with enhanced IFN-γ production and formation of mature hepatic granulomas. No modulation of anti-inflammatory cytokines.	[103]
<i>Bursaria aplera</i> Ramirez	Bursaceae		Podephyllotoxin	<i>L. mexicana</i>	MEPA (T, 0.408 mg/mL in cream, 200µm/day, 8 weeks)	<i>In vitro</i> , promastigote apoptosis and decrease of mitochondrial membrane potential. <i>In vivo</i> , reduction in lesion size and parasite burden. Increase of Th1 cytokines TNF-α and IFN-γ, and decrease of Th2 cytokines IL-4 and IL-10 in sera of mice.	[104]
<i>Rhynchosyris retusa</i> , <i>Tephala curculoides</i> , <i>Safranum nepalense</i>	Orobanchaceae	India Aruachal Pradesh	NA	<i>L. donovani</i>	Fractions (25-62-250µg/mL, 48h)	Rhynchosyris retusa roots extracts was active against intracellular amastigotes with low cytotoxicity.	[65]
<i>Physalis angulata</i>	Solanaceae	Brazil	NA	<i>L. amazonensis</i>	AEPA (100µg/ml, 72h)	AEPA increase ROS which induced leishmania cell death by apoptosis. AEPa increased macrophage activation state and promoted synthesis of Superoxide anion (O <sub>2</sub> <sup>-</sup> ).	[76]
<i>Euterpe oleracea</i> "Açai"	Arecaceae	Brazil	Anthocyanins, phenolic compounds	<i>L. amazonensis</i> <i>L. infantum</i>	Clarified Açai juice (dilutions 1:12.5, 1:25, 1:50, 24-72h)	Clarified Açai juice increased ROS levels and externalization of PS marking apoptosis. Reduce amastigote load inside cells for <i>L. amazonensis</i> and <i>L. infantum</i> . It lead to strong reduction of IL-17 levels in infected cells. K17.K27	[77]
<i>Tetradenia riparia</i> (Hochstetter) Codd	Lamiaceae	Africa	NA	<i>L. amazonensis</i>	TEO (300mg/mL, 24h)	Reversion of parasite mediated inhibition of IFN-γ secretion, blocking of the induction of IL-10, IL-4 and IL-5, and inhibition of secretion of IL-1β, IL-17, IL-33 and TNF-α.	[73]
<i>Croton callicara</i> Berth. "sacaca"	Euphorbiaceae	Brazil	Trans-dehydrocotin (DCTN), trans-oleon (CTN) and acetylacetic acid (AAA)	<i>L. amazonensis</i>	DCTN/CTN or AAA (9.38-150µg/mL, 24h-72h)	Inhibition of trypanothione reductase enzyme.	[71]
<i>Stachyrrhiza caymenensis</i> (Rich.) Vahl.	Verbenaceae	Brazilian and Peruvian Amazon	Verbascoside, isoverbascoside (ratio 7:3)	<i>L. amazonensis</i>	BUF extract (0.5-500µg/mL, 24-72h)	Selective inhibition of parasite Arginase.	[69]
<i>Zingiber zerumbet</i> (L.) Smith (ginger)	Zingiberaceae	various	Zerumbone	<i>L. donovani</i>	Zerumbone (0.1-50µM, 48h)	Increased ROS, led to DNA condensation and PS externalization followed by apoptosis.	[78]
<i>Syzgium cumini</i> (L.) Skeels "jambolão"	Myrtaceae	Brazil	α-pinene	<i>L. amazonensis</i>	SEO or α-pinene (12.5-100µg/ml, 48h)	Immunomodulatory activity by increase of NO secretion and phagocytic and lysosomal activity.	[74]
<i>Platonia insignis</i> Mart. "bacurizero"	Cusciaceae	Brazil	Lupeol	<i>L. amazonensis</i>	Fractions of Lupeol (6.25-800µg/mL, 48h) On Intra-Amastigotes (1, 12, and 14 LC50)	Led to increased lysosomal volume and phagocytic capacity of macrophages.	[75]
46 plants	varying	Peru (Loreto)	NA	<i>L. donovani</i>	Extracts (0.78-100µg/ml, 48h)	Of the 46 plants, 15 extracts showed an activity against <i>Leishmania</i> parasites.	[66]
<i>Stachyrrhiza caymenensis</i>	Verbenaceae	Brazil	Verbascoside	<i>L. amazonensis</i>	Verbascoside (2.34-300µM)	Inhibition of parasite arginase, leading to reduced protective oxidative mechanism with impaired trypanothione synthesis.	[72]
<i>Alternanthera brasiliana</i> (L.) Kunze, <i>Eugenia uniflora</i> L., <i>Jatropha gossypifolia</i> , <i>Schinus molle</i> , <i>Schinus molle</i> , <i>terebinthifolia</i> Raddei	Amaranthaceae, Myrtaceae, Euphorbiaceae, Anacardiaceae	Atlantic forest (Brazil)	Tricallene type terpenoids schinol and masticadienol acid (S, terebinthifolia), sesquiterpene atracylon, glucosylated flavonoids including quercetin (E. uniflora)	<i>L. amazonensis</i>	Extracts (0.4-100 µg/mL)	<i>E. uniflora</i> extracts contained quercetin already reported as an arginase inhibitor.	[70]
<i>Alga laemanni</i>	Lamiaceae	Turkey	Hirpagide, 8-O-acetylhirpagide, cis-melicostide, trans-melicostide, dihydromelicostide, verbascoside, galactosylmyricetin, isoorientin.	<i>L. donovani</i>	Pure compounds (0.123- 90 µg/ml)	The firdiol glucoside 8-O-acetylhirpagide and verbascoside were the most active against <i>L. donovani</i> .	[67]
46 plants	varying	Japan	NA	<i>L. donovani</i>	Extracts (0.123-90 µg/mL, 72h)	The study revealed over 80% of extracts with some anti-leishmanial activity.	[68]

**MPM** : Murine Peritoneal Macrophages ; **MPF** : Murine Peritoneal Fluid cells ; **MFC-5** : human fetal lung fibroblast ; **HUVEC** : human umbilical vein endothelial cells ; **J774** : Cell line of murine peritoneal macrophages ; **L.6** : cell line of rat skeletal myoblasts ; **RAW** : macrophage cell line ; **VERO** : kidney epithelial cell line  
**PTR1** : Pentidine reductase 1 ; **APRT** : adenosine phosphoribosyltransferase, **LPG** : lipophosphoglycan ; **GP83** Glycoprotein 83 ; **MEBA** : Methanol Bark extract ; **PEN** : Pentalinostrol  
**AEPA** : Aqueous extract of *Physalis angulata* ; **TREO** : Triptaria Essential Oil ; **NA** : Not Assessed

## Discussion

This review aimed to identify specific strategies of drug development by looking at current advances in drug discovery. We chose to only include studies that were either performed *in vivo* or on amastigotes *in vitro* as amastigotes are the form that are found inside host cells and are responsible for the disease. We have excluded screenings of compounds on promastigotes since it is known screening on amastigotes leads to a good hit-to-success ratio but screenings on promastigotes often fail in later stages of drug development due to false positivity [100].

As regarding treatments, monotherapies are recommended by WHO as first line treatments with different authorized molecules among different parts of the world. Liposomal Amphotericin B (L-AMB) figures among the most efficient treatments, although it has numerous issues regarding its necessity for hospitalization, cost, and its availability throughout the world. Indeed, many countries do not have access to L-AMB, and recent reports of resistant strains have only confirmed the necessity to change strategies in drug development if we do not want to face a crisis like the current therapeutic failures of antibiotics.

In order to counter problems of drug resistance, combination of authorized drugs has emerged as a key strategy to efficiently and with reduced costs, develop new treatment regimens. Although most combinations indeed reduced dosage, toxicity and increased efficiency, combination of L-AMB with SSG or Miltefosine [22] or combination of intralesional Glucantime with oral itraconazole [24] offered no benefit over monotherapy. In the case of Miltefosine and Pentamidine combination, an additive effect of treatment was observed, but it also gave rise to additive side effects and cost, rendering this treatment unusable [23]. Overall, the development of combination treatments still needs a lot of trial in order to determine which combinations are effective, and which are the optimal doses and posology for these treatment regimens. Despite this reduction of cytotoxicity and cost because of reduced doses, it does not allow the elimination of both these problems since they are inherent to the used molecules and would need the development of alternative compounds to be resolved.

The formulation in nanocarriers such as liposomes had proven efficient in the case of Amphotericin B, efficiently reducing toxicity, but increasing cost of the treatment. This was partially because current formulations rely on animal derived cholesterol. Processing of this cholesterol to render it free of mammal prions and ready for injection is very expensive, thus it has been proposed to replace the liposome carrier of Amphotericin B by a new lipid derived from plant stigmasterol (DSHemsPC). This formulation did not reduce AMB in target organs or efficiency in the reduction of inflammation and parasite burden in mice, making it a promising alternative for liposomal formulations [45].

Formulations in nanoparticles has allowed for a decrease of toxicity by delaying liberation of the compound, allowed targeting to specific organs or cell types and allowed for modifications in the route of administration [84–87]. Nanoparticle formulation can be combined with either strategy of improvement of existent molecules, like deliver combination therapies like AMB and paromomycin orally [101] or AMB and miltefosine topically [102]. It can also help effectively deliver natural molecules [28].

Overall, since nanoparticules are carriers, they are a very versatile tool for treatment improvement and can come as a last improvement on already better treatments against leishmaniasis, although this comes with an important raise of cost.

Drug repositioning, like nanoparticle formulations, had already proven its use in the case of neglected tropical diseases as discussed previously with for example miltefosine. Compounds cited in this review were repositioned from the fight against other pathogens, aiming for common pathways to block or inhibit, but also from diseases that had nothing to do with infection. Only one of these repositioned drugs, fexinidazole, has undergone clinical trials after promising results *in vivo* in mice. This anti-trypanosomatid targeting a homolog of nitroreductase in *Leishmania*, has shown a good effect but led to multiple relapses, causing the trial to be terminated because of lack of efficiency [54]. The sterol synthesis pathway is one other promising target, and several approved drugs against other diseases are known to act on this pathway. Andrade-Neto *et al.* have proposed the combination of two sterol pathway inhibitors acting at different stages of sterol conversion, leading to the decrease of IC50 values for miconazole when used in combination with imipramine, and thus seeming like an interesting combination strategy acting at different levels of one pathway [53].

Repositioning allows for great time and money saving in the process of drug development, as compounds have already received authorization for human application. Although it can sometimes be complicated to foresee the effects of the drug when it has immunomodulatory properties, like in the case of simvastatin that allowed for parasite burden reduction in both susceptible Balb/c and resistant C57/Bl6 mice, contrary to pravastatin that increased survival of susceptible mice, but worsened the condition of resistant mice [63].

As immunity is so important in disease progression, and current treatments present mechanisms of action revolving around the parasite, it has been often proposed to combine classical treatments with immunomodulating compounds in order to skew host response in a more favorable way, either by stimulating pro-inflammatory environment or by avoiding excessive response in the case of cutaneous lesions. If certain of these strategies have led to treatment duration decrease, or treatment dosage decrease, lowering side effects and cost at the same time, others have shown no effect [78]. Moreover,

some treatments actually increased incidence of adverse effects, as in the case of pentoxifylline supplementation [76]. In the case of combination with imiquimod, while combination with Glucantime on *L. major* infections showed better cure rate [72], combination with SSG on *L. braziliensis* showed a tendency but no statistical significance [75]. Multiple articles have sought to increase Th1 responses by favoring a Pro-inflammatory environment, though there have also been trials that inhibited Th1 responses to limit local inflammation and reduce tissue damage in response to cutaneous infection [79,80]. Although immunomodulation is a very promising strategy in the fight against leishmaniasis, up to date there are no immunomodulatory treatments available that show complete efficiency on their own, without an anti-leishmanial chemotherapy associated. Furthermore, the development of immunostimulation could lead to the identification of treatments efficient on a range of different pathogens, as activation of the immune system is not specific to one microbe in particular, like actual treatments are.

A multitude of articles screening for novel anti-leishmanial drugs in plants have been published over the course of the last years. Among these articles, there are different approaches as to the selection of these plants, but one of the more promising approaches, allowing for possible time saving and money saving is the ethnobotanical approach. All over the world, scientists have tried to use this approach to identify new anti-leishmanial compounds. Starting from surveys and interrogation of the local population, most plants have various indications against a large variety of symptoms, ranging from inflammation to thrombosis or aphrodisiacs [81]. Thus, it is no wonder that not every ethnobotanical study ends up giving favorable results or confirming ethnopharmacological use of plants. If overall, most extracts were shown to have low toxicity, some studies revealed fractions with important CC50 values, which has led them to be unusable on macrophages [103,104]. Highlighting the importance of testing on intracellular amastigotes, Girardi *et al.* showed that while compounds showed activity on promastigotes and axenic amastigotes, none of the extracts were active against intracellular macrophages at a concentration lower than their CC50 [105]. If numerous studies have screened these compounds, few elucidate their mechanism of action. Furthermore, it is not always possible to narrow down the effects of an extract to one unique molecule, as sometimes several compounds can act synergistically. Overall, the ethnobotanical approach still seems to be quite promising as it allows for the valorization of the vast biodiversity and gives access to highly represented compounds that could be way cheaper to produce. The commercialization of natural products meets current demands of a more conscious and "safe" way of treating diseases, and would lead to easier commercialization of products that often have low cytotoxicity and possibly immunomodulatory properties.

## Acknowledgments

This work was supported by the Fondation pour la Recherche Médicale, grant number **ECO201806006733**, to A.M.

## References

1. Pigott DM, Bhatt S, Golding N, Duda KA, Battle KE, Brady OJ et al. (2014) Global distribution maps of the leishmaniasis. *Elife* 3: e02851.
2. WHO (2021) Leishmaniasis.
3. CDC (2020) Parasites - Leishmaniasis.
4. Reguera RM, Morán M, Pérez-Pertejo Y, García-Estrada C, Balaña-Fouce R (2016) Current status on prevention and treatment of canine leishmaniasis. *Vet Parasitol* 227: 98-114.
5. Velez R, Gállego M (2020) Commercially approved vaccines for canine leishmaniasis: a review of available data on their safety and efficacy. *Tropical Medicine & International Health* 25: 540-557.
6. Organization WH (2010) Control of the leishmaniasis. World Health Organization, Tech Rep Ser xii-xiii, 1.
7. Ponte-Sucre A, Gamarro F, Dujardin JC, Barrett MP, López-Vélez R, García-Hernández R et al. (2017) Drug resistance and treatment failure in leishmaniasis: A 21st century challenge. *PLoS Negl Trop Dis* 11: e0006052.
8. Frézard F, Demicheli C, Ribeiro RR (2009) Pentavalent antimonials: new perspectives for old drugs. *Molecules* 14: 2317-2336.
9. Moreira VR, de Jesus LCL, Soares RP, Silva LDM, Pinto BAS, Melo MN et al. (2017) Meglumine Antimoniate (Glucantime) Causes Oxidative Stress-Derived DNA Damage in BALB/c Mice Infected by *Leishmania (Leishmania) infantum*. *Antimicrob Agents Chemother* 61:
10. Braga SS (2019) Multi-target drugs active against leishmaniasis: A paradigm of drug repurposing. *Eur J Med Chem* 183: 111660.
11. Chawla B, Jhingran A, Panigrahi A, Stuart KD, Madhubala R (2011) Paromomycin affects translation and vesicle-mediated trafficking as revealed by proteomics of paromomycin - susceptible -resistant *Leishmania donovani*. *PLoS One* 6: e26660.
12. Shalev-Benami M, Zhang Y, Rozenberg H, Nobe Y, Taoka M, Matzov D et al. (2017) Atomic resolution snapshot of Leishmania ribosome inhibition by the aminoglycoside paromomycin. *Nat Commun* 8: 1589.
13. Yang G, Choi G, No JH (2016) Antileishmanial Mechanism of Diamidines Involves Targeting Kinetoplasts. *Antimicrob Agents Chemother* 60: 6828-6836.
14. van Griensven J, Diro E (2019) Visceral Leishmaniasis: Recent Advances in Diagnostics and Treatment Regimens. *Infect Dis Clin North Am* 33: 79-99.
15. Diro E, Blesson S, Edwards T, Ritmeijer K, Fikre H, Admassu H et al. (2019) A randomized trial of AmBisome monotherapy and AmBisome and miltefosine combination to treat visceral leishmaniasis in HIV co-infected patients in Ethiopia. *PLoS Negl Trop Dis* 13: e0006988.

16. Chungue CN, Gachihi G, Muigai R, Wasunna K, Rashid JR, Chulay JD et al. (1985) Visceral leishmaniasis unresponsive to antimonial drugs. III. Successful treatment using a combination of sodium stibogluconate plus allopurinol. *Trans R Soc Trop Med Hyg* 79: 715-718.
17. Santos MF, Alexandre-Pires G, Pereira MA, Marques CS, Gomes J, Correia J et al. (2019) Meglumine Antimoniate and Miltefosine Combined With Allopurinol Sustain Pro-inflammatory Immune Environments During Canine Leishmaniasis Treatment. *Front Vet Sci* 6: 362.
18. Manna L, Corso R, Galiero G, Cerrone A, Muzj P, Gravino AE (2015) Long-term follow-up of dogs with leishmaniasis treated with meglumine antimoniate plus allopurinol versus miltefosine plus allopurinol. *Parasit Vectors* 8: 289.
19. Kasabalis D, Chatzis MK, Apostolidis K, Xenoulis PG, Buono A, Petanides T et al. (2019) Evaluation of nephrotoxicity and ototoxicity of aminosidine (paromomycin)-allopurinol combination in dogs with leishmaniasis due to *Leishmania infantum*: A randomized, blinded, controlled study. *Exp Parasitol* 206: 107768.
20. de Moraes-Teixeira E, Aguiar MG, Soares de Souza Lima B, Ferreira LA, Rabello A (2015) Combined suboptimal schedules of topical paromomycin, meglumine antimoniate and miltefosine to treat experimental infection caused by *Leishmania (Viannia) braziliensis*. *J Antimicrob Chemother* 70: 3283-3290.
21. Hendrickx S, Van den Kerkhof M, Mabilille D, Cos P, Delputte P, Maes L et al. (2017) Combined treatment of miltefosine and paromomycin delays the onset of experimental drug resistance in *Leishmania infantum*. *PLoS Negl Trop Dis* 11: e0005620.
22. Wasunna M, Njenga S, Balasegaram M, Alexander N, Omollo R, Edwards T et al. (2016) Efficacy and Safety of AmBisome in Combination with Sodium Stibogluconate or Miltefosine and Miltefosine Monotherapy for African Visceral Leishmaniasis: Phase II Randomized Trial. *PLoS Negl Trop Dis* 10: e0004880.
23. Soto J, Soto P, Ajata A, Rivero D, Luque C, Tintaya C et al. (2018) Miltefosine Combined with Intralesional Pentamidine for *Leishmania braziliensis* Cutaneous Leishmaniasis in Bolivia. *Am J Trop Med Hyg* 99: 1153-1155.
24. Bashir U, Tahir M, Anwar MI, Manzoor F (2019) Comparison of Intralesional Meglumine Antimonite along with oral Itraconazole to Intralesional Meglumine Antimonite in the treatment of Cutaneous Leishmaniasis. *Pak J Med Sci* 35: 1669-1673.
25. Mitchell MJ, Billingsley MM, Haley RM, Wechsler ME, Peppas NA, Langer R (2021) Engineering precision nanoparticles for drug delivery. *Nat Rev Drug Discov* 20: 101-124.
26. Zhu Y, Liao L (2015) Applications of Nanoparticles for Anticancer Drug Delivery: A Review. *J Nanosci Nanotechnol* 15: 4753-4773.
27. da Gama Bitencourt JJ, Pazin WM, Ito AS, Barioni MB, de Paula Pinto C, Santos MA et al. (2016) Miltefosine-loaded lipid nanoparticles: Improving miltefosine stability and reducing its hemolytic potential toward erythrocytes and its cytotoxic effect on macrophages. *Biophys Chem* 217: 20-31.
28. Ray L, Karthik R, Srivastava V, Singh SP, Pant AB, Goyal N et al. (2020) Efficient antileishmanial activity of amphotericin B and piperine entrapped in enteric coated guar gum nanoparticles. *Drug Deliv Transl Res*
29. Afzal I, Sarwar HS, Sohail MF, Varikuti S, Jahan S, Akhtar S et al. (2019) Mannosylated thiolated paromomycin-loaded PLGA nanoparticles for the oral therapy of visceral leishmaniasis. *Nanomedicine (Lond)* 14: 387-406.

30. Valle IV, Machado ME, Araújo CDCB, da Cunha-Junior EF, da Silva Pacheco J, Torres-Santos EC et al. (2019) Oral pentamidine-loaded poly(d,l-lactic-co-glycolic) acid nanoparticles: an alternative approach for leishmaniasis treatment. *Nanotechnology* 30: 455102.
31. Téllez J, Echeverry MC, Romero I, Guatibonza A, Santos Ramos G, Borges De Oliveira AC et al. (2020) Use of liposomal nanoformulations in *antileishmania* therapy: challenges and perspectives. *J Liposome Res* 1-8.
32. Dar MJ, Din FU, Khan GM (2018) Sodium stibogluconate loaded nano-deformable liposomes for topical treatment of leishmaniasis: macrophage as a target cell. *Drug Deliv* 25: 1595-1606.
33. Singh PK, Jaiswal AK, Pawar VK, Raval K, Kumar A, Bora HK et al. (2018) Fabrication of 3-O-sn-Phosphatidyl-L-serine Anchored PLGA Nanoparticle Bearing Amphotericin B for Macrophage Targeting. *Pharm Res* 35: 60.
34. Asthana S, Gupta PK, Jaiswal AK, Dube A, Chourasia MK (2015) Targeted chemotherapy of visceral leishmaniasis by lactoferrin-appended amphotericin B-loaded nanoreservoir: *in vitro* and *in vivo* studies. *Nanomedicine (Lond)* 10: 1093-1109.
35. Tripathi P, Jaiswal AK, Dube A, Mishra PR (2017) Hexadecylphosphocholine (Miltefosine) stabilized chitosan modified Ampholipospheres as prototype co-delivery vehicle for enhanced killing of *L. donovani*. *Int J Biol Macromol* 105: 625-637.
36. Gupta PK, Jaiswal AK, Asthana S, Verma A, Kumar V, Shukla P et al. (2015) Self assembled ionically sodium alginate cross-linked amphotericin B encapsulated glycol chitosan stearate nanoparticles: applicability in better chemotherapy and non-toxic delivery in visceral leishmaniasis. *Pharm Res* 32: 1727-1740.
37. Gaspar MM, Calado S, Pereira J, Ferronha H, Correia I, Castro H et al. (2015) Targeted delivery of paromomycin in murine infectious diseases through association to nano lipid systems. *Nanomedicine* 11: 1851-1860.
38. Mehrizi TZ, Ardestani MS, Khamesipour A, Hoseini MHM, Mosaffa N, Anissian A et al. (2018) Reduction toxicity of Amphotericin B through loading into a novel nanoformulation of anionic linear globular dendrimer for improve treatment of *leishmania major*. *J Mater Sci Mater Med* 29: 125.
39. Asthana S, Jaiswal AK, Gupta PK, Dube A, Chourasia MK (2015) Th-1 biased immunomodulation and synergistic antileishmanial activity of stable cationic lipid-polymer hybrid nanoparticle: biodistribution and toxicity assessment of encapsulated amphotericin B. *Eur J Pharm Biopharm* 89: 62-73.
40. Abu Ammar A, Nasereddin A, Erekat S, Dan-Goor M, Jaffe CL, Zussman E et al. (2019) Amphotericin B-loaded nanoparticles for local treatment of cutaneous leishmaniasis. *Drug Deliv Transl Res* 9: 76-84.
41. Kumar R, Sahoo GC, Pandey K, Das V, Das P (2015) Study the effects of PLGA-PEG encapsulated amphotericin B nanoparticle drug delivery system against *Leishmania donovani*. *Drug Deliv* 22: 383-388.
42. Casa DM, Scariot DB, Khalil NM, Nakamura CV, Mainardes RM (2018) Bovine serum albumin nanoparticles containing amphotericin B were effective in treating murine cutaneous leishmaniasis and reduced the drug toxicity. *Exp Parasitol* 192: 12-18.
43. de Souza RM, Maranhão RC, Tavares ER, Filippin-Monteiro FB, Nicodemo AC, Morikawa AT et al. (2020) Lipid nanoparticles for amphotericin delivery in the treatment of American tegumentary leishmaniasis. *Drug Deliv Transl Res* 10: 403-412.



44. Zadeh Mehrizi T, Khamesipour A, Shafiee Ardestani M, Ebrahimi Shahmabadi H, Haji Molla Hoseini M, Mosaffa N et al. (2019) Comparative analysis between four model nanoformulations of amphotericin B-chitosan, amphotericin B-dendrimer, betulinic acid-chitosan and betulinic acid-dendrimer for treatment of *Leishmania major*: real-time PCR assay plus. *Int J Nanomedicine* 14: 7593-7607.
45. Iman M, Huang Z, Alavizadeh SH, Szoka FC, Jaafari MR (2017) Biodistribution and *In Vivo* Antileishmanial Activity of 1,2-Distigmasterylhemisuccinoyl-sn-Glycero-3-Phosphocholine Liposome-Intercalated Amphotericin B. *Antimicrob Agents Chemother* 61:
46. Soltani S, Forushani HM, Soltani S, Kahvaz MS, Foroutan M (2019) Antileishmanial activity of conventional and solid lipid nanoparticles of Amphotericin B on *Leishmania major*. *Infect Disord Drug Targets*
47. Sousa-Batista AJ, Cerqueira-Coutinho C, do Carmo FS, Albernaz MS, Santos-Oliveira R (2019) Polycaprolactone Antimony Nanoparticles as Drug Delivery System for Leishmaniasis. *Am J Ther* 26: e12-e17.
48. Reis LES, Fortes de Brito RC, Cardoso JMO, Mathias FAS, Aguiar Soares RDO, Carneiro CM et al. (2017) Mixed Formulation of Conventional and Pegylated Meglumine Antimoniate-Containing Liposomes Reduces Inflammatory Process and Parasite Burden in *Leishmania infantum*-Infected BALB/c Mice. *Antimicrob Agents Chemother* 61:
49. Kumar R, Sahoo GC, Pandey K, Das VNR, Topno RK, Ansari MY et al. (2016) Development of PLGA-PEG encapsulated miltefosine based drug delivery system against visceral leishmaniasis. *Mater Sci Eng C Mater Biol Appl* 59: 748-753.
50. Heidari-Kharaji M, Taheri T, Doroud D, Habibzadeh S, Badirzadeh A, Rafati S (2016) Enhanced paromomycin efficacy by solid lipid nanoparticle formulation against *Leishmania* in mice model. *Parasite Immunol* 38: 599-608.
51. Bezerra-Souza A, Fernandez-Garcia R, Rodrigues GF, Bolas-Fernandez F, Dalastra Laurenti M, Passero LF et al. (2019) Repurposing Butenafine as An Oral Nanomedicine for Visceral Leishmaniasis. *Pharmaceutics* 11:
52. Teixeira de Macedo Silva S, Visbal G, Lima Prado Godinho J, Urbina JA, de Souza W, Cola Fernandes Rodrigues J (2018) *In vitro* antileishmanial activity of ravuconazole, a triazole antifungal drug, as a potential treatment for leishmaniasis. *J Antimicrob Chemother* 73: 2360-2373.
53. Andrade-Neto VV, Pereira TM, Canto-Cavalheiro M, Torres-Santos EC (2016) Imipramine alters the sterol profile in *Leishmania amazonensis* and increases its sensitivity to miconazole. *Parasit Vectors* 9: 183.
54. Patterson S, Wyllie S, Norval S, Stojanovski L, Simeons FR, Auer JL et al. (2016) The anti-tubercular drug delamanid as a potential oral treatment for visceral leishmaniasis. *Elife* 5:
55. Gil Z, Martinez-Sotillo N, Pinto-Martinez A, Mejias F, Martinez JC, Galindo I et al. (2020) SQ109 inhibits proliferation of *Leishmania donovani* by disruption of intracellular  $Ca^{2+}$  homeostasis, collapsing the mitochondrial electrochemical potential ( $\Delta\Psi_m$ ) and affecting acidocalcisomes. *Parasitol Res* 119: 649-657.
56. Khanra S, Juin SK, Jawed JJ, Ghosh S, Dutta S, Nabi SA et al. (2020) *In vivo* experiments demonstrate the potent antileishmanial efficacy of repurposed suramin in visceral leishmaniasis. *PLoS Negl Trop Dis* 14: e0008575.

57. Varikuti S, Volpedo G, Saljoughian N, Hamza OM, Halsey G, Ryan NM et al. (2019) The Potent ITK/BTK Inhibitor Ibrutinib Is Effective for the Treatment of Experimental Visceral Leishmaniasis Caused by *Leishmania donovani*. *J Infect Dis* 219: 599-608.
58. El Hajj R, Bou Youness H, Lachaud L, Bastien P, Masquefa C, Bonnet PA et al. (2018) EAPB0503: An Imiquimod analog with potent *in vitro* activity against cutaneous leishmaniasis caused by *Leishmania major* and *Leishmania tropica*. *PLoS Negl Trop Dis* 12: e0006854.
59. Nandan D, Zhang N, Yu Y, Schwartz B, Chen S, Kima PE et al. (2018) Miransertib (ARQ 092), an orally-available, selective Akt inhibitor is effective against *Leishmania*. *PLoS One* 13: e0206920.
60. Collier MA, Peine KJ, Gautam S, Oghumu S, Varikuti S, Borteh H et al. (2016) Host-mediated *Leishmania donovani* treatment using AR-12 encapsulated in acetalated dextran microparticles. *Int J Pharm* 499: 186-194.
61. da Silva Rodrigues JH, Miranda N, Volpato H, Ueda-Nakamura T, Nakamura CV (2019) The antidepressant clomipramine induces programmed cell death in *Leishmania amazonensis* through a mitochondrial pathway. *Parasitol Res* 118: 977-989.
62. Lima ML, Abengózar MA, Náchter-Vázquez M, Martínez-Alcázar MP, Barbas C, Tempone AG et al. (2018) Molecular Basis of the Leishmanicidal Activity of the Antidepressant Sertraline as a Drug Repurposing Candidate. *Antimicrob Agents Chemother* 62:
63. Parihar SP, Hartley MA, Hurdal R, Guler R, Brombacher F (2016) Topical Simvastatin as Host-Directed Therapy against Severity of Cutaneous Leishmaniasis in Mice. *Sci Rep* 6: 33458.
64. Khadir F, Taheri T, Habibzadeh S, Zahedifard F, Gholami E, Heidari-Kharaji M et al. (2019) Antileishmanial effect of rapamycin as an alternative approach to control *Leishmania tropica* infection. *Vet Parasitol* 276: 108976.
65. Oryan A, Bemani E, Bahrami S (2018) Emerging role of amiodarone and dronedarone, as antiarrhythmic drugs, in treatment of leishmaniasis. *Acta Trop* 185: 34-41.
66. Volpedo G, Pacheco-Fernandez T, Holcomb EA, Cipriano N, Cox B, Satoskar AR (2021) Mechanisms of Immunopathogenesis in Cutaneous Leishmaniasis And Post Kala-azar Dermal Leishmaniasis (PKDL). *Front Cell Infect Microbiol* 11: 685296.
67. Gupta G, Oghumu S, Satoskar AR (2013) Mechanisms of immune evasion in leishmaniasis. *Adv Appl Microbiol* 82: 155-184.
68. Baxarias M, Martínez-Orellana P, Baneth G, Solano-Gallego L (2019) Immunotherapy in clinical canine leishmaniosis: a comparative update. *Res Vet Sci* 125: 218-226.
69. Khodabandeh M, Rostami A, Borhani K, Gamble HR, Mohammadi M (2019) Treatment of resistant visceral leishmaniasis with interferon gamma in combination with liposomal amphotericin B and allopurinol. *Parasitol Int* 72: 101934.
70. Murray HW, Brooks EB, DeVecchio JL, Heinzl FP (2003) Immunoenhancement combined with amphotericin B as treatment for experimental visceral leishmaniasis. *Antimicrob Agents Chemother* 47: 2513-2517.
71. Netea MG, Van der Meer JW, Suttmuller RP, Adema GJ, Kullberg BJ (2005) From the Th1/Th2 paradigm towards a Toll-like receptor/T-helper bias. *Antimicrob Agents Chemother* 49: 3991-3996.
72. Taslimi Y, Zahedifard F, Rafati S (2016) Leishmaniasis and various immunotherapeutic approaches. *Parasitology* 145: 497-507.
73. Goyonlo VM, Vahabi-Amlashi S, Taghavi F (2019) Successful treatment by adding thalidomide to meglumine antimoniate in a case of refractory anthroponotic mucocutaneous leishmaniasis. *Int J Parasitol Drugs Drug Resist* 11: 177-179.

74. Murray HW (2005) Interleukin 10 receptor blockade--pentavalent antimony treatment in experimental visceral leishmaniasis. *Acta Trop* 93: 295-301.
75. Miranda-Verastegui C, Tulliano G, Gyorkos TW, Calderon W, Rahme E, Ward B et al. (2009) First-line therapy for human cutaneous leishmaniasis in Peru using the TLR7 agonist imiquimod in combination with pentavalent antimony. *PLoS Negl Trop Dis* 3: e491.
76. Brito G, Dourado M, Guimarães LH, Meireles E, Schrieffer A, de Carvalho EM et al. (2017) Oral Pentoxifylline Associated with Pentavalent Antimony: A Randomized Trial for Cutaneous Leishmaniasis. *Am J Trop Med Hyg* 96: 1155-1159.
77. Ventin F, Cincurá C, Machado PRL (2018) Safety and efficacy of miltefosine monotherapy and pentoxifylline associated with pentavalent antimony in treating mucosal leishmaniasis. *Expert Rev Anti Infect Ther* 16: 219-225.
78. Murray HW, Flanders KC, Donaldson DD, Sypek JP, Gotwals PJ, Liu J et al. (2005) Antagonizing deactivating cytokines to enhance host defense and chemotherapy in experimental visceral leishmaniasis. *Infect Immun* 73: 3903-3911.
79. Macedo SR, de Figueiredo Nicolete LD, Ferreira AS, de Barros NB, Nicolete R (2015) The pentavalent antimonial therapy against experimental *Leishmania amazonensis* infection is more effective under the inhibition of the NF- $\kappa$ B pathway. *Int Immunopharmacol* 28: 554-559.
80. Schwartz J, Moreno E, Calvo A, Blanco L, Fernández-Rubio C, Sanmartín C et al. (2018) Combination of paromomycin plus human anti-TNF- $\alpha$  antibodies to control the local inflammatory response in BALB/ mice with cutaneous leishmaniasis lesions. *J Dermatol Sci* 92: 78-88.
81. Das A, Jawed JJ, Das MC, Sandhu P, De UC, Dinda B et al. (2017) Antileishmanial and immunomodulatory activities of lupeol, a triterpene compound isolated from *Sterculia villosa*. *Int J Antimicrob Agents* 50: 512-522.
82. Roy S, Dutta D, Satyavarapu EM, Yadav PK, Mandal C, Kar S et al. (2017) Mahanine exerts *in vitro* and *in vivo* antileishmanial activity by modulation of redox homeostasis. *Sci Rep* 7: 4141.
83. Dey S, Mukherjee D, Chakraborty S, Mallick S, Dutta A, Ghosh J et al. (2015) Protective effect of *Croton caudatus Geisel* leaf extract against experimental visceral leishmaniasis induces proinflammatory cytokines *in vitro* and *in vivo*. *Exp Parasitol* 151-152: 84-95.
84. Bhatnagar M, Sarkar N, Gandharv N, Apang O, Singh S, Ghosal S (2017) Evaluation of antimycobacterial, leishmanicidal and antibacterial activity of three medicinal orchids of Arunachal Pradesh, India. *BMC Complement Altern Med* 17: 379.
85. Vásquez-Ocmín P, Cojean S, Rengifo E, Suyyagh-Albouz S, Amasifuen Guerra CA, Pomel S et al. (2018) Antiprotozoal activity of medicinal plants used by Iquitos-Nauta road communities in Loreto (Peru). *J Ethnopharmacol* 210: 372-385.
86. Atay I, Kirmizibekmez H, Kaiser M, Akaydin G, Yesilada E, Tasdemir D (2016) Evaluation of *in vitro* antiprotozoal activity of *Ajuga laxmannii* and its secondary metabolites. *Pharm Biol* 54: 1808-1814.
87. Tasdemir D, MacIntosh AJJ, Stergiou P, Kaiser M, Mansour NR, Bickle Q et al. (2020) Antiprotozoal and antihelminthic properties of plants ingested by wild Japanese macaques (*Macaca fuscata yakui*) in Yakushima Island. *J Ethnopharmacol* 247: 112270.
88. Maquiaveli CDC, Oliveira E Sá AM, Vieira PC, da Silva ER (2016) *Stachytarpheta cayennensis* extract inhibits promastigote and amastigote growth in *Leishmania amazonensis* via parasite arginase inhibition. *J Ethnopharmacol* 192: 108-113.

89. Santos BM, Bezerra-Souza A, Aragaki S, Rodrigues E, Umehara E, Ghilardi Lago JH et al. (2019) Ethnopharmacology Study of Plants from Atlantic Forest with Leishmanicidal Activity. *Evid Based Complement Alternat Med* 2019: 8780914.
90. Lima GS, Castro-Pinto DB, Machado GC, Maciel MA, Echevarria A (2015) Antileishmanial activity and trypanothione reductase effects of terpenes from the Amazonian species *Croton cajucara Benth* (Euphorbiaceae). *Phytomedicine* 22: 1133-1137.
91. Maquiaveli CDC, Rochetti AL, Fukumasu H, Vieira PC, da Silva ER (2017) Antileishmanial activity of verbascoside: Selective arginase inhibition of intracellular amastigotes of *Leishmania (Leishmania) amazonensis* with resistance induced by LPS plus IFN- $\gamma$ . *Biochem Pharmacol* 127: 28-33.
92. Demarchi IG, Terron MS, Thomazella MV, Mota CA, Gazim ZC, Cortez DA et al. (2016) Antileishmanial and immunomodulatory effects of the essential oil from *Tetradenia riparia* (Hochstetter) Codd. *Parasite Immunol* 38: 64-77.
93. Rodrigues IA, Ramos AS, Falcão DQ, Ferreira JLP, Basso SL, Silva JRA et al. (2018) Development of Nanoemulsions to Enhance the Antileishmanial Activity of *Copaifera paupera* Oleoresins. *Biomed Res Int* 2018: 9781724.
94. Souza AC, Alves MMM, Brito LM, Oliveira LGC, Sobrinho-Júnior EPC, Costa ICG et al. (2017) *Platonia insignis* Mart., a Brazilian Amazonian Plant: The Stem Barks Extract and Its Main Constituent Lupeol Exert Antileishmanial Effects Involving Macrophages Activation. *Evid Based Complement Alternat Med* 2017: 3126458.
95. Da Silva BJM, Da Silva RRP, Rodrigues APD, Farias LHS, Do Nascimento JLM, Silva EO (2016) *Physalis angulata* induces death of promastigotes and amastigotes of *Leishmania (Leishmania) amazonensis* via the generation of reactive oxygen species. *Micron* 82: 25-32.
96. Da Silva BJM, Souza-Monteiro JR, Rogez H, Crespo-López ME, Do Nascimento JLM, Silva EO (2018) Selective effects of Euterpe oleracea (açai) on *Leishmania (Leishmania) amazonensis* and *Leishmania infantum*. *Biomed Pharmacother* 97: 1613-1621.
97. Mukherjee D, Singh CB, Dey S, Mandal S, Ghosh J, Mallick S et al. (2016) Induction of apoptosis by zerumbone isolated from *Zingiber zerumbet* (L.) Smith in protozoan parasite *Leishmania donovani* due to oxidative stress. *Braz J Infect Dis* 20: 48-55.
98. Gupta G, Peine KJ, Abdelhamid D, Snider H, Shelton AB, Rao L et al. (2015) A Novel Sterol Isolated from a Plant Used by Mayan Traditional Healers Is Effective in Treatment of Visceral Leishmaniasis Caused by *Leishmania donovani*. *ACS Infect Dis* 1: 497-506.
99. Nieto-Yañez OJ, Resendiz-Albor AA, Ruiz-Hurtado PA, Rivera-Yañez N, Rodriguez-Canales M, Rodriguez-Sosa M et al. (2017) *In vivo* and *In vitro* antileishmanial effects of methanolic extract from bark of *Bursera aptera*. *Afr J Tradit Complement Altern Med* 14: 188-197.
100. De Muylder G, Ang KK, Chen S, Arkin MR, Engel JC, McKerrow JH (2011) A screen against *Leishmania* intracellular amastigotes: comparison to a promastigote screen and identification of a host cell-specific hit. *PLoS Negl Trop Dis* 5: e1253.
101. Parvez S, Yadagiri G, Gedda MR, Singh A, Singh OP, Verma A et al. (2020) Modified solid lipid nanoparticles encapsulated with Amphotericin B and Paromomycin: an effective oral combination against experimental murine visceral leishmaniasis. *Sci Rep* 10: 12243.
102. Dar MJ, Khalid S, McElroy CA, Satoskar AR, Khan GM (2020) Topical treatment of cutaneous leishmaniasis with novel amphotericin B-miltefosine co-incorporated second generation ultra-deformable liposomes. *Int J Pharm* 573: 118900.

103. García Díaz J, Tuentler E, Escalona Arranz JC, Llauradó Maury G, Cos P, Pieters L (2019) Antimicrobial activity of leaf extracts and isolated constituents of *Croton linearis*. J Ethnopharmacol 236: 250-257.
104. Obbo CJD, Kariuki ST, Gathirwa JW, Olaho-Mukani W, Cheplogoi PK, Mwangi EM (2019) *In vitro* antiplasmodial, antitrypanosomal and antileishmanial activities of selected medicinal plants from Ugandan flora: Refocusing into multi-component potentials. J Ethnopharmacol 229: 127-136.
105. Girardi C, Fabre N, Paloque L, Ramadani AP, Benoit-Vical F, González-Aspajo G et al. (2015) Evaluation of antiplasmodial and antileishmanial activities of herbal medicine *Pseudelephantopus spiralis* (Less.) Cronquist and isolated hirsutinolide-type sesquiterpenoids. J Ethnopharmacol 170: 167-174.

# Objectifs de la Thèse

Les Leishmanioses sont aujourd'hui endémiques dans plus de 88 pays, et présentent ainsi un risque pour plus d'un milliard de personnes dans le monde. Il n'existe à l'heure actuelle aucun vaccin prévenant l'infection chez l'humain, et les traitements possèdent d'importantes limites, tant en matière de coût, qu'en matière de toxicité et d'efficacité quant à la prévention de rechutes. Ceci fait qu'il est aujourd'hui urgent de trouver des traitements alternatifs contre la leishmaniose. C'est en se basant sur ce constat que ce projet a commencé avec l'idée de cribler des plantes locales pour des extraits moins cytotoxiques que les traitements de référence et montrant un effet anti-*Leishmania*.

Les objectifs de cette thèse, débutée en 2018, se déclinent en 2 grandes parties.

La première consiste à la création de nouvelles souches rapportrices de *Leishmania*. Ceci afin d'obtenir des outils plus performants pour le suivi de l'infection *in vitro* par l'obtention de souches émettant de la fluorescence à différentes longueurs d'onde, et pour le suivi de l'infection *in vivo* par la création de souches capables d'émettre de la bioluminescence.

La seconde partie consiste à utiliser ces outils afin de continuer le crible sur les différents extraits de plante, afin d'en isoler des molécules possédant une activité anti-parasitaire et d'explorer leur efficacité ainsi que l'efficacité des dérivés des molécules d'intérêt isolées.



# Résultats





# Partie I : Création de nouvelles souches rapportrices de *Leishmania*

## I. Introduction

Afin d'élucider les mécanismes d'entrée, de persistance, de propagation et permettre un crible plus rapide et plus simple de nouvelles molécules anti-*Leishmania*, la création de souches rapportrices a révolutionné l'étude *in vitro* et *in vivo* de la leishmaniose. En effet, les techniques utilisées auparavant consistaient en la coloration au May-Grünwald Giemsa des leishmanies, ou en des techniques d'immunofluorescence, nécessitant la fixation des cellules étudiées. Avec l'apparition d'autres gènes rapporteurs, qui comme la  $\beta$ -galactosidase,  $\beta$ -lactamase, les protéines fluorescentes ou les enzymes permettant l'émission de bioluminescence (Dube, Gupta, & Singh, 2009) d'importants progrès ont pu être faits tant en matière de gain de temps qu'en matière de précision des mécanismes étudiés. La transfection a permis l'expression de ces différents gènes rapporteurs de façon transitoire, pendant quelques générations, ou de façon stable par insertion dans le génome des parasites, ce qui permet leur persistance au cours des générations.

L'expression de rapporteurs fluorescents a permis la visualisation des parasites *in vitro* en contournant la nécessité d'ajouter un substrat, ou de fixer les cellules pour le marquage, ce qui permet de faire des suivis de plus longue durée sur des cellules vivantes.

L'expression d'enzymes bioluminescentes comme la luciférase a été plus utilisée *in vivo* car en dépit de la nécessité d'ajouter un substrat, la luciférine, elle permet la visualisation des leishmanies dans des organes internes comme le foie et la rate, qui sont des organes cibles dans le cas des leishmanioses viscérales. L'utilisation des enzymes bioluminescentes a permis de mettre en place des suivis longitudinaux sur le même animal, car le sacrifice n'est pas nécessaire pour quantifier la charge parasitaire.

Il existe une multitude de fluorophores émettant à des longueurs d'onde différentes, et une multitude de luciférases permettant de l'émission de bioluminescence plus ou moins forte.

Au cours de cette thèse, nous avons cherché à produire des souches rapportrices fluorescentes autre que la GFP que nous possédions, afin de pouvoir élargir leur utilisation et contourner l'autofluorescence verte *in vitro*. Nous avons cherché à construire des souches plus performantes avec une émission de bioluminescence plus élevée que la souche *L. infantum*-Luc que nous possédons afin d'augmenter la quantité de signal reçue et contourner certains problèmes de limite de détection *in vitro* et *in vivo*. Finalement, nous avons réalisé la construction de souches doublement transformées pour exprimer de la fluorescence et de la bioluminescence en même temps, afin de garder une seule souche en culture pour les expérimentations aussi bien *in vitro* que *in vivo*.

## II. Matériel et Méthodes

### *Culture des souches de Leishmania*

Les *L. tarentolae* sont maintenues en culture à 26°C dans des flasques ventilées, en milieu Schneider's Complet. Les souches WT sont maintenues sans antibiotique de sélection, les souches transformées eFly-mCherry sont additionnés d'Hygromycine B à 100 µg/ml (1068701, GIBCO®).

### *Coloration des leishmanies*

Après une infection de 6h à une multiplicité d'infection de 20, les cellules BMDM ont été fixées et colorées au May-Grünwald (MG) et Giemsa (G) selon le protocole suivant : MG 3 minutes, 2 lavages PBS, MG ½ pendant 1 minute, 2 lavages PBS, G pendant 20 minutes. Les lames ont été observées au microscope Nikon Eclipse 50 i (objectif 100x A/1.25 à huile, caméra DS-Fi, Nikon).

### *Imagerie Bioluminescente in vivo et quantification*

Après inoculation de *L. infantum*, les souris ont été imagées une fois par semaine après injection intrapéritonéale de D-luciferin (PerkinElmer, 122799 XenoLight D-Luciferin, K+ Salt Bioluminescent Substrate) à 300 mg/kg, ou de 200µl de DTZ à 3mM (MedChem Express HY-

111382). L'injection a été réalisée 10 minutes avant d'anesthésier les souris dans une atmosphère de 3% isoflurane (Vetflurane), puis les souris ont été placées dans le PhotonIMAGER Optima (Biospace Lab), et l'anesthésie a été maintenue en utilisant 2,5% d'isoflurane pendant 5 minutes d'acquisition. Les images ont été analysées avec le logiciel M3Vision (Biospace Lab, Version 1.1.3.31192) avec des régions d'intérêt (ROI) autour du foie et de la rate pour quantifier l'émission de bioluminescence en photons/s/cm<sup>2</sup>/sr.

#### *PCR quantitative*

Des sections de foie (20mg) et de rate (10mg) ont été récupérées en Lysis buffer du kit Qiagen QIAmp DNA Mini Kit® et dissociées avec le Precellys® (2 x 30 sec, 15 sec break). L'extraction d'ADN a été réalisée selon le protocole Qiagen®. La PCR quantitative ciblant les minicercles de l'ADN du kinétoplaste utilise des amorces et des sondes décrites précédemment par *Mary et al.* (Mary, Faraut, Lascombe, & Dumon, 2004) et contient 20 pmol de sonde forward (5'-CTTTTCTGGTCCTCCGGGTAGG-3') et reverse (5'-CCACCCGGCCCTATTTTACACCAA-3') et 3.33 pmol de sonde TaqMan (FAM-TTTTTCGCAGAACGCCCTACCCGC-TAMRA). Le volume final est de 10µL, avec 2.5µL d'ADN, dans un automate StepONE system (ThermoFisher). Chaque expérimentation utilise des contrôles négatifs et une gamme standard obtenue de l'extraction d'AND de 2x10<sup>8</sup> parasites dilués en série au 1/10<sup>e</sup>, ce qui correspond à 50 000 à 0.05 parasites dans 2.5 µL. Le programme de PCR réalise deux étapes de température à 95°C et 60°C pendant 40 cycles.

### III. Résultats

#### *Tests de la souche sauvage*

Afin de déterminer la souche à transférer, nous avons fait des tests préliminaires d'infectivité des souches. Pour ce faire, nous avons testé 4 souches de parasites, LPN 05, 101, 388 et 432, classés du plus ancien au plus récemment isolé au CHU de Nice. Nous avons réalisé une infection de cellules BMDM à une MOI de 20 durant 6h, puis à 24h nous avons réalisé une

fixation et coloration au May-Grünwald Giemsa (MGG). La quantité de cellules infectées a été comptée, ainsi que le nombre moyen de leishmanies par cellules, sur un total de 100 cellules, en duplicat. Les résultats représentés ci-dessous indiquent que plus la souche est récente, plus elle infecte les BMDM. La souche la plus virulente LPN 432 a donc été choisie pour les futures transfections (Fig 6).

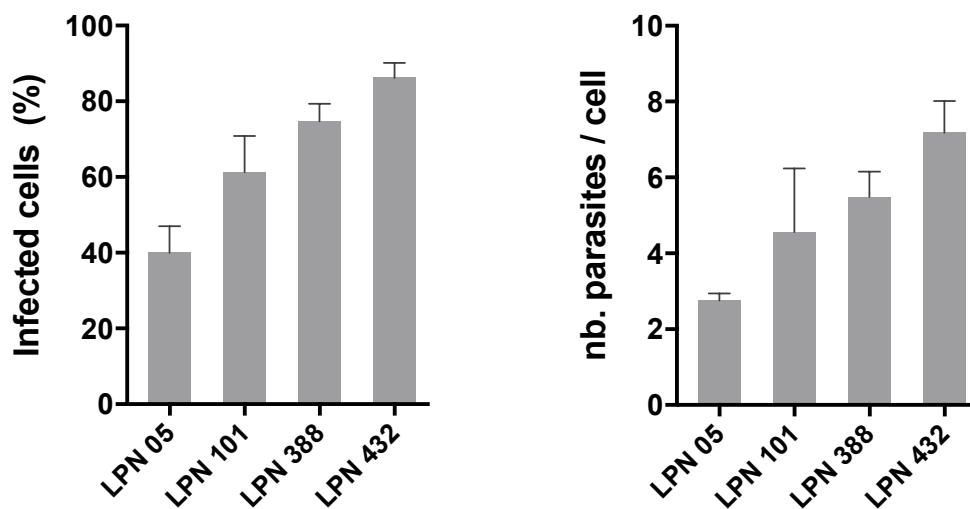


Figure 6 : Test d'infectivité de 4 souches sauvages isolées au CHU de Nice

Afin d'obtenir de nouvelles souches rapportrices utilisables avec un large éventail de techniques, nous avons choisi des rapporteurs fluorescents.

Le premier, mRuby est une protéine monomérique dérivée de l'anémone *Entacmaea quadricolor*, émettant de la fluorescence dans le rouge (longueur d'onde d'excitation à 558nm et d'émission à 605nm). Le second, mMaroon1, émet de la fluorescence dans le rouge lointain (longueur d'onde d'excitation à 609nm et d'émission à 657nm).

Nous avons choisi pour rapporteur bioluminescent le teLuc, qui est un mutant de la protéine nanoLuc trouvée dans la crevette marine *Oplophorus gracilirostris*. Comparé à la luciférase de luciole, cette luciférase permet une émission de bioluminescence plus intense, et la mutation pour obtenir le teLUC a permis d'obtenir une protéine émettant en plus une fluorescence shiftée vers le rouge-lointain. Le substrat du teLuc est un dérivé du substrat du nanoLuc, la Di-Phényl Terazine (DTZ). Des comparaisons ont montré que *in vitro*, le couple teLuc/DTZ permet

une émission de bioluminescence jusqu'à 1000 fois plus importante que le couple Luciférase de Luciole/Luciférine (Yeh *et al.*, 2017).

Enfin, nous avons voulu obtenir des souches exprimant à la fois de la bioluminescence et de la fluorescence, et nous avons essayé de transformer à l'aide des deux constructions obtenues précédemment une souche qui exprimerait le mMaroon1 et le teLuc, que nous n'avons malheureusement pas réussi à obtenir. Pour terminer, nous avons choisi le couple eFFly-mCherry. Le marqueur bioluminescent, la Luciférase de luciole, est utilisable avec un substrat luciférine très répandu pour l'imagerie *in vivo*, et la protéine fluorescente mCherry, peu intense en terme de fluorescence mais peu sensible au pH et qui émet de la fluorescence dans le rouge. Ces travaux font l'objet d'une publication sous forme d'article original, qui sera résumée ci-dessous.

Les constructions ont été réalisées à l'aide des vecteurs d'expression pLEXY, qui possèdent des séquences homologues à la séquence ADN de *Leishmania* codant pour l'ARN 18S permettant son insertion par recombinaison homologue. Le vecteur possède également un gène de résistance à un antibiotique pour permettre la sélection des clones transformés. Les gènes d'intérêt utilisés pour générer les souches rapportrices ont été amplifiés à l'aide d'amorces homologues en partie avec le vecteur et en partie avec l'insert, afin de pouvoir utiliser la technique Gibson Assembly IN-FUSION pour l'insertion dans le vecteur d'expression. Une fois le vecteur d'expression obtenu, des parasites *L. major* ou *L. infantum* ont été transfectés et sélectionnés pour l'expression des gènes d'intérêt.

Après transfection, nous avons tout d'abord vérifié par microscopie si la fluorescence était bien exprimée dans les promastigotes sélectionnés. Les souches mMaroon1, mRuby et mCherry permettaient une visualisation en microscopie confocale des promastigotes. Cependant, un suivi au cours du temps en cytométrie de flux a révélé que les mMaroon1 et mCherry exprimaient stablement la fluorescence même après un mois en culture, alors que les parasites mRuby perdaient l'expression de la fluorescence, tout en continuant à croître dans un milieu contenant l'antibiotique de sélection. Nous avons donc écarté la souche mRuby pour les expérimentations suivantes. Nous avons ensuite vérifié si l'insertion du transgène

avait eu un effet sur la croissance ou la mortalité de la souche eFFly-mCherry par rapport à la souche WT, ou sur la croissance et mortalité des souches teLuc et mMaroon1. Pour ce faire, nous avons réalisé un suivi sur 11 jours en cytométrie de flux, et regardant à différents temps la concentration en parasites/mL, et le pourcentage de leishmanies mortes avec le marqueur de mortalité DAPI. Les cinétiques de croissance et de mortalité étaient strictement identiques entre la souche non transformée et transformée eFFly-mCherry, et avaient un profil normal pour les souches teLuc et mMaroon1. Après avoir vérifié le comportement des souches, nous avons regardé leur fluorescence et leur bioluminescence *in vitro* sous forme promastigote à l'aide d'un suivi en cytométrie de flux. La fluorescence et la bioluminescence de toutes les souches était relativement stable sur les 4 premiers jours, avant l'atteinte du plateau de croissance, puis les deux paramètres ont vu leurs valeurs chuter avec l'augmentation de la mortalité, ce qui montre que les nouveaux gènes rapporteurs aussi bien bioluminescents que fluorescents sont de bons indicateurs de viabilité de la culture à l'état promastigote. La corrélation entre le nombre de leishmanies et la bioluminescence émise était très bonne ( $R^2 > 0,98$ ) pour toutes les souches.

Nous avons ensuite infecté des macrophages primaires issus de moelle osseuse de souris avec les parasites transformés à une multiplicité d'infection de 10 sur la nuit. L'observation en microscopie confocale après marquage de l'actine des cellules ainsi que de leur noyau a montré que les leishmanies eFFly-mCherry *L. infantum* et *L. major*, ainsi que les mMaroon1 *L. infantum* étaient capables d'infecter des cellules hôtes de souris, et que les parasites intracellulaires étaient bien visibles en fluorescence.

Le co-marquage des parasites avec les lysosomes a permis de mettre en évidence que certaines des leishmanies intracellulaires étaient contenues dans des vacuoles acides. Il est intéressant de noter que toutes les leishmanies ne colocalisent pas avec le lysotracker, ce qui pourrait être dû à leur temps passé dans le macrophage. Effectivement, l'infection sur 24h permet aux parasites d'entrer dans la cellule à différents temps, et donc d'observer des vacuoles plus ou moins acides. Les parasites mMaroon1 n'étaient pas visibles en colocalisation avec les lysosomes.

Nous avons ensuite regardé à 24h post infection, si le pourcentage de cellules infectées augmentait avec la multiplicité d'infection. Le pourcentage de cellules infecté a été suivi en

cytométrie en flux. Effectivement on peut observer une augmentation du pourcentage de cellules infectées en eFFly-mCherry, mais aussi une augmentation de la moyenne d'intensité de fluorescence. La moyenne d'intensité de fluorescence peut être prise comme un indicateur du nombre de parasites par cellules, car il augmente avec la quantité de signal fluorescent perçu.

De façon similaire, l'observation de la bioluminescence émise après ajout de luciférine par des cellules infectées avec *L. infantum*-eFFly-mCherry et teLuc à différentes MOI a montré une augmentation du signal avec l'augmentation de la quantité de leishmanies 24h post infection.

La construction de nouvelles souches *Leishmania* rapportrices permet l'obtention de plus en plus d'outils, et de contourner de plus en plus de limites de détection et de visualisation. Nous avons généré 4 souches rapportrices possédant chacune des avantages et des inconvénients. La configuration mRuby montrait une fluorescence très intense, cependant elle n'était pas stable au cours du temps.

Les parasites mMaroon1 montraient une fluorescence dans une longueur d'onde qui menait à peu de bruit de fond, cependant la sensibilité à l'acide de cette protéine n'a pas permis leur visualisation en forme amastigote en colocalisation avec des vésicules acides.

La construction teLuc permet une émission de bioluminescence très forte, mais le substrat DTZ est très instable, et difficilement soluble ce qui ne permet pas de contrôler la concentration. Enfin, la souche double rapportrice eFFly-mCherry émettait une bioluminescence correcte, et une fluorescence d'intensité moyenne qui permettait cependant sa visualisation *in vitro*.

Pour conclure, nous avons généré une souche doublement bioluminescente et fluorescente qui montre une bonne application *in vitro* et qui devra être testée *in vivo*.





# Article original

Soumis dans PLoS Neglected Tropical Diseases

## Generation and characterization of novel *Leishmania* reporter strains.

Alissa MAJOUR<sup>1</sup>, Alexandre PERRONE<sup>1</sup>, Loïc SIMON<sup>2</sup>, Pierre MARTY<sup>1,2</sup>, Grégory MICHEL<sup>1\*</sup>, Laurent BOYER<sup>1</sup>, Christelle POMARES<sup>1,2</sup>

<sup>1</sup> Université Côte d'Azur, INSERM U1065, Centre Méditerranéen de Médecine Moléculaire (C3M), Nice, France. <sup>2</sup> Service de Parasitologie-Mycologie, Centre Hospitalier Universitaire de Nice, Hôpital de l'Archet, Nice, France. \*Corresponding author : gregory.michel@univ-cotedazur.fr

### Abstract

Leishmaniasis is a neglected tropical disease, giving rise to up to a million new cases per year, among which up to 30 000 deaths. Current treatments are toxic, expensive, and face an increasing threat due to the apparition of resistance. Thus, the search for new treatments is a priority. The creation of reporter strains of *Leishmania* have revolutionized the screening of novel compounds, with fluorescence for *in vitro* studies and bioluminescence for *in vivo* adaptations and follow up in mice. We propose the creation of several reporter strains expressing either fluorescence, bioluminescence or both in order to adapt *Leishmania* parasites to a vast array of techniques ranging from microscopy and cytometry to bioluminescence follow-up *in vivo*. The mRuby strain we have generated failed to retain fluorescence expression over time. The mMaroon1 strain allowed for good visualization of promastigotes, but did not allow for amastigote colocalization with acid vacuoles, probably due to its high acid sensitivity. The telLuc expressing strain emitted the highest levels of *in vitro* bioluminescence, and the double reporter strain expressing mCherry red fluorescence and firefly luciferase emitted both correct fluorescence and bioluminescence.

In summary, eFFly-mCherry and teLuc are both promising strains for reporters of *Leishmania in vitro*, and should be further investigated *in vivo*.

## **Introduction**

Leishmaniasis is an uncontrolled neglected tropical disease transmitted by the bite of infected phlebotomine sandflies. It is endemic in over 98 countries, putting 350 million people at risk of infection and leading to 70 000 to 1 million new cases each year, among which 20-30 000 deaths occur annually [1]. Over 20 species of *Leishmania* exist, and they are responsible for different clinical manifestations ranging from asymptomatic infections to severe disease [2]. Cutaneous Leishmaniasis (CL) is the most frequent symptomatic form of the disease, responsible for self-healing skin lesions. It can be conferred by *L. major*. Muco-Cutaneous Leishmaniasis (MCL) provokes severe lesions to the nose and mouth mucosa, leaving patients with severe disfiguration in progressed stages of the disease. It can be conferred by *L. braziliensis*. The most severe form is Visceral Leishmaniasis (VL) which localizes in the liver and spleen and leads to death in the absence of treatment. This form can be conferred by *L. donovani* or *L. infantum*.

Current treatments for visceral leishmaniasis present important drawbacks, including high cost, toxicity, need for invasive administration and long duration of treatments. This is making them difficult to follow-up in low-income countries and today, we observe the emergence of resistance towards all approved treatments [3].

In order to search for new treatments, multiple tools have been developed over the years, including reporter strains of *Leishmania* expressing fluorescence for *in vitro* follow-up and bioluminescence for *in vivo* experimentation. Obtaining reporter strains can be achieved either by transient or by stable transfection. Stable integration into the genome through homologous recombination enables long-term gene expression, but is more time-consuming compared to episomal transfection. Indeed, episomal transfection can be used for expressing a gene for a few generations and necessitates a simple prokaryotic plasmid with leishmanial Intergenic Regions (IRs) and flanking multiple cloning sites only [4]. While episomal transfection can be used for short *in vitro* experiments, *in vivo* monitoring requires stable

transfection to ensure that the reporter gene can still be expressed several months after infection. Nowadays, stable integration is facilitated by commercial *Leishmania* specific vectors such as pXG [5], p6,5 [6] and pLEXY [7]. Indeed, stable transfection of *Leishmania* parasites with different reporter genes has totally renewed *in vitro* or *in vivo* studies which follow up disease progression in mice [8,9]. These improved parasites have made it possible to search for new treatments by testing a greater number of new compounds [10,11]. Using reporter genes for *in vitro* and *in vivo* drug [12], high-throughput screening [13,14], whole-animal non-invasive imaging for parasites [12] and for the study of several aspects of host–parasite interactions have been realized. *Leishmania* parasites transformed with fluorescent or luminescent reporters have been used to understand relapse [15] and evaluate vaccine candidates [16]. Moreover, reporter genes have allowed to discover, *in vitro* and *in vivo*, new localizations of *Leishmania* parasites like in the thymus [17].

In most cases, transfected parasites express only a fluorescent or bioluminescent reporter. Fluorescent parasites are usually limited to *in vitro* applications due to a high background noise *in vivo*. Even though some fluorescent constructions exist to bypass these problems, such as far-red shifted fluorescence and highly bright fluorochromes, *in vivo* use remains rare in the case of whole-animal imaging [18]. *In vitro* fluorescence can allow for parasite visualization and counting. Microscopy and flow cytometry remain good techniques to visualize fluorescent parasites under either promastigote or amastigote form. [19]. In order to compensate for this limited *in vivo* use, bioluminescent strains have proven to be most efficient. Bioluminescent reporter strains are based on the use of the couple Luciferase/Luciferin for detection. While Firefly luciferase is the most commonly used enzyme, a lot of brighter mutants were generated, like NanoLuc luciferase that is smaller in size and is optimized with different substrates [20].

In summary, both fluorescence and bioluminescence present important advantages for *in vitro* or *in vivo* experimentation, and a strain expressing both types of reporter genes could be used for a vast array of applications. Here, we propose the creation of different reporter constructs and their testing in *Leishmania* parasites to obtain novel reporter strains. To perform long time follow up of the infection, we used stable transfection protocol to insert

fluorescent and bioluminescent reporter genes and have evaluated advantages and drawbacks of each construction.

## **Material and Methods**

### **Mice and ethics statement**

Six- to eight-week-old female BALB/c mice were purchased from Charles River (France). Mice were maintained and handled according to the regulations of the European Union, the French Ministry of Agriculture and to FELASA (the Federation of Laboratory Animal Science Associations) recommendations. Experiments were approved by the CIEPAL-Azur ethic committee n°28, France (Protocol number: 2020071719136396 ). Mice have been integrated into experiments after a minimum of one week of acclimatization.

### **Isolation of Murine Bone marrow derived macrophages**

Female Balb/c mice aged 8-12 weeks were euthanized. Bone marrow was extracted from femurs with 25G needles, passed on filters and washed in RPMI medium 1640® (Invitrogen GIBCO®). Monocytes were then differentiated to macrophages on non-cell culture treated Petri dishes at 37°C for 6 days in BMDM medium (RPMI medium 1640® supplemented with 10% fetal calf serum and 1% Penicillin-streptomycin), in the presence of 100 ng/ml mouse M-CSF (Miltenyi Biotec). To detach macrophages, petri dishes were incubated at 37°C with PBS-EDTA (5mM) during 15 minutes, and macrophages were washed and counted in KOVA® Glasstic® Slide 10 (KOVA International).

### **Promastigote culture**

*L. infantum* promastigotes were obtained from a patient with visceral leishmaniasis acquired in the south of France, strain MON-1 (MHOM/FR/18/LPN432). *L. major* parasites have been collected on a Tunisian patient (MHOM/TU/17/LPN418). Promastigotes were grown at 26°C at pH 7.2, in Complete Schneider's medium (Schneider's Insect Medium, Sigma-Aldrich),

supplemented with 10% fetal calf serum (Biowest), 2% male human urine, 1% L-glutamine (Gibco), 1% HEPES and 1% Penicillin-streptomycin (Gibco). Passages were performed every 3 to 4 days when cultures reached late log-phase.

### **Generation of reporter gene constructs**

Expression vectors pLEXY hyg2.1 (EGE-272) and pLEXY neo2.1 (EGE-273) were purchased from Jena Bioscience. Plasmids containing the inserts of interest were purchased from Addgene. mRuby-H2B-6, pcDNA3.1-mMaroon1, pcDNA3-teLuc c-myc, pCDH-EF1a-eFFly-mCherry were gifts from Michael Davidson (Addgene plasmid # 55866 ; <http://n2t.net/addgene:55866> ; RRID:Addgene\_55866) [21], Michael Lin (Addgene plasmid # 83840 ; <http://n2t.net/addgene:83840> ; RRID:Addgene\_83840) [22], Huiwang Ai (Addgene plasmid # 100026 ; <http://n2t.net/addgene:100026> ; RRID:Addgene\_100026) [23] and Irmela Jeremias (Addgene plasmid # 104833 ; <http://n2t.net/addgene:104833> ; RRID:Addgene\_104833) [24] respectively.

The coding regions for all inserts were amplified by PCR using primers bearing homology to both insert and vector that are consigned in Table 1. For amplification, we used 35 cycles of 98°C for 10 seconds, 55°C for 15 seconds, 72°C for 1 minute in a Techne TC-5000 pcr thermal cycler. The PCR products were migrated on a 1% agarose gel and the amplification of the inserts plus primers were purified with QIAquick PCR purification Kit, Qiagen®. *Leishmania* expression vector pLEXY hyg2.1 conferring resistance to HygromycinB (HygB) or pLEXY neo2.1 conferring resistance to Geneticin (G418) were digested with the appropriate restriction enzymes (Table 1), then the insert was cloned by Gibson Assembly In-Fusion (Takara Bio) into the expression vector. The obtained result was transformed into XL-10 gold thermocompetent bacteria and plated on ampicillin-containing agar overnight, then resistant colonies were isolated, amplified and DNA was obtained following extraction. Following linearization of the expression vector by Swa I restriction enzyme, the insert containing DNA coding for 18S RNA flanking the coding sequence for the inserts and resistance marker was inserted into the 18S RNA coding region of *Leishmania* promastigotes by electroporation.

Insert	Forward primer	Reverse primer	Insert size	Vector	Restriction enzyme
mMaroon1	ACCAGATCTGCCATGGATGGTGAG CAAGGGCGAGG	TACCCTTAAGGCTAGCTTACTTGTA CAGCTCGTCCATGCC	735 bp	pLEXSY-neo2.1	Nco I / Nhe I
mRuby	CCTTGCCACCAGATCTGATCCACCG GTCGCCACC	AGGAGGAGGGCGGCCCTTACC CTCCGCCAGGC	681 bp	pLEXSY-neo2.1	Bgl II / Not I
teLuc	ACCAGATCTGCCATGGTGCCGCCA CCATGGTCTT	TACCCTTAAGGCTAGCATGCATGC TCGAGTTACAGATCCT	555 bp	pLEXSY-hyg2.1	Nco I / Nhe I
eFFly-mCherry	CTTGCCACCAGATCTATGGAAGAT GCCAAGAACATCAAG	GGCATGGACGAGCTGTACAAGTA AGGTACCCACCACCATCACCA	2427 bp	pLEXSY-hyg2.1	Bgl II / Kpn I

**Table 1 : Primers and restriction enzymes used to amplify inserts and linearize expression vectors for *Leishmania* reporter strains**

### Electroporation into *L. infantum* promastigotes

*L. infantum* promastigotes in exponential growth phase were suspended at  $1 \times 10^8$  parasites/mL in Electroporation Buffer (HEPES 21mM, NaCl 137mM, KCl 5mM, Na<sub>2</sub>HPO<sub>4</sub> 0,7mM and Glucose 6mM).

Transfections were performed by electroporation (Gene Pulser X cell System, Biorad) using 3 µg of DNA for  $1 \times 10^7$  promastigotes in 2mm cuvettes, 25 µF, 1.6 kV.

### Electroporation into *L. major* promastigotes

*L. major* promastigotes in exponential growth phase were transfected using the “Parasite” kit (Lonza) on an Amaxa – Nucleofactor 2b (Lonza) by electroporation following program X-001. Transfections were performed in 2mm cuvettes (100µl) using 10 µg of DNA for  $1 \times 10^7$  promastigotes in Nucleofactor® Solution.

### Selection of transformed *Leishmania* clones

Following electroporation, parasites were cultured in Complete Schneider’s medium for 2 days without antibiotics, followed by 1 week of culture under appropriate selection pressure (Hygromycin B or Geneticin), then limiting dilutions were performed under 100 µg/mL selection pressure starting at 30 parasites per well. To isolate unique clones, the last well containing promastigotes 15 days after the initial inoculation were selected. After collection and expansion of single colonies, cultures were aliquoted and frozen at -150°C in 90% fetal calf serum, 10% DMSO until use.

### ***In vitro* infection of macrophages**

Macrophages were seeded at a concentration of  $4 \times 10^4$  cells/well or  $4 \times 10^5$  cells/well for 96 or 12 well plates respectively. 4-day old *L. infantum* promastigote cultures were used for infection at different Multiplicities Of Infection (MOI) overnight. Plates were then washed twice with PBS to eliminate excess promastigotes in culture media and incubated in BMDM Medium at 37°C for 24h to 72h.

### **Microscopy visualization and staining**

Microscopy images were acquired on Nikon Confocal A1R Microscope with a 60x/oil magnification. Actin was labeled with Phalloidin-iFluor 488 reagent (Abcam, ab 176753) for lysotracker experiments, and Phalloidin-iFluor 647 reagent (Abcam, ad 176759) for amastigote visualization experiments, and used at 1/5000<sup>e</sup>. LysoTracker Deep Red (Invitrogen, L12492) was used following supplier's recommendations, at 1/2000<sup>e</sup>. Hoechst (fisher scientific) was used at 1/400<sup>e</sup>.

### **Characterization of the newly generated reporter strains**

At late log phase, parasites were counted and seeded in culture flasks in Complete Schneider's medium at a concentration of  $1 \times 10^6$  parasites/ml. Cultures were then left to grow for 11 days, and Flow Cytometry was performed every day for 4 days, then on day 8 and 11. Briefly, parasites were resuspended in 500  $\mu$ l of PBS, and DAPI (Sigma) was added to stain dead cells prior to analysis. Data was analyzed by MACSQuantify™ analysis software (version 2.13.0), and count/ml, percentage of Dapi+ dead cells, percentage and Mean Fluorescence Intensity (MFI) of mCherry<sup>+</sup> cells and mMaroon1<sup>+</sup> were reported. After assessing concentration of parasites,  $1 \times 10^6$  parasites were resuspended in PBS, and bioluminescent kinetics were determined after addition of Luciferin (20  $\mu$ l per 100  $\mu$ l, 30 mg/ml) or DTZ (10  $\mu$ l per 100  $\mu$ l, 3mM) with the Synergy2 Microplate Reader (BioTek).



## **Results**

### **Generation of reporter constructs for *Leishmania***

In order to obtain a strain expressing the selected reporter genes, we have generated a construction in an integrative constitutive expression vector pLEXY (Fig 1). This vector contains a bacterial backbone conferring resistance to the antibiotic Ampicillin (Amp<sup>R</sup>) that allows for bacterial selection. The eucaryotic region contains a multiple cloning site, and a resistance marker either to Hygromycin B or Geneticin antibiotic (Atb<sup>R</sup>) inserted between two homologous regions to 18S RNA of *Leishmania* (5'ssu and 3'ssu). After transformation of the different constructs consigned in table 2, we have evaluated the success of the transformation into *Leishmania* parasites. Following culture under the appropriate antibiotic depending on the construct (Hygromycin B or Geneticin), we have selected a number of clones from the limiting dilution technique.

For mRuby, we obtained 8 clones, with 4 clones showing a correct growth rate. Among these 4 clones, 2 were not fluorescent. For mMaroon1, we isolated 10 clones, all showing far-red fluorescence. Only 1 clone showed impaired growth. For teLuc, we isolated 21 clones, among which 4 clones showed growth defects. Rapid testing showed the 17 remaining clones were bioluminescent. 8 clones were selected for further testing, and we retained the most bioluminescent clone. For teLuc-mMaroon1 we used the most bioluminescent clone from the teLuc selections above. Among the 10 clones obtained after second transfection, all showed far-red fluorescence, but none showed emission of bioluminescence. Thus, we did not manage to obtain this double fluorescent and bioluminescent strain. Finally, 8 clones were selected after eFFly-mCherry *L. infantum* transformation, 5 of them showed correct growth rates. Every single isolated clone showed emission of red fluorescence and bioluminescence. For eFFly-mCherry *L. major*, 8 clones were obtained. We selected the 2 best growing clones, that were also fluorescent.

The best performing clones in terms of fluorescence intensity and bioluminescence emission were next used to characterize the newly transformed strains.

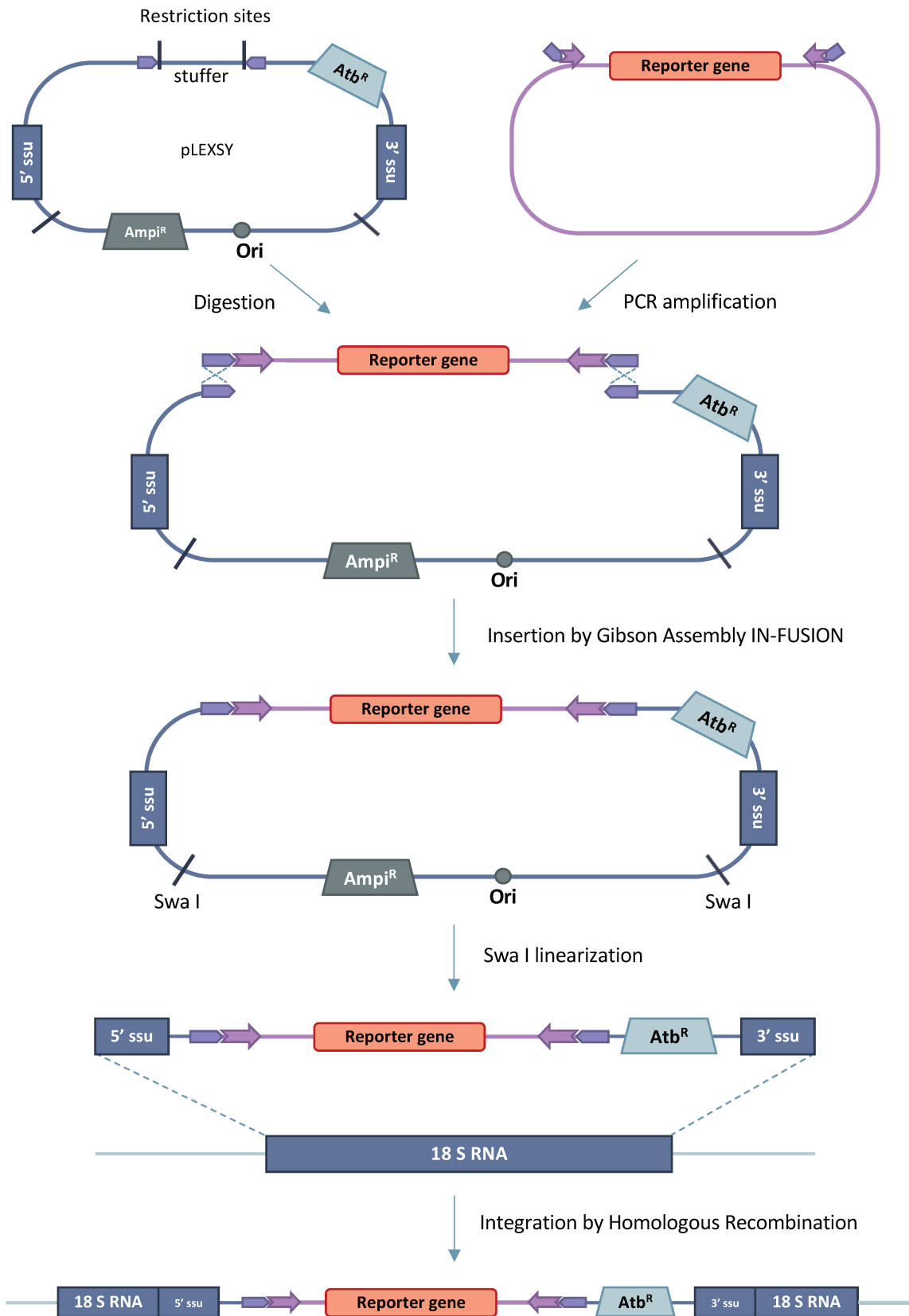


Figure 1 : Schematic illustration of *Leishmania* reporter genes construction steps

	Reporter gene	Description	<i>Leishmania</i> expression vector	<i>Leishmania</i> strains
Fluorescence	mRuby	Red Fluorescence	pLEXSY-neo-2.1	<i>L. infantum</i>
	mMaroon1	Far red Fluorescence		
Bioluminescence	teLuc	Enhanced Bioluminescence	pLEXSY-hyg-2.1	
Double	teLuc-mMaroon1	Far red Fluorescence and enhanced Bioluminescence	pLEXSY-hyg-2.1 and pLEXSY-neo-2.1	<i>L. infantum, L. major</i>
	eFFly-mCherry	Red Fluorescence and Bioluminescence	pLEXSY-hyg-2.1	

**Table 2 : Table of generated *Leishmania* reporter strains**

### **Insertion of fluorescent reporter genes allows for rapid verification of transfection success**

The transformation of *Leishmania* with the fluorescent reporter genes allowed for easy visual detection of the fluorescent protein inside parasites. Confocal microscopy showed that mMaroon1, mRuby and mCherry were correctly expressed in transfected parasites (Fig 2). However, if mCherry and mMaroon1 expression was stable inside a culture under antibiotic selection marker, the mRuby strains completely lost fluorescence despite the antibiotic over the course of 28 days, suggesting this fluorescent protein is unusable as a stably transfected reporter gene (Fig 3). Moreover, the intensity of the signal led to important overlap in other channels.

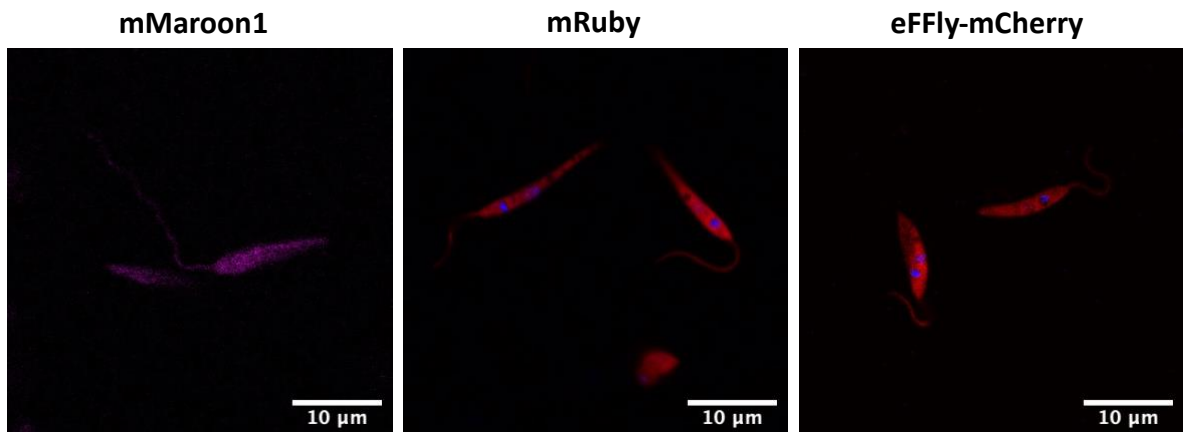


**Figure 2 : Confocal microscopy on *Leishmania infantum* promastigotes expressing fluorescent reporter genes**

The nuclei of *L. infantum* mMaroon1, mRuby and eFFly-mCherry strains were stained with Hoechst and appear in blue.

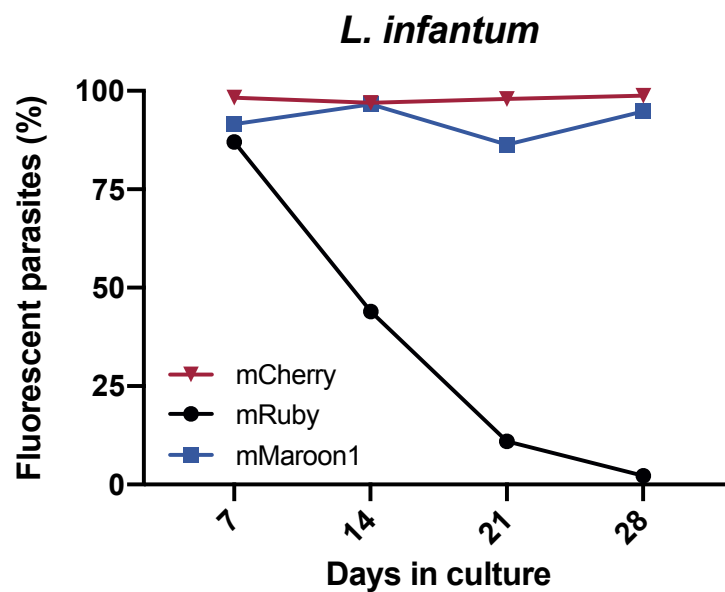


**Figure 3 : Follow-up of fluorescence in *L. infantum* promastigote culture**

Fluorescence percentage in cultures was assessed once a week in transformed cultures with mCherry, mRuby and mMaroon1 by flow cytometry.

**Insertion of reporter genes in *Leishmania* parasites does not alter growth or death, and leads to stable fluorescence or bioluminescence expression.**

In order to assess whether or not transfection with reporter genes altered growth or death in transformed *Leishmania* parasites, concentration and mortality were assessed over the course of 11 days in a WT *Leishmania* culture or in the transformed culture. Flow cytometry follow-up demonstrated eFFly-mCherry insertion did not alter growth or mortality in *L. infantum* (Fig 4A) or *L. major* (Fig 4B) cultures. Cultures transformed with teLuc (Fig 4C) or mMaroon1 (Fig 4D) showed a similar profile in growth and mortality, suggesting reporter gene insertion was not unfavorable for parasite growth and survival. Fluorescence was stably detected in promastigote cultures for the first 3 days, and decreased as mortality increased in eFFly-mCherry *L. infantum* (Fig 4E), *L. major* (Fig 4F) and mMaroon1 (Fig 4H). In eFFly-mCherry constructs, bioluminescence emission was fairly stable for the first 4 days, with culminating values at day 2, then decreased in a similar fashion as fluorescence both in *L. infantum* (Fig 4E) and in *L. major* (Fig 4F), suggesting eFFly-mCherry is a good reporter construct to visualize parasite death by the intermediate of either fluorescence or bioluminescence. In the case of teLuc, bioluminescence emission peaked higher even at lower parasite concentrations ( $1 \times 10^5$  parasites were tested in the case of teLuc, versus  $1 \times 10^6$  in the case of eFFly-mCherry to avoid signal overflow), with a peak emission at day 2, but bioluminescence values dropped faster than in the case of eFFly expressing cultures (Fig 4G). These results were compared to two existent *L. infantum* strains previously generated by Michel *et al.* [9], GFP and Luc *L. infantum* which showed similar results in growth, fluorescence and bioluminescence profiles (Supplemental Fig 1).

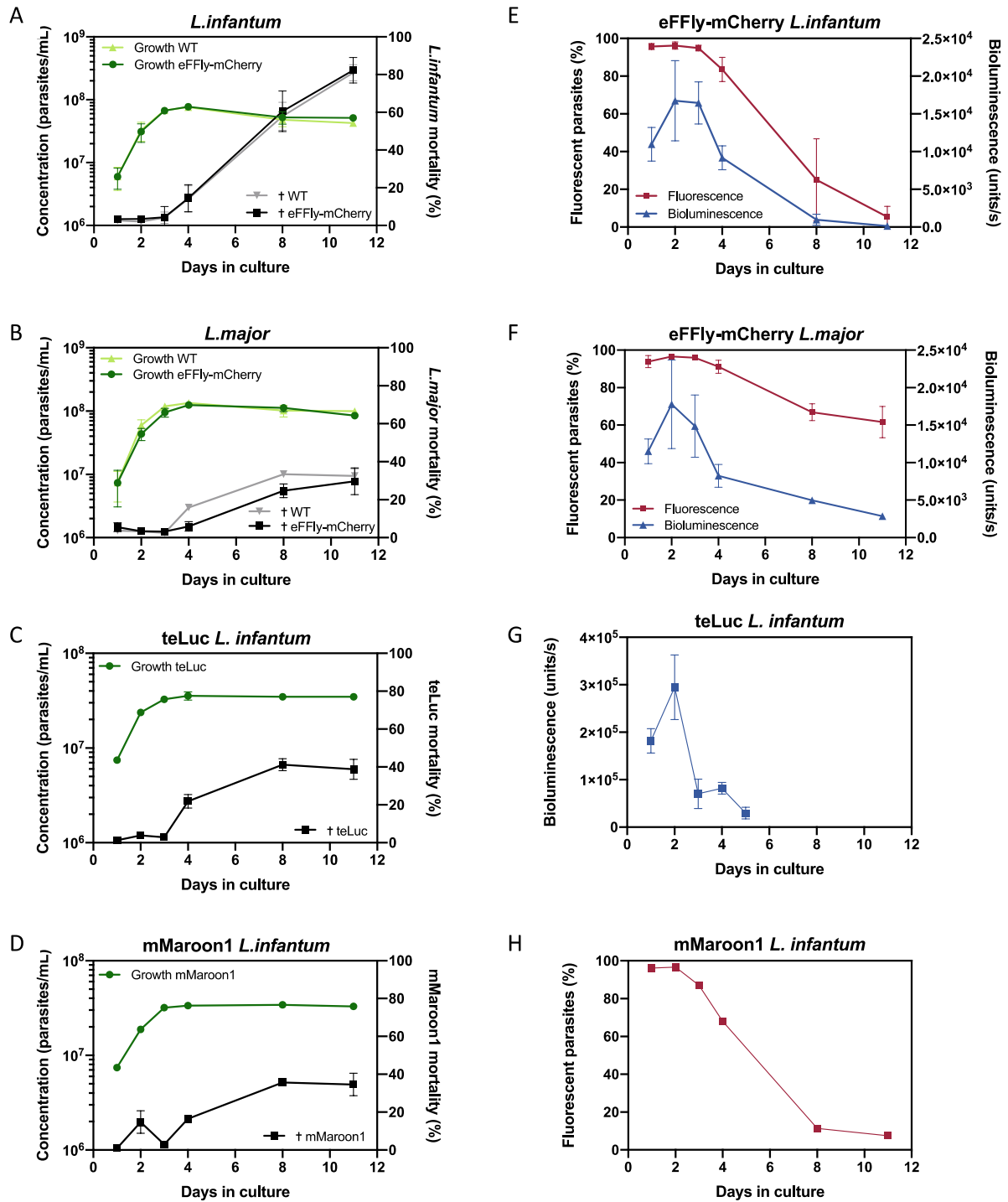


**Figure 4 : *In vitro* characterization of the *L. infantum* and *L. major* strains**

Following dilution to  $1 \times 10^6$  parasites/mL, we followed up promastigote cultures for 11 days by Flow Cytometry to assess growth curves and parasite mortality after DAPI staining of both WT and eFFly-mCherry *L. infantum* (A), and *L. major* (B), *teLuc L. infantum* (C) and *mMaroon1 L. infantum* strains (D). Emission of fluorescence over time was assessed by counting the percentage of fluorescent cells in culture among counted events by flow cytometry, and emission of bioluminescence over time was assessed by measuring photon emission of  $1 \times 10^6$  parasites after addition of luciferin in eFFly-mCherry *L. infantum* (E) or eFFly-mCherry *L. major* (F), or of  $1 \times 10^5$  parasites after DTZ addition in *teLuc L. infantum* (G). Fluorescence in *mMaroon1 L. infantum* was also assessed (H).

**Bioluminescence emission of reporter strains were strongly correlated to the quantity of parasites *in vitro***

We have also confirmed that concentration of parasites could be strongly correlated with an  $R^2$  superior or equal to 0.98 to bioluminescence emission in promastigote cultures, in teLuc *L. infantum* (Fig 5B) eFFly-mCherry *L. infantum* (Fig 5C) and eFFly-mCherry *L. major* (Fig 5D). At an equal quantity of  $10^6$  parasites, teLuc expressing promastigotes were 59 times more bioluminescent than eFFly-mCherry *L. infantum* (teLuc =  $355 \times 10^6$  ph/s/cm<sup>2</sup>/sr ; eFFly-mCherry =  $6 \times 10^6$  ph/s/cm<sup>2</sup>/sr) (Fig 5A). As a reference, we have included data on the previously generated Luc *L. infantum* strain. teLuc expressing promastigotes were 47 times more bioluminescent than Luc expressing parasites (Luc =  $7,5 \times 10^6$  ph/s/cm<sup>2</sup>/sr) (Supplemental Fig 3).

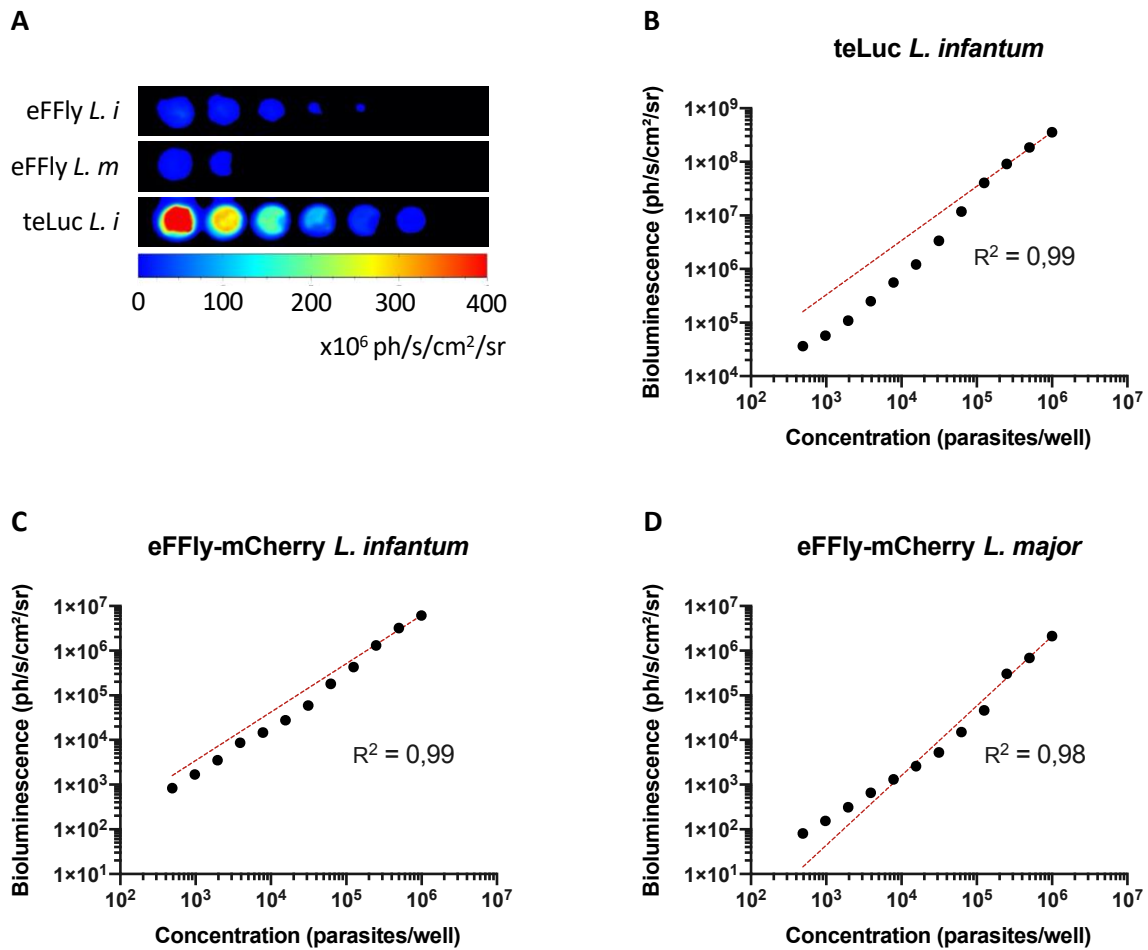


**Figure 5 : *in vitro* correlation between bioluminescence emission and concentration of *L. infantum* eFFly-mCherry, *L. major* eFFly-mCherry and *L. infantum* teLuc**

**(A)** Image of Bioluminescence emission of serially diluted bioluminescence-expressing parasites after addition of Luciferin or DTZ substrate

**(B-D)** Correlation between concentration and bioluminescence emission of promastigotes was assessed by serially diluting *L. infantum* teLUC **(B)**, *L. infantum* eFFly-mCherry **(C)**, or *L. major* eFFly-mCherry **(D)** starting with  $1 \times 10^6$  parasites.  $R^2$  represents the linear regression analysis. All values of fluorescence and bioluminescence are normalized to WT background emission.

### Transfected parasites are able to infect macrophages and are visible in fluorescence microscopy

We have verified that the mCherry and mMaroon1 fluorophores were sufficiently expressed to be visible both in the extracellular and intracellular form of *Leishmania* parasites. Confocal



microscopy on BMDM cells infected with an MOI of 10, 24 hours post infection, showed intracellular parasites were visible inside the cells, suggesting eFFly-mCherry and mMaroon1 parasites can be used for both promastigote and amastigote visualization (Fig 6).

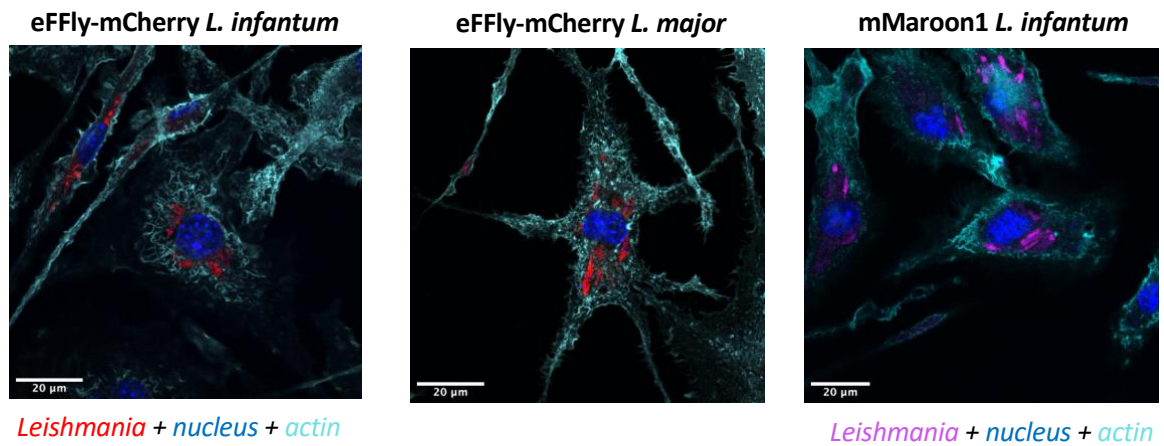


**Figure 6 : Confocal microscopy observation of eFFly-mCherry and mMaroon1 amastigotes**

*L. infantum* eFFly-mCherry, *L. major* eFFly-mCherry or *L. infantum* mMaroon1 amastigotes inside BMDM cells were stained with Hoechst and Phalloidin for BMDM cells, then observed by confocal microscopy.

Nuclei are stained in blue, actin is stained in cyan, and parasites emit either red (eFFly-mCherry) or far-red (mMaroon1) fluorescence.

### **Transfected parasites are able to penetrate into host cells and are located inside lysosome-fused vacuoles**

In order to verify if our newly transfected strains effectively localize inside phagocytic vacuoles, we stained infected BMDM cells with LysoTracker to observe lysosome-fused vacuoles and assess whether they colocalize with *L. infantum* parasites. Confocal microscopy revealed eFFly-mCherry *L. infantum* parasites inside BMDM cells, and showed that some of these intracellular parasites strongly colocalized with intense fluorescence emitted by LysoTracker staining, indeed confirming the localization of parasites inside acid parasitic vacuoles fused to lysosomes (Fig 7). mMaroon1 parasites were not visible in colocalization with lysosomes (data not shown).

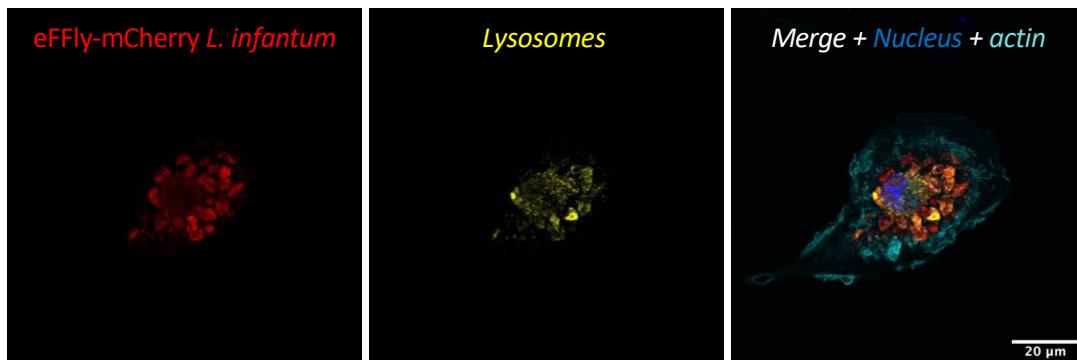


**Figure 7 : Confocal microscopy of *Leishmania* infected BMDM cells**

BMDM cells infected with eFFly-mCherry *L. infantum* parasites at an MOI of 10 for 24 hours. Images were taken by Confocal microscopy. Nuclei are stained with Hoechst and appear in blue, actin is stained with phalloidin and appears in cyan, lysosomes are stained with LysoTracker and appear yellow, and eFFly-mCherry *L. infantum* emit red fluorescence.

### **Reporter strains can be used for visualizing *in vitro* infection of host cells by fluorescence and bioluminescence**

Following evidence that the new reporter strain eFFly-mCherry *L. infantum* could penetrate inside host macrophages, we investigated the possibility of visualizing parasites inside macrophages by flow cytometry and with luciferase assay. Flow cytometry showed that eFFly-mCherry *L. infantum* allowed for visualization of differential infection between MOI 5, 10 and 20 (Fig 8A) with an increase in percentage of infected cells as MOI increased. Median of fluorescence can here be correlated to the quantity of parasites inside cells, and we can observe an increase in median of fluorescence for both reporter strains (Fig 8B) suggesting that both percentage of infected cells and number of parasites per cell increase with the MOI. This was confirmed by bioluminescence after addition of luciferin (Fig 8C) with a similar increase in emitted signal dependent on MOI, that was also seen after addition of substrate DTZ to teLuc expressing *L. infantum* (Fig 8D). Newly transformed strains performed as well as previously generated reporter strains GFP and Luc *L. infantum* (Supplemental Fig 2).

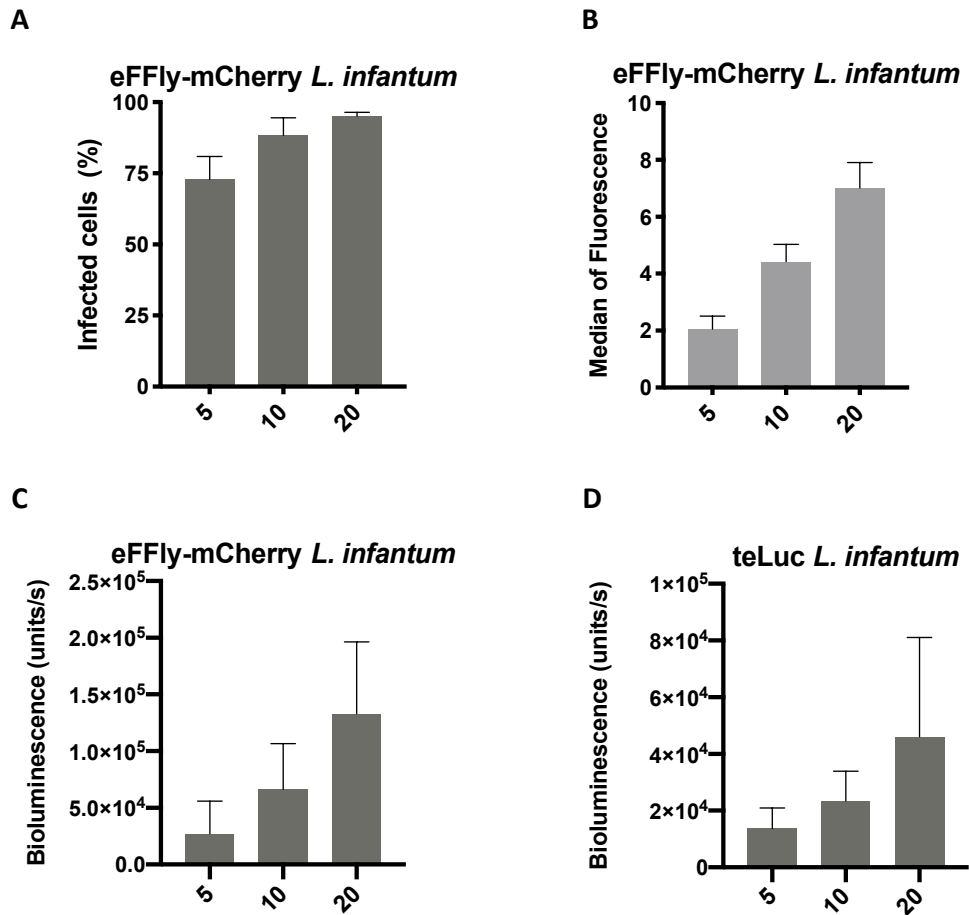


**Figure 8 : *In vitro* characterization of *L. infantum* eFFly-mCherry amastigotes**

Percentage of infected BMDM cells after 24h of infection at MOI 5 to 20 with eFFly-mCherry *L. infantum* as assessed by flow cytometry (A). Median of Fluorescence was quantified on infected cells, and represents an idea of the number of parasites per cell (B). Bioluminescence of eFFly-mCherry (C) or teLuc (D) inside BMDM cells in the same conditions of infection was measured after addition of luciferin substrate. Bioluminescence was acquired on Synergy Biotek machine with a gain of 255 for eFFly-mCherry amastigotes, and a gain of 135 for teLuc amastigotes to avoid signal overflow, hence the lower bioluminescent signal in teLuc parasites even though they are brighter than eFFly-mCherry parasites.

## Discussion

Reporter genes have revolutionized the study of disease progression in the case of leishmaniasis by offering time-saving, high sensitivity and high resolution tools for localization studies, longitudinal evolution of the disease as well as high throughput drug screening. The use of fluorescent markers has allowed the use of a vast array of techniques on *Leishmania*, such as cytometry [25], microscopy, *ex vivo* studies [26], and visualization inside infected sandflies [27]. Even though it is commonly limited to *in vitro* use, fluorescent markers can be used in the follow-up of cutaneous forms of leishmaniasis *in vivo* [28], and can also be tracked in deep-tissue with intravital imaging in mice [29].

In this article, we describe the generation of a number of different constructs, taking advantage of the pLEXSY configurations that allow for insertion into more than one *Leishmania* species, and from the IN-FUSION technique that allows for easy primer design and insert choice. Table 3 sums up the advantages and drawbacks of every strain that was generated for use in *Leishmania*.

	Reporter gene	Leishmania strains	Advantages	Drawbacks
Fluorescence	mRuby	<i>L. infantum</i>	High brightness (39,2), low sensitivity to pH (pKa=4,4)	Loses fluorescence expression even under antibiotic selection. High brightness leads to signal overlap
	mMaroon1		Far red fluorescence has low background noise in cells	Low brightness (8.8), sensitive to pH (pKa=6,2) rendering imaging complicated in amastigote form
Bioluminescence	teLuc		Brighter <i>in vitro</i> than Firefly luciferase	Unstable substrate with solubility issues. Expensive chemical substrate
Double	eFFly-mCherry	<i>L. infantum</i> , <i>L. major</i>	Low sensitivity to pH (pKa=4,5), double reporter genes allowing for <i>in vitro</i> and possible <i>in vivo</i> use	Medium brightness (15,4)

**Table 3 : Table of obtained *Leishmania* reporter strains with their advantages and drawbacks**

The mMaroon1 construct allowed for Far red fluorescence emission, that led to low background noise in cells, but with low brightness and high pH sensitivity. This construct was efficient in promastigotes, but signal was very faint inside host cells after infection, and was unobservable after 48 hours. Even though the pLEXSY configurations integrate DNA inside 18S

RNA coding regions, that should not be expressed differently between stages, we have observed an overall decrease in fluorescence in every fluorescent strain with amastigote transformation. Loss of signal could be due to the low brightness of mMaroon1, but is most likely to be due to this protein's sensitivity to acid. Indeed, pKa of mMaroon1 protein was of 6.2, meaning half the fluorescence intensity was lost at a pH 6.2. Seeing as *Leishmania* parasites colocalize with lysosomes, it is possible that fluorescence was lost due to the inherent properties of this fluorophore.

The mRuby red fluorescent protein compensated this pKa problem (pKa = 4.4) with very low pH sensitivity and high brightness. However, despite the choice of a configuration that allowed stable insertion by targeting 18S RNA, mRuby red fluorescence was lost over time even in the presence of antibiotic selection pressure in Geneticin (G418), contrary to the other fluorescent strains, that maintained fluorescence expression for at least 10 passages *in vitro*. Further investigation should be performed in order to verify if mRuby was really inserted into 18S RNA coding regions by sequencing, or if it was inserted then lost over time. Another explanation would be a lower expression of the protein by the parasite, which would explain why parasites retain resistance to G418 but lose red fluorescence.

While fluorescence can be a good reporter for a vast array of studies, some drug screenings can face the problem of interference of fluorescence with molecular structures such as flavanol aglycones, rendering screening by fluorescence difficult [28]. In this case, the use of another reporter gene such as bioluminescence could help bypass these limitations.

Firefly luciferase is the most commonly used luciferase enzyme, but there are a number of alternatives such as *Renilla*, *Oplophorus* and *Gaussia* Luciferase that use analog substrates [30]. Other mutant proteins derived from these luciferases, such as NanoLuc and teLuc have been generated and allow emission of bioluminescence that is brighter, even though new substrates are not always ideal for *in vivo* applications [31]. We have used teLuc, a nanoLuc mutant with bright, red shifted bioluminescence emission after the addition of the DTZ substrate that should be up to 1 000 times more bioluminescent than regular Firefly luciferase with luciferin [23]. Although very high bioluminescence was indeed observed *in vitro*, the DTZ substrate appeared difficult to solubilize in most classically used solvents, and is very unstable once it is solubilized. This could be challenging for further applications such as *in vivo* use,

where incorrect solubilization could lead to incorrect dosage and the need for chemical solvents might not be suitable for *in vivo* applications.

In summary, both fluorescence and bioluminescent have their own sets of limitations, and are complementary techniques that can be used for long term follow-up of the same animal, up to precise localization inside cell types. Thus, the generalization of double reporter strains can allow for a diversity of techniques to be used with the same transformed strain. We have tried to obtain a strain expressing both fluorescence and bioluminescence by first transfecting pLEXSY-hyg2.1/teLuc and selecting a single clone expressing high levels of bioluminescence. We next performed a second transfection with pLEXSY-neo2.1/mMaroon1, and tried selecting double reporter strains. Unfortunately, parasites appeared to be fluorescent after transfection but did no longer emit bioluminescence after substrate addition, suggesting that a subsequent transformation can eject the first present insert. This should be confirmed by sequencing. The double transfection of two separate plasmids is a very time-consuming process, as it requires the selection of a single clone expressing the first reporter gene, then a second round of transfection and selection to obtain a double construct. Seeing the second transfection might lead to the loss of the first insertion, it should be considered to use two different expression vectors targeting different sequences as they are already available [5–7]. However, to avoid loss of inserts and save the time of a second round in selection, it can be possible to combine two sequences of interest in the same expression vector configuration, as we did with eFFly-mCherry, that was already commercially available. eFFly-mCherry showed both good fluorescence with low pH sensitivity and bioluminescence emission. It was visible both in promastigote and amastigote form, colocalized with acidic vacuoles and could be followed by flow cytometry and bioluminescence, allowing for a change in technique of detection should there be any fluorescent interference or limit of detection in bioluminescence emission.

## Conclusion

Finally, we have taken profit of the multiple tools that exist today to generate *Leishmania* reporter strains expressing bioluminescence, fluorescence or both. From all the generated strains, the fluorescent strain mRuby did not show a stable insertion allowing for fluorescent expression throughout passages. mMaroon1 appeared as a good reporter strain for promastigote follow-up but failed to resist to the acidic pH inside macrophages, thus limiting its application in amastigote monitoring and highlighting the importance of pKa verification. teluc showed increased bioluminescence emission *in vitro* and could be a good candidate for *in vivo* application, however in our hands the substrate DTZ appeared difficult to solubilize and would not be injectable to mice. The double reporter strain teluc-mMaroon1 highlighted the possibility of gene loss in the case of insertion with the same expression vector targeting the same regions, even if 18S RNA is a repeated region. Finally, eFFly-mCherry appears to be a good candidate for further *in vitro* testing, with sustained fluorescence and bioluminescence that is visible in both *L. infantum* and *L. major*.

## **Acknowledgments**

This work was supported by the Fondation pour la Recherche Médicale, grant number ECO201806006733, to A.M.

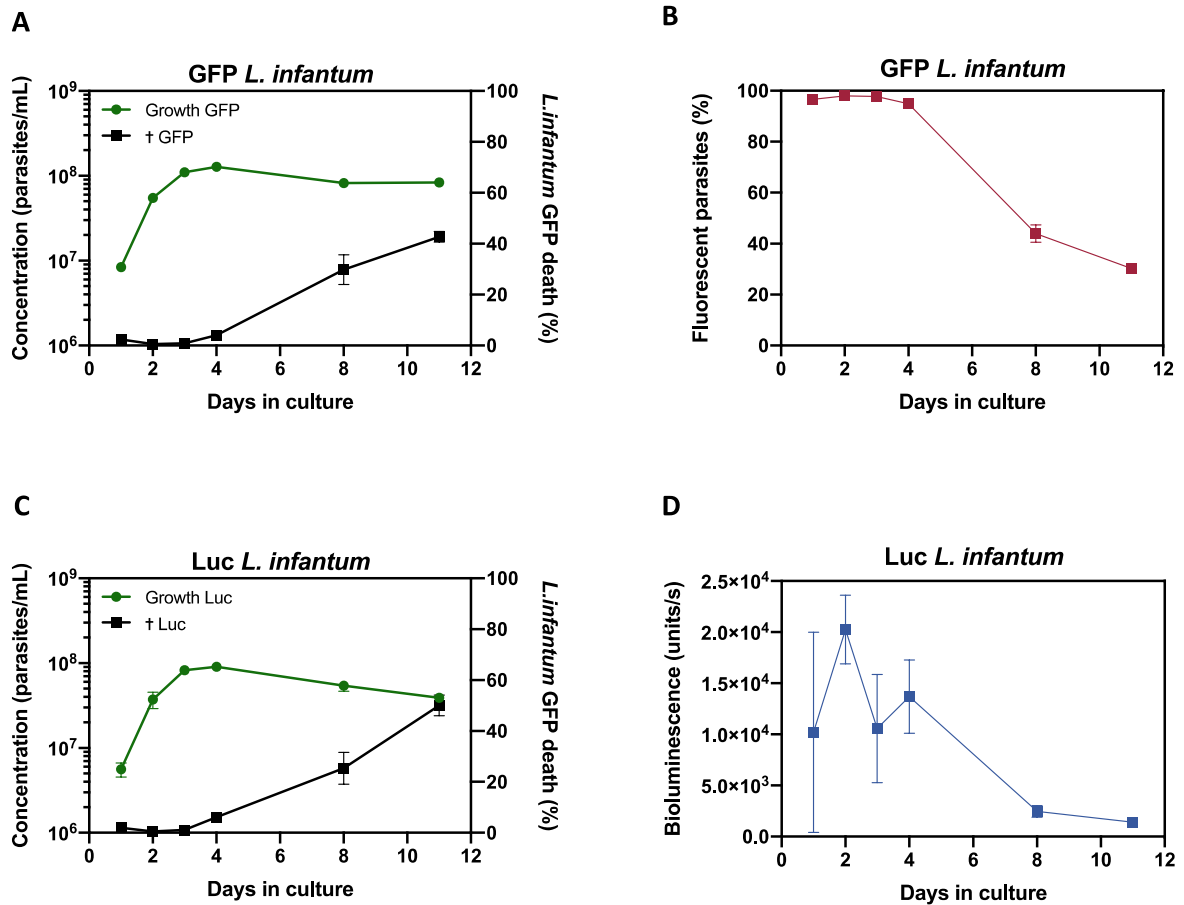
For flow cytometry, samples acquisition and data analysis were performed on the C3M Cytometry Core Facility financed by Conseil Général CG06 and Conseil Régional PACA.

We would like to thank Dr Thomas LAMONERIE (iBV - Neurodevelopment : Temporal functions of transcription factors in mouse brain development) for allowing us to use the electroporator.

We sincerely thank the GIS-IBISA multi-sites platform Microscopie Imagerie Côte d'Azur (MICA), and particularly the imaging site of C3M (INSERM U1065) supported by Conseil Régional, Conseil Départemental, and IBISA. The help of Marie Irondelle is acknowledged.

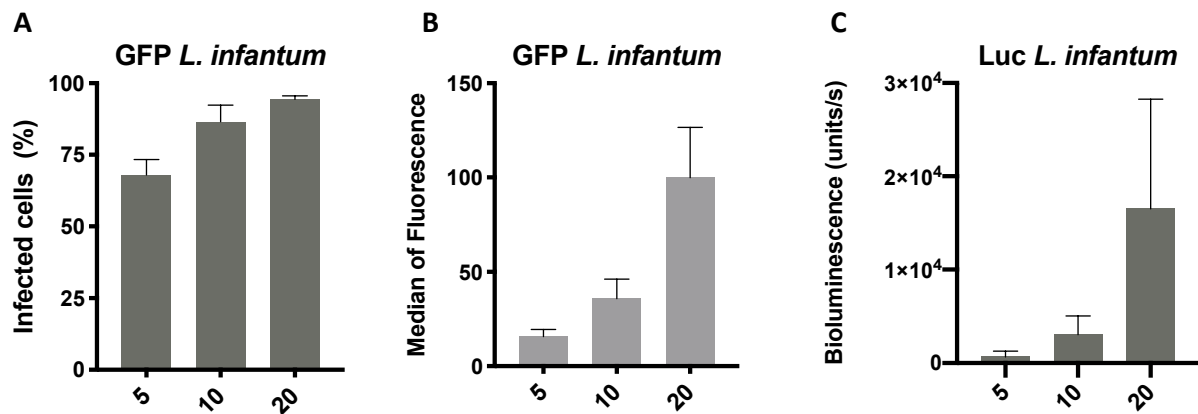


## Supplemental Material



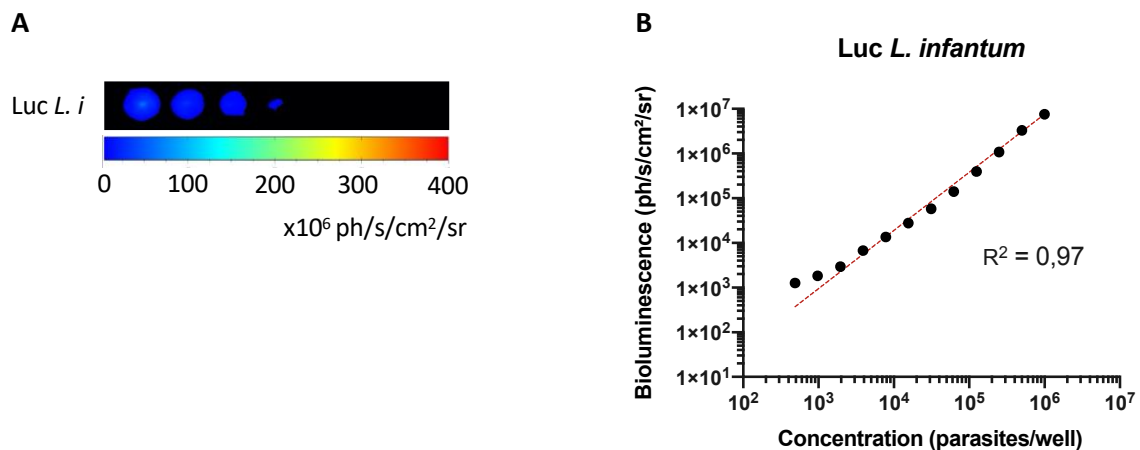
**Supplemental figure 1 : *In vitro* characterization of Luc and GFP *L. infantum* strains**

Following dilution to  $1 \times 10^6$  parasites/mL, we followed up promastigote cultures for 11 days by Flow Cytometry to assess growth curves and parasite mortality after DAPI staining of both GFP (**A**) and Luc (**C**) *L. infantum* strains. Emission of fluorescence over time was assessed by counting the percentage of fluorescent cells in culture among counted events by flow cytometry in GFP *L. infantum* (**B**). Emission of bioluminescence over time was assessed by measuring photon emission of  $1 \times 10^6$  parasites after addition of luciferin to Luc *L. infantum* (**D**).



**Supplemental figure 2 : *In vitro* characterization of the Luc and GFP *L. infantum* strains**

Percentage of infected BMDM cells after 24h of infection at MOI 1 to 20 with GFP *L. infantum* as assessed by flow cytometry **(A)**. Median of Fluorescence was quantified on infected cells, and represents an idea of the number of parasites per cell **(B)**. Bioluminescence of Luc *L. infantum* inside BMDM cells in the same conditions of infection was measured after addition of luciferin substrate **(C)**.



**Supplemental figure 3 : *in vitro* correlation between bioluminescence emission and concentration of Luc *L. infantum***

**(A)** Image of Bioluminescence emission of serially diluted bioluminescence-expressing parasites after addition of Luciferin substrate.

**(B)** Correlation between concentration and bioluminescence emission of promastigotes was assessed by serially diluting Luc *L. infantum* starting with  $1 \times 10^6$  parasites.  $R^2$  represents the linear regression analysis. All values of fluorescence and bioluminescence are normalized to WT background emission.

## References

1. WHO (2021) Leishmaniasis.
2. CDC (2020) Parasites - Leishmaniasis.
3. Ponte-Sucre A, Gamarro F, Dujardin JC, Barrett MP, López-Vélez R, García-Hernández R et al. (2017) Drug resistance and treatment failure in leishmaniasis: A 21st century challenge. *PLoS Negl Trop Dis* 11: e0006052.
4. Taheri T, Seyed N, Mizbani A, Rafati S (2016) *Leishmania*-based expression systems. *Appl Microbiol Biotechnol* 100: 7377-7385.
5. Vacas A, Sugden C, Velasco-Rodríguez Ó, Algarabel-Olona M, Peña-Guerrero J, Larrea E et al. (2017) Construction of Two mCherry Plasmids (pXG-mCherry) for Transgenic *Leishmania*: Valuable Tools for Future Molecular Analysis. *J Parasitol Res* 2017: 1964531.
6. Ertabaklar H, Çalışkan SÖ, Kolli B, Ertuğ S, Özbilgin A, Malatyali E et al. (2019) [Transfection of *Leishmania tropica* with green fluorescent protein (gfp) gene and investigation of the *in vitro* drug effect]. *Mikrobiyol Bul* 53: 213-223.
7. Majidiani H, Dalimi A, Ghaffarifard F, Pirestani M (2021) Multi-epitope vaccine expressed in *Leishmania tarentolae* confers protective immunity to *Toxoplasma gondii* in BALB/c mice. *Microb Pathog* 155: 104925.
8. Lang T, Goyard S, Lebastard M, Milon G (2005) Bioluminescent *Leishmania* expressing luciferase for rapid and high throughput screening of drugs acting on amastigote-harboring macrophages and for quantitative real-time monitoring of parasitism features in living mice. *Cell Microbiol* 7: 383-392.
9. Michel G, Ferrua B, Lang T, Maddugoda MP, Munro P, Pomares C et al. (2011) Luciferase-expressing *Leishmania infantum* allows the monitoring of amastigote population size, *in vivo*, *ex vivo* and *in vitro*. *PLoS Negl Trop Dis* 5: e1323.
10. Caridha D, Leed S, Cawfield A (2020) *In Vivo* Bioluminescent Monitoring of Parasites in BALB/c Mouse Models of Cutaneous Leishmaniasis Drug Discovery. *Methods Mol Biol* 2081: 81-106.
11. Caridha D, Parriot S, Hudson TH, Lang T, Ngundam F, Leed S et al. (2017) Use of Optical Imaging Technology in the Validation of a New, Rapid, Cost-Effective Drug Screen as Part of a Tiered *In Vivo* Screening Paradigm for Development of Drugs To Treat Cutaneous Leishmaniasis. *Antimicrob Agents Chemother* 61:
12. Agostino VS, Trinconi CM, Galuppo MK, Price H, Uliana SRB (2020) Evaluation of NanoLuc, RedLuc and Luc2 as bioluminescent reporters in a cutaneous leishmaniasis model. *Acta Trop* 206: 105444.
13. Vacchina P, Morales MA (2014) *In vitro* screening test using *Leishmania* promastigotes stably expressing mCherry protein. *Antimicrob Agents Chemother* 58: 1825-1828.

14. Jaiswal AK, Rao KB, Kushwaha P, Rawat K, Modukuri RK, Khare P et al. (2016) Development of *Leishmania donovani* stably expressing DsRed for flow cytometry-based drug screening using chalcone thiazolyl-hydrazone as a new antileishmanial target. *Int J Antimicrob Agents* 48: 695-702.
15. Álvarez-Velilla R, Gutiérrez-Corbo MDC, Punzón C, Pérez-Pertejo MY, Balaña-Fouce R, Fresno M et al. (2019) A chronic bioluminescent model of experimental visceral leishmaniasis for accelerating drug discovery. *PLoS Negl Trop Dis* 13: e0007133.
16. Ong HB, Clare S, Roberts AJ, Wilson ME, Wright GJ (2020) Establishment, optimisation and quantitation of a bioluminescent murine infection model of visceral leishmaniasis for systematic vaccine screening. *Sci Rep* 10: 4689.
17. Domínguez-Asenjo B, Gutiérrez-Corbo C, Pérez-Pertejo Y, Iborra S, Balaña-Fouce R, Reguera RM (2021) Bioluminescent Imaging Identifies Thymus, As Overlooked Colonized Organ, in a Chronic Model of *Leishmania donovani* Mouse Visceral Leishmaniasis. *ACS Infect Dis* 7: 871-883.
18. Li C, Tebo AG, Thauvin M, Plamont MA, Volovitch M, Morin X et al. (2020) A Far-Red Emitting Fluorescent Chemogenetic Reporter for *In Vivo* Molecular Imaging. *Angew Chem Int Ed Engl* 59: 17917-17923.
19. Dube A, Gupta R, Singh N (2009) Reporter genes facilitating discovery of drugs targeting protozoan parasites. *Trends Parasitol* 25: 432-439.
20. Berry SL, Hameed H, Thomason A, Maciej-Hulme ML, Saif Abou-Akkada S, Horrocks P et al. (2018) Development of NanoLuc-PEST expressing *Leishmania mexicana* as a new drug discovery tool for axenic- and intramacrophage-based assays. *PLoS Negl Trop Dis* 12: e0006639.
21. Day RN, Davidson MW (2009) The fluorescent protein palette: tools for cellular imaging. *Chem Soc Rev* 38: 2887-2921.
22. Bajar BT, Lam AJ, Badiie RK, Oh YH, Chu J, Zhou XX et al. (2016) Fluorescent indicators for simultaneous reporting of all four cell cycle phases. *Nat Methods* 13: 993-996.
23. Yeh HW, Karmach O, Ji A, Carter D, Martins-Green MM, Ai HW (2017) Red-shifted luciferase-luciferin pairs for enhanced bioluminescence imaging. *Nat Methods* 14: 971-974.
24. Ebinger S, Özdemir EZ, Ziegenhain C, Tiedt S, Castro Alves C, Grunert M et al. (2016) Characterization of Rare, Dormant, and Therapy-Resistant Cells in Acute Lymphoblastic Leukemia. *Cancer Cell* 30: 849-862.
25. Islek Z, Ucisik MH, Sahin F (2021) Novel dual-fluorescent flow cytometric approach for quantification of macrophages infected with *Leishmania infantum* parasites. *Parasitology* 1-7.
26. Domínguez-Asenjo B, Gutiérrez-Corbo C, Álvarez-Bardón M, Pérez-Pertejo Y, Balaña-Fouce R, Reguera RM (2021) *Ex Vivo* Phenotypic Screening of Two Small Repurposing

- Drug Collections Identifies Nifuratel as a Potential New Treatment against Visceral and Cutaneous Leishmaniasis. *ACS Infect Dis* 7: 2390-2401.
27. Diaz-Albiter HM, Regnault C, Alpizar-Sosa EA, McGuinness D, Barrett M, Dillon RJ (2018) Non-invasive visualisation and identification of fluorescent *Leishmania tarentolae* in infected sand flies. *Wellcome Open Res* 3: 160.
  28. Haghdoost S, Azizi M, Haji Molla Hoseini M, Bandehpour M, Mohseni Masooleh M, Yeganeh F (2020) Parasite Burden Measurement in the *Leishmania major* Infected Mice by Using the Direct Fluorescent Microscopy, Limiting Dilution Assay, and Real-Time PCR Analysis. *Iran J Parasitol* 15: 576-586.
  29. Zayats R, Uzonna JE, Murooka TT (2021) Visualizing the *In Vivo* Dynamics of Anti-*Leishmania* Immunity: Discoveries and Challenges. *Front Immunol* 12: 671582.
  30. Kirkpatrick A, Xu T, Ripp S, Sayler G, Close D (2019) Biotechnological advances in luciferase enzymes. editors. *Bioluminescence-Analytical Applications and Basic Biology*. IntechOpen.
  31. England CG, Ehlerding EB, Cai W (2016) NanoLuc: A Small Luciferase Is Brightening Up the Field of Bioluminescence. *Bioconjug Chem* 27: 1175-1187.

## Travaux complémentaires à l'étude des souches rapportrices de *Leishmania*

En parallèle de ces travaux, nous avons aussi transfecté des souches de *L. tarentolae*, une espèce trouvée chez le lézard qui n'est pas pathogène pour l'homme.

La vérification de la croissance après transfection a montré que l'insertion du transgène n'a eu aucun effet sur la pousse des parasites. La souche émettait la plus haute bioluminescence au jour 2 de la croissance, comme ce qui avait été observé pour les souches de *L. infantum* et *L. major* (Fig 7).

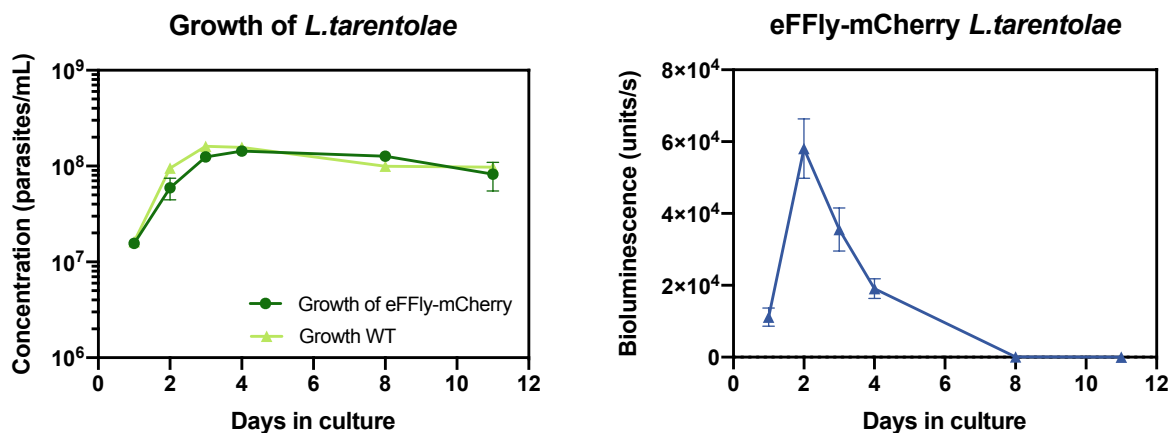


**Figure 7** : Croissance, mortalité et émission de bioluminescence de *L. tarentolae* WT et eFFly-mCherry. A gauche, croissance et mortalité d'une souche de *L. tarentolae* WT et transformée eFFly-mCherry. A droite, émission de bioluminescence de la souche de *L. tarentolae* eFFly-mCherry.

Les parasites *L. tarentolae* sont bien rouges en visualisation en microscopie, et émettent une fluorescence homogène dans la cellule (Fig 8).

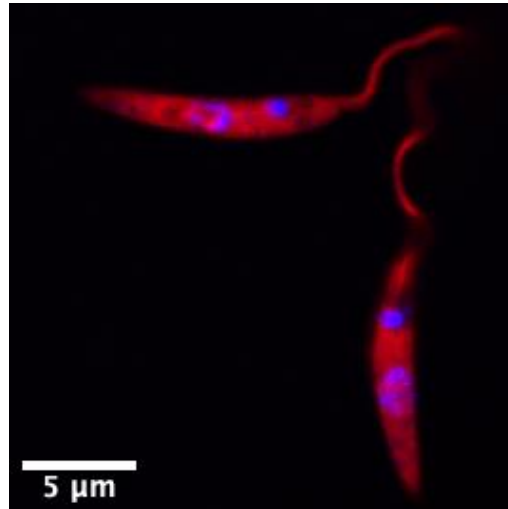


**Figure 8** : Promastigotes *L. tarentolae-eFFly-mCherry* en microscopie confocale.  
En rouge, le parasite, en bleu l'ADN marqué au Hoechst.

#### *Tests in vivo de la souche teLuc L. infantum*

Des essais *in vivo* avec la souche teLuc *L. infantum* ont été réalisés sur des souris Balb/c. Après injection dans la veine caudale de  $3 \times 10^6$ ,  $3 \times 10^7$ , ou  $3 \times 10^8$  leishmanies, les souris ont été imagées au jour 7 puis 14 post infection après injection de 200  $\mu$ l de DTZ à 3mM. A l'imagerie *in vivo*, nous n'avons observé aucun signal au niveau du foie ni de la rate (résultats non présentés).

Quinze jours post infection, les souris ont été sacrifiées et les rates et foies ont été récupérés. Après extraction d'ADN, les charges parasitaires ont été quantifiées dans les deux organes cibles et ont révélé que les souris étaient bien infectées avec des leishmanies, même si aucun signal n'était visible en imagerie *in vivo* après injection du substrat (Fig 9).

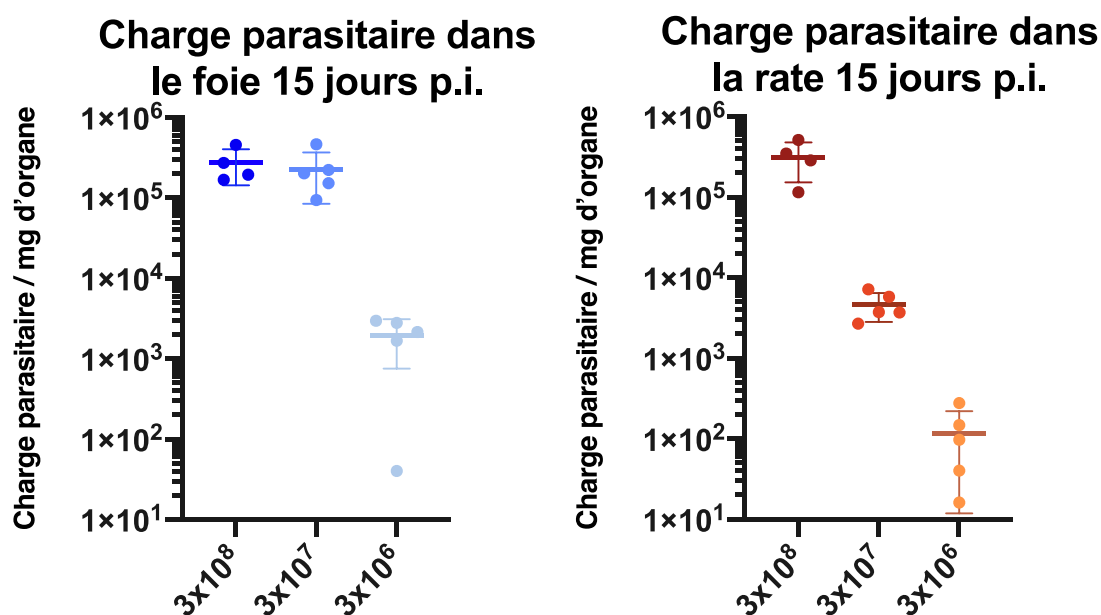


Figure 9 : Quantification par qPCR de la charge parasitaire dans le foie et la rate de souris infectées. L'infection a été réalisée 15 jours auparavant avec des quantités de leishmanies variables.

#### Tests *in vivo* de la souche eFFly-mCherry *L. infantum*

La souche double rapportrice eFFly-mCherry, caractérisée précédemment a également été injectée à des souris Balb/c. Afin de pouvoir mieux caractériser la souche eFFly-mCherry, nous l'avons comparée avec la souche Luc disponible au laboratoire. Nous avons donc injecté  $3 \times 10^8$  leishmanies dans la veine caudale des souris, puis réalisé des imageries 1, 7, 14, 21 et 28 jours post-infection. Les leishmanies Luc *L. infantum* et eFFly-mCherry se retrouvent bien au niveau du foie à 1 jour post infection, puis les parasites Luc se multiplient dans le foie jusqu'à 14 jours, puis diminuent et se localisent dans la rate à 28 jours, alors que les parasites eFFly-mCherry *L. infantum* ne sont plus visibles dès 7 jours post infection (Fig 10).



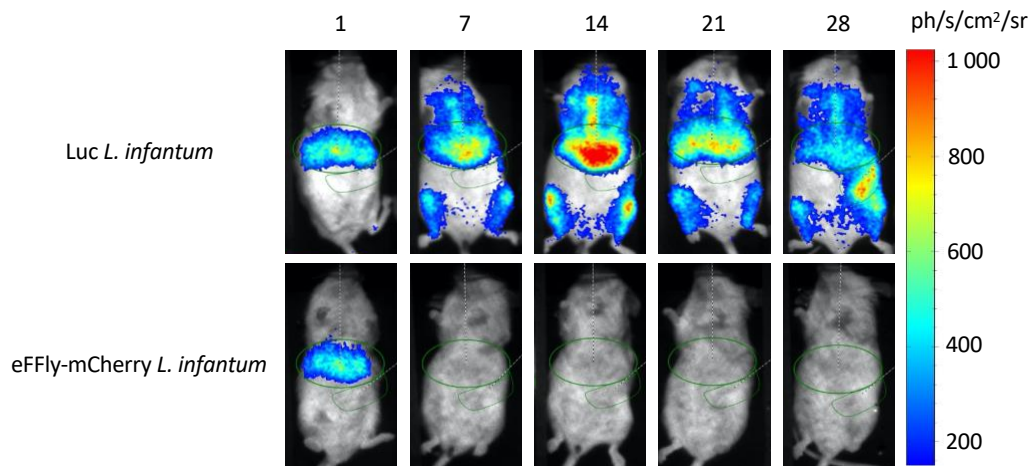


Figure 10 : Infection de souris Balb/c avec des *L. infantum* Luc et eFFly-mCherry

La quantification de ces données à l'aide des ROI sur le foie et sur la rate est montrée ci-dessous (Fig 11).

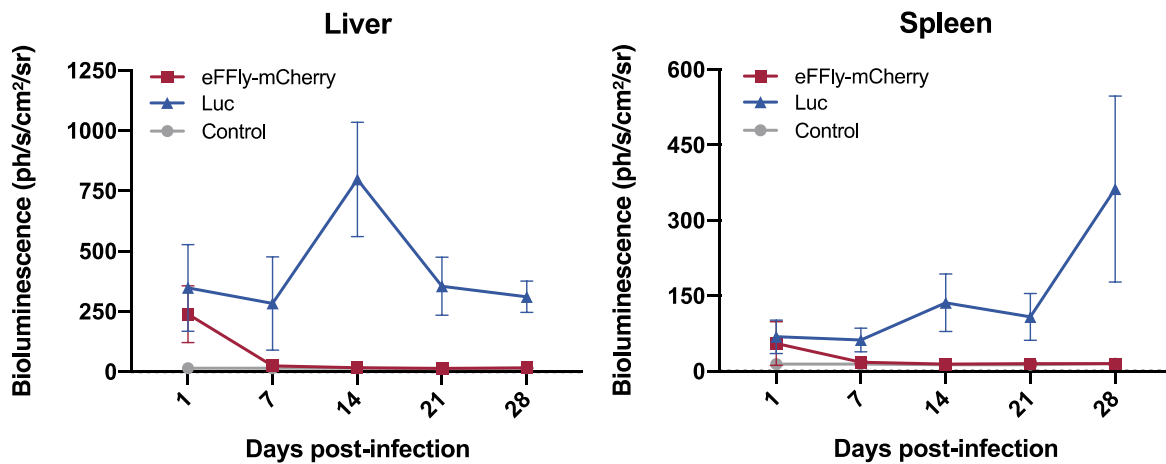


Figure 11 : Quantification de l'émission de bioluminescence au niveau du foie et de la rate de souris infectées par *L. infantum* Luc et eFFly-mCherry

Nous avons voulu regarder dans une expérimentation indépendante et sur des temps plus courts la cinétique de disparition du signal dans les souris infectées par eFFly-mCherry *L. infantum*. Le signal bioluminescent était toujours présent dans le foie des souris infectées à 1

jour post-infection, puis a chuté fortement, mettant encore en évidence des leishmanies à 3 jours mais plus à 6 jours (Fig 12).

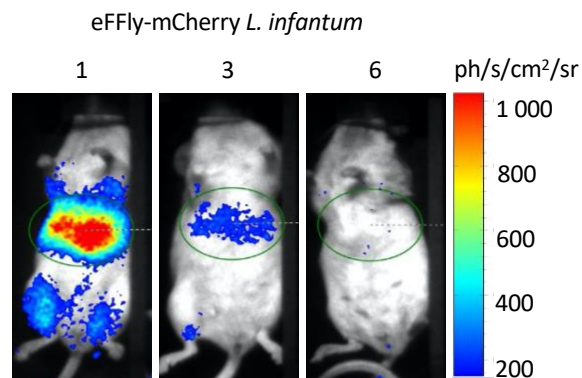


Figure 12 : Évolution de l'infection de souris Balb/c par *L. infantum* eFFly-mCherry sur des temps courts

La quantification de la charge parasitaire dans le foie par bioluminescence est montrée ci-dessous (Fig 13).

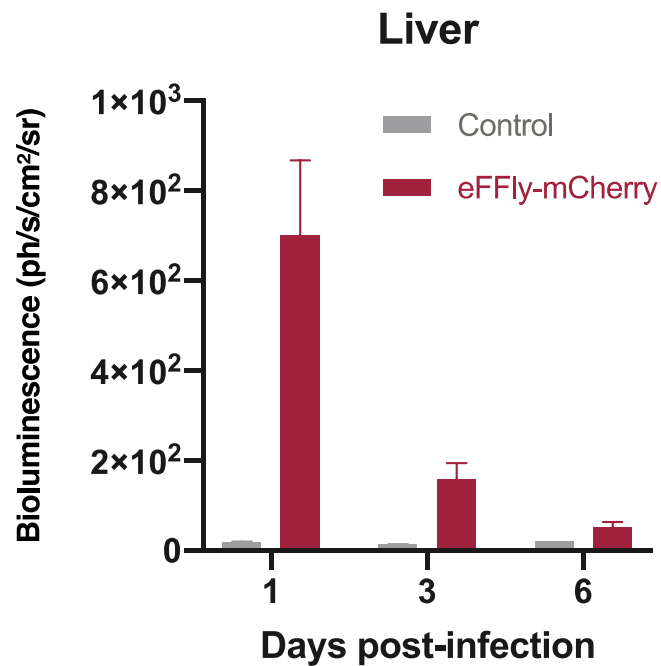


Figure 13 : Quantification de l'émission de bioluminescence dans le foie de souris infectées par *L. infantum* eFFly-mCherry.

## IV. Discussion

Face aux limites des traitements actuels contre la leishmaniose, tant au niveau du coût, de la toxicité et face à l'apparition croissante de résistances, il est aujourd'hui urgent de trouver des traitements alternatifs. L'arrivée des gènes rapporteurs pouvant être stablement exprimés par les parasites a montré un gain de temps et d'argent considérable, permettant des criblages à haut débit (Lang, Goyard, Lebastard, & Milon, 2005) et l'avancée constante en terme de génération de protéines fluorescentes améliorées et de luciférases permettant une émission de bioluminescence plus vive ne cesse d'agrandir l'étendue des possibilités. Nous avons réalisé des transfections afin d'obtenir 4 nouvelles souches fluorescentes, bioluminescentes ou doublement transformées. Les transgènes sélectionnés l'ont tous été pour améliorer la détection, ou la longueur d'onde d'émission de rapporteurs déjà disponibles dans *Leishmania*, et ont tous montré des avantages et des inconvénients complémentaires les uns des autres.

La construction mMaroon1 permettant une émission de fluorescence dans le rouge lointain, possédait une intensité basse, mais menait à très peu de bruit de fond dans les cellules. Cependant, sa sensibilité à l'acide n'a pas permis son utilisation pour visualiser la forme amastigote du parasite localisé dans des vacuoles acides. Pour compenser ce problème, nous avons réalisé une construction mRuby, très intensément fluorescente dans le rouge, avec un pKa de 4.4 traduisant une très faible sensibilité à l'acide. Cette construction a donné des promastigotes très fluorescents, mais l'émission de fluorescence n'a pas été maintenue au cours du temps. Il serait intéressant de vérifier la présence du transgène mRuby par séquençage, et de vérifier la présence de la protéine afin de voir pourquoi cette construction qui devrait être stablement insérée dans le génome pouvait conduire à une perte de la fluorescence.

La construction teLuc a permis une émission de bioluminescence très forte, à la fois dans la forme promastigote qu'amastigote, mais le substrat est complexe à dissoudre dans un solvant. Il n'est pas stable dans du DMSO et nécessite la suspension dans des solvants incompatibles avec le vivant, ou alors donne lieu à des solutions non homogènes. L'obtention d'une souche exprimant à la fois la fluorescence et la bioluminescence a été un échec une

première fois avec le mMaroon1-teLuc, car l'insertion du second transgène a remplacé le premier. La construction eFFly-mCherry, issu d'un seul plasmide donc d'une seule recombinaison, a montré de bons résultats *in vitro*.

Les souches eFFly-mCherry et teLuc ont donc été testées *in vivo*.

Si le teLuc avait pu être utilisé *in vivo* dans la littérature (Yeh *et al.*, 2017), la solubilisation du substrat de l'enzyme a posé un problème *in vivo* de détection entre nos mains. Effectivement, si la qPCR a permis de mettre en évidence une charge parasitaire importante au niveau du foie et de la rate de souris Balb/c 15 jours post-infection, aucun signal n'était visible en suivi de bioluminescence sur l'animal entier. Sachant que la souche teLuc émet plus de bioluminescence que des souches Luc classiques, et que les souches Luc ont été visualisables en imagerie *in vivo*, nous émettons l'hypothèse qu'il s'agit d'un problème d'accessibilité du substrat aux organes profonds.

Les parasites eFFly-mCherry nécessitent l'ajout de l'enzyme luciférine, qui est très facilement soluble dans le PBS. Nous n'avons pas observé de difficultés *in vivo* de mise en évidence de l'infection 1 jour post injection, cependant contrairement aux leishmanies Luc, les eFFly-mCherry *L. infantum* n'ont pas persisté au niveau du foie, et ce dès 7 jours post infection. Il sera nécessaire de réaliser des quantifications par qPCR pour confirmer l'élimination du parasite et écarter la possibilité d'une baisse de l'expression de la protéine eFFly qui mènerait à une réduction du signal bioluminescent.

## V. Conclusion et Perspectives

La génération d'une nouvelle souche rapportrice est un processus couteux en temps, qui ne donne pas toujours des constructions utilisables dans le système dans lequel elles ont été insérées. Sur les 5 constructions que nous avons essayé d'obtenir, 1 n'a pas aboutie à la double transformation souhaitée, 2 ont montré des limites dès les tests *in vitro* et les deux autres ont montré des problèmes lors des tests *in vivo*.

Cependant la mise au point des techniques de construction et de transformation nous ont permis d'avoir un protocole robuste pour le remplacement des gènes d'intérêt dans les

constructions, et il sera intéressant d'utiliser ces connaissances afin de générer un panel de nouvelles souches rapportrices dans le futur.

La souche la plus prometteuse reste la *L. infantum* teLuc car elle montre une bioluminescence très importante *in vitro*, qui pourrait permettre la mise en évidence de sites faiblement infectés dans l'animal, et peut être d'étudier les sanctuaires de persistance ou le portage asymptomatique si le problème de solubilité du substrat peut être résolu.

Actuellement, de nouveaux solvants sont disponibles et des tests préliminaires ont montré que la solubilité était bien meilleure dans ces conditions de solubilisation. Nous reprogrammerons donc des expérimentations afin de tester de nouveau la détection *in vivo* des parasites teLuc avec le nouveau solvant.

## **Partie II : Recherche de nouveaux composés immuno-stimulateurs contre *Leishmania***

Cette partie de la thèse contient des résultats confidentiels, car soumis à un dépôt de brevet. Les noms de toutes les molécules utilisées ont aussi été volontairement anonymisés afin de ne pas dévoiler la nature des composés. Pour le rapport, qui devra rester confidentiel à la suite d'une demande de la SATT Sud-Est, les correspondances avec les molécules sont indiquées dans ce tableau (Fig 14).

1	Acide palmitique
2	Harmame
3	Uvaol
6	Acide oléanolique
7	$\beta$ sitostérol
8	DL- $\alpha$ tocopherol acétate
9	$\alpha$ tocopherol
10	$\beta$ tocopherol
11	$\delta$ tocopherol
12	$\gamma$ tocopherol
13	$\alpha$ tocotrienol
14	$\beta$ tocotrienol
15	$\delta$ tocotrienol
16	$\gamma$ tocotrienol
17	$\alpha$ -tocopherol acétate
18	$\alpha$ -tocopherol succinate
19	Phytol
20	Oleyl alcohol
21	Trolox
22	Trolox méthyl éther
23	Acide garcinoïque
24	Succinate de phytyle
25	Maléate de phytyle
26	Succinate d' $\alpha$ -tocopherol
27	Maléate d' $\alpha$ -tocopherol
28	Succinate de $\delta$ -tocopherol
29	Succinate de l'ester isopropylique du trolox
30	Maléate de l'ester isopropylique du trolox

Figure 14 : Tableau des correspondances entre les numéros des molécules et leur nom.

## I. Introduction

Comme il a été mentionné dans l'introduction générale de la thèse, et dans la revue « Leishmaniasis : Strategies in treatment development » (cf. page 33 du manuscrit), il existe actuellement plusieurs traitements approuvés permettant le traitement de la leishmaniose. Ces traitements possèdent cependant d'importantes limitations. Le traitement de référence, préconisé par l'OMS pour le traitement des leishmanioses viscérales sur le pourtour du bassin méditerranéen est l'Amphotéricine B sous sa forme liposomale. Sa formulation liposomale est importante pour limiter la toxicité rénale du traitement, mais augmente aussi fortement le coût de production. Il est administré par voie intraveineuse, et nécessite une hospitalisation pour suivre le traitement. Si ce traitement limitait auparavant les risques de rechute et de non-réponse thérapeutique comparé à d'anciens traitements comme les antimoniés pentavalents (Sodium Stibogluconate et Meglumine antimoniate), on voit aujourd'hui apparaître de plus en plus de cas de résistance à l'Amphotéricine B (Ponte-Sucre *et al.*, 2017). Il devient donc urgent de découvrir de nouveaux traitements efficaces contre la leishmaniose. Parmi les stratégies de recherche de traitement actuels, la recherche de molécules naturelles, que ce soit au travers l'étude de composés couramment utilisés en médecine traditionnelle ou à travers l'étude de la biodiversité, possède une place de plus en plus importante. Effectivement, les végétaux représentent une grande partie de la biodiversité terrestre et beaucoup de composés utilisés aujourd'hui en médecine sont issus de plantes. De plus, c'est un sujet qui est dans l'air du temps, avec la montée de plus en plus importante de la consommation « Bio » et des remèdes naturels, moins « chimiques », et le souci de recyclage afin de préserver la planète.

Depuis 2015, mon équipe d'accueil au C3M travaille en collaboration avec l'Institut de Chimie de Nice (ICN). Dans un souci de valorisation de la végétation locale, et de recyclage de déchets végétaux issus de l'industrie de la parfumerie, l'équipe de l'ICN a récupéré des plantes, qui ont été extraites en fractions. Ces fractions ont ensuite servi à réaliser un crible visant à identifier des extraits :



1. Non cytotoxiques
2. Avec ou sans activité sur la forme extracellulaire promastigote de *L. infantum*
3. Avec une activité sur la forme amastigote intracellulaire de *L. infantum*, responsable de la maladie

L'organisation de ce crible nous permettra d'identifier des extraits qui peuvent être utilisés sur les cellules sans posséder de toxicité. Les tests sur la forme promastigote et amastigote permettront d'identifier 3 types de candidats actifs :

1. Ceux avec une activité sur la forme promastigote seulement : activité directe sur le parasite.
2. Ceux avec une activité sur la forme promastigote et amastigote : activité directe sur le parasite, avec possibilité d'agir sur la leishmanie intracellulaire (accessibilité des composés)
3. Ceux avec une activité sur la forme amastigote uniquement : activité possiblement indirecte sur le parasite, médiée par l'activité de la cellule hôte.

Ce crible ne permet donc pas seulement d'identifier des composés actifs, mais aussi potentiellement d'identifier des composés immuno-stimulateurs, dont l'activité anti-parasitaire est médiée par la cellule hôte.

Ceci est important car des composés qui ne ciblent pas directement les pathogènes, présentent un risque moins important d'aboutir à l'émergence de résistances.

Sur près de 150 plantes et extraits testés dans ce crible de 2017, qui font l'objet d'une thèse de science réalisée avant celle-ci par Aurélie Schwing (Schwing-Chaïb, 2018) les extraits cytotoxiques ont été écartés du crible de façon précoce. Par la suite, les extraits non toxiques ont été testés sur les promastigotes et amastigotes de *L. infantum*. 11 extraits ont montré une activité sur seulement la forme promastigote, 7 extraits avaient une activité sur la forme promastigote et amastigote, et 1 seul extrait n'était actif que sur la forme intracellulaire amastigote du parasite. Au cours de ma thèse, je me suis intéressé à ce dernier extrait intitulé CA-TM-0015 (Fig 15).

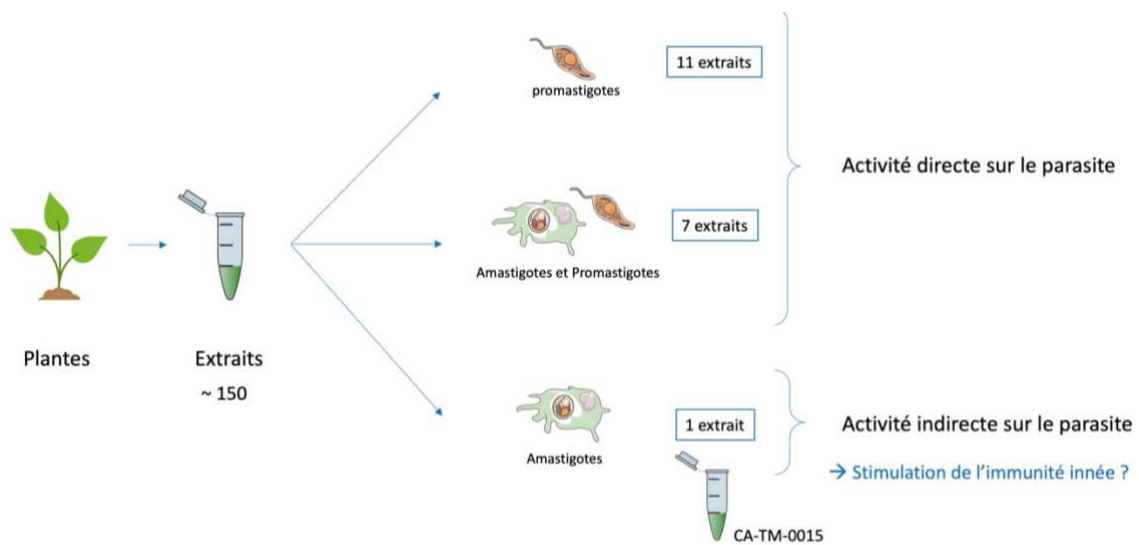
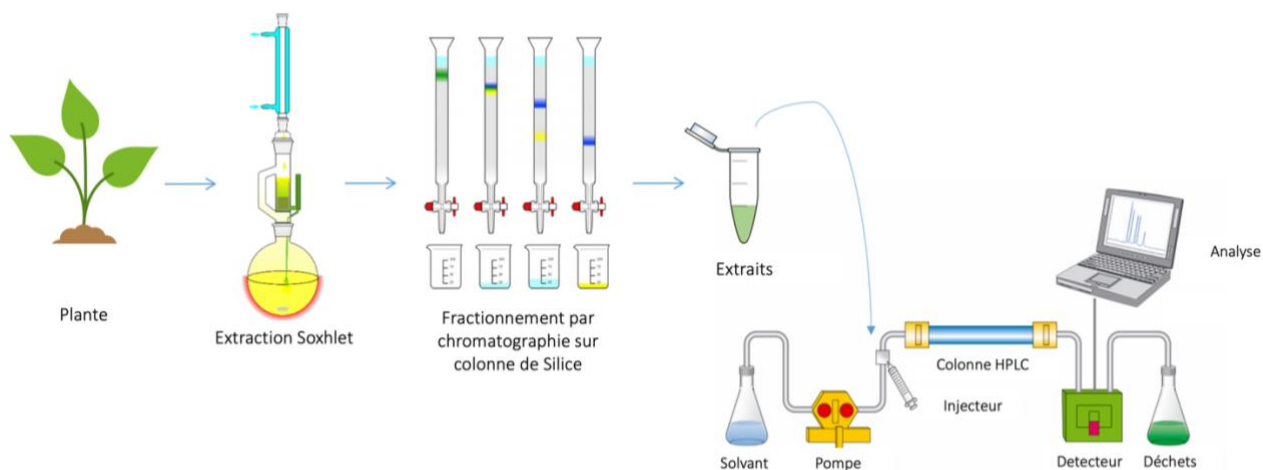


Figure 15 : Résumé du projet de thèse à l'origine des travaux présentés ici.

L'extrait CA-TM-0015 montrant une activité uniquement sur la forme amastigote, a été divisé en fractions afin de pouvoir éventuellement identifier la ou les molécules responsables de son activité. L'extraction a été réalisée à l'aide d'un extracteur de Soxhlet, qui consiste à faire macérer dans un solvant la drêche de la plante. Le mélange est ensuite chauffé, et le solvant s'évapore tandis que le liquide retombe par condensation dans le ballon et enrichit petit à petit le mélange en composés solubles issus de la drêche. L'extraction est suivie par un fractionnement par chromatographie sur colonne de silice, qui permet une séparation des composés contenus dans l'extrait. Les fractions sont ensuite passés sur une colonne HPLC (High Performance Liquid Chromatography) qui permet l'identification de pics correspondant à des molécules ou familles de molécules (Fig 16).



**Figure 16** : Schéma du procédé d'obtention des chromatogrammes HPLC.

L'identification par HPLC se base sur une technique de séparation des composés présents dans un extrait basé sur leur affinité avec le solvant utilisé. La détection est réalisée selon deux techniques : une lecture à 280nm, ainsi que l'utilisation d'un détecteur évaporatif à diffusion de lumière (ELSD). Le passage de l'extrait CA-TM-0015 a permis l'obtention du graphe suivant (Fig 17).

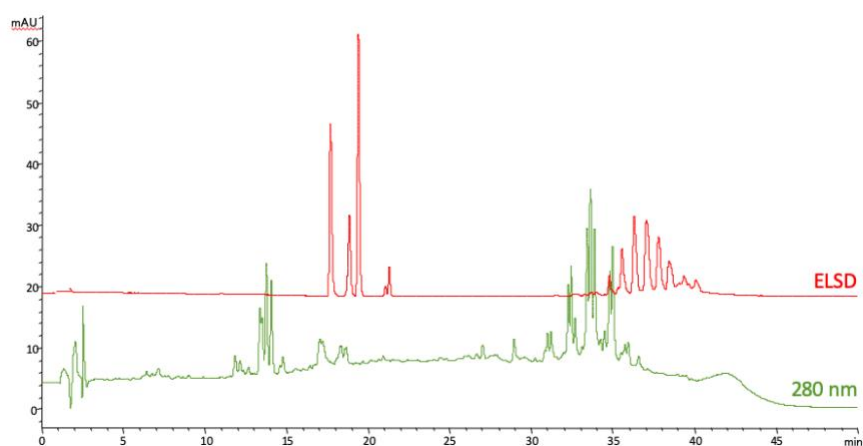


**Figure 17** : Chromatogramme HPLC de l'extrait CA-TM-0015.

Obtenu sur une colonne Luna® C18 (150 mm × 4,6 mm ; 5 µm) à 280 nm et avec ELSD ; gradient de solvants acidifiés à 0,1% d'acide formique : H<sub>2</sub>O, ACN, iPrOH

Lorsque l'on analyse les profils ELSD de la fraction CA-TM-0015, on remarque que deux grands groupes de pics ont pu être isolés. L'extrait CA-TM-0015 a ensuite été repassé en Chromatographie sur colonne de silice phase normale (cyclohexane et Et<sub>2</sub>O) afin d'obtenir les fractions A à G. Parmi celles-ci, les fractions C et E permettaient de séparer le plus efficacement les deux familles de pics obtenus en HPLC (Fig 18).

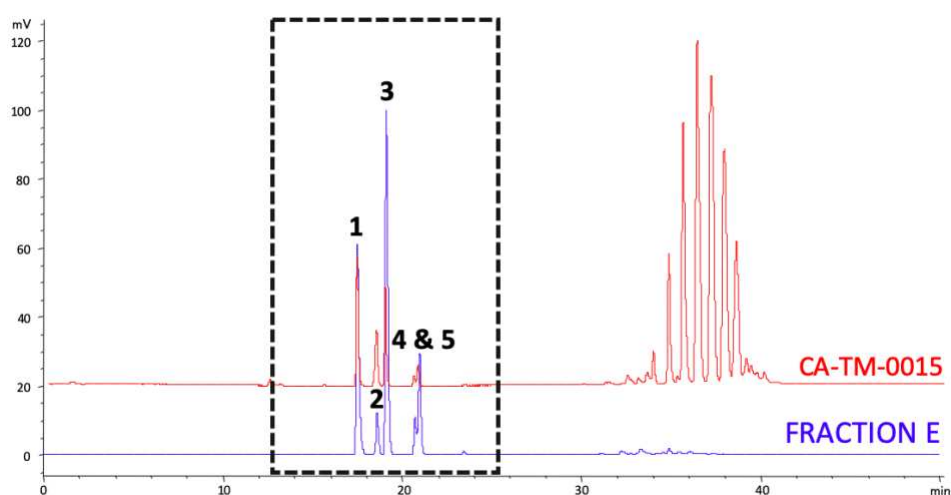
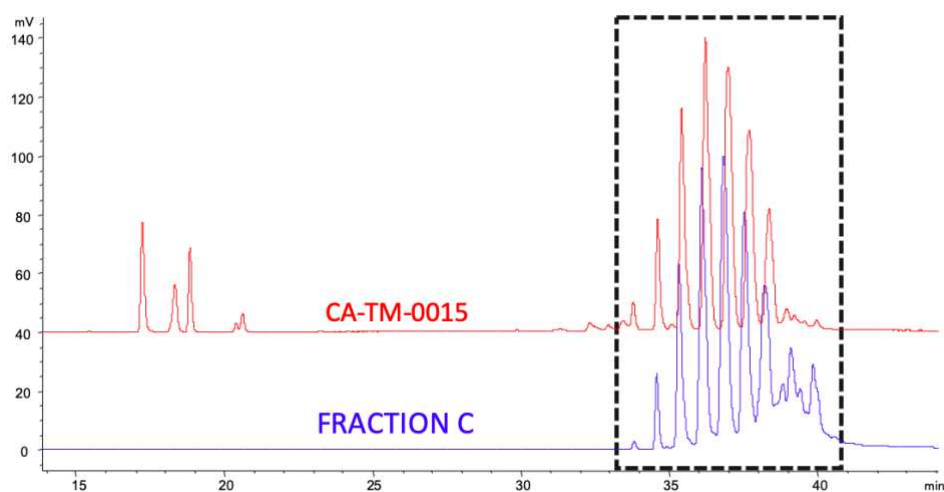


**Figure 18** : Chromatogramme HPLC des fractions C et E.

Obtenues sur une colonne Luna® C18 (150 mm × 4,6 mm ; 5 µm) avec ELSD

Dans les étapes suivantes, les fractions ont été passés en Chromatographie de partage centrifuge afin de séparer les pics contenus dans les fractions, pour obtenir 1 seul pic par condition (Fig 19).

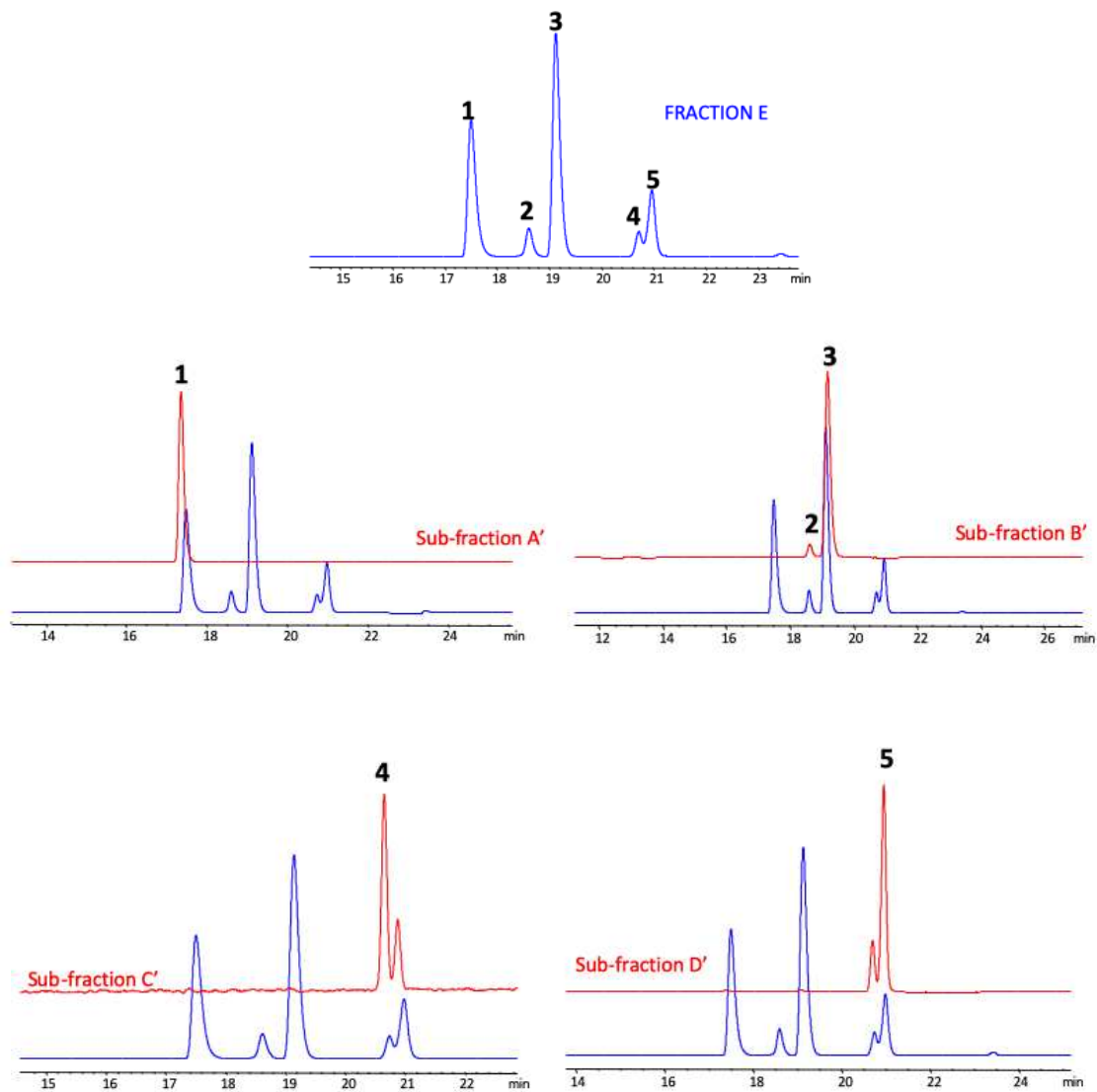


Figure 19 : Résultat de la chromatographie de partage centrifuge sur la séparation de la fraction E

Une fois qu'il n'y avait qu'un seul pic par chromatogramme, les molécules ont été identifiées par spectroscopie RMN (Résonance magnétique), et nous avons pu obtenir des fractions les molécules 1 à 8 qui seront testées dans la suite de ce manuscrit.

## II. Matériel et Méthodes

### *Culture des leishmanies Luc et teLuc L. infantum sous forme promastigote*

Les souches utilisées pour ces travaux ont été isolées sur des patients atteints de leishmaniose viscérale à Nice. Une souche de *L. infantum* MON-1 (MHOM/FR/94/LPN101) transformée pour exprimer stablement la luciférase Luc, et une souche de *L. infantum* MON-1 (MHOM/FR/18/LPN432) isolée à Nice en 2019, transformée pour exprimer stablement la luciférase teLuc ont été utilisées. Elles sont maintenues en culture à 26°C dans du milieu Schneider's Insect Medium (Référence : 2187504 Sigma®) supplémenté en NaHCO<sub>3</sub> 0.4g/L (Janssen chimica®), CaCl<sub>2</sub> 0.6g/L (Fluka Chemika®), Sérum de veau foetal (SVF) 10% (Référence : 10270-098, GIBCO®), Urine 2% (provenant d'un pool), HEPES 1mM pH=7,3 (Référence : 10110D, EUROMEDEX®), L-Glutamine 1% (Référence : 25030-024, GIBCO®), Pénicilline-Streptomycine 1% (Référence : 15140-122 GIBCO®), et de 0,1% de Rouge Phénol (Sigma, P0290). Les cultures sont diluées 2 fois par semaine, en début de phase stationnaire de croissance, à 1x10<sup>6</sup> leishmanies/mL. Le milieu de culture est additionné d'Hygromycine B à 100ug/mL (Référence : 1068701, GIBCO®) pour permettre la sélection des souches transformées.

### *Isolation et culture des macrophages murins primaires*

Les BMDM (Bone Marrow Derived Macrophages) proviennent de souris Balb/c, âgées de 8 à 12 semaines. Les souris sont euthanasiées par dislocation cervicale. Après dissection et récupération des fémurs, la moelle osseuse est récupérée par lavages successifs avec une seringue 25G, puis filtrées sur un tamis de 0,45 µM. Les cellules sont ensuite lavées, puis mises en culture à 37°C + CO<sub>2</sub> (5%), dans du milieu RPMI Medium 1640® (Référence : 21875, Invitrogen GIBCO®), supplémenté en SVF 10% (Référence : 10270-098, GIBCO®), Pénicilline/streptomycine (1%) (Référence : 15140-122 GIBCO®), et de M-CSF 100 ng/mL (Mouse M-CSF, Miltenyi Biotec). Les cellules sont maintenues en culture pendant 6 jours sur des boîtes en plastique non traité pour la culture cellulaire, afin d'induire leur différenciation en macrophages sous l'effet du M-CSF (100ng/ml). Ensuite, les cellules sont détachées au PBS-EDTA 5mM pendant 10 minutes, puisensemencées (400 000 cellules par puits dans les

plaques 12 puits, 30 000 cellules par puits dans les plaques 96 puits) sur la nuit pour une utilisation le lendemain.

#### *Préparation des extraits de plantes*

Les extraits ont été fournis par l'ICN à une concentration de 10mg/ml, suspendus dans du diméthylsulfoxyde (DMSO). Dès leur arrivée, les extraits sont répartis en petits volumes et congelés à -20°C afin d'éviter les successions de cycles de congélation/décongélation qui pourraient mener à la dégradation des molécules contenues dans les extraits.

#### *Tests de cytotoxicité des extraits et molécules*

Les extraits de plante sont testés à 100 µg/mL, incubés avec les cellules BMDM à 37°C + CO<sub>2</sub> (5%) pendant 48h. Les molécules pures sont testées à des concentrations allant de 1000 µM à 1,5µM par dilutions sérielles au ½. La viabilité des cellules est ensuite testée par ajout de 10% d'AlamarBlue HS™ (Invitrogen). La mesure de la viabilité est réalisée après 3h d'incubation à 37°C, en lisant la fluorescence (Excitation/Emission (nm) : 530-560 / 590) de la plaque dans le lecteur de plaques multi-mode Synergy™ 2 (BioTek®).

#### *Activité des extraits et molécules sur la forme promastigote*

Les extraits de plante sont testés à 100 µg/mL, incubés avec les cellules BMDM à 37°C + CO<sub>2</sub> (5%) pendant 48h. Les molécules pures sont testées à des concentrations allant de 1000 µM à 1,5 µM par dilutions sérielles au ½. La viabilité des promastigotes est testée grâce à l'ajout de 10µl d'une solution de 30 mg/mL de luciférine (D-Luciferin Potassium salt 1G, 122796, PerkinElmer SAS) par lecture de bioluminescence dans le lecteur de plaques multi-mode Synergy™ 2 (BioTek®).

#### *Activité des extraits et molécules sur la forme amastigote bioluminescente*

Onensemence 2x10<sup>4</sup> cellules BMDM par puits, en présence de 100 ng/ml de MCSF pour induire leur activation et différenciation en macrophages pendant 5 jours à 37°C. Après activation, on infecte les cellules à une MOI de 20 parasites par cellule. 6h plus tard, les cellules sont lavées puis laissées 48h à 37°C pour la transformation des parasites en amastigotes. Les

extraits et les molécules sont ajoutées à 100 µg/ml, et on incube à 37°C pendant 48h, puis on mesure la viabilité à l'aide de la luciférine, par mesure de bioluminescence (Photons/secondes) dans le lecteur de plaques multi-mode Synergy™ 2 (BioTek®).

#### *Tests de stabilité des molécules*

Les molécules pures commerciales sont initialement suspendues dans du DMSO à une concentration de 100 µg/mL. Pour la dégradation forcée, les molécules sont gardées pendant 1 semaine à 4°C, 50°C ou 100°C. Pour les expérimentations en condition de laboratoire, les molécules sont gardées à -20°C ou à température ambiante à l'abri de la lumière durant 66 jours. Les suspensions sont ensuite passées en Chromatographie liquide de haute performance (HPLC) dans un gradient d'élution 80% Acéto-nitrile, 20% Isopropanol, sur une colonne Luna C18 150 mm\*4,6 mm\*5 µm. Les chromatogrammes DEDL, 210 nm et 292 nm sont acquis, puis l'aire sous la courbe 292 nm est mesurée à l'aide du logiciel Agilent Chemstation avec l'aire sous la courbe de la molécule nouvellement reprise fixée à 100%. Ensuite, le rapport est réalisé afin d'obtenir le pourcentage de molécule présente dans la suspension.

#### *Cytokine Array*

Le cytokine array (R&D systems Proteome Profiler, Mouse cytokine Array Panel A, #ARY006) est composé d'un panel de 40 cytokines. Il a été réalisé en suivant les indications du fournisseur. Brièvement, 500 µl des échantillons sont mélangés avec le cocktail d'anticorps et incubés pendant une heure, puis sont ajoutés sur les membranes du cytokine array. La révélation des cytokines capturées par les anticorps de la membrane est réalisée à l'aide de la Streptavidine/HRP et de son substrat, qui mène à une émission de bioluminescence. La visualisation de la membrane a été réalisée à l'aide du Fujifilm LAS 4000 Gel Imager contrôlé par le logiciel ImageQuant LAS 4000. Le traitement des données a été fait avec le logiciel Multi Gauge v3. de Fujifilm.

#### *Infection et suivi des souris in vivo*

Des souris Balb/c femelles âgées de 6 semaines ont été infectées par voie intraveineuse avec



$3 \times 10^8$  parasites *L. infantum*-Luc en fin de phase exponentielle de croissance, 5 jours post-dilution. Les parasites ont été préalablement lavés 2 fois avec du PBS. Suivant l'infection, les souris ont été imagées aux jours indiqués après injection intrapéritonéale de D-luciférine (PerkinElmer, 122799 XenoLight D-Luciferin, K+ Salt Bioluminescent Substrate) à une concentration de 300 mg/kg. L'injection a été réalisée 10 minutes avant d'anesthésier les souris dans une atmosphère à 3.0% d'isoflurane (Vetflurane), puis les souris ont été placées dans le PhotonIMAGER Optima (Biospace Lab), et l'anesthésie a été maintenue à 2.5% isoflurane pendant les 5 minutes d'acquisition. Les images ont été analysées avec le logiciel M3Vision (Biospace Lab, Version 1.1.3.31192) en traçant des Régions d'Intérêt (ROI) autour du foie et de la rate afin de quantifier la bioluminescence émise en photons/s/cm<sup>2</sup>/sr.

### III. Résultats

#### Partie I. Crible initial

##### a. Cytotoxicité des molécules

Les structures des molécules de 1 à 8 sont représentées ci-contre (Fig 20) :

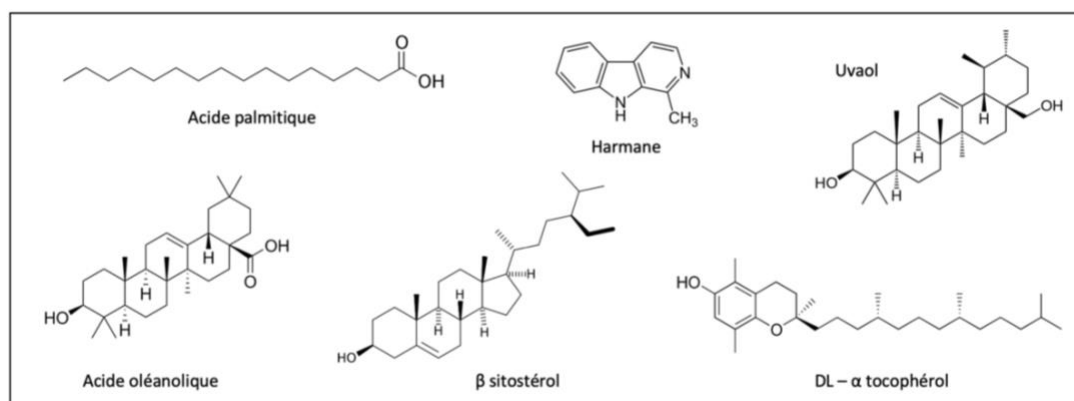
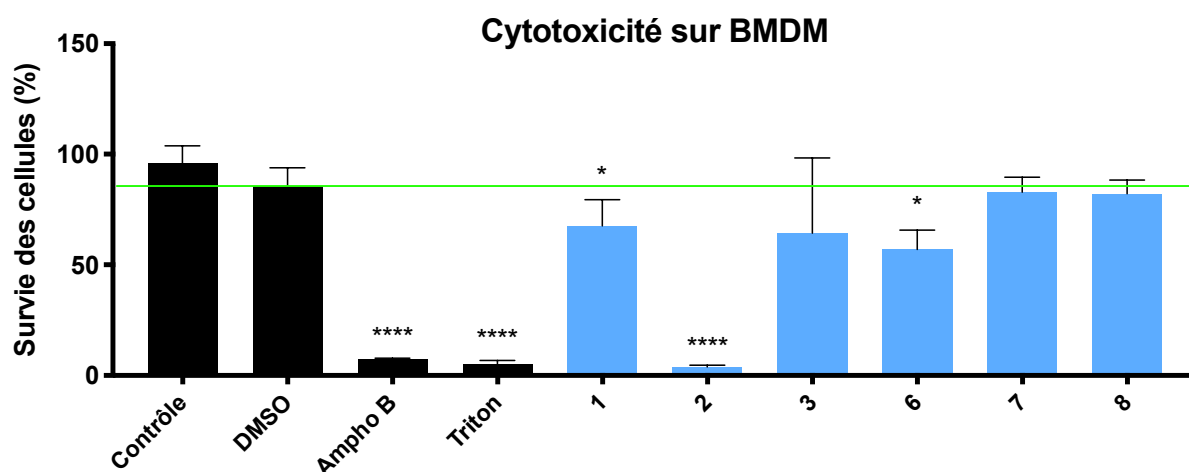


Figure 20 : Structure chimique des molécules 1 à 8

Nous avons testé ces molécules pour leur toxicité sur des cellules BMDM à une concentration de 100 µg/mL correspondant aux concentrations auxquelles les extraits de plantes ont été testé. Ceci nous a permis de mettre en évidence une absence de toxicité de la molécule 7 et 8, mais des toxicités variables pour les molécules de 1 à 6. La molécule 2 montrait une toxicité aussi forte que l'amphotéricine B, alors que les molécules 1 et 6 montraient une faible toxicité. La molécule 3 a montré une toxicité variable en fonction des expérimentations, ce qui était potentiellement dû au fait qu'elle forme des cristaux en DMSO et que la concentration n'est pas systématiquement identique, ce qui explique également l'écart-type plus important (Fig 21).



**Figure 21** : Cytotoxicité des molécules pures sur des cellules primaires BMDM murines.

n=3 ; Test Statistique : One-Way ANOVA (par rapport à la condition « DMSO »), non paramétrique, Kruskal-Wallis, Dunn non corrigé. P value \*=0,03 ; \*\*=0,002 ; \*\*\*=0,0002 \*\*\*\*=<0,0001

Afin de confirmer ces résultats sur cellules primaires murines, j'ai réalisé des tests de toxicité des molécules sur 2 autres types cellulaires humains. Dans un premier temps, des THP-1, une lignée monocyttaire humaine (Fig 22), et dans un second temps sur des PBMC, monocytes primaires circulants issus du sang de donneurs sains (Fig 23). Les résultats sur les trois types cellulaires étaient assez semblables, montrant les molécules 7 et 8 avec une faible toxicité, puis une toxicité plus ou moins importante sur les autres molécules. Après ces études, nous avons exclu la molécule 2 dû à sa forte toxicité sur tous les types cellulaires, similaire à l'Amphotéricine B. Nous n'avons donc plus testé cette molécule dans les expérimentations suivantes.

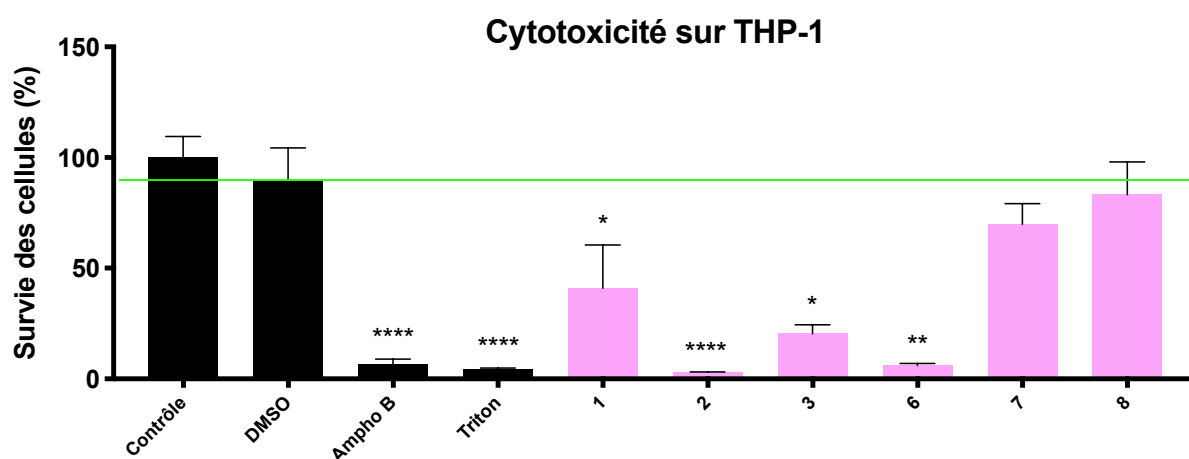


**Figure 22** : Cytotoxicité des molécules pures sur une lignée de cellules THP-1 humaines. n=2 ; Test Statistique : One-Way ANOVA (par rapport à la condition « DMSO »), non paramétrique, Kruskal-Wallis, Dunn non corrigé. P value \*=0,03 ; \*\*=0,002 ; \*\*\*=0,0002 \*\*\*\*=<0,0001

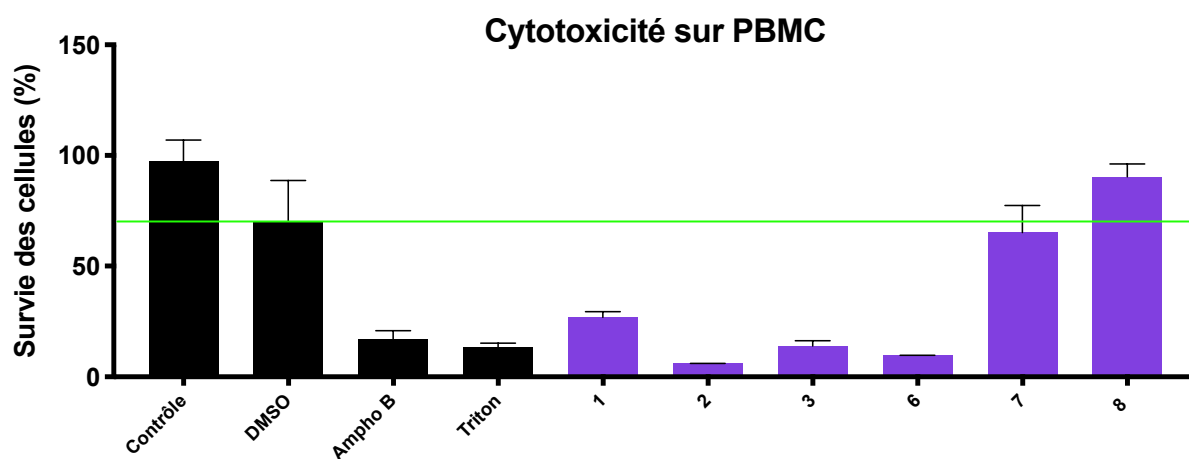


**Figure 23** : Cytotoxicité des molécules pures sur des PBMC primaires humains. n=1 ; Test Statistique : One-Way ANOVA (par rapport à la condition « DMSO »), non paramétrique, Kruskal-Wallis, Dunn non corrigé.

### b. Effet sur la forme promastigote

Dans un second temps, nous avons observé l'effet des molécules sur la forme promastigote de *L. infantum*, en utilisant la souche *L. infantum*-Luc disponible dans l'équipe. La molécule 1 semblait avoir un effet favorisant la croissance des parasites, car leur nombre double par rapport au contrôle. Les molécules 3 et 6 possèdent un effet anti-*Leishmania* sur la forme promastigote du parasite, alors que les molécules 7 et 8 n'ont aucun effet sur la viabilité des promastigotes (Fig 24).

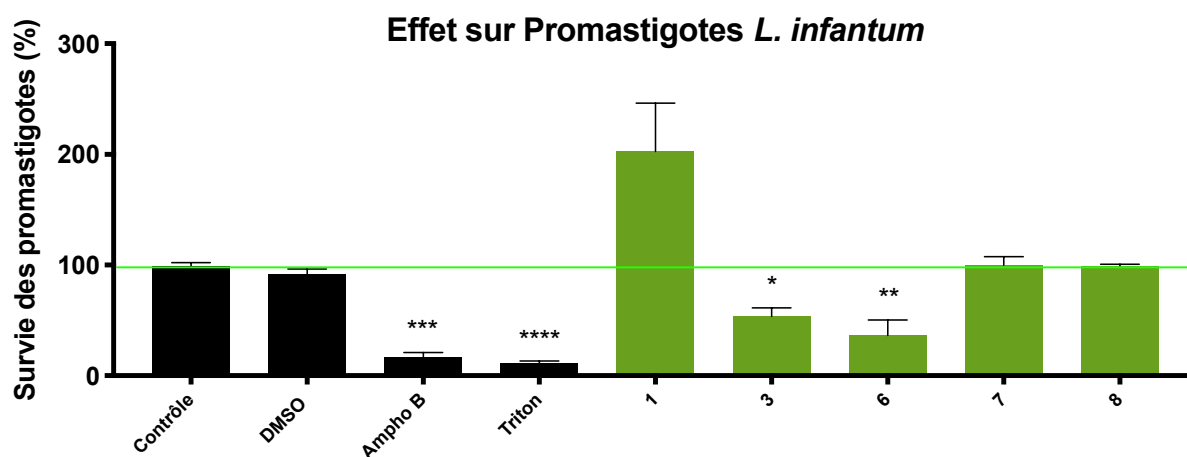


Figure 24 : Effet sur la forme promastigote de *L. infantum* des molécules pures.

n=3 ; Test Statistique : One-Way ANOVA (par rapport à la condition « Control »), non paramétrique, Kruskal-Wallis, Dunn non corrigé. P value \*=0,03 ; \*\*=0,002 ; \*\*\*=0,0002 \*\*\*\*=<0,0001

### c. Effet sur la forme amastigote

Nous avons ensuite observé la survie des parasites intracellulaires après une infection de BMDM. Nous retrouvons l'effet antiparasitaire des molécules 3 et 6, ainsi que l'augmentation de la survie des leishmanies en présence de la molécule 1. En revanche, la molécule 8 semble

montrer ici une diminution de viabilité des parasites, alors qu'elle n'avait aucun effet sur la forme extracellulaire promastigote du parasite. La molécule 8 se présente donc comme un candidat intéressant du fait de son activité uniquement sur la forme amastigote, similaire à celle de l'extrait CA-TM-0015 dont les molécules ont été isolées (Fig 25).

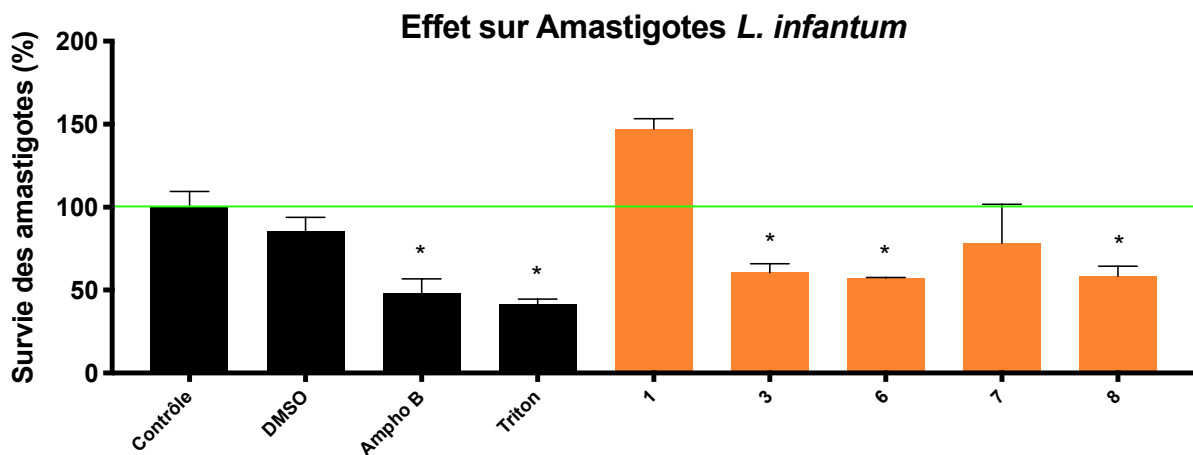


Figure 25 : Effet sur la forme amastigote de *L. infantum* dans des BMDM des molécules pures. n=1 ; La survie des amastigotes a été mesurée par bioluminescence après ajout de luciférine

#### d. Effet sur la sécrétion de cytokines

Une fois que nous avons isolé la molécule 8 comme un potentiel candidat pour une molécule anti-parasitaire, nous avons voulu regarder si cette molécule exerçait son effet par une modulation immunitaire, vu qu'elle ne semble pas avoir d'effet direct sur le parasite, mais que l'effet semble être médié par la cellule hôte. Pour ce faire, nous avons réalisé un Cytokine Array afin de comparer la sécrétion de cytokines entre une condition contrôle et additionnée de Molécule 8.

Nous avons représenté l'effet de la molécule seule sur les BMDM afin d'observer quels étaient les changements observés dans la sécrétion de cytokines.

On peut observer une augmentation dans la sécrétion de composés chémo-attractants lorsque les BMDM sont traités avec la molécule 8. On observe une modulation plus hétérogène des cytokines pro-inflammatoires, avec une augmentation d'IFN- $\gamma$ , mais une diminution d'IL-2 et de TNF- $\alpha$ , qui sont des cytokines très régulées au cours de l'infection à *Leishmania*. Parmi les cytokines anti-inflammatoires, la plus fortement réprimée était l'IL-1ra, un antagoniste de l'IL-1 $\beta$  (Fig 26).

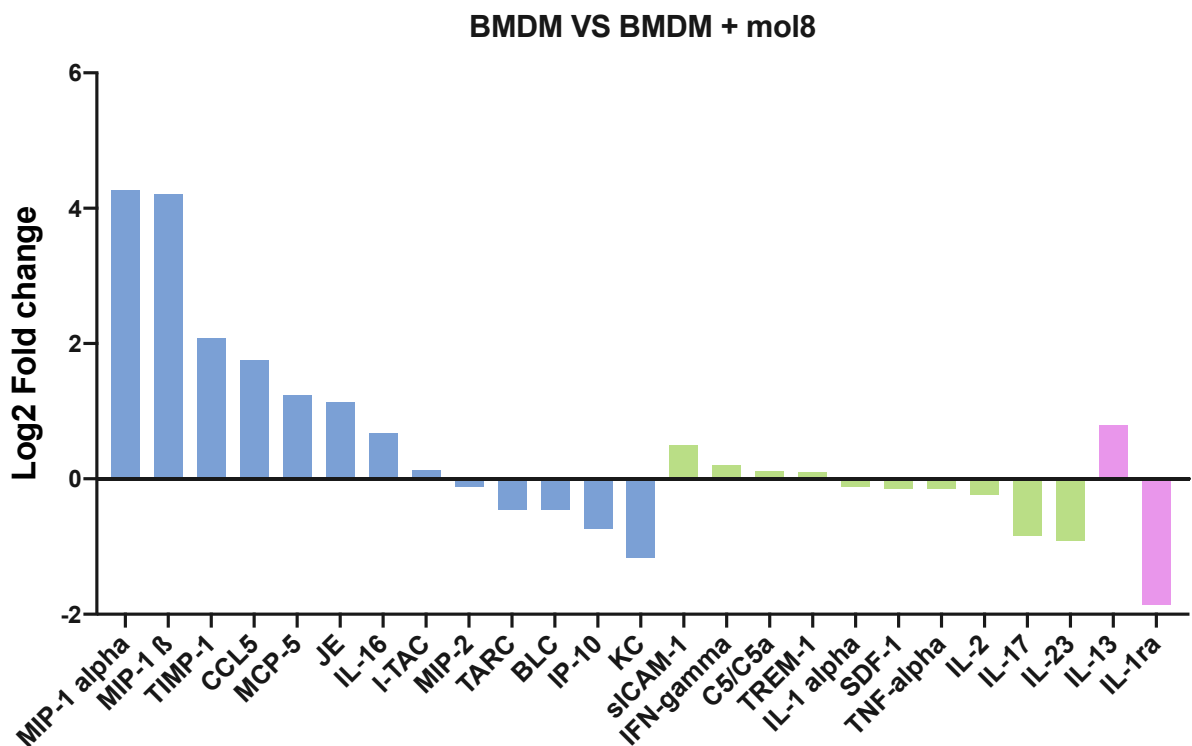


**Figure 26 :** Modifications induites par la molécule 8 sur la sécrétion de cytokines par des BMDM.

Le cytokine array a été réalisé sur surnageant de cellules BMDM traitées pendant 48h avec la molécule8. En bleu, les chémokines, en vert, les cytokines pro-inflammatoires et en rose les cytokines anti-inflammatoires.

Partant du postulat que les chémokines interviennent dans la réponse immunitaire adaptative en recrutant d'autres cellules immunitaires au site de l'infection, nous nous sommes intéressés aux cytokines de l'immunité innée Pro et Anti-inflammatoires. La protéine la plus

fortement réprimée étant l'antagoniste au récepteur de l'IL-1, l'IL-1ra, nous avons quantifié de façon plus précise la variation d'IL-1ra à l'aide d'une technique d'ELISA sandwich (Fig 27). On observe ici que la molécule 8 est capable de diminuer la sécrétion d'IL-1ra en condition normale. L'infection augmente fortement la sécrétion d'IL-1ra par les cellules, et le traitement avec la molécule 8 en contexte d'infection permet de revenir à des valeurs basales de quantité d'IL-1ra.

Ainsi, la molécule 8 possède la capacité de moduler la sécrétion cytokinique par les cellules BMDM, et semble donc posséder les caractéristiques d'un immuno-modulateur.

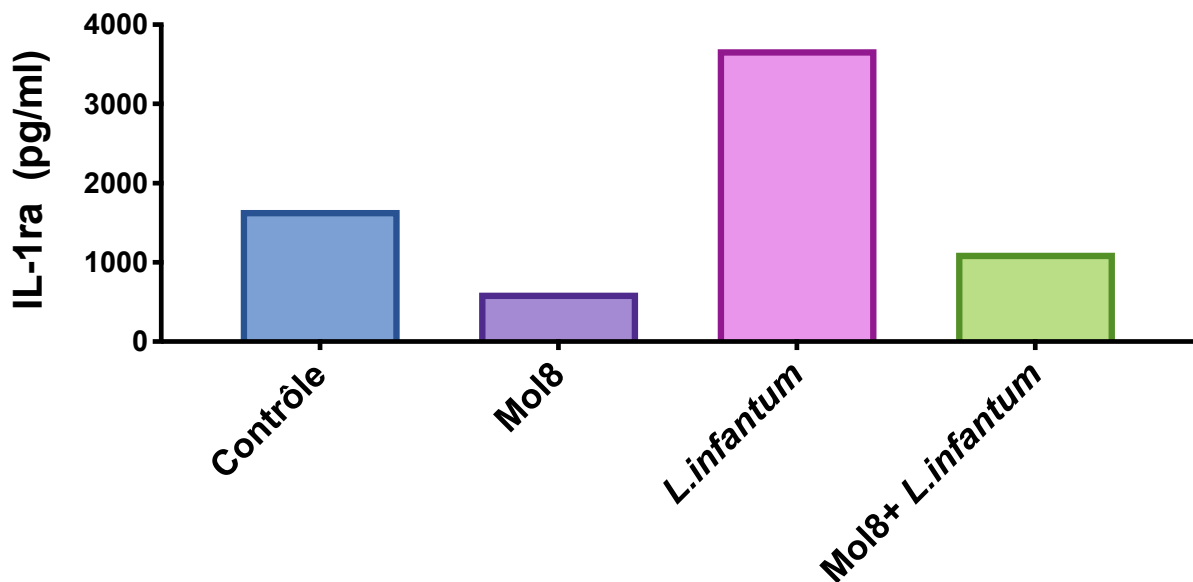


Figure 27 : Quantification par ELISA sandwich de l'IL-1ra dans les surnageants de cellules BMDM.



## Partie II. Stabilité de la Molécule 8

L'un des points limitants pour l'utilisation des traitements anti-*Leishmania*, surtout dans les pays en voie de développement, est également la conservation des composés. Nous avons donc voulu vérifier si la molécule 8 était stable et facilement conservable en regardant dans un premier temps sa stabilité en fonction de l'exposition à la température.

Pour ce faire, nous avons mis en place un suivi par HPLC en collaboration avec l'ICN. La quantité de molécule 8 dans l'échantillon a été mesurée après une resuspension à 100 µg/mL au départ (Fig 28).

La technique d'HPLC se base sur la séparation dans une colonne avec une phase stationnaire composée de chaînes de carbone, de molécules mises en suspension dans un mélange de solvants. Les molécules contenues dans la solution injectée seront entraînées par le flux du solvant, puis resteront plus ou moins longtemps dans la colonne en fonction de leur polarité. Ici les molécules les plus polaires sortent en premier, entraînées par le solvant polaire alors que les composés apolaires interagiront avec les chaînes carbonées contenues dans la colonne. A la sortie, les composés passent devant un détecteur, qui permet la génération de pics correspondant à présence de molécules.

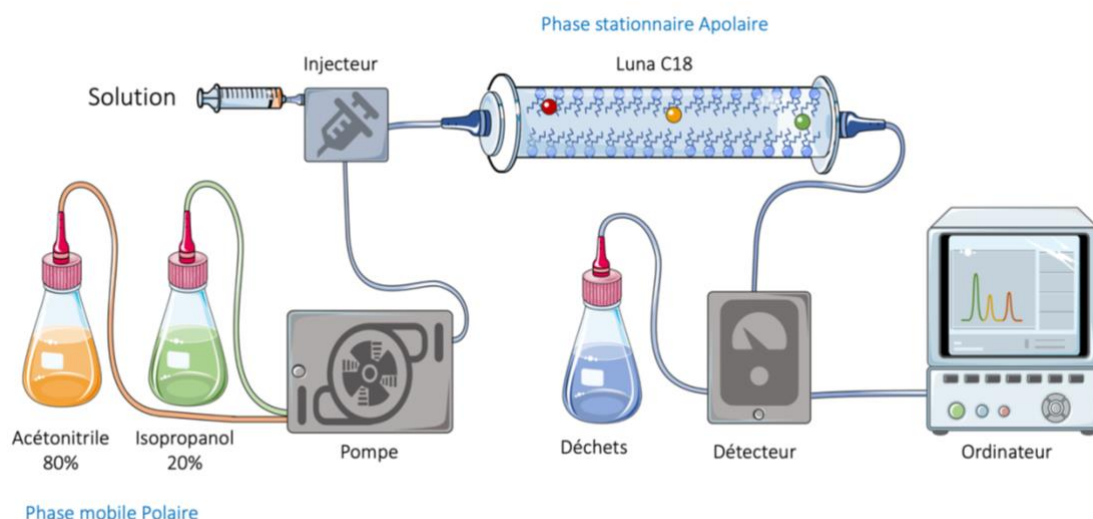


**Figure 28** : Schéma de la technique de chromatographie sur colonne HPLC.

Cette technique a été utilisée pour caractériser la stabilité de la molécule 8.

La caractérisation de la molécule 8 en HPLC nous a permis d'observer entre 2 et 4 minutes le pic correspondant au DMSO, et le pic correspondant à la molécule 8 vers 9m30. Les trois couleurs de courbes correspondent à trois lectures différentes : à 210 nm les structures absorbant en UV tel que les cycles et les chromophores (bleu), en ELSD les structures n'absorbant pas en UV tel que les chaînes carbonées (vert), et la mesure à 292 nm correspondant au maximum d'absorption de la molécule 8 (rouge) (Fig 29).

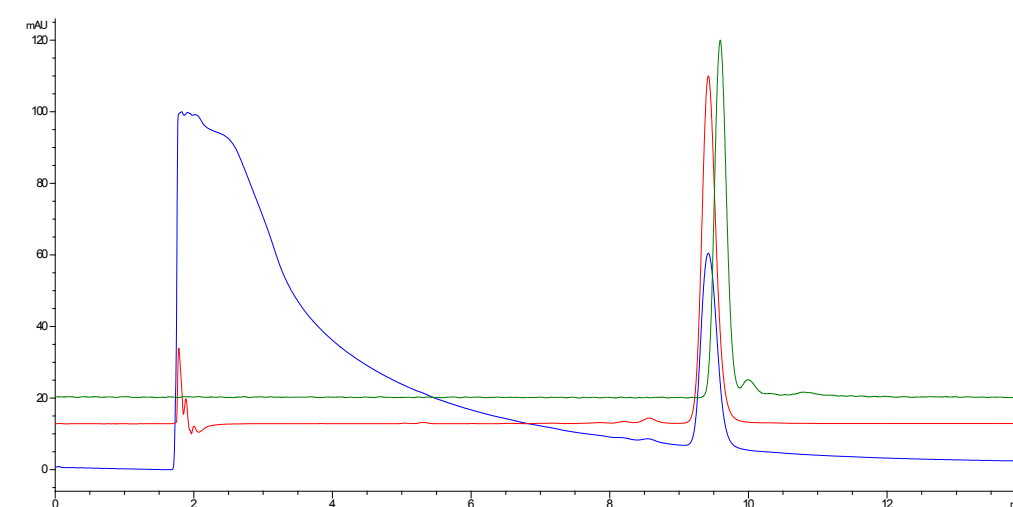


**Figure 29** : Chromatogramme HPLC classique de la Molécule 8.

210 nm : Structures absorbant en UV (cycles) ; ELSD : Structures n'absorbant pas en UV (chaînes carbonées) ; 292 nm : Maximum d'absorption de la molécule 8

On peut observer entre 2 et 4 minutes le pic correspondant au DMSO, puis vers 9m30 un pic unique correspondant à la molécule 8.

Une fois le profil HPLC normal de la molécule 8 obtenu, nous avons voulu savoir s'il était possible, en soumettant cette molécule à différentes conditions de température, d'observer un changement dans le profil HPLC obtenu. Nous avons soumis la molécule à des températures de 50°C et 100°C, en plus de la condition contrôle gardée à 4°C pendant 7 jours, puis nous avons repassé l'échantillon en HPLC. On peut remarquer ici la présence d'une multitude de pics avant le pic de la molécule 8 à 9m30, correspondant à des produits de

dégradation de la molécule 8, que nous n'avons pas lorsque la molécule était gardée à 4°C (Fig 30).

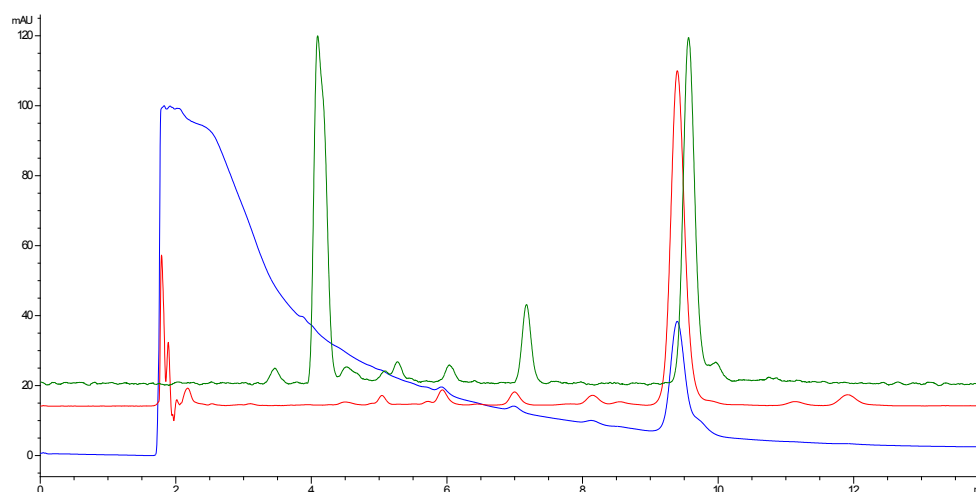


**Figure 30** : Chromatogramme HPLC de la Molécule 8 après 7 jours à 100°C.

210 nm : Structures absorbant en UV (cycles) ; ELSD : Structures n'absorbant pas en UV (chaines carbonées) ; 292 nm : Maximum d'absorption de la molécule 8.

A l'aide du calcul de l'aire sous la courbe, nous avons pu rapporter ces valeurs au pourcentage de molécule présent par rapport au pourcentage initial (Fig 31).

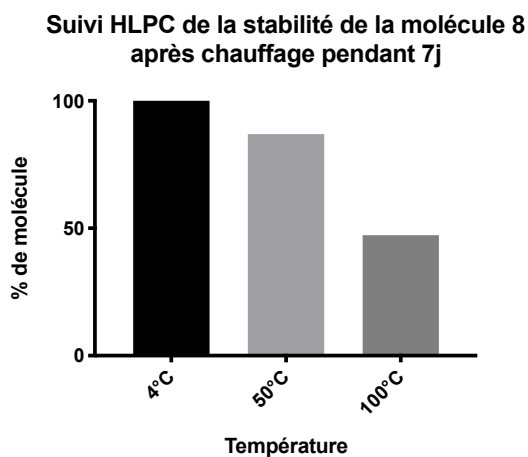


**Figure 31** : Quantification de la stabilité de la molécule 8 en suivi HPLC.

La molécule a été resuspendue à 100 µg/mL, puis soumise à différentes conditions de température.

Après avoir démontré que l'on peut suivre le pourcentage de molécule présent, ainsi que l'apparition de produits de dégradation à l'aide de la méthode d'HPLC, nous avons regardé la stabilité de la molécule dans des conditions d'utilisation normale au laboratoire, en la laissant à température ambiante ou en la soumettant à des cycles de congélation/décongélation successifs (Fig 32).

On peut voir sur la figure que la molécule 8 est très stable dans des conditions d'utilisation normales au laboratoire. On a une tendance à la décroissance du pourcentage de molécule au bout de la 5<sup>e</sup> décongélation, et au bout d'un mois à température ambiante. Ainsi, afin de s'assurer de l'intégrité de la molécule, nous avons réalisé une répartition par petits volumes et nous avons veillé à ne jamais dépasser 5 congélations/décongélation.

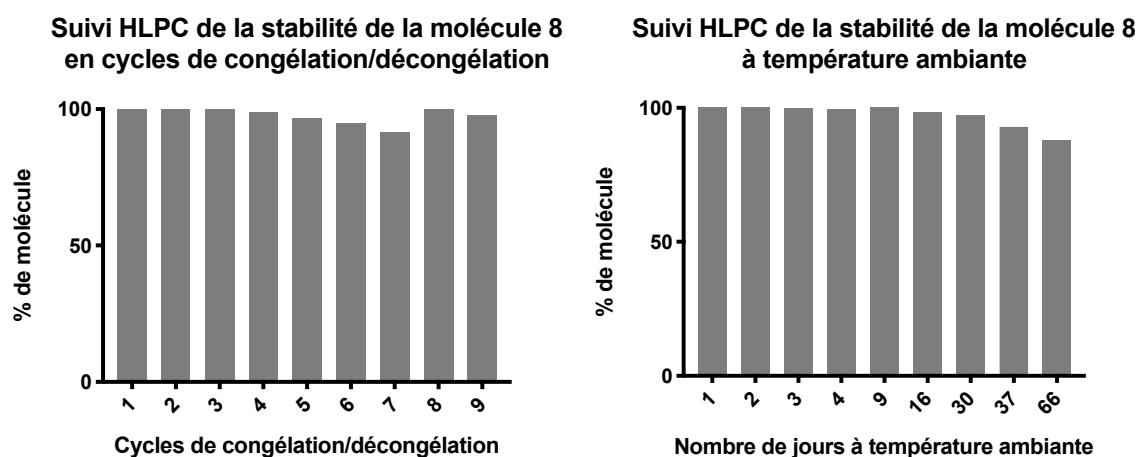


Figure 32 : Intégrité de la molécule 8 au cours du temps.

Après 9 cycles de congélation/décongélation (gauche) ou à température ambiante pendant 66 jours (droite)

### Partie III. Dérivés de la molécule 8

Une fois que la molécule 8 avait été identifiée comme un bon candidat, avec une activité anti-*Leishmania* sur la forme amastigote intracellulaire de *L. infantum*, l'ICN nous a fourni des dérivés de cette molécule afin d'identifier des formes soit moins toxiques, soit plus actives sur les parasites. Les dérivés représentaient les tocophérols, les tocotriénols avec des chaînes carbonées saturées, des dérivés acétate et succinate de la molécule 8 initiale. Il y avait également des formes sans chaîne carbonée et des chaînes carbonées sans cycle pour identifier quelle partie de la molécule médie l'activité anti-*Leishmania* (Fig 33).

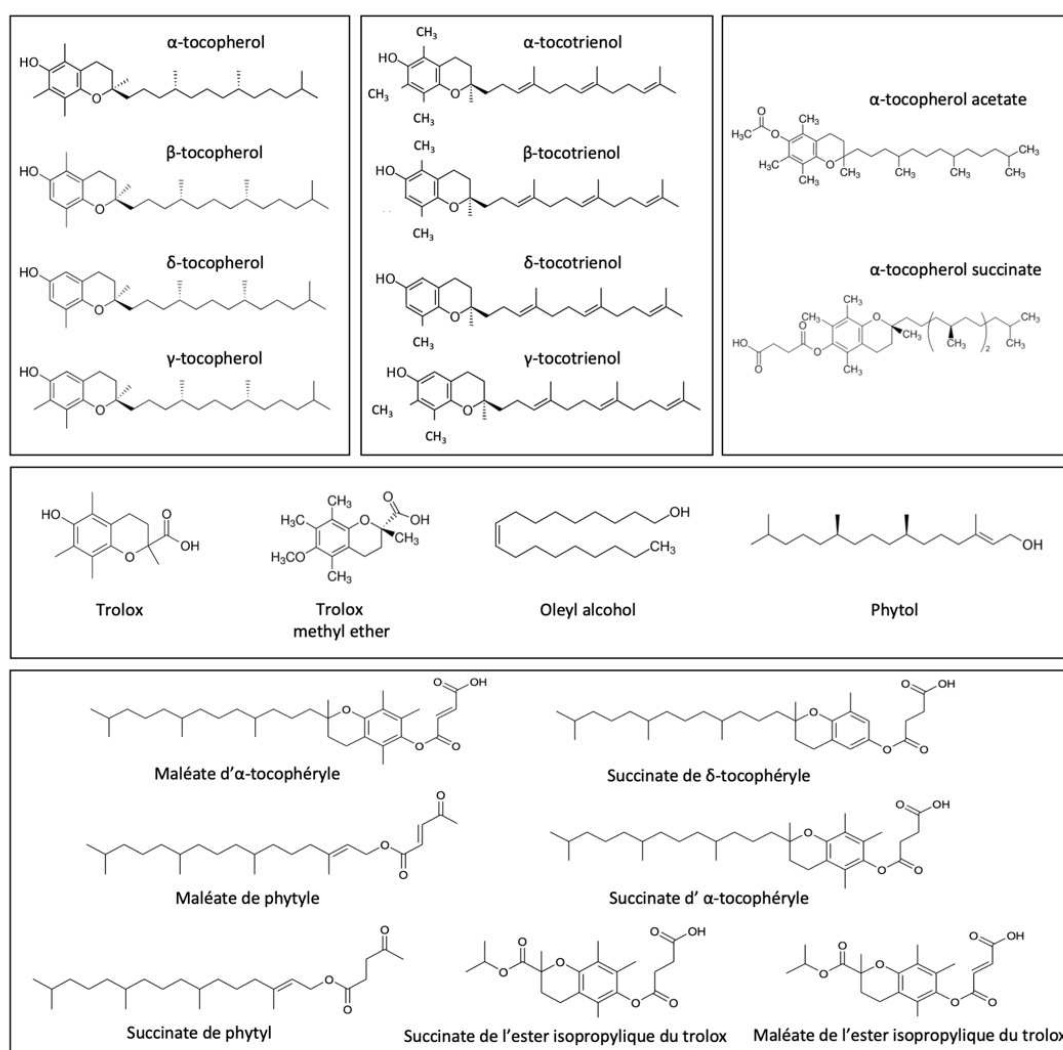
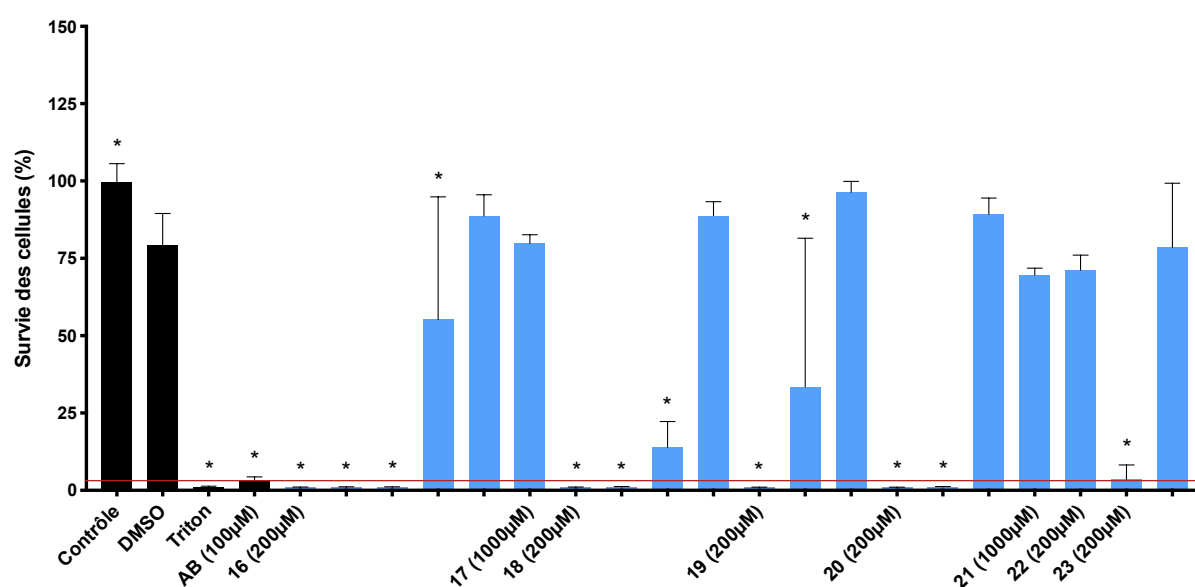
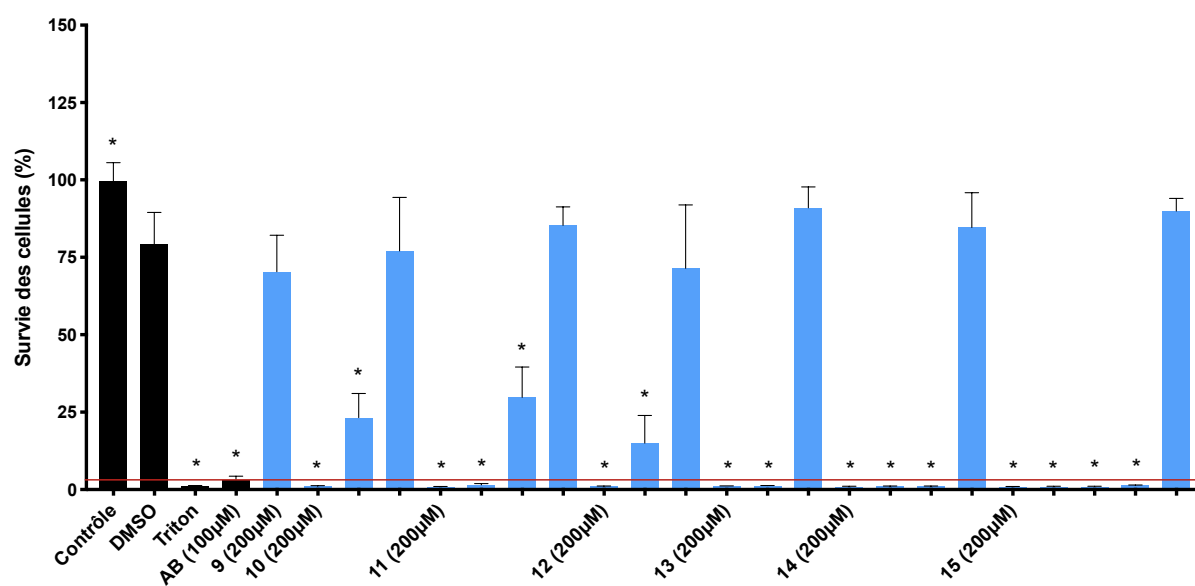
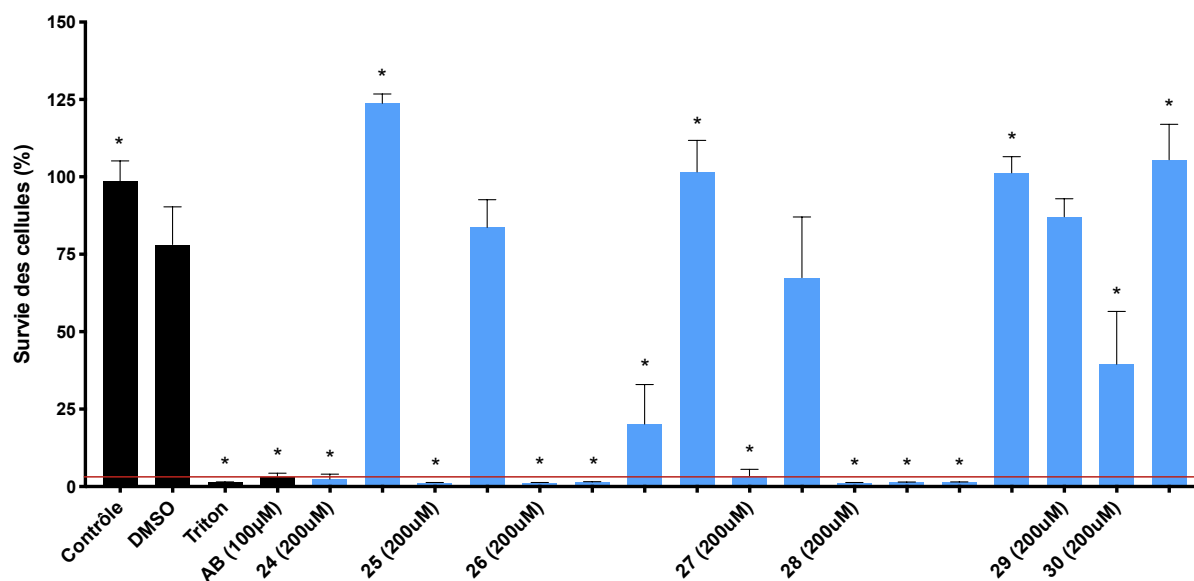


Figure 33 : Structure des dérivés de la molécule 8

### a. Cytotoxicité des dérivés sur cellules BMDM

Dans un premier temps, nous avons déterminé la toxicité des molécules. Cette fois, nous avons cherché à préciser les études en réalisant des dilutions sérielles au demi des molécules depuis 200  $\mu$ M, en montant jusqu'à 1000  $\mu$ M lorsque le dérivé ne montrait aucune toxicité sur la cellule. La plupart des dérivés ont montré une cytotoxicité plus importante que la molécule 8, sauf les molécules 9, 17, 21, 22 et 29 (Fig 34).





**Figure 34** : Cytotoxicité des dérivés sur cellules BMDM

n=3 ; Concentration des extraits : Dilutions au 1/2 à partir de 200 µM ou 1000 µM  
 Test statistique utilisé : Ordinary One-Way ANOVA (par rapport à la condition « DMSO »),  
 comparaisons multiples. Correction Dunnett test \* = <math>< 0,0001</math>  
 La barre rouge correspond à la toxicité du traitement de référence Amphotéricine B

#### b. Effet des dérivés sur la forme promastigote de *L. infantum*

Nous avons ensuite regardé l'effet anti-parasitaire des molécules sur la forme promastigote de *L. infantum*. Nous avons ici utilisé les parasites *L. infantum* teLuc, étant donné que cette souche est plus bioluminescente et permet une meilleure détection des signaux faibles. Comme on pouvait s'y attendre, la plupart des dérivés de la molécule 8, à l'instar de celle-ci, n'ont pas d'effet sur la forme promastigote du parasite. On peut cependant noter que les molécules 20 et 23 ont quant à elles un effet anti-*Leishmania* (Fig 35).

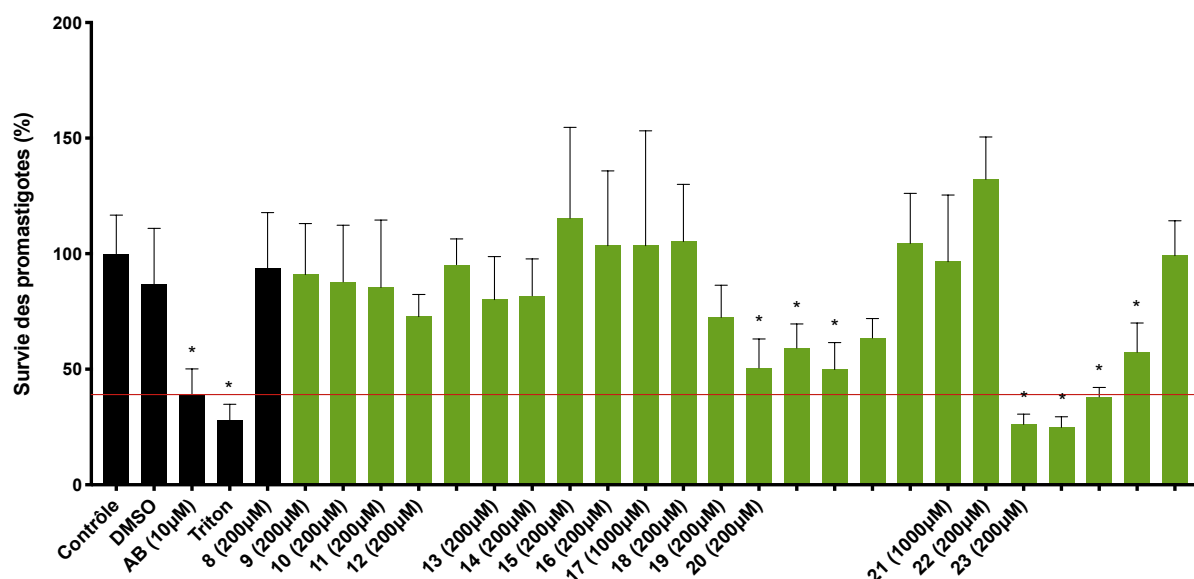


**Figure 35** : Effet des molécules pures sur la forme promastigote de *L. infantum*

n=3 ; Concentration des extraits : Dilutions au 1/2 à partir de 200 µM ou 1000 µM.

Test statistique utilisé : One-Way ANOVA (par rapport à la condition « DMSO »), non paramétrique, Kruskal-Wallis, Dunn non corrigé. \*= $<0,05$ .

La barre rouge correspond à la toxicité du traitement de référence Amphotéricine B

### c. Calcul de l'Indice de Sélectivité

Les tests de cytotoxicité sur les cellules BMDM ainsi que les tests d'activité contre la forme promastigote de *L. infantum* nous ont par la suite permis de réaliser un tableau récapitulatif de ces résultats, ainsi que de calculer l'indice de sélectivité des composés sur les promastigotes. L'indice de sélectivité correspond à la division de la valeur de  $CC_{50}$  par  $IC_{50}$ . Ainsi cet indicateur rend compte de l'efficacité d'un composé par rapport à sa toxicité. Si l'indice de sélectivité est supérieur à 1, le composé est toxique sur la cellule alors qu'il n'est pas actif contre le pathogène. Plus il sera donc proche de 0, plus le composé sera efficace contre le pathogène à des concentrations non cytotoxiques. Les indices de sélectivité de chaque dérivé sont indiqués dans le tableau ci-contre (Fig 36) :



	Cytotoxicité CC <sub>50</sub> (μM)	Promastigote IC <sub>50</sub> (μM)	Promastigote SI
8	> 1000	> 1000	Nd.
9	> 200	> 200	Nd.
10	77,69		> 1
11	44,52		
12	68		
13	63,3		
14	30,43		
15	16,86		
16	26,57		
17	> 1000	> 1000	
18	37,74	> 200	> 1
19	~ 97,12		
20	63,3	16,54	0,26
21	> 1000	> 1000	Nd.
22	> 200	> 200	
23	~ 108,2	21,77	0,2
24	~ 174,9	En cours	
25	121,1		
26	~ 46,71		
27	113,9		
28	~ 42,20		
29	> 200		
30	~ 195,7		

**Figure 36** : Tableau récapitulatif des valeurs de CC<sub>50</sub>, IC<sub>50</sub> et SI

L'IC<sub>50</sub> est calculée pour la forme promastigote et a servi pour le calcul de l'indice de sélectivité des dérivés de la molécule 8 (SI = IC<sub>50</sub> / EC<sub>50</sub>)

Sur la première partie de molécules testées, de 9 à 23, la majorité des molécules ont montré un SI supérieur à 1, indiquant qu'elles sont plus toxiques sur les cellules que sur les promastigotes. Certaines molécules, comme la 9, 17, 21 et 22 ont un indice de sélectivité « Nd. », car elles ne sont ni toxiques sur les BMDM ni actives contre la forme promastigote.

Seules les molécules 20 et 23 ont montré un SI inférieur à 1, indiquant qu'elles possèdent un effet anti-parasitaire sans montrer de toxicité sur les BMDM.

La seconde partie des dérivés de 24 à 30 ont été obtenus plus tard. Les valeurs de  $CC_{50}$  ont déjà été calculées, cependant les expérimentations pour déterminer leur effet sur la forme promastigote restent à réaliser.

## Partie IV. Premiers essais *in vivo*

Dans le cadre de la collaboration avec la SATT Sud-Est, nous avons obtenu une pré-maturation pour le projet de recherche sur la molécule 8, et une pré-maturation de la part de l'Université Cote d'Azur, Académie 4, ce qui nous a permis de réaliser une première série d'expérimentations *in vivo* afin de déterminer si l'effet anti-*Leishmania* de la molécule est visible dans l'organisme entier dans un modèle murin de leishmaniose viscérale. Pour ce faire, nous avons testé 2 façons différentes d'administrer la molécule : en traitement préventif ou curatif.

### a. Prévention

Le premier protocole de prévention visait à savoir si la prise de molécule 8 pouvait prévenir ou diminuer l'installation de l'infection dans le foie et dans la rate de souris Balb/c. Les souris ont été traitées pendant 5 jours par voie orale (gavage) avec des doses croissantes de molécule 8. Nous avons donc administré aux souris des doses de 2000, 4000 et 6000mg/kg administrées de façon cumulée sur 5 jours de gavage par voie orale (400, 800 et 1200 mg/kg/jour respectivement pour les doses cumulées). Après pré-traitement, les souris ont été infectées par voie Intra Veineuse (IV) avec  $3 \times 10^8$  leishmanies *L. infantum*-Luc. La bioluminescence émise a été monitorée entre J1 et J38 post infection afin d'observer l'installation de l'infection.

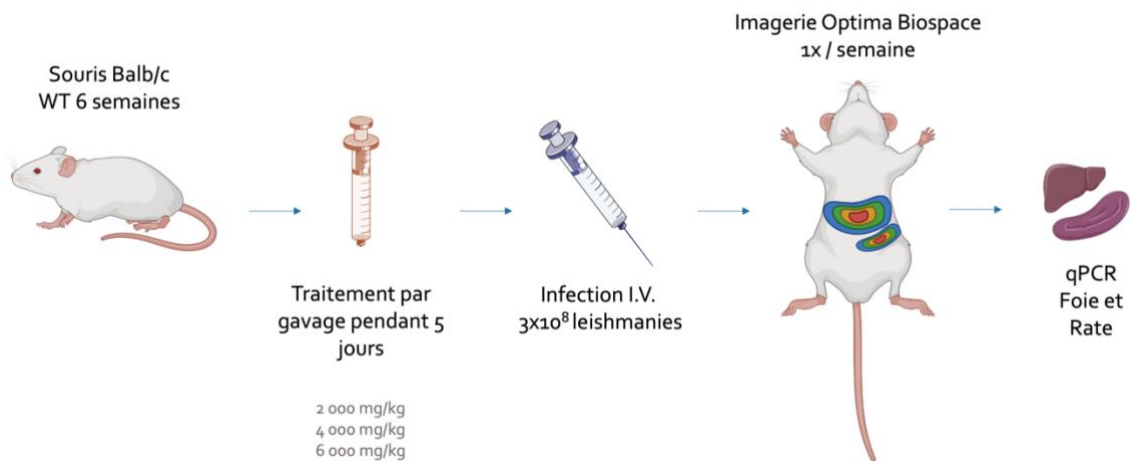


Schéma créé avec BioRender et SMART - Servier medical art

Figure 37 : Schéma expérimental du protocole de prévention à l'aide de la molécule 8

On peut observer que globalement, les souris pré-traitées avec la molécule 8 ont une charge parasitaire moins importante dans le foie et dans la rate par rapport aux contrôles. L'image montre des souris représentatives de chaque groupe (Fig 37), et l'émission de bioluminescence a été quantifiée dans le foie et dans la rate (Fig 38). On peut observer que comparé à la condition contrôle, le traitement à 6000 mg/kg avec la molécule 8 mène à une diminution par 2 de la bioluminescence quantifiée dans le foie à J18 et dans la rate à J38, indiquant que le pré-traitement a eu un effet sur l'installation de l'infection dans ces souris.

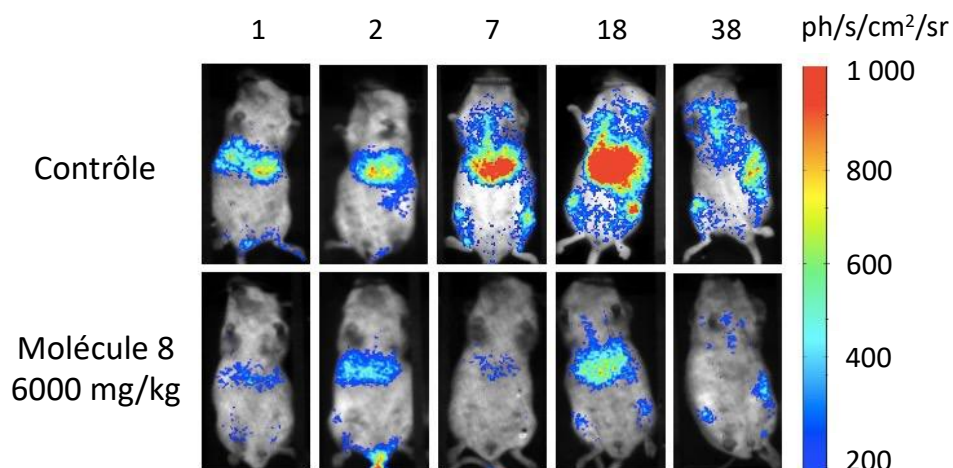
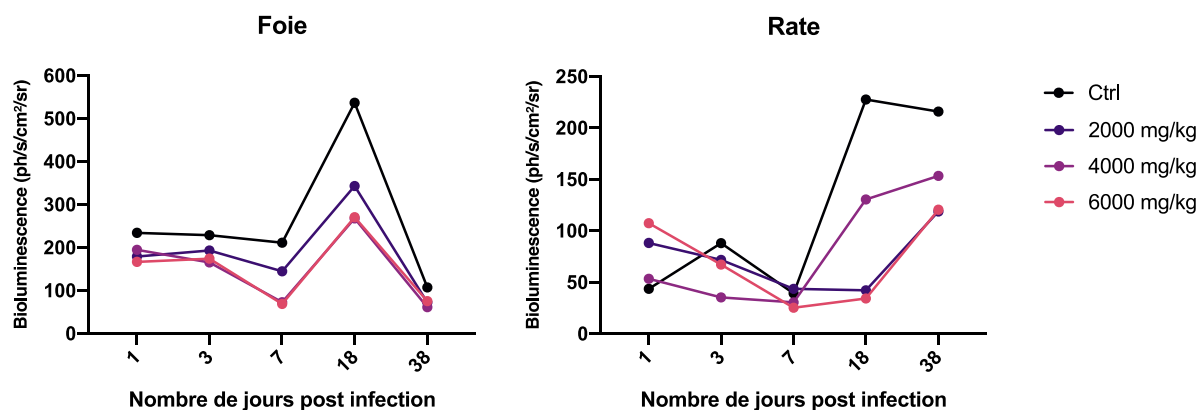


Figure 38 : Souris représentatives des groupes traités ou non avec la molécule 8 après infection à *L. infantum*



**Figure 39** : Effet du pré-traitement avec la Molécule 8 sur l'infection de souris à *L. infantum*

La bioluminescence émise a été quantifiée sur le foie et la rate de souris pré-traitées pendant 5 jours avec la molécule 8. Pour chaque groupe, la courbe représente la moyenne de 3 souris pour les conditions pré-traitées, et 2 souris dans la condition contrôle.

#### b. Traitement

Le second protocole visait à déterminer si dans un modèle de leishmaniose viscérale installée, le traitement curatif avec la molécule 8 était efficace à des doses de 2000, 4000 et 6000mg/kg administrées de façon cumulée sur 5 jours de gavage par voie orale. Des souris Balb/c âgées de 6 semaines ont été infectées par voie IV avec  $3 \times 10^8$  leishmanies *L. infantum*-Luc. La bioluminescence émise au niveau du foie a été contrôlée à 3 semaines post-infection, lorsque les leishmanies ont commencé leur installation dans la rate mais que l'infection dans le foie est encore visible. Le gavage a été réalisé pendant 5 jours puis nous avons observé la bioluminescence dans les organes avant le gavage, puis à 3, 11 et 18 jours post gavage (Fig 39).

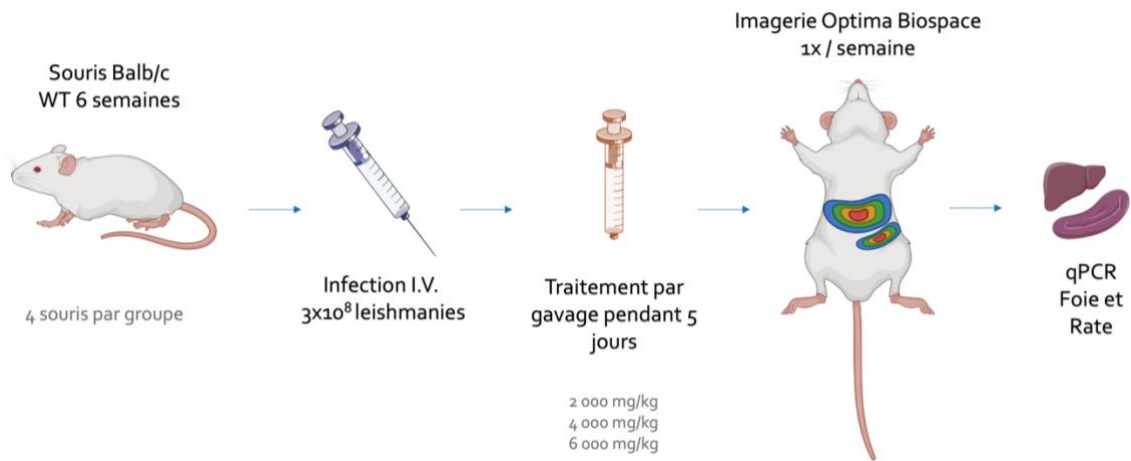
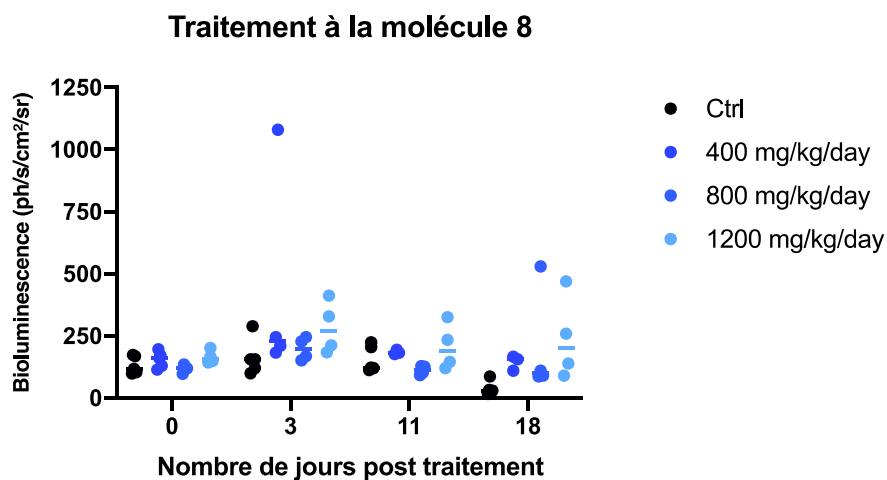


Schéma créé avec BioRender et SMART - Servier medical art

**Figure 40** : Schéma expérimental du protocole de traitement de souris avec la molécule 8

Nous avons pu observer que dans ces conditions, il n'y avait aucune différence entre les groupes contrôle et les groupes traités.



**Figure 41** : Effet du traitement avec la Molécule 8 sur l'infection de souris à *L. infantum*

La bioluminescence émise a été quantifiée sur souris entières traitées pendant 5 jours avec la molécule 8, qui avaient été infectées à *L. infantum* 3 semaines auparavant. Pour chaque groupe traité, 3-5 souris sont suivies au cours du temps.

## IV. Discussion

En l'absence de vaccin préventif contre la leishmaniose humaine, la chimiothérapie est la seule option disponible pour lutter contre cette maladie. Cependant, le nombre de composés anti-*Leishmania* disponibles en clinique reste relativement faible. Un problème majeur dans le développement de nouveaux composés potentiellement efficaces contre la leishmaniose est la recherche de fonds (Craig *et al.*, 2021). En effet, les populations principalement touchées étant généralement assez pauvres, les grandes entreprises pharmaceutiques considèrent la leishmaniose comme un marché de niche. Pourtant, les changements climatiques en cours aboutissent à une expansion des zones d'endémies et c'est pour cela que l'OMS considère la leishmaniose comme une maladie réémergente et que la mise au point de nouveaux traitements est aujourd'hui nécessaire (Short, Caminade, & Thomas, 2017). Le processus de découverte des molécules comprend de nombreuses étapes avant d'aboutir à un nouveau médicament pour traiter une maladie spécifique, et ce processus est coûteux et prend du temps. Par conséquent, de nombreuses stratégies ont été développées pour optimiser le coût en temps et en argent.

La première consiste à utiliser des banques de molécules et tester automatiquement un grand nombre de molécules chimiques. Dans ce type d'approche, des techniques automatisées sont utilisées pour tester des composés. Les échanges hydrogène/deutérium couplés à la spectrométrie de masse (HDX-MS) et aux bibliothèques de fragments sont des techniques qui jouent un rôle essentiel dans cette stratégie. HDX-MS est une approche bien adaptée pour étudier les altérations de la conformation des protéines induites par la liaison de petites molécules aux ligands (Marciano, Dharmarajan, & Griffin, 2014). Les progrès récents de la microscopie automatisée ont la capacité d'augmenter le débit des criblages en remplaçant les observations microscopiques manuelles laborieuses par une imagerie à haut débit, et cette technique est utilisée avec succès dans le dépistage *in vitro* d'organismes entiers contre les parasites kinétoplastides vivants (Siqueira-Neto *et al.*, 2012). Les outils bio-informatiques qui prédisent le potentiel du composé en tant que médicament, tels que les règles de Lipinski (Lipinski, Lombardo, Dominy, & Feeney, 2001), ainsi que d'autres outils qui prédisent l'interaction de ce composé avec les protéines (tests d'amarrage), fournissent des données

solides pour aider à choisir des tests cellulaires à effectuer et permettre l'exclusion de certains composés s'ils ne présentent pas de bons résultats *in silico*. Les bibliothèques de fragments de molécules permettent également d'identifier des composés plus petits qui se lient à différentes parties d'une cible biologique et permet ainsi de trouver rapidement des familles de composés et de fragments utilisables pour traiter les maladies. La justification principale d'utiliser les banques est que les hits identifiés donnent accès à un espace chimique plus large tout en criblant un nombre limité de composés (Schulz, Landström, Bright, & Hubbard, 2011). La seconde approche réutilise ou modifie des molécules existantes. Pour cela, les plateformes de familles de gènes, les bibliothèques de composés, les modèles informatiques, la biologie structurale et les tests cellulaires et biochimiques sont largement utilisés pour évaluer si une molécule existante peut être redirigée comme traitement contre la leishmaniose (Lage *et al.*, 2018).

Enfin la troisième approche consiste à étudier les médicaments qui sont connus pour cibler une voie de signalisation cellulaire impliqué dans la destruction des leishmanies (Moffat, Vincent, Lee, Eder, & Prunotto, 2017).

Nous avons développé dans notre laboratoire une stratégie supplémentaire en utilisant les déchets de la parfumerie. Dans un contexte grandissant d'économie circulaire, et de renforcement des démarches écoresponsable au sein de notre société, l'utilisation des parties de plantes non utilisés en parfumerie nous a paru être une bonne alternative. C'est ainsi qu'une plante locale, l'argousier, a été sélectionnée pour son effet anti-*Leishmania*. Après séparation des différents composés chimiques de cette plante et leur caractérisation, par l'ICN, une série de test *in vitro* a permis d'évaluer leur cytotoxicité, leur effet sur la forme promastigote extracellulaire du parasite et sur la forme amastigote intracellulaire. Plus d'une dizaine de fractions ont montré une action directe sur la forme promastigote. Les molécules contenues dans ces fractions seront intéressantes pour les formulations de crèmes préventives, qui pourront être utilisées dans les zones d'endémie. Mais seulement une molécule, la molécule 8, a permis d'obtenir une diminution de la charge parasitaire dans les cellules hôtes, sans avoir d'effet direct sur les promastigotes. Les résultats du profil cytokinique ont montré qu'en présence de la molécule 8, il y avait une immunomodulation de la réponse cellulaire face à la présence de parasites. Nous avons pu observer une



augmentation de chémokines recrutant des macrophages et des cellules NK (MIP-1 $\alpha$ , MIP-1 $\beta$ , CCL5), et des monocytes inflammatoires (MCP-5 et JE), et une diminution du recrutement de neutrophiles (MIP-2 et KC). Les neutrophiles sont les premières cellules recrutées au site de l'infection (Elmahallawy, Alkhaldi, & Saleh, 2021). Elles ont un rôle très dépendant de l'espèce de la leishmanie dans la progression de la maladie, qui peut être protecteur comme dans le cas de *L. amazonensis*, ou être à l'origine d'une progression de l'inflammation comme dans le cas des parasites conférant une forme viscérale, *L. donovani* ou *L. infantum* (Gabriel, McMaster, Girard, & Descoteaux, 2010). La régulation des cytokines des voies Th1 et Th2 ne permet pas de mettre en évidence un biais vers l'une ou l'autre de ces voies, mais plutôt un équilibre, nécessaire à la bonne résolution de l'infection. La diminution de cytokines attirant des cellules nuisibles pour la résolution de l'infection comme les neutrophiles, et la diminution des cytokines de la voie Th17 qui possède également un rôle controversé, nous permettent d'émettre l'hypothèse que la molécule 8 semble avoir un rôle prometteur dans le cours de l'infection (Rossi & Fasel, 2018).

Même si, pour l'instant, les traitements basés sur l'activation du système immunitaire de l'hôte se sont avérés peu efficaces dans le contrôle de la leishmaniose viscérale par rapport à une chimiothérapie conventionnelle (Ratnapriya, Keerti, Yadav, Dube, & Sahasrabudde, 2021), l'intérêt d'avoir une molécule avec des effets stimulateurs de l'immunité de l'hôte paraît être une solution au problème de résistance qui apparaît dans les traitements actuels (Ponte-Sucre *et al.*, 2017).

Pour mieux comprendre comment fonctionne la molécule 8 nous avons étudié les dérivés de ce composé. Cette stratégie nous a permis d'isoler des molécules proches et de déterminer quelle partie de la molécule pouvait être responsable de l'élimination des leishmanies intracellulaires. L'étude *in vitro* de notre molécule d'intérêt s'est poursuivie par une étude *in vivo*. La première difficulté a été de choisir la voie d'administration. La première voie était la possibilité d'ajouter notre molécule d'intérêt à l'eau de boisson. Le problème est que cette molécule est très peu soluble dans l'eau, et que nous ne pouvions contrôler la quantité exacte de molécule ingérée par chaque souris. La mauvaise solubilité en eau de la molécule 8 est aujourd'hui en cours d'étude dans le laboratoire. Le problème a été le même lorsque nous avons voulu utiliser des croquettes supplémentées avec notre molécule d'intérêt, puisque

sous l'effet de la hiérarchie créée dans chaque cage, la prise de nourriture différentielle pouvait aboutir à une grande variabilité inter-individu. C'est pour cela que nous avons choisi d'utiliser la méthode de gavage des souris, afin de mieux contrôler l'ingestion de notre molécule. D'après les premiers résultats, la molécule 8 semble avoir un effet préventif au développement de l'infection. Mais cette étude *in vivo* nécessitera encore certains ajustements tel que la fréquence du gavage, les quantités fournies et la nécessité ou non d'arrêter le traitement après l'infection réalisée. Des études en cours permettront certainement de répondre à ces questions.

Finalement, les parasites *Leishmania* ont donc été utilisés comme modèle dans ma thèse, mais les travaux présentés devront certainement être adaptés et étudiés dans d'autres modèles de pathogènes intracellulaire afin de pouvoir déposer un brevet sur des traitements capables de moduler la réponse immunitaire de l'hôte, permettant ainsi l'élimination d'un grand nombre de pathogènes. En effet, des études sur des bactéries intracellulaires comme *Salmonella* ou *Listeria*, devront être réalisées. La réalisation de ces études sera normalement facilitée par le fait que la culture des bactéries par rapport aux leishmanies prend moins de temps et que leur cycle de vie est en général plus simple. En effet, la recherche de nouveaux traitements contre la leishmaniose nécessite de prendre en compte les 2 états principaux des leishmanies, promastigote et amastigote, ce qui fait que le nombre de tests à effectuer est deux fois plus important. Un dépôt de brevet est donc entrepris mais nécessitera de pouvoir fournir des résultats complémentaires sur d'autres pathogènes dans les mois à venir.



# Conclusion et perspectives



Au cours de ma thèse, j'ai eu l'occasion d'étudier le parasite *Leishmania infantum*, responsable de la leishmaniose viscérale. Cette maladie, en dépit de l'existence de traitements, fait encore 30 000 morts par an, principalement à cause de la mauvaise accessibilité au traitement dans les pays en voie de développement. En effet, l'observance du traitement n'est pas toujours respectée car les personnes malades doivent se déplacer à l'hôpital pour des injections invasives des composés, qui sont en plus de cela toxiques. Le traitement le plus efficace et le moins toxique est l'amphotéricine B sous sa forme liposomale, mais le coût élevé de cette formulation limite son application aux pays les plus riches. Outre ces problèmes de prix, de toxicité et d'administration invasive, des résistances à tous les traitements disponibles apparaissent aujourd'hui (Ponte-Sucre *et al.*, 2017).

C'est pour cela qu'il est aujourd'hui indispensable de trouver de nouveaux traitements.

Dans la recherche de traitements contre la leishmaniose, deux grandes problématiques se posent : il faut de nouvelles molécules antiparasitaires pour lutter contre la maladie, et il faut des outils permettant d'identifier des composés anti-*Leishmania* de façon simple et rapide, afin de pouvoir cribler un nombre important de composés.

En intégrant ces deux problématiques, ma thèse a été divisée en deux grands axes :

- Construire de nouvelles souches rapportrices de *Leishmania*
- Trouver de nouveaux composés anti-microbiens pour lutter contre le parasite

La construction de nouvelles souches rapportrices a été un projet long, intégrant beaucoup d'étapes : le choix des vecteurs d'expression, le choix des gènes rapporteurs, l'élaboration des plasmides et leur construction, la transformation et l'intégration des constructions dans les leishmanies puis leur sélection, et enfin les tests des souches obtenues.

De la construction à l'obtention d'une souche prête pour les tests *in vitro* il faut compter 1 mois et demi lorsque toutes les étapes se passent sans encombre, car la sélection d'un seul clone par technique de dilution limite, et l'amplification de ce dernier sont des étapes longues lorsque l'on se base sur le cycle de vie de *Leishmania*.

Nous avons rencontré d'importants problèmes dans la sélection des souches fluorescentes, avec des problèmes de pKa et de sensibilité à l'acide de la protéine mMaroon1, la perte de la

protéine mRuby au cours des générations. Pour l'instant, la meilleure alternative fluorescente reste la souche GFP précédemment caractérisée. Les souches bioluminescentes ou doublement transformées ont montré de bons résultats *in vitro* mais ont montré des limites d'utilisation *in vivo*. L'accessibilité du substrat pour la souche teLuc n'a pas permis d'observer de signal bioluminescent dans l'animal. En ce qui concerne la souche eFFly-mCherry, la durée de persistance dans l'animal semble être limitée. En somme, la souche teLuc est très prometteuse, mais il faudra résoudre le problème de solubilité du substrat afin de possiblement obtenir un signal bien plus important que la souche Luc, qui reste aujourd'hui la meilleure alternative.

Cependant, même si nous n'avons pas pour le moment obtenu une souche capable de dépasser les problématiques actuelles des souches rapportrices de *Leishmania*, la mise en place du protocole de construction des inserts avec la méthode d'IN-FUSION permet un gain de temps considérable, et nécessite seulement la commande d'un insert et son amplification avec des amorces homologues, puis l'étape d'assemblage, réduisant le temps nécessaire pour la construction. A l'aide de ces protocoles et des outils disponibles, une étudiante en master poursuivra la création de souches rapportrices afin d'essayer d'obtenir une souche doublement transformée, efficace *in vivo* et *in vitro*.

Le travail réalisé dans le cadre de l'identification de nouvelles molécules anti-*Leishmania* est sans doute le projet qui m'a le plus appris. La collaboration avec les Chimistes de l'ICN m'a donné la possibilité d'assister à des extractions de plantes, et de me familiariser avec une discipline autre que la biologie. Si le projet initial partait d'une idée de crible bioguidé, et d'identification de nombreuses molécules à tester sur *Leishmania infantum*, nous avons obtenu très tôt dans le projet un hit intéressant, la molécule 8, et nous avons interrompu le crible afin de nous concentrer sur cette molécule prometteuse.

Grâce à la collaboration et l'échange avec l'ICN, j'ai eu la possibilité de réaliser moi-même les expérimentations de stabilité de la Molécule 8 en HPLC, et ainsi d'obtenir des connaissances techniques sur les méthodes utilisées pour identifier et caractériser les composés.

Notre collaboration avec la SATT Sud-Est m'a aussi permis de voir comment il était possible de valoriser les résultats issus de la recherche, et actuellement, un dépôt de brevet est en

cours. Cependant, étant donné que la leishmaniose est un marché de niche, nous nous sommes heurtés à des limitations dans l'intérêt de différentes compagnies quant à l'application sur la leishmaniose. Finalement, les composés que nous cherchons à identifier dans ce crible sont des composés non actifs sur la forme promastigote, mais actifs sur la forme amastigote intracellulaire. Ceci sous-entend que nous essayons d'identifier des composés sans activité directe sur le parasite, car ces composés peuvent donner lieu à l'apparition de résistances, mais que nous cherchons à stimuler l'activité anti-microbienne de la cellule en identifiant des immuno-stimulateurs. De ce fait, nous avons mis en évidence que la molécule 8 est capable de moduler la sécrétion cytokinique. Il serait intéressant de poursuivre les études mécanistiques sur ce composé afin d'identifier les voies d'action de cette molécule et leur effet sur les voies classiques d'élimination de pathogènes intracellulaires, l'Oxide Nitrique (NO) et les Espèces Réactives de l'Oxygène (ROS). Le caractère immunomodulateur de cette molécule laisserait présager que son activité n'est pas spécifique à *Leishmania*, mais pourrait être généralisée à d'autres pathogènes. Ainsi *Leishmania infantum* nous sert de modèle pour identifier des composés immuno-stimulateurs, qui pourront ensuite être testés sur d'autres intracellulaires. D'un point de vue valorisation, son utilisation potentielle contre la maladie de Lyme a été une des pistes suggérées.

Les premiers essais *in vivo* ont permis de montrer que la molécule 8 ne semblait pas avoir d'effet en traitement pendant une semaine, sur une infection installée chez la souris. Cependant, en pré-traitement, elle a montré une diminution de la charge parasitaire dans les souris à des doses de 2 000 à 6 000 mg/kg. Ces résultats préliminaires devront être reproduits sur un nombre plus important de souris, cependant nous devons auparavant résoudre le problème de solubilité de la molécule, afin de mieux contrôler les doses administrées. Nous sommes actuellement en train d'étudier la possibilité de formuler cette molécule sous forme de croquettes. L'étude de brevetabilité de la SATT Sud-Est a révélé que des dérivés de la molécule 8 se trouvaient déjà dans certaines marques de nourriture pour chiens souffrant de Leishmaniose « Advance Veterinary Diets Leishmaniasis » de Affinity Pet care même s'il s'agissait de suppléments, et pas directement de composés favorisant la réduction de la charge parasitaire. Nous proposons ici d'utiliser ce composé en plus grande quantité, au vu de



sa très faible toxicité, et de préconiser ces croquettes en prise préventive dans des zones endémiques de la maladie. Il est cependant intéressant de noter et de garder en tête que certaines études ont mis en évidence une croissance favorisée du parasite en présence de la molécule 8 chez des hamsters (Garg, Singh, & Dube, 2004) et qu'il est donc important de surveiller l'effet de cette supplémentation à long terme dans l'animal.

Au cours de ma thèse, j'ai également rédigé une revue de la littérature sur les différentes stratégies de recherche de traitement contre la leishmaniose, qui m'ont permis de me familiariser avec un nombre important de méthodes visant à améliorer l'efficacité d'un composé. Ainsi, l'une des pistes pour la solubilisation de la molécule 8 pourrait être son intégration dans des liposomes composés de lipides d'origine végétale (Iman, Huang, Alavizadeh, Szoka, & Jaafari, 2017), ce qui limiterait son coût tout en favorisant son administration. De plus, il pourrait être envisagé de combiner cette molécule avec des traitements de référence afin de limiter la concentration des chémo-thérapies et donc limiter le coût et les effets secondaires néfastes tout en appliquant cette molécule dans le cadre de traitements.

Finalement, la collaboration avec l'ICN sera poursuivie à l'issue de cette thèse afin de poursuivre le crible de composés. La mise en place récente d'un protocole permettant la séparation sur plaque de fractions entières de plante, puis le test biologique sur la forme promastigote et amastigote de *Leishmania* pourrait être appliquée dans le futur, afin d'accélérer encore plus la recherche de nouvelles molécules en contournant les étapes longues de fractionnement aujourd'hui nécessaires (voir article en collaboration annexé : « New method for screening anti-Leishmania compounds in plants extracts by HPTLC-bioautography »).

En somme, mon projet de thèse m'a permis de travailler en collaboration avec le monde de la chimie et de la valorisation de la recherche. J'ai pu adresser les deux grands problèmes de disponibilité de souches rapportrices et de molécules anti-*Leishmania* au cours de mon projet, qui se poursuivra à l'issue de cette thèse avec d'autres étudiant-e-s.

# Bibliographie



- Alcover, M. M., Riera, M. C., & Fisa, R. (2021). Leishmaniosis in Rodents Caused by *Leishmania infantum*: A Review of Studies in the Mediterranean Area. *Front Vet Sci*, *8*, 702687. doi:10.3389/fvets.2021.702687
- Alemayehu, B., & Alemayehu, M. (2017). Leishmaniasis: a review on parasite, vector and reservoir host. *Health Science Journal*, *11*(4), 1.
- Bourdoiseau, G. (2015). La leishmaniose canine à *Leishmania Infantum* actualités épidémiologiques–applications. *Bulletin de l'Académie Vétérinaire de France*.
- CDC. (2020). Parasites - Leishmaniasis. Retrieved from <https://www.cdc.gov/parasites/leishmaniasis/epi.html>
- Chagas, A. C., Oliveira, F., Debrabant, A., Valenzuela, J. G., Ribeiro, J. M. C., & Calvo, E. (2014). Lundep, a sand fly salivary endonuclease increases *Leishmania* parasite survival in neutrophils and inhibits XIa contact activation in human plasma. *PLoS pathogens*, *10*(2), e1003923.
- Craig, E., Calarco, A., Conte, R., Ambrogi, V., d'Ayala, G. G., Alabi, P., . . . Kima, P. E. (2021). Thermoresponsive Copolymer Nanovectors Improve the Bioavailability of Retrograde Inhibitors in the Treatment of *Leishmania* Infections. *Front Cell Infect Microbiol*, *11*, 702676. doi:10.3389/fcimb.2021.702676
- Dias, Á. F. L. R., Ayres, E. D. C. B. S., de Oliveira Martins, D. T., Maruyama, F. H., de Oliveira, R. G., de Carvalho, M. R., . . . Sousa, V. R. F. (2020). Comparative study of the use of miltefosine, miltefosine plus allopurinol, and allopurinol in dogs with visceral leishmaniasis. *Exp Parasitol*, *217*, 107947. doi:10.1016/j.exppara.2020.107947
- Dipineto, L., Manna, L., Baiano, A., Gala, M., Fioretti, A., Gravino, A. E., & Menna, L. F. (2007). Presence of *Leishmania infantum* in red foxes (*Vulpes vulpes*) in southern Italy. *J Wildl Dis*, *43*(3), 518-520. doi:10.7589/0090-3558-43.3.518
- Dube, A., Gupta, R., & Singh, N. (2009). Reporter genes facilitating discovery of drugs targeting protozoan parasites. *Trends Parasitol*, *25*(9), 432-439. doi:10.1016/j.pt.2009.06.006
- Elmahallawy, E. K., Alkhalidi, A. A. M., & Saleh, A. A. (2021). Host immune response against leishmaniasis and parasite persistence strategies: A review and assessment of recent research. *Biomedicine & Pharmacotherapy*, *139*, 111671.
- Gabriel, C., McMaster, W. R., Girard, D., & Descoteaux, A. (2010). *Leishmania donovani* promastigotes evade the antimicrobial activity of neutrophil extracellular traps. *The Journal of Immunology*, *185*(7), 4319-4327.
- Garg, R., Singh, N., & Dube, A. (2004). Intake of nutrient supplements affects multiplication of *Leishmania donovani* in hamsters. *Parasitology*, *129*(Pt 6), 685-691. doi:10.1017/s0031182004006055
- Iatta, R., Furlanello, T., Colella, V., Tarallo, V. D., Latrofa, M. S., Brianti, E., . . . Schunack, B. (2019). A nationwide survey of *Leishmania infantum* infection in cats and associated risk factors in Italy. *PLoS neglected tropical diseases*, *13*(7), e0007594.
- Iman, M., Huang, Z., Alavizadeh, S. H., Szoka, F. C., & Jaafari, M. R. (2017). Biodistribution and In Vivo Antileishmanial Activity of 1,2-Distigmasterylhemisuccinoyl-sn-Glycero-3-Phosphocholine Liposome-Intercalated Amphotericin B. *Antimicrob Agents Chemother*, *61*(9). doi:10.1128/AAC.02525-16
- Lage, O. M., Ramos, M. C., Calisto, R., Almeida, E., Vasconcelos, V., & Vicente, F. (2018). Current Screening Methodologies in Drug Discovery for Selected Human Diseases. *Mar Drugs*, *16*(8). doi:10.3390/md16080279

- Lang, T., Goyard, S., Lebastard, M., & Milon, G. (2005). Bioluminescent Leishmania expressing luciferase for rapid and high throughput screening of drugs acting on amastigote-harboring macrophages and for quantitative real-time monitoring of parasitism features in living mice. *Cell Microbiol*, 7(3), 383-392. doi:10.1111/j.1462-5822.2004.00468.x
- Lipinski, C. A., Lombardo, F., Dominy, B. W., & Feeney, P. J. (2001). Experimental and computational approaches to estimate solubility and permeability in drug discovery and development settings. *Adv Drug Deliv Rev*, 46(1-3), 3-26. doi:10.1016/s0169-409x(00)00129-0
- Mancianti, F. (2004). Feline leishmaniasis: what's the epidemiological role of the cat. *Parassitologia*, 46(1-2), 203-206.
- Marciano, D. P., Dharmarajan, V., & Griffin, P. R. (2014). HDX-MS guided drug discovery: small molecules and biopharmaceuticals. *Curr Opin Struct Biol*, 28, 105-111. doi:10.1016/j.sbi.2014.08.007
- Mary, C., Faraut, F., Lascombe, L., & Dumon, H. (2004). Quantification of Leishmania infantum DNA by a real-time PCR assay with high sensitivity. *J Clin Microbiol*, 42(11), 5249-5255. doi:10.1128/JCM.42.11.5249-5255.2004
- Michel, G., Pomares, C., Ferrua, B., & Marty, P. (2011). Importance of worldwide asymptomatic carriers of Leishmania infantum (L. chagasi) in human. *Acta tropica*, 119(2-3), 69-75.
- Michel, G. (2011). *Leishmaniose à Leishmania infantum: portage asymptomatique, vaccination par voie endonasale et apport de la bioluminescence*. Aix-Marseille 2.
- Moffat, J. G., Vincent, F., Lee, J. A., Eder, J., & Prunotto, M. (2017). Opportunities and challenges in phenotypic drug discovery: an industry perspective. *Nat Rev Drug Discov*, 16(8), 531-543. doi:10.1038/nrd.2017.111
- Olivier, M., Atayde, V. D., Isnard, A., Hassani, K., & Shio, M. T. (2012). Leishmania virulence factors: focus on the metalloprotease GP63. *Microbes and infection*, 14(15), 1377-1389.
- Pennisi, M. G., Hartmann, K., Lloret, A., Addie, D., Belák, S., Boucraut-Baralon, C., . . . Hosie, M. J. (2013). Leishmaniosis in cats: ABCD guidelines on prevention and management. *Journal of feline medicine and surgery*, 15(7), 638-642.
- Ponte-Sucre, A., Gamarro, F., Dujardin, J. C., Barrett, M. P., López-Vélez, R., García-Hernández, R., . . . Papadopoulou, B. (2017). Drug resistance and treatment failure in leishmaniasis: A 21st century challenge. *PLoS Negl Trop Dis*, 11(12), e0006052. doi:10.1371/journal.pntd.0006052
- Ratnapriya, S., Keerti, Yadav, N. K., Dube, A., & Sahasrabudhe, A. A. (2021). A Chimera of Th1 Stimulatory Proteins of Leishmania donovani Offers Moderate Immunotherapeutic Efficacy with a Th1-Inclined Immune Response against Visceral Leishmaniasis. *Biomed Res Int*, 2021, 8845826. doi:10.1155/2021/8845826
- Reithinger, R., Mohsen, M., Aadil, K., Sidiqi, M., Erasmus, P., & Coleman, P. G. (2003). Anthroponotic cutaneous leishmaniasis, Kabul, Afghanistan. *Emerging Infectious Diseases*, 9(6), 727.
- Rose, K., Curtis, J., Baldwin, T., Mathis, A., Kumar, B., Sakthianandeswaren, A., . . . Handman, E. (2004). Cutaneous leishmaniasis in red kangaroos: isolation and characterisation of the causative organisms. *Int J Parasitol*, 34(6), 655-664. doi:10.1016/j.ijpara.2004.03.001
- Rossi, M., & Fasel, N. (2018). How to master the host immune system? Leishmania parasites have the solutions. *International immunology*, 30(3), 103-111.

Schulz, M. N., Landström, J., Bright, K., & Hubbard, R. E. (2011). Design of a fragment library that maximally represents available chemical space. *J Comput Aided Mol Des*, 25(7), 611-620. doi:10.1007/s10822-011-9461-x

Schwing-Chaïb, A. (2018). *Études des relations entre leishmanioses et cancers: Leishmania infantum: recherche de sanctuaires de persistance et criblage in vitro de nouvelles molécules actives*. Aix-Marseille.

Short, E. E., Caminade, C., & Thomas, B. N. (2017). Climate Change Contribution to the Emergence or Re-Emergence of Parasitic Diseases. *Infect Dis (Auckl)*, 10, 1178633617732296. doi:10.1177/1178633617732296

Siqueira-Neto, J. L., Moon, S., Jang, J., Yang, G., Lee, C., Moon, H. K., . . . Freitas-Junior, L. H. (2012). An image-based high-content screening assay for compounds targeting intracellular *Leishmania donovani* amastigotes in human macrophages. *PLoS Negl Trop Dis*, 6, e1671. doi:10.1371/journal.pntd.0001671

Virbac. (2018). La leishmaniose canine. Retrieved from <https://fr.virbac.com/home/toutes-les-maladies/quest-ce-que-leishmaniose-chien.html?preventiframercaching=1>

Vinet, A. F., Fukuda, M., Turco, S. J., & Descoteaux, A. (2009). The *Leishmania donovani* lipophosphoglycan excludes the vesicular proton-ATPase from phagosomes by impairing the recruitment of synaptotagmin V. *PLoS pathogens*, 5(10), e1000628.

WHO. (2021). Leishmaniasis. Retrieved from <https://www.who.int/news-room/fact-sheets/detail/leishmaniasis>

WHO. (2010). *Control of the Leishmaniasis*. Retrieved from [http://books.google.fr/books?id=0CMKNN0jp3wC&hl=&source=gbs\\_api](http://books.google.fr/books?id=0CMKNN0jp3wC&hl=&source=gbs_api)

WHO. (2017). Unveiling the neglect of leishmaniasis. Retrieved from [https://apps.who.int/mediacentre/infographic/neglected-tropical-diseases/Unveiling\\_the\\_neglect\\_of\\_leishmaniasis\\_infographic.pdf?ua=1](https://apps.who.int/mediacentre/infographic/neglected-tropical-diseases/Unveiling_the_neglect_of_leishmaniasis_infographic.pdf?ua=1)

Yeh, H. W., Karmach, O., Ji, A., Carter, D., Martins-Green, M. M., & Ai, H. W. (2017). Red-shifted luciferase-luciferin pairs for enhanced bioluminescence imaging. *Nat Methods*, 14(10), 971-974. doi:10.1038/nmeth.4400



# Annexes





# Collaboration sur des articles

“New method for screening anti-*Leishmania* compounds in plants extracts by HPTLC-bioautography” – Accepted – Journal of Chromatography B – 2021

“Identification of adipocytes as target cells for *Leishmania infantum* parasites” – Published – Scientific Reports – 2021

“*Leishmania* infection: Misdiagnosis as cancer and tumor-promoting potential” – Published – Acta Tropica – 2019

“*Escherichia coli* Rho GTPase-activating toxin CNF1 mediates NLRP3 inflammasome activation via p21-activated kinases-1/2 during bacteraemia in mice” – Published – Nature Microbiology - 2021



# New method for screening anti-*Leishmania* compounds in plants extracts by HPTLC-bioautography

Valentin Hilaire, Grégory Michel, Alissa Majoor, Francis Hadji-Minaglou, Anne Landreau, Xavier Fernandez

## **Résumé**

Les parasites du genre *Leishmania* sont responsables de leishmanioses, un groupe de maladies affectant 12 million de personnes dans les zones tropicales et subtropicales. Actuellement, quelques traitements sont disponibles, mais ils sont chers et causent de nombreux effets secondaires. La recherche de nouveaux traitements dans le monde végétal semble être une voie prometteuse. Ces travaux présentent un test original HPLC contre *Leishmania infantum* afin de cribler de nouvelles molécules issues d'extraits de plante. La technique utilise des protozoaires transformés stablement avec le gène de la Luciférase, ce qui permet l'observation de l'autobiogramme en bioluminescence. Nous avons développé différents protocoles afin de tester les deux formes du parasite : la forme promastigote, et la forme intracellulaire amastigote. Ces deux formes se multiplient dans des conditions très différentes, ce qui a nécessité la mise en place de deux protocoles distincts. Pour la forme promastigote, la technique d'autobiographie directe a été choisie, alors que pour la forme amastigote intracellulaire, l'autobiographie par immersion (les cellules parasitées étant contenues dans une couche d'agar) a été nécessaire. L'amphotéricine B a été choisie comme drogue de référence pour ces tests. Le développement de ces deux protocoles a permis de mettre en évidence des zones d'activité sur l'autobiogramme, permettant un crible rapide et peu coûteux des molécules avec des propriétés antiparasitaires contenues dans des extraits naturels.



## New method for screening anti-*Leishmania* compounds in plants extracts by HPTLC-bioautography

Valentin Hilaire<sup>a, b</sup>, Gregory Michel<sup>c</sup>, Alissa Majoor<sup>c</sup>, Francis Hadji-Minaglou<sup>a</sup>, Anne Landreau<sup>b, d</sup>, Xavier Fernandez<sup>b, \*</sup>

<sup>a</sup> BotaniCert, 4 traverse Dupont, 06130 Grasse, France

<sup>b</sup> Université Côte d'Azur, CNRS, Institut de Chimie de Nice, UMR 7272, Nice, France

<sup>c</sup> Université Côte d'Azur, Inserm, U1065, C3M, Nice, France

<sup>d</sup> Univ Angers, Univ Brest, GEIHP, SFR ICAT, F-49000 Angers, France

### ARTICLE INFO

#### Keywords:

HPTLC  
*Leishmania infantum*  
 Direct Bioautography  
 Agar overlay  
 Plant extracts screening  
 Anti-*Leishmania*

### ABSTRACT

*Leishmania* genus is responsible for leishmaniasis, a group of diseases affecting 12 million people in the tropical and subtropical zone. Currently, the few drugs that are available to treat this disease are expensive and cause many side effects. Searching for new therapeutics from plant species seems to be a promising path. This work proposes an original HPTLC test against parasites, in particular on *Leishmania infantum*, to screen new molecules from plant extracts. The technique uses protozoa transformed to express the luciferase gene to observe the bioautogram in bioluminescence. We have developed two different test protocols based on the two dimorphic stages of the parasite. The free promastigote stage, and an intracellular stage parasitizing macrophage cells called the amastigote stage. These two stages only survive under extremely different conditions which required the development of two very different test protocols. For the promastigote free stage of the protozoa, the direct bioautography technique was chosen while for the intracellular amastigote stage, bioautography by immersion (agar overlay) was required. Amphotericin B was chosen as the reference compound for this assay. The development of each of these two tests made it possible to clearly detect areas of activity on the bioautogram, allowing a rapid and inexpensive screening of the antiparasitic properties of molecules in natural extracts.

### 1. Introduction

Leishmaniasis are vector parasites of reticuloendothelioses. The causative agent is a flagellated protozoan belonging to the genus *Leishmania*. Leishmaniasis is considered by the WHO (World Health Organization) to be an emerging, uncontrolled, and neglected disease [1]. They represent the second highest cause of mortality and the fourth cause of morbidity from tropical diseases. The number of cases worldwide is very high (estimated at 12 million). There are more than twenty species of *Leishmania* around the world, leading either to an asymptomatic carriage, or to various clinical manifestations such as a simple skin papule, a spreading of the mucous membranes of the face or even a visceral stage which is lethal without treatment. The number of therapeutic molecules currently available is limited and they have significant undesirable side-effects [2]. The number of molecules authorized for the treatment of leishmaniasis is very low. Most of these molecules are

from synthetic origin and are shared with other diseases. For example, amphotericin B was originally used as an antifungal [3]. However, this molecule is very expensive and has many side effects. In addition, resistance to molecules has appeared in parasites and cases of relapse have been described [4,5,6,7]. Furthermore, plants have always been a common source of drugs, either in traditional medical practices or as sources for purified active pharmaceuticals. The WHO considers more than 60% of the world's population predominately relied on plant-derived treatments in front line treatments [8]. Therefore, research of new antileishmanial drugs focusing on the use of plants seems a promising pathway.

Actual screening in vitro methods for anti-leishmanial compounds are 96 well plates assays. Detection methods can be microscopy [9,10] or coloring agents such as resazurin [11], MTT [12], or Alamar Blue® [13]. Some have modified *Leishmania* parasites transfecting  $\beta$ -lactamase gene in order to follow the apparition of a colorimetric compound [14,

\* Corresponding author at: Groupe MVBV, Institut de Chimie de Nice, UMR 7272 Université de Nice-Sophia Antipolis / CNRS, Parc Valrose, 06108 Nice Cedex 2, France.

E-mail address: [xavier.fernandez@unice.fr](mailto:xavier.fernandez@unice.fr) (X. Fernandez).

<https://doi.org/10.1016/j.jchromb.2021.123061>

Received 9 June 2021; Received in revised form 15 November 2021; Accepted 24 November 2021

1570-0232/© 2021

15]. These microwell screening techniques are well suited to screening libraries of pure molecules. However, these techniques are not efficient for studying plant extracts which are complex mixtures of molecules. Usually, the identification of new active plants compounds requires the preparation of various extracts of plants before assessing the activity of each molecule in the extract. Numerous bio-guided fractionation steps are ultimately necessary which are extremely time-consuming and costly in materials, reagents, and labor [16].

The aim of this work was to present a faster and more effective screening strategy for anti-*Leishmania* bioassays of plant extracts. We have succeeded in developing an HPTLC-bioautography method, including a new biological activity screening test [17,18]. This method has never been adapted to protozoa. Each molecule of the extract can therefore be evaluated separately from each other and the tedious steps of conventional bioguided fractionation are eliminated. The method has been described and adapted to each of the parasite lifecycle, promastigote and amastigote.

## 2. Material and methods

### 2.1. High-performance thin-layer chromatography

All solvents used for plate preparation were of analytical grade from Carlo Erba Reagents (Cornaredo MI, Italy). Amphotericin B (fungizone® from Bristol-Myers Squibb (New York, USA)) solution (100 µg/ml) was applied with CAMAG ATS4 (Muttentz, BL, Switzerland) on pre-washed (MeOH/H<sub>2</sub>O (8/4 ; v/v)) HPTLC silica gel plates 60 F254 Merck (Darmstadt, Hesse, Germany) on four spots with different concentrations (2 µl, 4 µl, 6 µl and 8 µl applications). Plates were developed with MeOH/H<sub>2</sub>O (90/10 ; v/v) mobile phase on CAMAG ADC2. Photos of the developed plate were taken with CAMAG TLC Visualizer 2 at 366 nm.

For the separation of the plant extracts, a raw methanolic extract (1/10 ; v/v) of a plant and a non-polar fraction of this extract were applied on a prewashed HPTLC plate in two separate spots (2 µl). The plate was developed with toluene/acetone (4/1 ; v/v) mobile phase. Photos of the derivatized (Natural Products reagent) plate were taken with CAMAG TLC Visualizer 2 under visible light.

### 2.2. In vitro inhibition test on promastigote stage

*Leishmania infantum* MON-1 parasites (MHOM / FR / 94 / LPN101) were isolated from a patient with visceral leishmaniasis in the Nice region. and 1.6 kb of the firefly luciferase coding region has been added to its genome [19].

Preparation of Culture Medium: The promastigote stage was cultured in Schneider's Insect Medium® from Sigma Aldrich (Saint-Louis, MI, USA). In To this medium the following were added: 0.4 g/L of NaHCO<sub>3</sub> from Acros Organics (Antwerp, Belgium), 0.6 g/L of CaCl<sub>2</sub> from Fluka chemie (Buchs, Switzerland), 10% of fetal calf serum, 10 ml of a human urine pool, 0.1% of phenol red from Sigma Aldrich (Saint-Louis, MI, USA), 1 % 1 M HEPES pH 7.3, 1% of respectively penicillin and streptomycin, 1% L-glutamine all three from GIBCO Thermo Fisher (Waltham, USA).

Verification of bioluminescence: 1 ml of parasite suspension at 1.10<sup>7</sup> parasites/ml (p/ml) was collected and centrifuged. The pellet was resuspended in 100 µl of complete schneider medium added to 100 µl of luciferin from Perkin (Waltham, USA) 8 mg/ml. The suspension was placed in a well of a 96-well microplate stirred for 5 s and read by luminescence (Gen5 (BioTek, Winooski, USA)).

The developed HPTLC plate was immersed in the parasite suspension at 1.10<sup>7</sup>p/ml using a narrow development and soaking tank 100 × 100 mm from Bionis (Houdan, Yvelines, France), and placed in a wet atmosphere box in the incubator at 26 °C for 6 h. After these 6 h, the plate was immersed in a solution of luciferin at 8 mg/ml and read

directly in the Fuji LAS4000® from Fujifilm Life Science (Valhalla, NY, United States) in luminescence mode with a time of exposure of 50 s.

### 2.3. In vitro inhibition test on amastigote stage

THP-1 cells (ATCC® TIB-202™) are derived from a pre-monocytic human cell line, derived from a child with leukemia. They were cultivated in RPMI Medium 1640® Invitrogen GIBCO® medium from GIBCO Thermo Fisher (Waltham, USA) to which 10% fetal calf serum, 1% glutamine, 1% sodium pyruvate, and 1% penicillin and streptomycin all four from GIBCO Thermo Fisher (Waltham, USA) have been added.

To avoid adhesion to the walls of the culture flasks, cells have been activated with vitamin D<sub>3</sub>. THP-1 cells were activated with 100 µl of vitamin D<sub>3</sub> at 250 ng/ml. The activation time was three days long. Activated THP-1 cells were infected by parasites in the promastigote stage. by introducing 20 promastigote parasites into the cell culture for one THP-1 cell (MOI 20). The infection time was 24 h.

A total of 20 ml of Ficoll® from Cytiva (Marlborough, USA) was placed in respectively two 50 ml centrifuge tubes and the suspension of infected THP-1 cells was split in two (2 × 20 ml) and each half was deposited delicately on the surface of Ficoll® using a pipette. Each of the tubes were centrifuged at 2000 rpm for 30 min (acceleration 1 and braking 0). Cells were collected at the Ficoll® / medium interface and washed twice with sterile PBS. The pellet was collected and suspended in 10 ml of THP-1 medium. The cells were counted using a Glasstick® slide from Kova international (Garden Grove, USA).

The developed plate was placed in a 100 mm × 100 mm wet box. The suspension was diluted or concentrated to obtain a final concentration of 1.10<sup>8</sup> cells in 5 ml of THP-1 medium. This mix was added to 5 ml of liquefied 1.2% agar and homogenized to be finally poured onto the plate. The plate was incubated at 37 °C for 24 h. At the end of these 24 h, the agar was covered with luciferin solution at 8 mg/ml and 20 min later the dish was photographed in luminescence mode during 50 s placed in the Fuji LAS4000®.

## 3. Results and discussion

### 3.1. Choice of the HPTLC-bioautography method

Among other screening methods, HPTLC-bioautography has been chosen because in this technique the constituents of complex mixtures are first separated by high performance thin layer chromatography (HPTLC), which is already widely used in phytochemistry for quality control, followed directly by the contact with microorganisms. After revelation, spots appear on the bioautogram corresponding to molecules exhibiting an anti-parasitic activity. In addition, the chromatography step will allow to separate molecules that could have antagonistic effects inside the plant extract and whose activity had not been yet revealed. Likewise, this process will also separate the molecules whose activity could have resulted from a synergy with others various compounds. This method was therefore particularly suitable for the discovery of new, active, pure compounds to promote as future drug candidates. Three types of bioautography currently exist [20]. Two of them have been used in this assay development.:

The first method is direct bioautography, in which the microorganism of interest is applied directly onto the developed HPTLC plate surface.

The second bioautography method used is agar overlay: a layer of agar seeded with a given concentration of microorganisms was poured and gelled directly on the plate where the plant extracts had been separated. The active molecules included in the extracts then diffused off the plate and through the agar to interacted with microorganisms.

### 3.2. Methods adaptation to parasite stages

As the parasite exists in two different stages, the search for active molecules therefore took place in two different ways. The survival conditions of promastigotes being less demanding than those of amastigotes, thus direct bioautography was chosen for the promastigotes (Fig. 1).

Conversely, the agar overlay technique proved to be the best option for attest inhibition of amastigotes. This method fixes the cells and nourishes them properly during this time (Fig. 2).

For this development, a strain of *Leishmania* transfected with the gene encoding the enzyme luciferase [19] was used. Thus, the viability of the parasites was directly proportional to the number of photons picked up by the detector of the Synergy II plate reader when the *Leishmania* parasites are brought into contact with the luciferase substrate, luciferin. This molecule is oxidized by luciferase resulting in the production of photons. When the parasites are dying, the photon emission is no longer possible and the decrease in luminescence is directly proportional to the antileishmanial activity of the molecule on the parasites [19].

### 3.3. Test with a standard

The test was developed with an amphotericin B standard as a positive control, which is the gold standard in the treatment of leishmaniasis. The amphotericin B stock solution was chosen at a concentration of 100 µg / ml. Deposits of increasing volumes were made on the plate: 2 µl, 4 µl, 6 µl and 8 µl. The plate was then developed using the mobile phase: MeOH / H<sub>2</sub>O (90/10; v / v) allowing the migration of amphotericin B.

### 3.4. Development of in vitro inhibition test on promastigote stage

Since HPTLC-bioautography has never been developed for protozoa, the first step in development was to ascertain that promastigotes could survive on the Silica gel plate by doing a test plate with just one spot of amphotericin B and luminescence revelation. Once this step was successful, the adequate concentration to have a sufficiently bright background was searched and set at 10<sup>7</sup> parasites/ml. At this concentration, the active areas were clearly visible. The luciferin concentration was set at 8 mg/ml. Several contact time assays were carried out to find the optimal contact time between the eluted plate and the parasite. It has been found that 6 h was a good compromise between having a fast test and suitable results. Migrated amphotericin B treated under these conditions showed black areas on a luminescent background. Evaluation of the different concentrations of this latter has permitted to determine its proper limit of detection for this test. In fact, the lowest concentration deposited (2 µl in a final solution of 100 µg/ml, i.e. 200 ng deposited on the plate) did not produce visible black spot on the plate while the 2 times higher concentration allowed it (400 ng deposited on the plate) (Fig. 3).

### 3.5. Development in vitro inhibition test on amastigote stage.

In contrast to most anti-*Leishmania* screening methods, this method uses live, in-host, amastigotes. Usually, to screen the anti-leishmanial activities on the amastigote stage, many scientists use axenic *Leishmania* parasites, which are free forms of the parasite simply approaching the amastigote stage. This use is now criticized [23] because these forms do not exactly mimic the metabolism of the real amastigote stage which is intracellular. For several years now, the C3M research labora-



Fig. 1. Process for promastigotes testing. Plant is extracted and applied on the plate which is developed with proper mobile phase, immersed in parasitic culture and kept in contact for 6H. Revelation is operated by dipping the plate in 8 mg/ml luciferin solution.

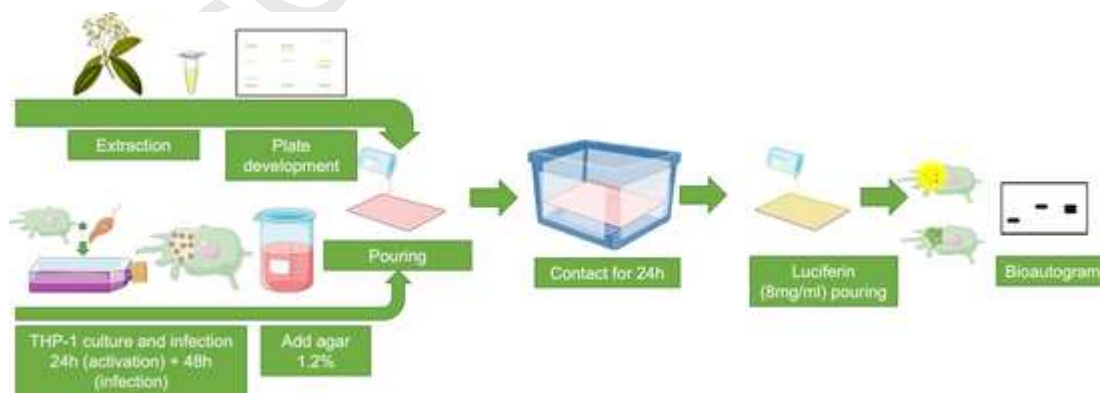
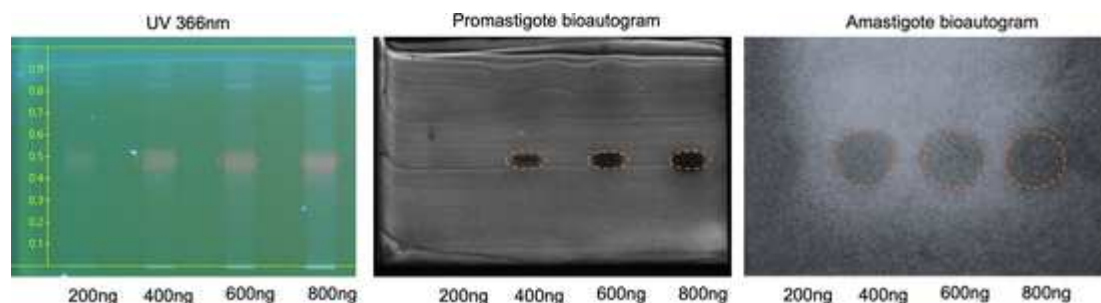


Fig. 2. Process for amastigotes testing. Plant is extracted and applied on the plate which is developed with proper mobile phase. THP-1 cells are activated in vit D<sub>3</sub> for 24H and infected with promastigotes for 48H. Agar 1.2% is added to the THP-1 broth and poured on the plate. The plate is kept in contact for 24H then luciferin solution (8 mg/ml) is poured on it for the revelation step.



**Fig. 3.** HPTLC-bioautogram on *Leishmania infantum* promastigote stage. Four different volumes of amphotericin B solution (100  $\mu\text{g/ml}$ ) have been applied on the plate (2  $\mu\text{l}$ , 4  $\mu\text{l}$ , 6  $\mu\text{l}$  and 8  $\mu\text{l}$ ). Promastigote stage test: plates have been developed in MeOH/H<sub>2</sub>O (90/10 ; v/v). Plate is immersed in *Leishmania* solution (10<sup>7</sup>/ml) and photo is taken with FUJIFILM LAS400. Amastigote stage test: plates have been developed in MeOH/H<sub>2</sub>O (90/10 ; v/v). Plate was covered by agar containing infected THP-1 cells (10<sup>7</sup>/plate) and photo is taken with FUJIFILM LAS400. Dark zones on both bioautograms show the antileishmanial effect of amphotericin.

tory is working on real amastigote stages that mimic reality more faithfully. However, these stages are extremely delicate to produce and maintain. As the amastigote stage of the parasite can only survive in a host cell, the test conditions have had to be adapted. Longer time was needed for the penetration of the molecule towards and inside the cell to make contact with the parasite, but the THP-1 cells did not survive this time on the silica surface (maybe the nutrient was not enough), therefore agar overlay bioautography was chosen. This method has allowed the cell to remain in a viable environment during the entire contact time. As before, the test was developed with a plate containing several deposits of an amphotericin B solution (100  $\mu\text{g/ml}$ ) of increasing volumes. After all these steps, an 8 mg/ml luciferin solution was poured over the agar before revelation. Kinetic curve has been done to register the delay caused by the luciferin to diffuse through agar and reach the amastigote stage. The plateau of the curve was reached after 20 min. Finally, the plates were then photographed 20 min after the luciferin pouring. Dark spots corresponded to inhibition zones of amastigote parasites (Fig. 4).

This stage has required a much more advanced test development methodology than the promastigote stage given that the development time was much longer. Indeed, many difficulties were overcome during the development of this test, in particular, first the challenge to obtain living and infected cells in the agar gel and then specifically to find the right concentration of cells allowing to obtain an exploitable signal.

### 3.6. Tests on plant extracts

To achieve the development of the test, these methods were carried out also on plant extracts to ascertain the correct progress and the appearance of active molecules in complex matrices. The test was carried out on a total methanolic plant extract as well as on a fraction containing only the non-polar molecules. This plant contains antibacterial compounds and has been screened for anti-leishmanian activity. One molecule in particular was targeted by this test. It is a terpenoid-type compound (revealed in violet with anisaldehyde) and eluting at  $R_f = 0.5$  with the toluene / acetone (4/1; v / v) mobile phase.

A dark spot is visible at  $R_f = 0.5$  after incubation with both promastigote and amastigote stage test methods. These two methods have thus successfully revealed a single compound which shows anti-leishmanian activity for further study (Fig. 4).

### 3.7. Advantages and limits

On both obtained bioautograms, a dark spot (at  $R_f = 0.5$ ) has indicated a zone where a molecule with anti-leishmanian activity has migrated. This molecule has showed an activity on both stages of the parasite because of the dark spot appearing on both bioautograms. From these results, the plant extracts evaluation has attested that the assays' methods were suitable for use in the research of natural anti-leishmanian compounds.

One issue is that activity zones appeared slightly diffuse for the amastigote assay. One solution could be to further optimize mobile phase conditions inducing a greater selectivity to obtain an improved separation of the compounds from each plant extract. Otherwise, an alternative could be to use a direct bioautographic method with small amount of agarose (e.g. 0.05%) in the cell suspension in order to fix more medium on the silica plate.

## 4. Conclusion

This work has enabled the development of an innovative HPTLC-Bioautography assay to identify anti-leishmanian compounds in crude plant extracts. These types of microorganisms have never been used before in this type of biochemical test. It constitutes a new tool in the search for new natural molecules in the fight against both stages of leishmaniasis: searching for systemic medicines to treat the human disease using the amastigote stage test and for topical medicines to prevent the infection of the parasite using the promastigote stage test. As this test works properly, even at the amastigote stage, these methods could be applied to other intracellular pathogenic microorganisms.

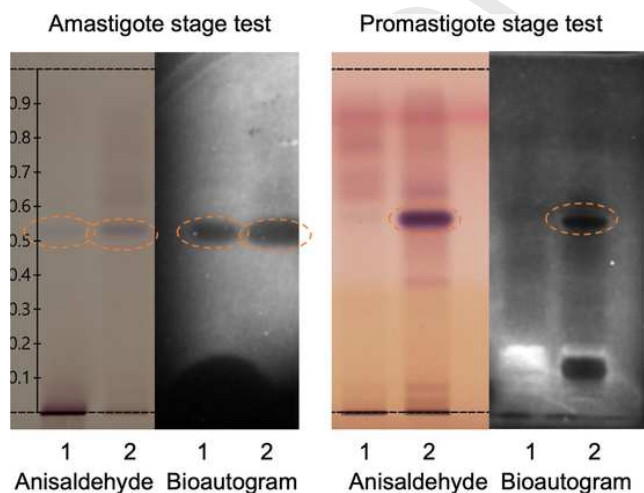


**Fig. 4.** HPTLC-bioautograms on plant extracts 1 and 2. Both bioautographic tests (amastigote stage and promastigote stage) were carried out on both plant extract. Plates were developed with toluene/acetone (4/1 ; v/v) mobile phase.



## Declaration of Competing Interest

The authors declare that they have no known competing financial interests or personal relationships that could have appeared to influence the work reported in this paper.

## Acknowledgement

Authors greatly acknowledge the French Association Nationale de la Recherche et de la Technologie (ANRT) for supporting the CIFRE partnership Botanicert - Université Côte d'Azur.

## References

- [1] N. Feasey, M. Wansbrough-Jones, D.C.W. Mabey, A.W. Solomon, Neglected tropical diseases, *Br. Med. Bull.* 93 (2010) 179–200, <https://doi.org/10.1093/bmb/ldp046>.
- [2] S. Burza, S.L. Croft, M. Boelaert, Leishmaniasis, *Lancet*. 392 (2018) 951–970, [https://doi.org/10.1016/S0140-6736\(18\)31204-2](https://doi.org/10.1016/S0140-6736(18)31204-2).
- [3] N.R.H. Stone, T. Bicanic, R. Salim, W. Hope, Liposomal Amphotericin B (AmBisome®): A Review of the Pharmacokinetics, Pharmacodynamics, Clinical Experience and Future Directions, *Drugs*. 76 (2016) 485–500, <https://doi.org/10.1007/s40265-016-0538-7>.
- [4] A.A. Kassardjian, K.M. Yim, S. Rabi, T.Z. Liang, G.H. Kim, M.T. Ochoa, M.V. Sattah, I.Z. Ahronowitz, Diffuse cutaneous leishmaniasis and HIV co-infection: A case report and review of the literature, *J. Cutan. Pathol.* (2021) cup.13993, <https://doi.org/10.1111/cup.13993>.
- [5] T.R. de Moura, M.L.B. Santos, J.M. Braz, L.F.V.C. Santos, M.T. Aragão, F.A. de Oliveira, P.L. Santos, Â.M. da Silva, A.R. de Jesus, R.P. de Almeida, Cross-resistance of *Leishmania infantum* isolates to nitric oxide from patients refractory to antimony treatment, and greater tolerance to antileishmanial responses by macrophages, *Parasitol. Res.* 115 (2016) 713–721, <https://doi.org/10.1007/s00436-015-4793-4>.
- [6] S. Hendrickx, P.J. Guerin, G. Caljon, S.L. Croft, L. Maes, Evaluating drug resistance in visceral leishmaniasis: The challenges, *Parasitology*. 145 (2018) 453–463, <https://doi.org/10.1017/S0031182016002031>.
- [7] A.W. Pountain, S.K. Weidt, C. Regnault, P.A. Bates, A.M. Donachie, N.J. Dickens, M.P. Barrett, Genomic instability at the locus of sterol C24-methyltransferase promotes amphotericin B resistance in *Leishmania* parasites, *PLoS Negl. Trop. Dis.* 13 (2019) 1–26, <https://doi.org/10.1371/journal.pntd.0007052>.
- [8] A.G. Atanasov, B. Waltenberger, E.M. Pferschy-Wenzig, T. Linder, C. Wawrosch, P. Uhrin, V. Temml, L. Wang, S. Schwaiger, E.H. Heiss, J.M. Rollinger, D. Schuster, J.M. Breuss, V. Bochkov, M.D. Mihovilovic, B. Kopp, R. Bauer, V.M. Dirsch, H. Stuppner, Discovery and resupply of pharmacologically active plant-derived natural products: A review, *Biotechnol. Adv.* 33 (2015) 1582–1614, <https://doi.org/10.1016/j.biotechadv.2015.08.001>.
- [9] I. Roquero, J. Cantizani, I. Cotoillo, M.P. Manzano, A. Kessler, J.J. Martín, C.W. Mcnamara, Novel chemical starting points for drug discovery in leishmaniasis and Chagas disease, *IJP Drugs Drug Resist.* 10 (2019) 58–68, <https://doi.org/10.1016/j.ijpdr.2019.05.002>.
- [10] J.L. Siqueira-neto, O. Song, H. Oh, J. Sohn, G. Yang, J. Jang, J. Cechetto, C.B. Lee, S. Moon, A. Genovesio, T. Christophe, L.H. Freitas-junior, Antileishmanial High-Throughput Drug Screening Reveals Drug Candidates with New Scaffolds, *PLoS Negl Trop Dis.* 4 (2010) 1–9, <https://doi.org/10.1371/journal.pntd.0000675>.
- [11] D. Paape, A.S. Bell, W.P. Heal, J.A. Hutton, R.J. Leatherbarrow, E.W. Tate, D.F. Smith, Using a Non-Image-Based Medium-Throughput Assay for Screening Compounds Targeting N-myristoylation in Intracellular *Leishmania* Amastigotes, *PLoS Negl Trop Dis.* 8 (2014), <https://doi.org/10.1371/journal.pntd.0003363>.
- [12] S. Khanra, Y.P. Kumar, J. Dash, R. Banerjee, In vitro screening of known drugs identified by scaffold hopping techniques shows promising leishmanicidal activity for suramin and netilmicin, *BMC Res. Notes.* (2018) 1–6, <https://doi.org/10.1186/s13104-018-3446-y>.
- [13] M. Ohashi, J. Agyapong, F. Ayertey, M. Amoabosompem, K.D. Kwofie, R. Adegle, M. Mamfe, K. Baffuor, A. Owusu, I. Tuffour, P. Atchoglo, T. Uto, F. Aboagye, A. Ampomah, R.A. Alexander, K.N. William, K. Anyan, I. Ayi, D. Adjei, B. Kwadwo, A. Koram, D. Edoh, S. Yamaoka, Y. Shoyama, In vitro antiprotozoan activity and mechanisms of action of selected Ghanaian medicinal plants against Trypanosoma, Leishmania, and Plasmodium parasites, *Phytotherapy.* (2018) 1–14, <https://doi.org/10.1002/ptr.6093>.
- [14] S. Mandal, M. Maharjan, S. Ganguly, M. Chatterjee, S. Singh, F.S. Buckner, R. Madhubala, High-throughput screening of amastigotes of *Leishmania donovani* clinical isolates against drugs using a colorimetric  $\beta$ -lactamase assay, *Indian J Exp Biol.* 47 (2011) 475–479.
- [15] F.S. Buckner, A.J. Wilson, Colorimetric assay for screening compounds against *Leishmania* amastigotes grown in macrophages, *Am. J. Trop. Med. Hyg.* 72 (2005) 600–605.
- [16] A. Urbain, C.A. Simões-Pires, Thin-Layer Chromatography for the Detection and Analysis of Bioactive Natural Products, in: *Encycl. Anal. Chem.*, Wiley, 2020: pp. 1–29. <https://doi.org/10.1002/9780470027318.a9907.pub2>.
- [17] I.M. Choma, E.M. Grzelak, Bioautography detection in thin-layer chromatography, *J. Chromatogr. A.* 1218 (2011) 2684–2691, <https://doi.org/10.1016/j.chroma.2010.12.069>.
- [18] T.T. Häbe, M. Jamshidi-Aidji, J. Macho, G.E. Morlock, Direct bioautography hyphenated to direct analysis in real time mass spectrometry: Chromatographic separation, bioassay and mass spectra, all in the same sample run, *J. Chromatogr. A.* 1568 (2018) 188–196, <https://doi.org/10.1016/j.chroma.2018.07.002>.
- [19] G. Michel, B. Ferrua, T. Lang, M.P. Maddugoda, P. Munro, Luciferase-Expressing *Leishmania infantum* Allows the Monitoring of Amastigote Population Size, In Vivo, Ex Vivo and In Vitro, *PLoS Negl Trop Dis.* 5 (2011) 1–7, <https://doi.org/10.1371/journal.pntd.0001323>.
- [20] K. Ciura, S. Dziomba, J. Nowakowska, M.J. Markuszewski, Thin layer chromatography in drug discovery process, *J. Chromatogr. A.* 1520 (2017) 9–22, <https://doi.org/10.1016/j.chroma.2017.09.015>.



# Identification of adipocytes as target cells for *Leishmania infantum* parasites

Aurélie Schwing, Didier F. Pisani, Christelle Pomares, Alissa Majoor, Sandra Lacas-Gervais, Jennifer Jager, Emmanuel Lemichez, Pierre Marty, Laurent Boyer & Grégory Michel

## **Résumé**

*Leishmania infantum* est l'espèce responsable de la leishmaniose viscérale, transmise par la morsure de phlébotomes femelles. Selon l'OMS, l'incidence annuelle estimée de nouveaux cas de leishmaniose est d'un million, résultant en 30 000 morts par an. Les traitements recommandés incluent l'amphotéricine B, mais au cours des dernières années, les cas de rechutes se sont multipliés. Ces rechutes remettent en cause l'efficacité des traitements actuels et soulèvent la question de l'existence de sites de persistance des parasites. En effet, *Leishmania* peut persister chez l'humain pendant de longues périodes, même après un traitement concluant. Plusieurs sites de persistance ont déjà été identifiés et nommés « Safe-targets ». Sachant que le tissu adipeux a été proposé comme un sanctuaire de persistance pour plusieurs pathogènes, nous avons cherché à vérifier si *Leishmania infantum* pouvait être présent dans ce tissu. Nous avons démontré *in vitro* et *in vivo* que *Leishmania infantum* est capable d'infecter des adipocytes. Dans l'ensemble, nos résultats suggèrent que les adipocytes peuvent être un « Safe-target » pour *Leishmania infantum*.



OPEN

# Identification of adipocytes as target cells for *Leishmania infantum* parasites

Aurélie Schwing<sup>1,2,3</sup>, Didier F. Pisani<sup>4</sup>, Christelle Pomares<sup>1,2</sup>, Alissa Majoor<sup>2</sup>, Sandra Lacas-Gervais<sup>5</sup>, Jennifer Jager<sup>2</sup>, Emmanuel Lemichez<sup>6</sup>, Pierre Marty<sup>1,2</sup>, Laurent Boyer<sup>2</sup> & Grégory Michel<sup>2</sup>✉

*Leishmania infantum* is the causative agent of visceral leishmaniasis transmitted by the bite of female sand flies. According to the WHO, the estimated annual incidence of leishmaniasis is one million new cases, resulting in 30,000 deaths per year. The recommended drugs for treating leishmaniasis include Amphotericin B. But over the course of the years, several cases of relapses have been documented. These relapses cast doubt on the efficiency of actual treatments and raise the question of potential persistence sites. Indeed, *Leishmania* has the ability to persist in humans for long periods of time and even after successful treatment. Several potential persistence sites have already been identified and named as safe targets. As adipose tissue has been proposed as a sanctuary of persistence for several pathogens, we investigated whether *Leishmania infantum* could be found in this tissue. We demonstrated both in cell cultures and in vivo that *Leishmania infantum* was able to infect adipocytes. Altogether our results suggest adipocytes as a 'safe target' for *Leishmania infantum* parasites.

*Leishmania infantum* (*L. infantum*) is the causative agent of visceral leishmaniasis and is transmitted by the bite of female sand flies. According to the WHO, the estimated annual incidence is one million new cases, resulting in 30,000 deaths per year<sup>1</sup>. The outcome of infection can be variable, ranging from an asymptomatic form in immunocompetent individuals to obvious disease<sup>2</sup>. These clinical features depend on the species and the immune response of the host<sup>3</sup>. Symptomatic leishmaniasis is characterized by 3 main forms: cutaneous (CL), mucocutaneous (MCL) and visceral leishmaniasis (VL). CL is a chronic infection with ulcerative skin lesion occurring at the site of inoculation. MCL is generally the result of parasite dissemination from the skin to the naso-oro-pharyngeal mucosa. VL is the most serious form of leishmaniasis and typically leads to death in a few months in the absence of treatment. It is characterized by irregular fever, weight loss, hepatosplenomegaly, lymphadenopathies and pancytopenia. Currently, there is no human vaccine and treatments are expensive, with WHO guidelines recommending the use of just a few drugs, such as Amphotericin B<sup>4</sup>. Over time, several cases of relapses have been documented<sup>5,6</sup>, which thus call into question the efficiency of current treatments<sup>5,7</sup> and raise the unsolved question of host sites allowing parasite persistence. Indeed, *Leishmania* has the ability to persist in humans for long periods of time, even after successful treatment<sup>8</sup>. Several potential persistence sites have already been identified and named as safe targets. These include immature myeloid precursor cells, monocytes, sialoadhesin-positive stromal macrophages of the bone marrow, hepatocytes and fibroblasts<sup>8</sup>. Previously, *L. infantum* persistence and development has been demonstrated in intra-abdominal adipose tissue of intraperitoneally infected mice<sup>9</sup>. Moreover, adipose tissue has been proposed as a sanctuary of persistence for bacteria such as *Mycobacterium* (*M.*) *tuberculosis*<sup>10</sup> or *M. canettii*<sup>11</sup>, *Coxiella burnetii*<sup>12</sup>, viruses such as Human or Simian Immunodeficiency Virus<sup>13,14</sup>, and parasites such as *Trypanosoma* (*T.*) *cruzi* or *T. brucei* and *Plasmodium* spp.<sup>15,16</sup>. Here, we address the issues of whether *L. infantum* infects adipose tissues and whether adipocytes represent host cells for these parasites.

## Results

***L. infantum* is found in the adipose tissue of infected mice.** First, we investigated whether *L. infantum* was present in brown (BAT) and white (WAT) adipose tissue of infected mice. For this purpose, BALB/c mice were intravenously inoculated with LUC-*L. infantum* as previously described<sup>9</sup>. Although bioluminescent parasites were used in this study, parasite burden in adipose tissue was insufficient to obtain an exploitable signal

<sup>1</sup>Université Côte d'Azur, CHU, Inserm, C3M, Nice, France. <sup>2</sup>Université Côte d'Azur, Inserm, C3M, Nice, France. <sup>3</sup>Université Aix-Marseille, Marseille, France. <sup>4</sup>Université Côte d'Azur, CNRS, LP2M, Nice, France. <sup>5</sup>Université Côte d'Azur, Centre Commun de Microscopie Appliquée, Nice, France. <sup>6</sup>Institut Pasteur, CNRS UMR2001, Unité des Toxines Bactériennes, 75015 Paris, France. ✉email: gmichel@univ-cotedazur.com

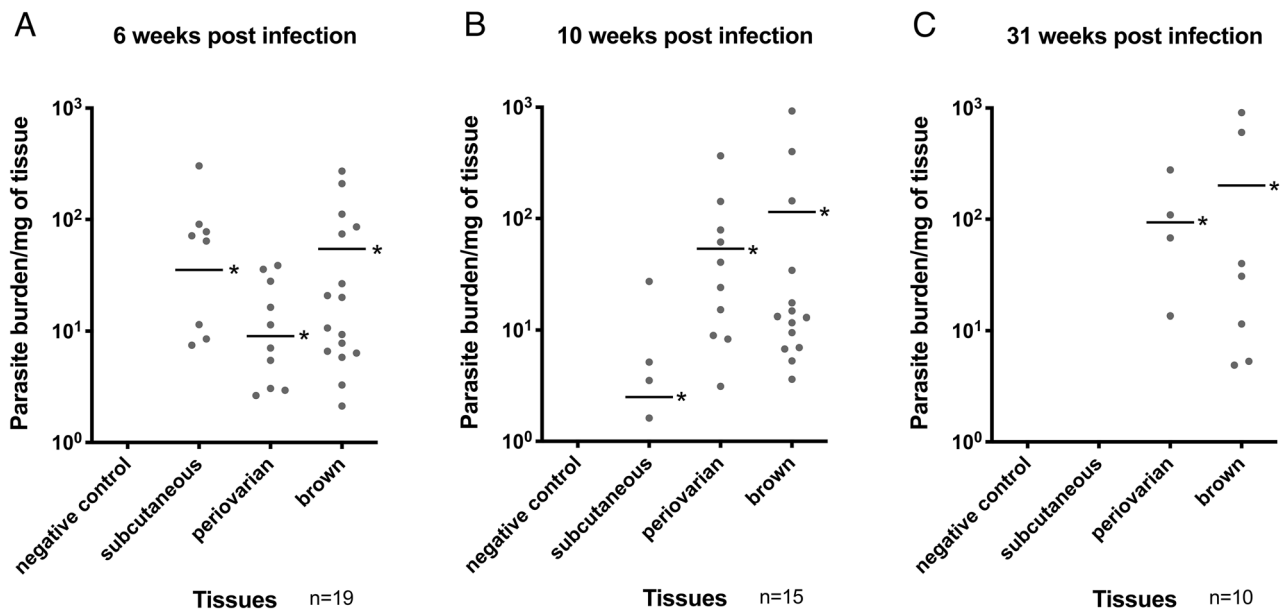


**Figure 1.** *L. infantum* parasites are present in adipose tissue from BALB/c mice. Subcutaneous, periovarian, and brown adipose tissue (25 mg) from mice inoculated with *L. infantum* were collected after different periods of time (6 (A), 10 (B) and 31 weeks post infection (C)), DNA was extracted in a 100  $\mu$ L volume and the presence of *L. infantum* DNA was determined by qPCR using a 2.5  $\mu$ L DNA extract. Results represent parasite burden per milligram of tissue with SEM. \* $p < 0.05$ . qPCR negative samples are not shown on graphs.

and allow in vivo monitoring of infection. Mice were thus sacrificed 6, 10 and 31 weeks post infection (p.i.). Tissue samples were analyzed for the presence of *L. infantum* by qPCR, which confirmed chronic infection in the spleen and liver (Fig. S1). At 6 weeks p.i., subcutaneous and periovarian BAT and WAT presented parasite burden which remained high in BAT 10 weeks p.i. In subcutaneous tissue, between 6 and 10 weeks p.i., parasite burden decreased then totally disappeared after 31 weeks (Fig. 1). In contrast, the percentage of mice with positive parasite burden in BAT remained higher than 70%. These results indicated the persistence of *L. infantum* in BAT after infection by the intravenous route. Furthermore, we performed histological sections on different tissues from the same infected mice in order to visualize parasites by immunolabelling. 40 weeks p.i., the presence of *L. infantum* parasites in all types of adipose tissue could be observed (Fig. 2). This raised the question of whether parasites contained in adipose tissue were alive and endowed with the capacity to infect. We thus performed an adoptive transfer experiment by intravenously injecting naive mice with BAT homogenate from infected mice. 34 weeks post-transfer we were able to detect parasite DNA by qPCR in the liver, spleen and BAT of secondary-infected mice (Fig. S2). Taken together, our results show that *L. infantum* parasites present in the adipose tissue of mice kept their infectivity.

***L. infantum* is present in adipocyte-enriched fractions.** To assess whether *L. infantum* was present in adipocytes or other cell types, we separated an adipocyte-enriched fraction from the stromal vascular fraction (SVF). WAT and BAT from 4 mice infected intravenously were isolated and floating fractions enriched in adipocytes were obtained. The samples were pooled in order to increase the number of parasites and improve detection by qPCR. Separation between adipocytes and stromal cells was checked by amplification of adipocyte marker mRNA (Fig. 3A). As expected, expression of perilipin 1, a protein coating the lipid droplet and abundantly expressed only in white and brown adipocytes<sup>17</sup>, Uncoupling Protein 1 (UCP-1) Mitochondrial protein responsible for thermogenic respiration, a specialized capacity of brown adipose tissue, as well as adiponectin, a glycoprotein adipocyte-specific factor<sup>18</sup>, were specifically detected in the adipocyte fraction. As no parasite DNA was detected in the SVF of each kind of adipose tissue (Fig. 3B), these results demonstrated the localization of *L. infantum* in adipocytes.

***L. infantum* can infect both murine and human adipocytes in vitro.** We next evaluated in vitro, the ability of *L. infantum* to infect white, brown and brite adipocytes derived from primary mouse pre-adipocytes. Brite adipocytes are similar to classical brown adipocytes although they are derived from WAT. Primary pre-adipocytes from BALB/c mice were collected in subcutaneous (SC) white adipose tissue and differentiated into white and brite adipocytes. Pre-adipocytes from BAT were differentiated into brown adipocytes. 24, 48 and 72h post-infection, observation of the cells suggested the presence of intracellular parasites. This infection was observed in all types of adipocytes, and indicated the ability of *L. infantum* to infect and survive in murine adipocytes in vitro (Fig. 4). Given that *L. infantum* targets macrophages, bone marrow-derived macrophages (BMDM) were taken as a positive control for infection (Fig. S3). We subsequently observed the presence of parasites in human white and brite adipocytes differentiated from human adipose tissue stromal cells (Fig. S4)<sup>19</sup>. Specificity

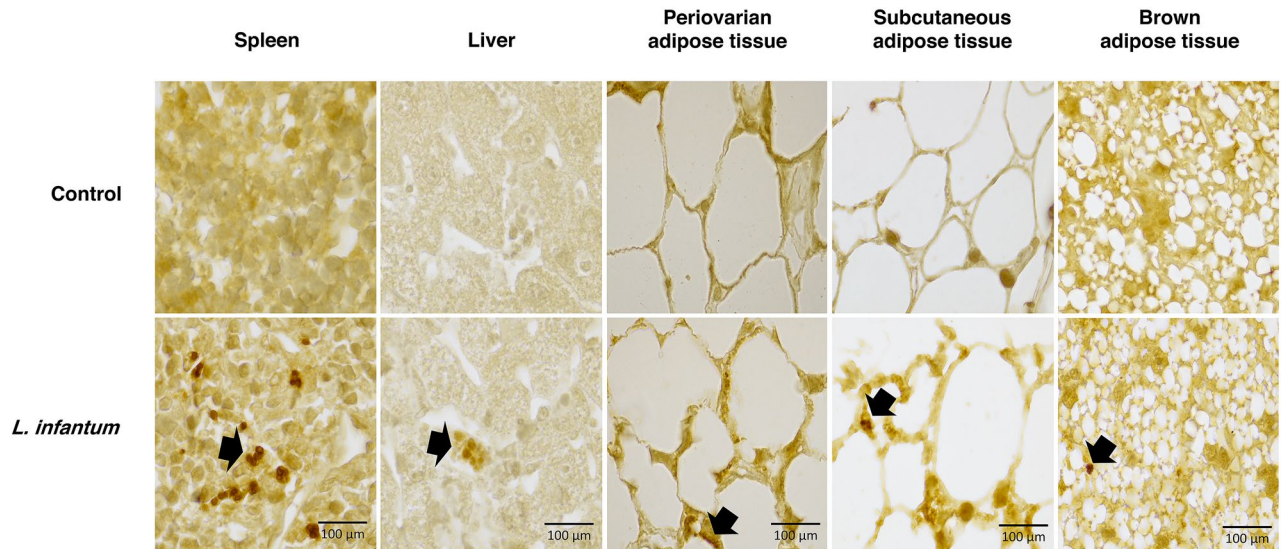
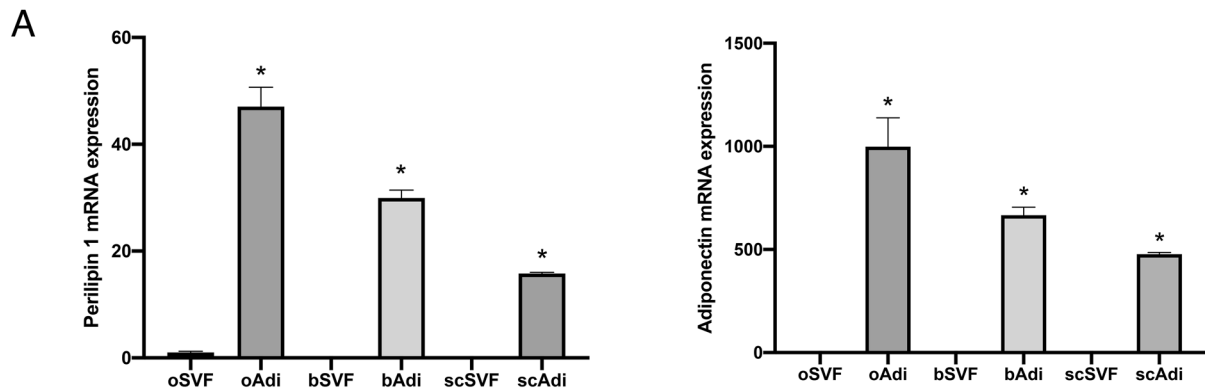


**Figure 2.** Immuno-labeled histological sections of tissues from BALB/c mice infected with *Leishmania infantum*, 40 weeks post infection. The presence of *Leishmania infantum* was determined in sections of different paraffin-embedded adipose tissue using rabbit anti-*Leishmania* polyclonal antibodies. Parasites were revealed using biotin-conjugated antibodies and peroxidase-labeled streptavidin. Labeled *Leishmania infantum* appear in orange/brown in adipocyte tissue (black arrows).



**B**

Samples		Amplification by qPCR of <i>L. infantum</i>
Adipocytes enriched fraction (Adi)	Negative control	-
	Subcutaneous AT (scAdi)	+
	Periovarian AT (oAdi)	
	Brown AT (bAdi)	
SVF	Negative control	-
	Subcutaneous (scSVF)	
	Periovarian (oSVF)	
	Brown (bSVF)	

**Figure 3.** (A) mRNA expression of Perilipin 1 and Adiponectin determined by RT-qPCR in the stroma vascular fraction (SVF) and the adipocyte fraction from scAdi, oAdi and bAdi of BALB/c mice in brown and white adipocytes (subcutaneous and periovarian) and stromal vascular fractions. Perilipin-1 and Adiponectin mRNA expression were used as a control for adipocyte purification. Histograms represent mean + sem of 4 mice. (B) Detection by qPCR of *Leishmania infantum* in adipose tissue fractions. DNA was extracted in a 100  $\mu$ L volume and the presence of *L. infantum* DNA was determined by qPCR using a 2.5  $\mu$ L DNA extract. \* $p < 0.05$ .

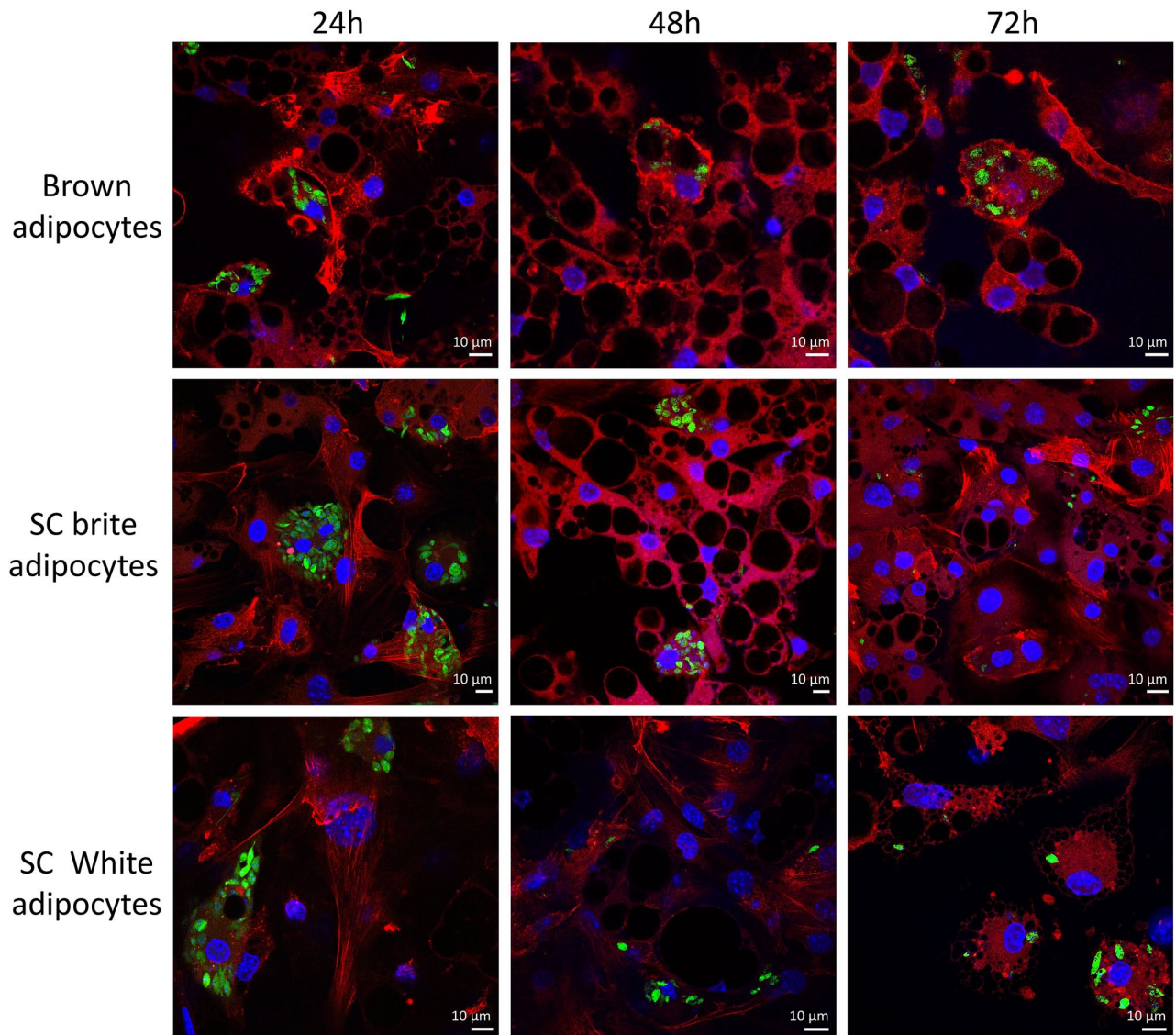


**Figure 4.** Confocal microscopy of BALB/C adipocytes infected *in vitro* with GFP-*L. infantum*. Adipocytes of pre-adipocyte murine origin were infected after 7 days of differentiation with 10 GFP-*Leishmania*/cells. Red: phalloidin-Txred, Blue: Dapi, Green: GFP-leish. Images were acquired with Nikon Confocal A1R software (NIS-Elements Confocal) from Nikon (<https://www.microscope.healthcare.nikon.com>). Images were merged with ImageJ bundled with Java 1.8.0\_172 (<https://imagej.nih.gov/ij/>). Images were assembled with Adobe Photoshop 2020 (<https://www.adobe.com/>).

of *in vitro* differentiated adipocytes was assessed by qPCR for both adipocytes isolated from mouse and human donors (Fig. S5). To confirm the intracellular localization of *L. infantum* parasites in brown adipocytes, we performed an electron microscopy experiment. *L. infantum* parasites were indeed found inside a vacuole within lipid droplet-containing cells (Fig. 5). Moreover, using confocal microscopy we found GFP-*L. infantum* parasites inside 3T3-L1 adipocytes (Fig. S6). Altogether, by combining confocal and electron microscopy approaches, we confirmed the ability of *L. infantum* to parasitize adipocytes. Here we provide *in vivo* and *in vitro* evidence demonstrating that adipocytes are *bona fide* host cells for *L. infantum* parasites.

## Discussion

*Leishmania* persistence in humans is a critical medical problem but their sanctuaries remain undetermined. Adipose tissue has been recently hypothesized as a reservoir for several intracellular pathogens that are able to induce relapses<sup>10–15</sup>. Moreover, we previously highlighted the presence of *L. infantum* in intra-abdominal fat in BALB/c mice<sup>9</sup>. Here, we investigated whether or not adipocytes could be infected and if the adipose tissue could be a sanctuary of persistence for *L. infantum*.

Our results have shown the presence of *L. infantum* in murine subcutaneous, periovarian, dorsal and predominantly in brown adipose tissue. These results show that *L. infantum* parasites can be found both in white and brown adipose tissue regardless of their different physiological roles, even though persistence in white

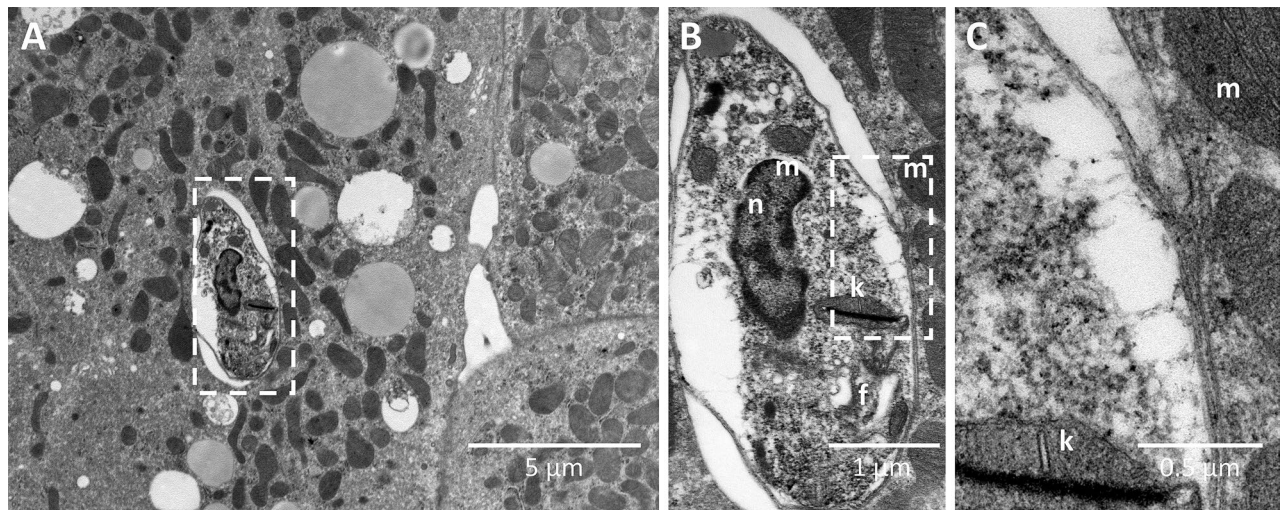


**Figure 5.** (A–C) Electron microscopy of in vitro infected brown adipocytes by GFP-*L. infantum* with different magnification (nucleus (n), flagella (f), kinetoplast (k), mitochondrion (m)).

adipose tissue is shorter. Mechanisms leading to the elimination of parasites in white adipose tissue over time would be of interest to study.

As mentioned in the results section, parasite burden in adipose tissue was insufficient for bioluminescence detection using the previously generated LUC-*L. infantum* parasites, thus we could not follow-up the infection in vivo. It would be interesting in the future to generate new highly bioluminescent strains allowing detection of few parasites, in order to characterize persistence in adipose tissue, and possibly shed light on other possible persistence sites.

As adipose tissue also contains macrophages, we investigated by qPCR the presence of parasites in an adipocyte-enriched fraction. Because presence of *L. infantum* parasites was demonstrated only in this fraction and not in the macrophage-containing SVF fraction, we analyzed by electron microscopy the infection of adipocytes by *L. infantum* parasites. For that purpose, we used adipocytes differentiated from murine pre-adipocytes isolated from stromal vascular cells. Visualization of electron microscopy data, 48h post infection has shown entrance and presence of a vacuole around *L. infantum* parasites. Interestingly, we could not find vacuoles containing multiple parasites. It would be interesting to perform further experiments to assess whether or not parasites are able to multiply in adipocytes.

Indeed, as it has been shown for *Mycobacterium tuberculosis*<sup>10</sup>, we can hypothesize that within the adipocytes *L. infantum* is in a dormancy state waiting for a better time to exit its host cell. Moreover, transfer of BAT from previously infected BALB/c to naive mice led to development of infection. This indicates that the *L. infantum* parasites present in BAT are infectious parasites, able to infect the liver, spleen and BAT of naive mice. We have shown that, in vitro, *L. infantum* can infect mouse and human adipocytes equally. Furthermore, BAT has been discovered recently in human adults in several anatomical regions<sup>20,21</sup>, thus, we suppose that *L. infantum* can similarly infect humans, as is described for rodents herein.

Another advantage for the parasite to infect adipocytes is that these cells are not professional phagocytes with inherent antimicrobial activities compared to macrophages, which are typically considered to be the host cell reservoir for *Leishmania* parasites. Nevertheless, it has been demonstrated that dermal adipocytes displayed antimicrobial activity<sup>22</sup>. Also, it will be interesting to evaluate this in white, brite and brown adipocytes to tentatively correlate antimicrobial capacity to the variation of persistence duration between these tissues. Our results further suggest that treatments with poor access to adipose tissue would be poorly effective at resolving the infection and would likely be followed by relapses. Further studies will be necessary to determine in humans whether adipocytes could be a reservoir for *L. infantum*. These findings could have an impact on future treatment development, taking into account drug bioavailability in newly found persistence sites to avoid relapses.

## Methods

**Mice and ethics statement.** Design and realization of animal experiments follow the ARRIVE guidelines. Female BALB/c mice were purchased from Charles River (France). Mice were maintained and handled according to the regulations of the European Union, the French Ministry of Agriculture and to FELASA (Federation of Laboratory Animal Science Associations) recommendations. Experiments were approved by the ethics committee of the Nice School of Medicine, France (Protocol number: 2017-56).

**Statistical analysis.** GraphPad Prism 9 was used for statistical analysis. Significance was determined by analysis of variance (ANOVA) using a Bonferroni correction for multiple comparisons. A p-value < 0.05 was considered significant.



***L. infantum* culture.** *L. infantum* MON-1 (MHOM/FR/94/LPN101), was isolated from a patient with Mediterranean visceral leishmaniasis contracted in the Nice area (South of France). We used this isolate to generate a recombinant *L. infantum*—expressing the Green Fluorescent Protein reporter (GFP-*L. infantum*) and *L. infantum*—expressing the Luciferase reporter (LUC-*L. infantum*)<sup>9</sup>. *L. infantum* promastigotes were routinely grown at 26 °C in Schneider's Insect Medium (Sigma<sup>®</sup>) supplemented with NaHCO<sub>3</sub> 0.4 g/L (Janssen chimica<sup>®</sup>), CaCl<sub>2</sub> 0.6 g/L (Fluka Chemika<sup>®</sup>), Fetal Bovine Serum 10% (Gibco<sup>®</sup>), 10 mL urine pool for 500 mL of medium, Phenol Red 0.1%, Hepes 10 mM pH 7.3, penicillin/streptomycin 1% (Gibco<sup>®</sup>), and L-Glutamine 1% (Gibco<sup>®</sup>).

**Parasite preparation and inoculation in mice.** Briefly the promastigote forms were washed three times in PBS, and  $2 \times 10^8$  parasites were injected by intravenous route in 200  $\mu$ L of PBS. Control mice were injected with 200  $\mu$ L of PBS.

**Minced BAT tissue from infected BALB/c.** BAT from infected BALB/c mice was sampled and freshly minced using a potter. The minced infected BAT was injected by intraperitoneal route in naive BALB/c mice.

**Separation of an adipocyte-enriched fraction and a stromal vascular fraction (SVF).** Briefly BAT and WAT were minced and then digested for 45 min at 37 °C in collagenase type 2. The tissue digest was passed through 250  $\mu$ m nylon sheets. Floating adipocytes were separated from the SVF after decantation. The floating fraction corresponding to the adipocyte-enriched fraction was carefully removed.

**Quantification of parasites by quantitative PCR.** Each sample of Adipose tissue, liver and spleen (25 mg) was put in a sterile tube of Lysing Kits (Precellys<sup>®</sup>), and then homogenized by Precellys<sup>®</sup> ( $2 \times 30$  s, with a break of 15 s) in lysis buffer of the Qiagen Kit QIAmp DNA Mini Kit<sup>®</sup>. DNA extraction was conducted according to the recommendations of Qiagen<sup>®</sup>. The extracts were kept at -20 °C for conservation. Quantitative PCR was implemented for detection and quantification of *L. infantum* targeting minicircle kinetoplast DNA (kDNA). Primers and probes previously described by Mary et al.<sup>5</sup> containing 20 pmol of each forward (5'-CTTTTCTGG TCCTCCGGGTAGG-3') and reverse (5'-CCACCCGGCCCTATTTTACACCAA-3') primer and 3.33 pmol TaqMan probe (FAM-TTTTCGCGAGAACGCCCTACCCGC-TAMRA) were used for *Leishmania* screening and quantification<sup>5</sup>. The assays were performed with a final volume of 10  $\mu$ L, including the 2.5  $\mu$ L DNA sample. A standard curve was obtained from the primary DNA extraction source of  $2.5 \times 10^7$  parasites and diluted serially at a 1/10 rate, which corresponded to 50,000 to 0.05 parasites in 2.5  $\mu$ L. The PCR program was implemented with two temperature steps of 95 °C and 60 °C for 40 cycles. The standard curve and a pair of negative controls were used for each assay.

**Histology and microscopic observation.** Organs were fixed in 4% PFA (ParaFormAldehyde). Samples were embedded in paraffin automatically with the spin tissue processor STP120 (ThermoFisher<sup>®</sup>). The tissue processor STP120 uses alcohol to remove water from tissues and replace it with a medium that allows sectioning of tissue. Thin sections (2.5  $\mu$ m) were cut with a Microtome Microme HM340E (Leica BIOSYSTEMS<sup>®</sup>). Sections were deparaffinized by immersing 3 $\times$  in xylene, rehydrated by successive immersion in ethanol solutions of different percentages (100%, 95%, 70%, 50%) and in water. Unmasking was conducted boiling in 10 mM Sodium Citrate buffer (pH 6.0). Endogenous peroxidase activity was blocked by a solution of 3.0% hydrogen peroxide. The immuno-histochemistry labeling consisted of a primary human antibody directed against *Leishmania*. This antibody was recognized by an anti-human goat antibody, which was recognized by biotinylated anti-goat, the signal was amplified and revealed by Streptavidin-HRP. The brightfield microscope was an Eclipse Ci upright stand (Nikon, Japan), using objectives 20 $\times$  dry NA 0.40. Acquisitions were done with a DS—Ri 1 camera (Nikon, Japan).

**Mouse primary pre-adipocyte purification and differentiation.** The method for generating white, brite and brown adipocytes from stromal vascular fraction (SVF) cells was adapted from a previous publication<sup>23</sup>. Briefly, fat deposits were sampled, minced and then digested for 45 min at 37 °C in DMEM (Lonza, BE12-707F) containing 2 mg/mL collagenase A (Roche Diagnostics, 11088793011) and 20 mg/mL BSA (Sigma-Aldrich Chemie GmbH, A7030). The digestion was successively filtrated through 250, 100 and 27  $\mu$ m nylon sheets, and finally centrifuged at 500 $\times$ g for 5 min. The pellet containing the SVF was cleared from red blood cells using specific buffer (Sigma) before being plated and maintained in DMEM containing 10% (v/v) fetal calf serum (FCS) until confluence. Differentiation was induced by supplementation with 1  $\mu$ M dexamethasone (Sigma-Aldrich Chemie GmbH, D4902), 0.5 mM isobutylmethylxanthine (Sigma-Aldrich Chemie GmbH, I5879) and 860 nM insulin (Invitrogen, 12585014) for 2 days. Cells were then maintained for 7–10 days in presence of 100 nM insulin for white adipogenesis or a mixture containing 100 nM insulin, 1  $\mu$ M rosiglitazone (BertinPharma, 71740) and 0.2 nM triiodothyronine (Sigma-Aldrich Chemie GmbH, T6397) for brown or brite adipogenesis.

**Differentiation and generation of 3T3 adipocytes.** 3T3-L1 fibroblasts were grown at 7% CO<sub>2</sub> and 37 °C on coverslips in 35 mm dishes in DMEM, 25 mM glucose, and 10% calf serum, and 1% Penicillin–Streptomycin, and induced to differentiate in adipocytes. Briefly, 2 days after confluence, medium was changed for DMEM, 25 mM glucose, 1% Penicillin–Streptomycin, and 10% fetal calf serum (FCS) supplemented with isobutylmethylxanthine (0.25 mM), dexamethasone (0.25  $\mu$ M), insulin (5  $\mu$ g/mL), and pioglitazone (10  $\mu$ M). The medium was removed after 2 days and replaced with DMEM, 25 mM glucose, 1% Penicillin–Streptomycin, and 10% FCS

supplemented with insulin (5 µg/mL) and pioglitazone (10 µM) for 2 days. Then the 3T3-L1 adipocytes were fed every 2 days with DMEM, 25 mM glucose, 1% Penicillin–Streptomycin, and 10% FCS.

**Differentiation and generation of macrophages.** For BMDM (Bone Marrow Derived Macrophage), mouse femurs were removed and purified from the surrounding muscles and connective tissue. Under sterile conditions, the bone marrow was flushed by pressure after needle penetration in epiphyses with BMDM medium containing RPMI and deplemented FBS 10% and gentamycin 0.001%. The cells were centrifuged (400×g, 5 min) and resuspended in BMDM medium supplemented with M-CSF 10 ng/mL. Cells were seeded at  $5 \times 10^5$  cells/well.

Blood monocytes were isolated from human healthy blood samples (leukoplatelet layer, Etablissement Français du Sang) using EasySep™ Human Monocyte Enrichment Kit (STEMCELL Technologies) according to manufacturer's instructions. Macrophage differentiation was induced by human M-CSF (Peprotech, 100 pg/mL, 5 days).

**Human adipocytes differentiation.** Human adipose tissue primary progenitor cells were from a previous study<sup>19</sup> and differentiated as follow. Cells were cultivated in DMEM containing 10% FCS until confluence. When the cells reached confluence, they were induced to differentiate for 3 days in DMEM/Ham's F12 (1:1) media supplemented with 10 µg/mL transferrin, 10 nM insulin, 0.2 nM triiodothyronine, 1 µM dexamethasone and 500 µM isobutyl-methylxanthine. The cells were next differentiated into white adipocytes using a media supplemented with 10 µg/mL transferrin, 10 nM insulin, 0.2 nM triiodothyronine or into brite adipocytes in the same media supplemented with 100 nM rosiglitazone.

**Isolation and analysis of RNA.** Total RNA was extracted using a TRI-Reagent kit (Euromedex) according to the manufacturer's instructions. Reverse transcription-polymerase chain reaction (RT-PCR) was performed using M-MLV-RT (Promega). SYBR qPCR premix Ex Taq II from Takara (Ozyme) was used for quantitative PCR (qPCR), and assays were run on a StepOne Plus ABI real-time PCR instrument (PerkinElmer Life and Analytical Sciences). The expression of selected genes was normalized to that of the 36B4 (RPLP0, Ribosomal Protein Lateral Stalk Subunit P0) and TBP (TATA-box protein) housekeeping genes and then quantified using the comparative-ΔCt method. Primer sequences are available upon request.

**In vitro infection.** The BMDM and adipocytes of pre-adipocyte murine origin were infected after 7 days of differentiation with a ratio of 10:1 GFP-*L. infantum* per cell. Human adipocytes were infected after 14 days of differentiation with a ratio of 10:1 GFP-*L. infantum* per cell. 3T3 cells were infected 8 days after their differentiation with a ratio of 10:1 GFP-*L. infantum* per cell.

**Epifluorescence and confocal microscopy.** For epifluorescence acquisition, we used the EVOS FL microscope (AMF-4302-EU; Labtech, France), using the 10× dry Ph and 20× dry FL objectives. Acquisitions were done with a Sony ICK285AL monochrome CCD, 2/3" 1360 × 1024, 1.4 Megapixel camera (Labtech, France). For confocal microscopy, F-actin was labeled with phalloidin-TRITC (red), and the nuclei were labeled with DAPI (blue). *Leishmania*-GFP parasite are green. The fluorescent signals were analyzed with a Nikon confocal microscope using a × 60 magnification lens.

**Electron microscopy.** For ultrastructural analysis, cells were fixed in 1.6% glutaraldehyde in 0.1 M phosphate buffer (pH 7.4) at 4 °C, rinsed in 0.1 mol/L cacodylate buffer, and fixed for 1 h in 1% osmium tetroxide and 1% potassium ferrocyanide in 0.1 mol/L cacodylate buffer to enhance the staining of membranes. Cells were rinsed in cold distilled water, quickly dehydrated in cold ethanol, and lastly embedded in epoxy resin. Contrasted ultrathin sections (70 nm) were analyzed under a JEOL 1400 transmission electron microscope (EM) mounted with a Morada Olympus charge-coupled device camera.

Received: 1 March 2021; Accepted: 29 September 2021

Published online: 28 October 2021

## References

1. WHO. *The WHO Leishmaniasis Fact Sheet* (World Health Organization, 2018).
2. Michel, G., Pomares, C., Ferrua, B. & Marty, P. Importance of worldwide asymptomatic carriers of *Leishmania infantum* (*L. chagasi*) in human. *Acta Trop.* **119**, 69–75 (2011).
3. Marty, P. *et al.* A century of leishmaniasis in Alpes-Maritimes, France. *Ann. Trop. Med. Parasitol.* **101**, 563–574 (2007).
4. WHO. Control of the leishmaniases. *Who Tech. Rep. Ser.* **949**, 1–185 (2010).
5. Mary, C., Faraut, F., Lascombe, L. & Dumon, H. Quantification of *Leishmania infantum* DNA by a real-time PCR assay with high sensitivity. *J. Clin. Microbiol.* **42**, 5249–5255 (2004).
6. Haque, L. *et al.* A rare case of visceral leishmaniasis in an immunocompetent traveler returning to the United States from Europe. *PLoS Negl. Trop. Dis.* **12**, e0006727 (2018).
7. Tatarelli, P. *et al.* Visceral leishmaniasis in hematopoietic cell transplantation: Case report and review of the literature. *J. Infect. Chemother.* **24**, 990–994 (2018).
8. Bogdan, C. Mechanisms and consequences of persistence of intracellular pathogens: Leishmaniasis as an example. *Cell Microbiol.* **10**, 1221–1234 (2008).

9. Michel, G. *et al.* Luciferase-expressing *Leishmania infantum* allows the monitoring of amastigote population size, in vivo, ex vivo and in vitro. *PLoS Negl. Trop. Dis.* **5**, e1323 (2011).
10. Neyrolles, O. *et al.* Is adipose tissue a place for *Mycobacterium tuberculosis* persistence. *PLoS ONE* **1**, e43 (2006).
11. Bouzid, F. *et al.* *Mycobacterium canettii* infection of adipose tissues. *Front. Cell Infect. Microbiol.* **7**, 189 (2017).
12. Bechah, Y. *et al.* Persistence of *Coxiella burnetii*, the agent of Q fever, in murine adipose tissue. *PLoS ONE* **9**, e97503 (2014).
13. Erlandson, K. M. & Lake, J. E. Fat matters: Understanding the role of adipose tissue in health in HIV infection. *Curr. HIV/AIDS Rep.* **13**, 20–30 (2016).
14. Damouche, A. *et al.* Adipose tissue is a neglected viral reservoir and an inflammatory site during chronic HIV and SIV infection. *PLoS Pathog.* **11**, e1005153 (2015).
15. Tanowitz, H. B., Scherer, P. E., Mota, M. M. & Figueiredo, L. M. Adipose tissue: A safe haven for parasites. *Trends Parasitol.* **33**, 276–284 (2017).
16. Ferreira, A. V. *et al.* Evidence for *Trypanosoma cruzi* in adipose tissue in human chronic Chagas disease. *Microbes Infect.* **13**, 1002–1005 (2011).
17. Sztalryd, C. & Brasaemle, D. L. The perilipin family of lipid droplet proteins: Gatekeepers of intracellular lipolysis. *Biochim. Biophys. Acta Mol. Cell Biol. Lipids* **1862**, 1221–1232 (2017).
18. Fang, H. & Judd, R. L. Adiponectin regulation and function. *Compr. Physiol.* **8**, 1031–1063 (2018).
19. Giroud, M. *et al.* miR-125b affects mitochondrial biogenesis and impairs brite adipocyte formation and function. *Mol. Metab.* **5**, 615–625 (2016).
20. van Marken Lichtenbelt, W. D. *et al.* Cold-activated brown adipose tissue in healthy men. *N. Engl. J. Med.* **360**, 1500–1508 (2009).
21. Virtanen, K. A. *et al.* Functional brown adipose tissue in healthy adults. *N. Engl. J. Med.* **360**, 1518–1525 (2009).
22. Zhang, L. J. *et al.* Innate immunity. Dermal adipocytes protect against invasive *Staphylococcus aureus* skin infection. *Science* **347**, 67–71 (2015).
23. Pisani, D. F. *et al.* Visfatin expression analysis in association with recruitment and activation of human and rodent brown and brite adipocytes. *Adipocyte* **5**, 186–195 (2016).

## Acknowledgements

We acknowledge Dr Véronique Corcelle and the C3M animal room facility. We thank Maéva Gesson, Marie Iron-delle and the C3M imaging facility (Côte d'Azur Microscopy and Imaging Platform, MICA). We acknowledge the University's CCMA Electron Microscopy facility supported by the Université de Nice Sophia-Antipolis, Région Provence Alpes-Côte d'Azur, Conseil Départemental 06, and Gis Ibsa and we thank Alyssia Mari for technical help. We also thank Jerome Gilleron and the C3M Immuno-histology facility. We acknowledge the IDEX UCA-JEDI Academie 4 for financial support. We also thank Abby Cuttriss of UCA for english corrections. We acknowledge financial support by the Conseil Départemental des Alpes-Maritimes and Conseil Régional PACA. This work was supported by a Grant from the Société Francophone du Diabète (SFD)/Pierre Fabre Médicament 2017. The funders had no role in the design of the study, in the collection, analyses, or interpretation of data, in the writing of the manuscript, or in the decision to publish the results.

## Author contributions

E.L., L.B., P.M., C.P. and G.M. designed in vitro experiments and analyzed results. A.S., D.F.P., J.J. and G.M. performed in vitro experiments. S.L.G., A.M. and G.M. designed and performed electron microscopy. A.S., A.M. and G.M. wrote the paper. All authors reviewed the manuscript.

## Competing interests

The authors declare no competing interests.

## Additional information

**Supplementary Information** The online version contains supplementary material available at <https://doi.org/10.1038/s41598-021-00443-y>.

**Correspondence** and requests for materials should be addressed to G.M.

**Reprints and permissions information** is available at [www.nature.com/reprints](http://www.nature.com/reprints).

**Publisher's note** Springer Nature remains neutral with regard to jurisdictional claims in published maps and institutional affiliations.



**Open Access** This article is licensed under a Creative Commons Attribution 4.0 International License, which permits use, sharing, adaptation, distribution and reproduction in any medium or format, as long as you give appropriate credit to the original author(s) and the source, provide a link to the Creative Commons licence, and indicate if changes were made. The images or other third party material in this article are included in the article's Creative Commons licence, unless indicated otherwise in a credit line to the material. If material is not included in the article's Creative Commons licence and your intended use is not permitted by statutory regulation or exceeds the permitted use, you will need to obtain permission directly from the copyright holder. To view a copy of this licence, visit <http://creativecommons.org/licenses/by/4.0/>.

© The Author(s) 2021

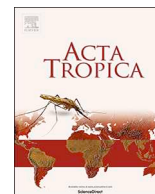


# Leishmania infection: Misdiagnosis as cancer and tumor-promoting potential

Aurélie Schwing, Christelle Pomares, Alissa Majoor, Laurent Boyer, Pierre Marty, Grégory Michel

## **Résumé**

Au regard de la prévalence des cancers et de la leishmaniose, la présence de ces deux pathologies dans le même tissu pourrait être complètement fortuite. L'issue clinique des deux maladies dépend de l'immunité innée et adaptative, et dans les deux cas, ces maladies sont caractérisées par une réponse Th1 insuffisante. Par conséquent, l'environnement cytokinique Th2 résultant de la progression de la leishmaniose pourrait promouvoir la prolifération de cellules tumorales, et vice versa. D'autre part, les aspects cliniques de formes sub-cliniques de leishmaniose cutanée ou viscérale peuvent ressembler à des néoplasmes, menant parfois à des diagnostics erronés. Dans cette revue, nous présentons les récentes découvertes sur l'association entre leishmaniose et affections malignes. Nous incluons des patients HIV positifs, négatifs et des patients dont le statut HIV n'était pas établi. La ressemblance dans les aspects cliniques a mené au diagnostic erroné de carcinome cellulaire squameux, lymphome B et T, tumeurs et granulomes oraux et intranasaux dans des cas de leishmaniose. Par conséquent, la leishmaniose devrait être considérée dans le diagnostic de cancers dans des zones où le parasite est endémique, ou dans des patients ayant voyagé vers des régions endémiques. Nous avons également listé des articles montrant que *Leishmania* pouvait promouvoir le développement de cancers dans des patients immunodéprimés et immunocompétents. Les mécanismes potentiels supportant cet effet sont discutés.



## Leishmania infection: Misdiagnosis as cancer and tumor-promoting potential

Aurélie Schwing<sup>a,b,c</sup>, Christelle Pomares<sup>a,b</sup>, Alissa Majoro<sup>a</sup>, Laurent Boyer<sup>a</sup>, Pierre Marty<sup>a,b</sup>, Grégory Michel<sup>a,\*</sup>

<sup>a</sup> Université Côte d'Azur, Inserm, C3M, Nice Cedex 3, France

<sup>b</sup> Parasitologie-Mycologie, Centre Hospitalier Universitaire L'Archet, Nice Cedex 3, France

<sup>c</sup> Aix Marseille université, Marseille, France

### ARTICLE INFO

#### Keywords:

Cancer  
Leishmania  
Tumor-promoting

### ABSTRACT

Given the prevalence of cancer and leishmaniasis worldwide, the presence of these two pathologies in the same tissue sample may be merely fortuitous. The clinical outcome of both diseases is under the control of innate and adaptive immunity, and in both cases these progressive diseases are characterized by an impaired host Th1 response. As a consequence, the Th2 cytokine microenvironment occurring in progressive leishmaniasis may potentially promote tumor cell proliferation and *vice versa*. On the other hand, clinical aspects of subclinical cutaneous or visceral leishmaniasis sometimes closely resemble those observed in various neoplasms thus leading to misdiagnosis. In this review, we present recent findings on the association between leishmaniasis and malignant disorders. Our review includes HIV positive, HIV negative subjects and patients whose HIV status has not been established. Leishmaniasis mimicking a malignant disorder was confirmed and extended to unreported neoplastic disorders including squamous cell carcinoma, T-cell and B-cell lymphoma, oral and intranasal tumors and granulomas. Thus, leishmaniasis should be considered in the differential diagnosis and course of various cancers in *Leishmania* endemic areas or in patients with travel history to these areas. We also listed recent reports showing that *Leishmania* can promote cancer development in immunocompromised as well as in immunocompetent patients. The potential mechanisms supporting this promoting effect are discussed.

### 1. Introduction

Leishmaniasis is a disease induced in humans by protozoan parasites from more than twenty different *Leishmania* species (WHO, 2018). The vector, a female phlebotomine sand fly, transmits parasites during blood feeding. The common clinical forms of leishmaniasis are visceral Leishmaniasis (VL), cutaneous Leishmaniasis (CL) and to a lesser extent muco-cutaneous Leishmaniasis (MCL). The outcome of infection can be variable, ranging from an asymptomatic form to obvious disease with intermediate cases of subclinical forms (Michel et al., 2011). In humans, CL appears as a localized lesion, with a long self-healing process. After healing, a depressed scar remains. MCL is generally the result of the parasite dissemination from the skin to the naso-oro-pharyngeal mucosa of certain species from the New World *Leishmania* subgenus (Burza et al., 2018). This dissemination occurs through lymphatic or blood vessels from a CL papule to the nasal mucosa. The most severe form, VL, is fatal if untreated and represents the second largest parasitic killer in the world after malaria (DebRoy et al., 2017). Leishmaniasis, classified as a neglected tropical disease, is widespread worldwide except for

Oceania. According to the WHO, the estimated annual incidence of leishmaniasis is one million new cases, resulting in 30 000 deaths per year (WHO, 2018). In parallel, besides the numerous cases of leishmaniasis, there are about 14 million new cases of cancer each year, which represents the second leading cause of death in the world (McGuire, 2016). Therefore, due to their frequency, an association between leishmaniasis and neoplastic disorders is likely to occur by chance. However, a growing number of studies speculate on a possible causal association between Leishmaniasis infection and the subsequent appearance of malignancy (Al-Kamel, 2017). We will review the literature in order to assess whether or not this hypothetical link is present. We shed in light that *Leishmania* infection can mimic cancer symptoms resulting in misdiagnosis, but also highlight that *Leishmania* can be found in neoplastic disorders in various clinical situations. The possible mechanisms underlying how leishmaniasis could promote cancer progression and *vice versa* are discussed.

\* Corresponding author.

E-mail address: [gmicHEL@unice.fr](mailto:gmicHEL@unice.fr) (G. Michel).

<https://doi.org/10.1016/j.actatropica.2018.12.010>

Received 18 October 2018; Received in revised form 3 December 2018; Accepted 6 December 2018

Available online 07 December 2018

0001-706X/ © 2018 Published by Elsevier B.V.

**Table 1**  
Human Cutaneous leishmaniasis mimicking cancer disorder.

<i>Leishmania</i> species	Clinical expression	Cancer mimicking	Investigation method for <i>leishmania</i>	Sample	Country	References
<i>L. braziliensis</i>	CL	Squamous cell carcinoma	Microscopy	Biopsy	Brazil	(Quintella et al., 2011)
<i>L. donovani</i> complex	MCL	Intranasal tumor	Histopathological examination and PCR	Tumoral mass	Turkey	(Gul et al., 2016)
<i>L. infantum</i>	CL	Squamous cell carcinoma	Microscopy	Biopsy	Iran	(Khorsandi-Ashtiani et al., 2009)
<i>L. major</i>	MCL	Intranasal tumor	Microscopy and PCR	Biopsy	Spain	(Ramos et al., 2015)
	CL	Carcinoma	Microscopy	lesion smears	Spain/Bolivia	(Cobo et al., 2016)
<i>L. mexicana</i>		Squamous cell carcinoma		Biopsy	Syria	(Sabri et al., 2009)
nd		Squamous cell carcinoma		Biopsy	United States	(Oetken et al., 2017)
	MCL	T-cell lymphoma	Serological Assays and PCR	Serum, biopsy	Brazil	(Nicodemo et al., 2017)
		Oral cancer	Biopsy and microscopy	Biopsy	Italy	(Celentano et al., 2015)
	Subclincic	Granulomas	Microscopy	Biopsy	Saudi Arabia	(Al-Qahtani et al., 2012)
	MCL	Squamous carcinoma	Microscopy and PCR	Biopsy	Turkey	(Akcali et al., 2008)

**Table 2**  
Human Visceral leishmaniasis mimicking cancer disorder (nd : not documented).

<i>Leishmania</i> species	Cancer mimicking	Investigation method for <i>leishmania</i>	Sample	Country	References
<i>L. donovani</i>	Lymphoma	Microscopy, peripheral blood culture	Bone marrow aspiration	India	(Kawakami et al., 1996)
	Histiocytosis	Microscopy and Serology		Saudi Arabia	(Sheikha et al., 1993)
	Nasopharyngeal tumor	Microscopy	Biopsy	India	(Naik et al., 1978)
<i>L. infantum</i>	Lymphoma	Microscopy, PCR and Serology	Bone marrow aspiration	Spain	(Evers et al., 2014)
	Cutaneous spindle-cell pseudotumors	Microscopy, culture		nd	(Perrin et al., 1993)
nd	B-cell lymphoma	Microscopy		Italy	(Orlandi and Malfitano, 2014)
	Adrenal Cystic Mass		Biopsy	Greece	(Brenner et al., 2000)

## 2. Leishmaniasis and cancer: diseases with similar symptoms

Sometimes, physical aspects as well as clinical parameters of CL and VL closely resemble those observed in various neoplasms (Tables 1 and 2). For example, lymphoma symptoms including enlarged lymph nodes, fever, sweating and chills, weight loss, extreme tiredness and swollen abdomen are clearly similar to those observed in VL (Kawakami et al., 1996; Evers et al., 2014). In a same way, CL lesions can resemble cutaneous cancers. Tables 1 and 2 present data from 18 clinical studies on leishmaniasis that masqueraded as a neoplastic disorder including 14 of them that were not mentioned in a previous review (Kopterides et al., 2007). Reported clinical cases indicated that subclinical forms of MCL and CL due to *L. infantum* and *L. major* can be misdiagnosed as various cancers including oral carcinomas, squamous cell carcinomas, T-cell lymphomas and granuloma tumors (Table 1). In the same way, sub-clinical forms of VL were misdiagnosed as lymphomas, histiocytosis, nasopharyngeal tumors, cutaneous spindle-cell pseudotumors and adrenal cystic masses (Table 2). Subclinical VL cases were characterized by clinical manifestations such as lymphadenopathy or two or more mild symptoms associated with at least one positive biological test (Badaro et al., 1986). In every case, *Leishmania* parasites were found in biopsies by anatomopathological studies. Therefore, Leishmaniasis can sometimes be misdiagnosed, and this misdiagnosis can lead either to surgical interventions or to the administration of an inadequate treatment (corticosteroids) and can delay the correct diagnosis and treatment (Orlandi and Malfitano, 2014; Gul et al., 2016).

## 3. The *Leishmania* and cancer link: does Leishmaniasis promote cancer development?

In humans, clinical expression of leishmaniasis ranged from sub-clinical to symptomatic forms. In this chapter, we focused only on clinical cases where leishmaniasis and tumor cells were observed in the

same biological sample. Leishmaniasis cases arising in patients previously diagnosed with various cancers and treated with anti-cancer chemotherapy for months have been reviewed previously (Kopterides et al., 2007). Indeed, although local immune suppression induced by malignant disorders may promote leishmaniasis development, it is more likely that immunosuppression induced by long-term anti-cancer drug therapy is responsible for parasite expansion (Fishman, 2011). In these cases, clinical data suggested that leishmaniasis may manifest itself in a more severe clinical course with unfavorable prognostic. In our review, numerous cases that speculate on a possible causal association between leishmaniasis infection and appearance of malignancy have been studied. Among the 28 presented cases, 14 cases were published after 2007 (Kopterides et al., 2007). Moreover, co-presence of leishmaniasis and cancer is represented with 5 new cases. Those 33 clinical cases with the co-presence at cancer diagnosis time, of tumor cells and *Leishmania* parasites in humans are summarized in Tables 3–5.

### 3.1. In HIV + patients

Seven cases of co-presence of leishmaniasis and cancer, originated from HIV + patients, are reported in this review. In HIV + subjects, VL was associated in three cases with squamous carcinoma and in one case, either with Burkitt lymphoma or dermatofibroma (Table 3). In HIV + individuals, as previously reported, the parasite multiplication can simply result from the immunosuppression due to the HIV-induced loss of *Leishmania* specific CD4 + T cells (Akuffo et al., 2018). However, participation of tumor cells to parasite expansion via local tumor-induced decrease of Th1 compartment, leading to a facilitated parasite growth, cannot be totally ruled out.

### 3.2. In HIV- patients

In HIV- humans, cutaneous leishmaniasis was associated with basal

**Table 3**  
Leishmaniasis in HIV + patients diagnosed with cancer.

<i>Leishmania</i> species	Clinical expression	Cancer	Investigation method for <i>leishmania</i>	Sample	Country	References
<i>L. donovani</i>	Subclinical	Conjunctival Squamous Carcinoma	Microscopy	Biopsy	Guatemala	(Bielory et al., 2011)
<i>L. donovani</i>	VL	Burkitt lymphoma			nd	(Boutros et al., 2006)
<i>L. infantum</i>	Subclinical	Squamous cell carcinoma	Histopathology, Microscopic examination		Italy	(Donati et al., 2013)
<i>L. infantum</i>					Spain / Morocco	(Armengot-Carbó et al., 2012)
<i>L. infantum</i>	MCL	Kaposi's sarcoma	Microscopy, isoenzymatic methods		France	(Michiels et al., 1994)
<i>L. infantum</i>	VL		Microscopy, culture, serology	Bone marrow aspiration, biopsy	Mediterranean countries	(Taillan et al., 1992)
nd		Dermatofibroma	Microscopy		Spain	(Castellano et al., 1999)
nd	Subclinical	Cutaneous Kaposi's sarcoma			Spain / Mexico	(Albrecht et al., 1994)

cell carcinoma, ocular epidermoid carcinoma or basal cell carcinoma and visceral leishmaniasis was co-present with lymphoblastic leukemia, lymphoma or osteosarcoma (Tables 4,5). In patients whose HIV status was not documented, CL or VL were associated mainly with leukemia and myeloma (Tables 4,5). Interestingly, on some occasions, a non-response to leishmaniasis therapy was observed. This lack of response was attributed to the presence of tumor cells, and excision of these cells restored the sensitivity of *Leishmania* to current treatments (Jewell and Giles, 1996; Asilian et al., 2012). Moreover, the development of cancer in leishmaniasis scars could occur several years after apparent healing. Therefore, the possible role of CL as a predisposing factor for skin cancer should be taken into account (Suster and Ronnen, 1988; Asilian et al., 2012).

### 3.3. In animals

In Table 6, we specifically pinpointed clinical cases of co-localization of *Leishmania* parasites and tumor cells in dogs. In these cases, dog visceral Leishmaniasis was mainly associated with transmissible venereal tumor or less frequently with histiocytic tumor, non-histiocytic lymphoma or squamous cell carcinoma.

The co-presence of Leishmaniasis and tumor cells in immunocompetent host (HIV - patients or dogs) at the time of cancer diagnosis raises the question of the reciprocal influence of cancer development and *Leishmania* proliferation (Tables 3–6).

## 4. Leishmaniasis triggered modulation of anti-cancer immunity

Studies in mouse models as well as in humans have demonstrated that the control of parasite proliferation in target organs depends on innate and adaptive immunity developed by the host. Type 1 adaptive

immunity characterized by IFN- $\gamma$ , IL-2, TNF- $\alpha$  and IL-12 production by CD4 + T-cell subsets, delayed-type hypersensitivity (DTH) and CD8 + T cells with suppressor antibody activity, confers protection against infection. By contrast, development of type 2 (Th2 cells) adaptive immunity, characterized by IL-4, IL-5 and IL-10 production by CD4 + T-cell subsets, antibody production and T suppressor DTH cells, leads to uncontrolled parasite proliferation in target organs (Kumar et al., 2017). Recently, Th17 subsets in conjunction with Th1 subsets have been shown to play an important role in the defense against various pathogens or in the control of cancer development, but these responses can be suppressed by T regulatory cells (T regs) recruited by the growing tumors (Steer et al., 2010). Generally, mixed Th1/Th2 responses were observed in response to parasite infection, but only hosts mounting a Th1 dominant response were able to contain parasite multiplication (Bretscher et al., 2002). Following parasite inoculation, most humans control parasite proliferation and become asymptomatic carriers. Thus, people developing patent disease represent only the tip of the iceberg (Michel et al., 2011). Immune suppression in healthy subjects such as that occurring in HIV + or in long-term immunosuppressive or anti-cancer therapy, results in some cases in the reactivation of parasite multiplication (Marty et al., 2007). Leishmaniasis also affects the activation and function of macrophages and dendritic cells and is responsible for chronic inflammation. Interestingly enough, chronic inflammation promotes cancer through multiple mechanisms like genomic instability and DNA damage which may cause genetic and epigenetic mutations initiating cancer (Schetter et al., 2010). Of note, like Leishmaniasis, progressive cancers alone can in some cases be associated with tumor specific Th2 response and regression of Th1 response (Bretscher et al., 2001; Ivanova and Orekhov, 2015). Moreover, many types of cancers take advantage of the immunomodulating activities of cytokines because of their capacity to act

**Table 4**  
Human Cutaneous leishmaniasis in patients diagnosed with cancer.

<i>Leishmania</i> species	Clinical expression	Cancer	Investigation method for <i>leishmania</i>	Sample	Country	References
<i>L. braziliensis</i>	MCL	Ocular Epidermoid carcinoma	Microscopic examination	Biopsy	Brazil	(Matayoshi et al., 2000)
<i>L. infantum</i>	Diffuse CL	Sézary syndrome	Microscopic examination and PCR		Spain	(Giavedoni et al., 2014)
	CL	Chronic lymphocytic leukaemia	Skin culture		Italy	(Jewell and Giles, 1996)
	MCL	Kaposi's sarcoma	Microscopy and isoenzymatic methods		France	(Michiels et al., 1994)
<i>L. mexicana</i>	Diffuse CL	Epidermoid cancer	Microscopy and PCR		Mexico	(Blum-Domínguez et al., 2017)
nd	CL	Basal Cell Carcinoma	Leishmanin skin tests		Iran	(Asilian et al., 2012)
			nd (30 years after the primary lesion)		Turkey	(Unlü et al., 2007)
		Necrotic leukaemic lesion	Microscopic examination		Turkey	(Paydaş and Zorludemir, 2000)
		Basal Cell Carcinoma			United Kingdom	(Rayatt and Moss, 2000)
					United Kingdom	(Czechowicz et al., 1999)
		Squamous Cell Carcinoma			Iran	(Friedman et al., 2003)
		Basal Cell Carcinoma			Israel	(Suster and Ronnen, 1988)



**Table 5**  
Human Visceral leishmaniasis in patients diagnosed with cancer.

<i>Leishmania</i> species	Clinical expression	Cancer	Investigation method for <i>Leishmania</i>	Sample	Country	References
<i>L. chagasi</i>	VL	Acute lymphoblastic leukemia	Serology	Blood sample	Brazil	(de Vasconcelos et al., 2014)
<i>L. donovani</i>	Subclinical	Distal femoral osteosarcoma	Microscopy	Biopsy	Greece	(Papanastasiou et al., 2016)
		Multiple myeloma	<i>Leishmania</i> -specific polymerase chain reaction (PCR) analysis		Italy	(Piro et al., 2012)
		Hodgkin's Lymphoma	Microscopy		Brazil	(Domingues et al., 2009)
<i>L. infantum</i>	VL	Acute myeloblastic leukemia	Microscopic examination, Indirect immunofluorescence test	Bone marrow aspiration	Nepal	(Sah et al., 2002)
		B-Cell Acute Lymphoblastic Leukemia	Microscopy, PCR and <i>in vitro</i> cultivation	Serum and bone marrow aspirate	Morocco	(El Youssi et al., 2015)
		Splenic Marginal Zone Lymphoma		Bone marrow aspiration	France	(Vase et al., 2012)
nd	Subclinical	Acute lymphoblastic leukemia	Microscopy	Bone marrow aspiration, biopsy	Iran	(Fakhar et al., 2008)
		Kaposi's sarcoma	Microscopy, culture, serology		Mediterranean countries	(Taïllan et al., 1992)
		Dermatofibroma	Microscopy	Biopsy	Spain	(Castellano et al., 1999)
		Cutaneous Kaposi's sarcoma			Spain / Mexico	(Albrecht et al., 1994)

on gene expression and to down-regulate immune responses that can eliminate cancer cells. Thus, many tumor cells secrete the immunosuppressive IL-10 cytokine with a concomitant decrease in the capacity to trigger protective Th1 responses. Consequently, Th2 micro environment together with chronic inflammation observed in obvious Leishmaniasis may facilitate cancer setting and progression and *vice versa*.

**5. Discussion**

In this review, we analyzed clinical cases of *Leishmania* infection in relationship with cancers. As in some cases development of atypical CL or VL physically and clinically resembles various cancer developments (Albrecht et al., 1994; Galluzzi et al., 2018), *Leishmania* infection was misdiagnosed and some patients received either anti-tumoral therapy before biopsy or underwent surgery. As a consequence, *Leishmania* infection worsened, until the right diagnosis was established and adequate *Leishmania* treatment was initiated (Al-Qahtani et al., 2012). These data confirmed that atypical CL can mimic various other skin disorders. Therefore, CL should be considered in patients with non-healing and/or unusual dermatological lesions especially in endemic countries and in individuals travelling in endemic regions. In addition, CL should be considered in transplanted patients who traveled or lived in endemic areas and display atypical cutaneous lesions whose clinical initial appearance suggested cancer development (Ramos et al., 2015). Cancers and leishmaniasis are very common diseases occurring worldwide (WHO, 2018; McGuire, 2016). Therefore, the unrelated coexistence of both pathologies in the same host can at first glance be expected. The outcome of both diseases is under the control of innate immunity including macrophages and natural killer cells, and of adaptive immunity including CD4/CD8 cells and regulatory T-cells (Melssen and Slingluff, 2017) and (da Silva Santos and Brodskyn, 2014). The development of a Th1 dominant response by CD4 + T-cells generally leads to the containment of both pathologies whereas the impairment of Th1 responses leads to parasite proliferation in target organs or uncontrolled cancer progression (Rodrigues et al., 2016) (Melssen and Slingluff, 2017). Presence of *Leishmania* and/or tumor cells, prolonged inflammatory signaling and defects in anti-inflammatory mechanisms can lead to chronic inflammation and benefit tumor development and/or parasite proliferation. Therefore, *Leishmania* chronic infection and/or cancer development are able to create a microenvironment that could promote parasite growth and/or cancer progression. As a consequence, environment generated following *Leishmania* infection can promote cancer progression and *vice versa*. Of note, the fact that the anti-cancer drug Miltefosine also displays a strong leishmanicidal effect suggests that mechanisms supporting parasite or cancer growth are at least partially similar (Tiwari et al., 2018). The notion that chronic inflammation may induce, promote or influence susceptibility to carcinogenesis is not novel (Parisi et al., 2018). Indeed, coinfection with multiple pathogens has been shown to accelerate cancer development in certain cases (Yasunaga and Matsuoka, 2018). For example, parasitic or bacterial infection is a risk factor for adult T cell leukemia lymphoma induced by human T cell leukemia virus type 1. Similarly, Epstein-Barr virus and malaria are closely associated with endemic Burkitt lymphoma (Yasunaga and Matsuoka, 2018). These findings indicate that these oncogenic pathogens can overcome host barriers against cancer development. Actually, it is estimated that 15% of cancers worldwide can be attributed to infection with oncogenic pathogens.

Here, we listed articles reporting on the co-localization of VL or CL with various cancers in HIV + human hosts, in humans whose HIV status was not documented, in HIV- patients and dogs (Tables 3–6). As immunosuppression alone in HIV + patients can promote Leishmaniasis development or can induce Kaposi's sarcoma and increase the risk of various cancers, the association of both pathologies evolving independently can be possible. In all human cases, subclinical or

**Table 6**  
Visceral leishmaniasis in dogs diagnosed with cancer (nd = not documented).

<i>Leishmania</i> species	Clinical expression	Cancer	Investigation method for <i>leishmania</i>	Sample	Country	References
<i>L. infantum</i>	Asymptomatic	Transmissible venereal tumor	Intratumoral fine needle aspirates, microscopy	Biopsy	Spain	(Kegler et al., 2013)
	VL	Extranodal lymphoma	Bone marrow aspirate, IFAT (immunofluorescent antibody test)	Bone marrow aspirate	Italia	(Foglia Manzillo et al., 2008)
	VL	Transmissible venereal tumor	Cytological examination, IFAT, PCR	Biopsy, Lymph node aspirate	Italia	(Catone et al., 2003)
nd	Asymptomatic	Nonhistiocytic Canine Tumors	IFAT, Microscopy	Serum and cutaneous Nodules aspirates		(Albanese et al., 2002)
			Microscopy, serology	Biopsy		(Ferro et al., 2013)

symptomatic forms of Leishmaniasis were observed. This would suggest that only progressive leishmaniasis could promote cancer development and consequently that asymptomatic *Leishmania* carriage does not display a potential indirect oncogenic power. However, the great number of asymptomatic carriers in endemic areas (Michel et al., 2011), aging population and possible immunosuppression (HIV, cancers, transplantation) represent potential factors that could initiate parasite reactivation or trigger disease by *de novo* infection. This could therefore promote cancer development (Torres-Guerrero et al., 2017). Although no association between asymptomatic carriage and tumor development has yet been studied, it is not excluded that asymptomatic carriage may increase the risk of cancer development. In addition, a tumor-induced parasite growth cannot be totally excluded. In this case, the micro-environment created by progressive cancers in asymptomatic carriers and the immunosuppressive effect of cancer therapies could lead to parasite reactivation, which in turn could promote cancer growth. This synergy would be extremely detrimental for the host. However, the lack of studies showing a direct effect of cancer on Leishmaniasis development and previous studies showing the oncogenic power of pathogens such as *Plasmodium falciparum* (Yasunaga and Matsuoka, 2018) indicate that subclinical or symptomatic Leishmaniasis can promote cancer growth. As a consequence, patients with subclinical or obvious leishmaniasis can be at higher risk of developing various cancers and thus would necessitate a particular treatment regimen. Further studies are however necessary to precise the impact of *Leishmania* infection on cancer development in Leishmaniasis endemic areas.

## Acknowledgement

We thank Bernard Ferrua for his assistance at all stages of the writing, especially for his comments that have greatly improved the manuscript, and Emmanuel Lemichez.

## References

- Akcali, C., Baba, M., Inaloz, S., Seckin, D., Uzun, S., 2008. Cutaneous leishmaniasis mimicking squamous cell carcinoma. *Ann. Acad. Med. Singapore* 37 (5), 435–436.
- Akuffo, H., Costa, C., van Griensven, J., Burza, S., Moreno, J., Herrero, M., 2018. New insights into leishmaniasis in the immunosuppressed. *PLoS Negl. Trop. Dis.* 12 (5), e0006375.
- Albanese, F., Poli, A., Millanta, F., Abramo, F., 2002. Primary cutaneous extragenital canine transmissible venereal tumour with *Leishmania*-laden neoplastic cells: a further suggestion of histiocytic origin. *Vet. Dermatol.* 13 (5), 243–246.
- Albrecht, H., Stellbrink, H.J., Gross, G., Berg, B., Helmchen, U., Mensing, H., 1994. Treatment of atypical leishmaniasis with interferon gamma resulting in progression of Kaposi's sarcoma in an AIDS patient. *Clin. Investig.* 72 (12), 1041–1047.
- Al-Kamel, M.A., 2017. Leishmaniasis and Malignancy: A review and perspective. *Clin. Skin Cancer* 2, 54–58.
- Al-Qahtani, M.S., Malik, N.W., Jamil, S., Mekki, T.E., 2012. Diagnostic dilemma of primary mucosal leishmaniasis. *Saudi Med. J.* 33 (11), 1234–1238.
- Armengot-Carbó, M., Carmona-Ramón, R., Rodrigo-Nicolás, B., Ferrando-Marco, J., 2012. [Unsuspected visceral leishmaniasis infiltrating a squamous cell carcinoma]. *Actas Dermosifiliogr.* 103 (4), 321–323.
- Asilian, A., Momeni, I., Khosravani, P., 2012. Basal cell carcinoma superimposed on a cutaneous leishmaniasis lesion in an immunocompromised patient. *J. Res. Med. Sci.* 17 (1), 108–110.
- Badaro, R., Jones, T.C., Carvalho, E.M., Sampaio, D., Reed, S.G., Barral, A., Teixeira, R., Johnson, W.D.J., 1986. New perspectives on a subclinical form of visceral leishmaniasis. *J. Infect. Dis.* 154 (6), 1003–1011.
- Bielory, B.P., Lari, H.B., Mirani, N., Kapila, R., Fitzhugh, V.A., Turbin, R.E., 2011. Conjunctival squamous cell carcinoma harboring *Leishmania* amastigotes in a human immunodeficiency virus-positive patient. *Arch. Ophthalmol.* 129 (9), 1230–1231.
- Blum-Domínguez, S.D., Martínez-Vázquez, A., Núñez-Oreza, L.A., Martínez-Hernández, F., Villalobos, G., Tamay-Segovia, P., 2017. Diffuse cutaneous leishmaniasis (DCL) and visceral leishmaniasis (VL) concurrent with cancer: Presentation of a case. *Gac. Med. Mex.* 153 (1), 121–124.
- Boutros, N., Hawkins, D., Nelson, M., Lampert, I.A., Naresh, K.N., 2006. Burkitt lymphoma and Leishmaniasis in the same tissue sample in an AIDS patient. *Histopathology* 48 (7), 880–881.
- Brenner, D.S., Jacobs, S.C., Drachenberg, C.B., Papadimitriou, J.C., 2000. Isolated visceral leishmaniasis presenting as an adrenal cystic mass. *Arch. Pathol. Lab. Med.* 124 (10), 1553–1556.
- Bretscher, P.A., Ismail, N., Menon, J.N., Power, C.A., Uzonna, J., Wei, G., 2001. Vaccination against and treatment of tuberculosis, the leishmaniasis and AIDS: perspectives from basic immunology and immunity to chronic intracellular infections. *Cell. Mol. Life Sci.* 58 (12–13), 1879–1896.
- Bretscher, P.A., Hamilton, D., Ogunremi, O., 2002. What information is needed to design effective vaccination against intracellular pathogens causing chronic disease? *Expert Rev. Vaccines* 1 (2), 179–192.
- Burza, S., Croft, S.L., Boelaert, M., 2018. Leishmaniasis *Lancet* 392 (10151), 951–970.
- Castellano, V.M., Rodríguez-Peralto, J.L., Alonso, S., Gómez-De la Fuente, E., Ibarrola, C., 1999. Dermatofibroma parasitized by *Leishmania* in HIV infection: a new morphologic expression of dermal Kala Azar in an immunodepressed patient. *J. Cutan. Pathol.* 26 (10), 516–519.
- Catone, G., Marino, G., Poglayen, G., Gramiccia, M., Ludovisi, A., Zanghi, A., 2003. Canine transmissible venereal tumour parasitized by *Leishmania infantum*. *Vet. Res. Commun.* 27 (7), 549–553.
- Celentano, A., Ruoppo, E., Mansueto, G., Mignogna, M.D., 2015. Primary oral leishmaniasis mimicking oral cancer: a case report. *Br. J. Oral Maxillofac. Surg.* 53 (4), 396–398.
- Cobo, F., Rodríguez-Granger, J., Gómez-Camarasa, C., Sampedro, A., Aliaga-Martínez, L., Navarro, J.M., Fernández, J.G., 2016. Localized mucosal leishmaniasis caused by *Leishmania infantum* mimicking cancer in the rhinolaryngeal region. *Int. J. Infect. Dis.* 5054–5056.
- Czechowicz, R.T., Millard, T.P., Smith, H.R., Ashton, R.E., Lucas, S.B., Hay, R.J., 1999. Reactivation of cutaneous leishmaniasis after surgery. *Br. J. Dermatol.* 141 (6), 1113–1116.
- da Silva Santos, C., Brodskyn, C.I., 2014. The Role of CD4 and CD8 T cells in human cutaneous Leishmaniasis. *Front. Public Health* 2165.
- de Vasconcelos, G.M., Azevedo-Silva, F., Dos Santos Thuler, L.C., Pina, E.T., Souza, C.S., Calabrese, K., Pombo-de-Oliveira, M.S., 2014. The concurrent occurrence of *Leishmania chagasi* infection and childhood acute leukemia in Brazil. *Rev. Bras. Hematol. Hemoter.* 36 (5), 356–362.
- DebRoy, S., Prosper, O., Mishoe, A., Mubayi, A., 2017. Challenges in modeling complexity of neglected tropical diseases: a review of dynamics of visceral leishmaniasis in resource limited settings. *Emerg. Themes Epidemiol.* 1410.
- Domingues, M., Menezes, Y., Ostronoff, F., Calixto, R., Florencio, R., Sucupira, A., Souto-Maior, A.P., Ostronoff, M., 2009. Coexistence of Leishmaniasis and Hodgkin's lymphoma in a lymph node. *J. Clin. Oncol.* 27 (32), e184–5.
- Donati, P., Paolino, G., Panetta, C., Muscardin, L., Cota, C., Giuliani, M., 2013. Visceral leishmaniasis revealed by a squamous cell carcinoma in an HIV-1 infected patient. *Infection* 41 (2), 575–578.
- El Youssi, H., Touaoussa, A., Bergui, I., Bougrine, N., Moncef, AmraniH., 2015. Visceral leishmaniasis and acute lymphoblastic leukemia B: what is the relationship? *Pan Afr. Med. J.* 20053.
- Evers, G., Pohlen, M., Berdel, W.E., Thoennissen, N.H., Titze, U., Köhler, G., Weckesser, M., Anthoni, C., Mesters, R.M., 2014. Visceral leishmaniasis clinically mimicking lymphoma. *Ann. Hematol.* 93 (5), 885–887.
- Fakhar, M., Asgari, Q., Motazedian, M.H., Monabati, A., 2008. Mediterranean visceral leishmaniasis associated with acute lymphoblastic leukemia (ALL). *Parasitol. Res.* 103 (2), 473–475.
- Ferro, S., Palmieri, C., Cavicchioli, L., De Zan, G., Aresu, L., Benali, S.L., 2013. *Leishmania* amastigotes in neoplastic cells of 3 nonhistiocytic canine tumors. *Vet. Pathol.* 50 (5),

- 749–752.
- Fishman, J.A., 2011. Infections in immunocompromised hosts and organ transplant recipients: essentials. *Liver Transpl.* 17 (Suppl. 3), S34–7.
- Foglia Manzillo, V., Pagano, A., Guglielmino, R., Gradoni, L., Restucci, B., Oliva, G., 2008. Extranodal gamma-delta-T-cell lymphoma in a dog with leishmaniasis. *Vet. Clin. Pathol.* 37 (3), 298–301.
- Friedman, R., Hanson, S., Goldberg, L.H., 2003. Squamous cell carcinoma arising in a *Leishmania* scar. *Dermatol. Surg.* 29 (11), 1148–1149.
- Galluzzi, L., Ceccarelli, M., Dotallevi, A., Menotta, M., Magnani, M., 2018. Real-time PCR applications for diagnosis of leishmaniasis. *Parasit. Vectors* 11 (1), 273.
- Giavedoni, P., Pau-Charles, L., Mascaró, J.M., Alsina-Gibert, M., García-Herrera, A., Estrach, T., 2014. Disseminated cutaneous leishmaniasis in a patient with Sézary syndrome. *J. Am. Acad. Dermatol.* 71 (5), e213–4.
- Gul, H.C., Tosun, F., Karakas, A., Koru, O., Onguru, O., Mert, G., Besirbellioglu, B.A., Eyigun, C.P., 2016. A case of mucosal leishmaniasis: Mimicking intranasal tumor with perforation of septum. *J. Microbiol. Immunol. Infect.* 49 (4), 604–607.
- Ivanova, E.A., Orekhov, A.N., 2015. T helper lymphocyte subsets and plasticity in autoimmunity and cancer: an overview. *Biomed Res. Int.* 2015, 327470.
- Jewell, A.P., Giles, F.J., 1996. Cutaneous manifestation of leishmaniasis 40 years after exposure in a patient with chronic lymphocytic leukaemia. *Leuk. Lymphoma* 21 (3–4), 347–349.
- Kawakami, A., Fukunaga, T., Usui, M., Asaoka, H., Noda, M., Nakajima, T., Hashimoto, Y., Tanaka, A., Kishi, Y., Numano, F., 1996. Visceral leishmaniasis misdiagnosed as malignant lymphoma. *Intern. Med.* 35 (6), 502–506.
- Kegler, K., Habierski, A., Hahn, K., Amarilla, S.P., Seehusen, F., Baumgärtner, W., 2013. Vaginal canine transmissible venereal tumour associated with intra-tumoural *Leishmania* spp. amastigotes in an asymptomatic female dog. *J. Comp. Pathol.* 149 (2–3), 156–161.
- Khorsandi-Ashtiani, M.T., Hasibi, M., Yazdani, N., Paydarfar, J.A., Sadri, F., Mirashrafi, F., Kouhi, A., 2009. Auricular leishmaniasis mimicking squamous cell carcinoma. *J. Laryngol. Otol.* 123 (8), 915–918.
- Kopterides, P., Mourtzoukou, E.G., Skopelitis, E., Tsavaris, N., Falagas, M.E., 2007. Aspects of the association between leishmaniasis and malignant disorders. *Trans. R. Soc. Trop. Med. Hyg.* 101 (12), 1181–1189.
- Kumar, R., Bhatia, M., Pai, K., 2017. Role of Cytokines in the Pathogenesis of Visceral Leishmaniasis. *Clin. Lab.* 63 (10), 1549–1559.
- Marty, P., Izri, A., Ozon, C., Haas, P., Rosenthal, E., Del Giudice, P., Godenir, J., Coulibaly, E., Gari-Toussaint, M., Delaunay, P., Ferrua, B., Haas, H., Pratlong, F., Le Fichoux, Y., 2007. A century of leishmaniasis in Alpes-Maritimes, France. *Ann. Trop. Med. Parasitol.* 101 (7), 563–574.
- Matayoshi, S., Baddina-Caramelli, C., Goldbaum, M., Takei, L.M., Honda, M., Kara-José, N., 2000. Epidermoid carcinoma arising in an ocular *Leishmania* lesion. *Br. J. Ophthalmol.* 84 (11), 1331–1332.
- McGuire, S., 2016. World Cancer Report 2014. World Health Organization, international agency for research on cancer, WHO Press, Geneva, Switzerland, pp. 2015.
- Melssen, M., Slingluff, C.L., 2017. Vaccines targeting helper T cells for cancer immunotherapy. *Curr. Opin. Immunol.* 4785–4792.
- Michel, G., Pomares, C., Ferrua, B., Marty, P., 2011. Importance of worldwide asymptomatic carriers of *Leishmania infantum* (*L. chagasi*) in human. *Acta Trop.* 119 (2–3), 69–75.
- Michiels, J.F., Monteil, R.A., Hofman, P., Perrin, C., Fuzibet, J.G., Lefichoux, Y., Loubière, R., 1994. Oral leishmaniasis and Kaposi's sarcoma in an AIDS patient. *J. Oral Pathol. Med.* 23 (1), 45–46.
- Naik, S.R., Vinayak, V.K., Talwar, P., Sehgal, S., Mehra, Y.N., Dutta, B.N., Chhuttani, P.N., 1978. Visceral leishmaniasis masquerading as a nasopharyngeal tumour. Report of a case. *Trans. R. Soc. Trop. Med. Hyg.* 72 (1), 43–45.
- Nicodemo, A.C., Duailibi, D.F., Feriani, D., Duarte, M.I.S., Amato, V.S., 2017. Mucosal leishmaniasis mimicking T-cell lymphoma in a patient receiving monoclonal antibody against TNF $\alpha$ . *PLoS Negl. Trop. Dis.* 11 (9), e0005807.
- Oetken, T., Hiscox, B., Orengo, I., Rosen, T., 2017. Cutaneous leishmaniasis mimicking squamous cell carcinoma. *Dermatol. Online J.* 23 (1).
- Orlandi, E.M., Malfitano, A., 2014. Visceral leishmaniasis mimicking Richter transformation. *Leuk. Lymphoma* 55 (12), 2952–2954.
- Papanastasiou, J., Mavrogenis, A.F., Flevas, D., Megaloikononimos, P.D., Kolimianakis, E., Iakovidou, I., Papagelopoulos, P.J., Demertzis, N., 2016. *Leishmania* infection of a Knee Megaprosthesis. *J. Bone Jt. Infect.* 150–153.
- Parisi, L., Gini, E., Baci, D., Tremolati, M., Fanuli, M., Bassani, B., Farronato, G., Bruno, A., Mortara, L., 2018. Macrophage polarization in chronic inflammatory diseases: killers or builders. *J. Immunol. Res.* 2018, 8917804.
- Paydas, S., Zorlutdemir, S., 2000. Leukaemia cutis and leukaemic vasculitis. *Br. J. Dermatol.* 143 (4), 773–779.
- Perrin, C., Michiels, J.F., Bernard, E., Hofman, P., Rosenthal, E., Loubiere, R., 1993. Cutaneous spindle-cell pseudotumors due to *Mycobacterium gordonae* and *Leishmania infantum*. An immunophenotypic study. *Am. J. Dermatopathol.* 15 (6), 553–558.
- Piro, E., Kropp, M., Cantaffa, R., Lamberti, A.G., Carillio, G., Molica, S., 2012. Visceral leishmaniasis infection in a refractory multiple myeloma patient treated with bortezomib. *Ann. Hematol.* 91 (11), 1827–1828.
- Quintella, L.P., Cuzzi, T., de Fátima Madeira, M., Valette-Rosalino, C.M., de Matos Salgueiro, M., de Camargo Ferreira e Vasconcellos, E., Mouta-Confort, E., Lambert Passos, S.R., de Oliveira Schubach, A., 2011. Cutaneous leishmaniasis with pseudoepitheliomatous hyperplasia simulating squamous cell carcinoma. *Am. J. Dermatopathol.* 33 (6), 642–644.
- Ramos, A., Muñoz, E., García-Domínguez, J., Martínez-Ruiz, R., Chicharro, C., Baños, I., Suarez-Massa, D., Cuervas-Mons, V., 2015. Mucosal leishmaniasis mimicking squamous cell carcinoma in a liver transplant recipient. *Transpl. Infect. Dis.* 17 (3), 488–492.
- Rayatt, S.S., Moss, A.L., 2000. Cutaneous leishmaniasis. *Br. J. Plast. Surg.* 53 (5), 443–445.
- Rodrigues, V., Cordeiro-da-Silva, A., Laforge, M., Silvestre, R., Estaquier, J., 2016. Regulation of immunity during visceral *Leishmania* infection. *Parasit. Vectors* 9118.
- Sabri, A., Khatib, L., Kanj-Sharara, S., Husseini, S.T., Nuwayri-Salti, N., Semaan, R., Rameh, C., 2009. Leishmaniasis of the auricle mimicking carcinoma. *Am. J. Otolaryngol.* 30 (4), 285–287.
- Sah, S.P., Rijal, S., Bhadani, P.P., Rani, S., Koirala, S., 2002. Visceral leishmaniasis in two cases of leukemia. *Southeast Asian J. Trop. Med. Public Health* 33 (1), 25–27.
- Schetter, A.J., Heegaard, N.H., Harris, C.C., 2010. Inflammation and cancer: interweaving microRNA, free radical, cytokine and p53 pathways. *Carcinogenesis* 31 (1), 37–49.
- Sheikha, A., Aljanadi, M., Malik, J., Abdalla, R., Alamari, O., Alshehri, M., 1993. Visceral leishmaniasis with a very-low degree of bone-marrow parasitemia, mimicking malignant histiocytosis. *Int. J. Oncol.* 3477–3480.
- Steer, H.J., Lake, R.A., Nowak, A.K., Robinson, B.W., 2010. Harnessing the immune response to treat cancer. *Oncogene* 29 (48), 6301–6313.
- Suster, S., Ronnen, M., 1988. Basal cell carcinoma arising in a *Leishmania* scar. *Int. J. Dermatol.* 27 (3), 175–176.
- Taillan, B., Marty, P., Schneider, S., Telle, H., Fuzibet, J.G., Rosenthal, E., Rahal, A., Lefichoux, Y., Dujardin, P., 1992. Visceral leishmaniasis involving a cutaneous Kaposi's sarcoma lesion and free areas of skin. *Eur. J. Med.* 1 (4), 255.
- Tiwari, N., Gedda, M.R., Tiwari, V.K., Singh, S.P., Singh, R.K., 2018. Limitations of current therapeutic options, possible drug targets and scope of natural products in control of Leishmaniasis. *Mini Rev. Med. Chem.* 18 (1), 26–41.
- Torres-Guerrero, E., Quintanilla-Cedillo, M.R., Ruiz-Esmenjaud, J., Arenas, R., 2017. Leishmaniasis: a review. *F1000Res* 6750.
- Unlü, R.E., Altun, S., Ssensöz, O., 2007. *Leishmania* scar: a risk factor for the development of basal cell carcinomas. *J. Craniofac. Surg.* 18 (3), 708–710.
- Vase, M.Ø., Hellberg, Y.K., Larsen, C.S., Petersen, E., Schaumburg, H., Bendix, K., Ravel, C., Bastien, P., Christensen, M., d'Amore, F., 2012. Development of splenic marginal zone lymphoma in a HIV-negative patient with visceral leishmaniasis. *Acta Haematol.* 128 (1), 20–22.
- WHO, 2018. The Who Leishmaniasis Fact Sheet. World Health Organization.
- Yasunaga, J.I., Matsuoka, M., 2018. Oncogenic spiral by infectious pathogens: cooperation of multiple factors in cancer development. *Cancer Sci.* 109 (1), 24–32.



# ***Escherichia coli* Rho GTPase-activating toxin CNF1 mediates NLRP3 inflammasome activation via p21-activated kinases-1/2 during bacteraemia in mice**

Océane Dufies, Anne Doye, Johan Courjon, Cédric Torre, Grégory Michel, Céline Loubatier, Arnaud Jacquet, Paul Chaintreuil, Alissa Majoor, Rodolphe R. Guinamard, Alexandre Gallerand, Pedro H. V. Saavedra, Els Verhoeven, Amaury Rey, Sandrine Marchetti, Raymond Ruimy, Dorota Czerucka, Mohamed Lamkanfi, Bénédicte F. Py, Patrick Munro, Orane Visvikis and Laurent Boyer

## **Résumé**

Les inflammasomes sont des plateformes de signalisation assemblées en réponse à une infection ou inflammation stérile par des « pattern recognition receptors » (PRR) cytosoliques. L'activation par l'inflammasome de la caspase-1 qui en découle est indispensable pour la défense de l'hôte contre les pathogènes. Au cours de l'infection, NLRP3, un PRR appelé aussi cryopyrine, déclenche l'assemblage de la caspase-1 activatrice de l'inflammasome par le biais du recrutement de la protéine ASC et Nek7. L'activation de l'inflammasome NLRP3 est étroitement régulé au niveau transcriptionnel et post-traductionnel. Malgré l'importance de la régulation de l'inflammasome NLRP3 dans les maladies auto-inflammatoires et infectieuses, peu de choses sont connues sur le mécanisme contrôlant l'activation de NLRP3 et la signalisation en aval qui régule l'assemblage de l'inflammasome NLRP3. Nous avons précédemment démontré que la toxine d'*Escherichia coli* « Cytotoxic necrotizing factor-1 » (CNF-1) activatrice de la Rho-GTPase était capable d'activer la caspase-1, mais le mécanisme reste à élucider. Ici, nous démontrons le rôle de l'inflammasome NLRP3 dans la détection de toxines bactériennes et de facteurs de virulence activant les Rho-GTPases de l'hôte. Nous montrons que cette activation dépend de l'activité de cette toxine sur la Rho GTPase Rac2. Nous démontrons également que l'inflammasome NLRP3 est activé par une cascade de signalisation qui implique les Kinases p21-activées 1 et 2 (Pak1/2) et de la phosphorylation de Thr 659 de NLRP3 par Pak-1, nécessaire pour l'interaction NLRP3-Nek7, l'activation de l'inflammasome et la maturation de la cytokine IL-1 $\beta$ . De plus, l'inhibition de l'axe Pak-NLRP3 diminue la clairance bactérienne dans les souris de bactéries *E. coli* UTI89 exprimant le CNF-1. Dans l'ensemble, nos résultats démontrent que Pak1 et Pak2 sont des régulateurs critiques de l'inflammasome NLRP3, et révèlent le rôle de l'axe de signalisation Pak-NLRP3 *in vivo* au cours de bactériémies chez la souris.



# *Escherichia coli* Rho GTPase-activating toxin CNF1 mediates NLRP3 inflammasome activation via p21-activated kinases-1/2 during bacteraemia in mice

Océane Dufies<sup>1</sup>, Anne Doye<sup>1</sup>, Johan Courjon<sup>1,2</sup>, Cédric Torre<sup>1</sup>, Gregory Michel<sup>1</sup>, Celine Loubatier<sup>1</sup>, Arnaud Jacquet<sup>1</sup>, Paul Chaintreuil<sup>1</sup>, Alissa Major<sup>1</sup>, Rodolphe R. Guinamard<sup>1</sup>, Alexandre Gallerand<sup>1</sup>, Pedro H. V. Saavedra<sup>3</sup>, Els Verhoeyen<sup>1,4</sup>, Amaury Rey<sup>1,4</sup>, Sandrine Marchetti<sup>1</sup>, Raymond Ruimy<sup>1,2</sup>, Dorota Czerucka<sup>5,6</sup>, Mohamed Lamkanfi<sup>3</sup>, Bénédicte F. Py<sup>4</sup>, Patrick Munro<sup>1</sup>, Orane Visvikis<sup>1</sup> and Laurent Boyer<sup>1,6</sup> ✉

**Inflammasomes are signalling platforms that are assembled in response to infection or sterile inflammation by cytosolic pattern recognition receptors. The consequent inflammasome-triggered caspase-1 activation is critical for the host defence against pathogens. During infection, NLRP3, which is a pattern recognition receptor that is also known as cryopyrin, triggers the assembly of the inflammasome-activating caspase-1 through the recruitment of ASC and Nek7. The activation of the NLRP3 inflammasome is tightly controlled both transcriptionally and post-translationally. Despite the importance of the NLRP3 inflammasome regulation in autoinflammatory and infectious diseases, little is known about the mechanism controlling the activation of NLRP3 and the upstream signalling that regulates the NLRP3 inflammasome assembly. We have previously shown that the Rho-GTPase-activating toxin from *Escherichia coli* cytotoxic necrotizing factor-1 (CNF1) activates caspase-1, but the upstream mechanism is unclear. Here, we provide evidence of the role of the NLRP3 inflammasome in sensing the activity of bacterial toxins and virulence factors that activate host Rho GTPases. We demonstrate that this activation relies on the monitoring of the toxin's activity on the Rho GTPase Rac2. We also show that the NLRP3 inflammasome is activated by a signalling cascade that involves the p21-activated kinases 1 and 2 (Pak1/2) and the Pak1-mediated phosphorylation of Thr 659 of NLRP3, which is necessary for the NLRP3-Nek7 interaction, inflammasome activation and IL-1 $\beta$  cytokine maturation. Furthermore, inhibition of the Pak-NLRP3 axis decreases the bacterial clearance of CNF1-expressing UTI89 *E. coli* during bacteraemia in mice. Taken together, our results establish that Pak1 and Pak2 are critical regulators of the NLRP3 inflammasome and reveal the role of the Pak-NLRP3 signalling axis in vivo during bacteraemia in mice.**

Uropathogenic *E. coli* is the leading causative agent of bacteraemia<sup>1</sup>. It is therefore fundamental to decipher the mechanisms that determine the fate of this pathogen in the blood. The innate immune sensing of *E. coli* is mediated by pattern recognition receptors (PRRs), mainly by Toll-like receptor-4 (TLR4), which detects bacterial lipopolysaccharides (LPS). LPS are the principal component of the external membrane of both pathogenic and non-pathogenic *E. coli* and, therefore, pattern-triggered immunity does not seem to be sufficient to gauge the pathogenic potential of microorganisms. As TLR4 is activated by both live and dead bacteria, pattern-triggered immunity is certainly important for monitoring the quantity of bacteria, but is not sufficient to determine their quality<sup>2</sup>. One strategy to determine microbial pathogenicity is the detection of virulence factor activities that are specific to pathogens<sup>3</sup>. Virulence factors of uropathogenic *E. coli* include CNF1, which is a Rho-GTPase-targeting toxin. The CNF1 toxin bears enzymatic activity that is responsible for the post-translational deamidation

of a specific glutamine residue on a subset of Rho GTPases, namely Rac, Cdc42 and RhoA<sup>4-6</sup>. This modification destroys the intrinsic and GTPase-activating-protein- (GAP)-regulated ability of these Rho GTPases to hydrolyse GTP, conferring dominant positive mutant characteristics to Rho proteins<sup>4-6</sup>. This modification increases GTP-bound activated Rho proteins and the activation of their downstream signalling pathways<sup>6</sup>. By modulating the host cytoskeleton, these virulence factors confer to bacteria invasion properties and the ability to modulate inflammatory responses<sup>7-10</sup>. Among the virulence factors, there are more than 30 that target Rho GTPases. They are either activators or inhibitors of Rho GTPases, both of which activate caspase-1 (refs. <sup>11,12</sup>).

Inflammasomes are signalling platforms that are assembled by cytosolic PRRs that activate caspase-1. NLRP3 oligomerizes on infection or cellular damage, and recruits ASC, Nek7 and caspase-1 to form the NLRP3 inflammasome. This assembly results in ASC speck formation, cleavage of pro-caspase-1 into active caspase-1 and

<sup>1</sup>Université Côte d'Azur, Inserm, C3M, Nice, France. <sup>2</sup>Université Côte d'Azur, CHU Nice, Nice, France. <sup>3</sup>Department of Internal Medicine and Pediatrics, Ghent University, Ghent, Belgium. <sup>4</sup>CIRI, Centre International de Recherche en Infectiologie, Université de Lyon, Inserm U1111, Université Claude Bernard Lyon 1, CNRS UMR5308, ENS de Lyon, Lyon, France. <sup>5</sup>Centre Scientifique de Monaco, Monaco, Monaco. <sup>6</sup>LIA ROPSE, Laboratoire International Associé Université Côte d'Azur, Centre Scientifique de Monaco, Nice, France. ✉e-mail: [laurent.boyer@univ-cotedazur.fr](mailto:laurent.boyer@univ-cotedazur.fr)

the maturation of pro-IL-1 $\beta$  into IL-1 $\beta$ . The NLRP3 inflammasome assembly is controlled by both the priming by TLR ligands and activation signals. Furthermore, the NLRP3 inflammasome assembly is regulated by phosphorylation and ubiquitination events<sup>13,14</sup>. Despite a variety of identified NLRP3 activators, the upstream signalling pathways that control NLRP3 post-translational modifications and activation mechanisms remain unclear<sup>14</sup>. Interestingly, toxins that inactivate Rho GTPases activate the Pyrin inflammasome through the modification of its phosphorylation status by the PKN1/2 kinases. The Pyrin inflammasome has been shown to detect toxins that inhibit Rho GTPases, but information about the sensing of toxins that activate Rho GTPases through inflammasomes is lacking<sup>15,16</sup>. In this Article, we used the CNF1 toxin as a model of the Rho-GTPase-activating virulence factor to demonstrate the role of the Pak–NLRP3 axis in sensing CNF1 activity and controlling the clearance of bacteria during bacteraemia.

## Results

**CNF1-triggered immunity requires NLRP3.** We set up an assay to monitor the CNF1-triggered activation of caspase-1 using a FAM-YVAD-FMK (FAM-FLICA) probe. Primary bone-marrow-derived macrophages (BMDMs) isolated from BALB/c mice were treated with CNF1 and analysed using confocal microscopy. Cells with dots of FAM-FLICA staining corresponding to ASC specks were counted (Extended Data Fig. 1a). This unbiased screen revealed that NLRP3 is the major NLR involved in CNF1-triggered caspase-1 activation (Fig. 1a). The role of NLRP3 in this pathway was confirmed in BMDMs isolated from C57BL/6J mice bearing ASC–citricine knockin using flow cytometry (Extended Data Fig. 1b,c). In this assay, we quantified the percentage of cells with ASC specks as previously described<sup>17,18</sup>. These data revealed the conserved role of NLRP3 in the response to CNF1 in macrophages isolated from both BALB/c and C57BL/6J background.

Next, we investigated the role of NLRP3 in CNF1-triggered immunity. Co-treatment of BMDMs isolated from wild-type (WT) mice with the CNF1 toxin together with the NLRP3 inhibitor MCC950 was sufficient to block caspase-1 activity, demonstrating that the CNF1 toxin is an NLRP3 activator (Fig. 1b,c). Importantly, the number of FAM-FLICA<sup>+</sup> cells was substantially reduced in BMDMs that were treated with catalytically inactive mutant CNF1<sup>C866S</sup>. This result provided evidence that CNF1 toxin activity is monitored by NLRP3, rather than the pattern of the toxin<sup>3</sup>. Furthermore, CNF1-triggered maturation and secretion of IL-1 $\beta$  and activation of caspase-1 was impaired in NLRP3-knockout BMDMs (Fig. 1d and Supplementary Fig. 1). By contrast, CNF1 treatment did not affect the secretion of IL-6 or TNF- $\alpha$ , two cytokines that are not regulated by inflammasomes (Fig. 1d and Supplementary Fig. 1). Activation of the NLRP3 inflammasome is often associated with pyroptosis<sup>19</sup>. To investigate whether CNF1 triggered pyroptosis, we measured propidium iodide incorporation (Extended Data Fig. 2a), lactate dehydrogenase (LDH) release (Extended Data Fig. 2b) and gasdermin D (GSDMD) cleavage (Extended Data Fig. 2c). In contrast to nigericin, we did not observe any of these pyroptosis markers after CNF1 treatment and we observed a similar level of CNF1-triggered caspase-1 activation and IL-1 $\beta$  maturation/secretion in WT and GSDMD-knockout macrophages (Extended Data Fig. 2d,e). We subsequently tested the role of the NLRP3 inflammasome regulator Nek7 in CNF1-triggered immunity. Transfection of *Nlrp3* or *Nek7* short interfering RNA (siRNA) in BMDMs inhibited CNF1-triggered IL-1 $\beta$  maturation (Extended Data Fig. 3a,b). K<sup>+</sup> efflux is an upstream event for NLRP3 inflammasome activation and Nek7 requires K<sup>+</sup> efflux for NLRP3 inflammasome assembly<sup>14,20</sup>. We observed that KCl treatment was sufficient to inhibit CNF1-triggered caspase-1 cleavage (Extended Data Fig. 3c). Importantly, we confirmed that the KCl treatment did not inhibit CNF1 toxin activity towards Rho GTPase activation using a glutathione S-transferase (GST)–Pak–Rac-binding domain

(RBD) pull-down assay (Extended Data Fig. 3d). We next investigated whether other toxins that target Rho GTPases have the ability to activate the NLRP3 inflammasome. Dermonecrotic toxin (DNT) from *Bordetella* has transglutaminase activity towards Rho GTPases that enables the constitutive activation of Rho GTPases<sup>6,10</sup>. We observed that purified recombinant DNT triggered the activation of caspase-1 in WT macrophages, but not in NLRP3-knockout macrophages (Extended Data Fig. 4a). We next tested whether the NLRP3 activation was triggered specifically by virulence factors activating Rho GTPases using NLRP3 inflammasome reconstitution in HEK293T cells<sup>21</sup>. Cells were transfected with plasmids encoding the DNT toxin or the injected bacterial virulence factors YopE from *Yersinia* containing a GAP domain that enables inactivation of the Rho GTPases<sup>6</sup>. We observed NLRP3-dependent IL-1 $\beta$  maturation when cells were transfected with the Rho-GTPase-activating toxin DNT, but not when cells were transfected with the Rho GTPase inhibitor YopE (Extended Data Fig. 4b). The expression of the virulence factor SopE from *Salmonella* containing a guanine nucleotide exchange factor (GEF) domain activating Rac and Cdc42 (refs. 6,22) or the expression of the GEF domain of the Dbl exchange factor (Dbl<sup>495–826</sup>)<sup>23</sup> were sufficient to trigger NLRP3-dependent IL-1 $\beta$  maturation (Extended Data Fig. 4b,c). Taken together, we showed that the activation of Rho GTPases by toxins and virulence factors triggered the activation of the NLRP3 inflammasome and that Rac has a major role in this pathway.

**Activation of the NLRP3 inflammasome by CNF1 relies on Rac2 and the Pak serine–threonine kinases.** Although the CNF1 toxin is a Rho GTPases activator and Rac2 is a haematopoietic-specific Rho GTPase that is involved in the innate immune response to the CNF1 toxin<sup>24</sup>, the contribution of Rac1 and Rac2 in this process is still unknown. To investigate the role of Rac in the CNF1-triggered NLRP3 inflammasome activation, we knocked down *Rac1* and/or *Rac2* using siRNA in BMDMs. Interestingly, *Rac1* knockdown resulted in an increase in the level of CNF1-triggered IL-1 $\beta$  maturation whereas *Rac2* knockdown was sufficient to block it (Fig. 2a). We tested whether activated GTP-bound Rac2 levels would increase when *Rac1* was targeted by siRNA. The GST–Pak–RBD pull-down analysis showed an increase in activated Rac2 when *Rac1* was knocked-down using siRNA (Fig. 2b). These data demonstrate the critical role of Rac2 in CNF1-triggered IL-1 $\beta$  maturation (Fig. 2a,b). To determine the molecular mechanism of the caspase-1 activation, we used a system of NLRP3 inflammasome reconstitution in HEK293T cells. This analysis showed that CNF1 is sufficient for the NLRP3 inflammasome activation-triggered caspase-1 cleavage and that the co-treatment of CNF1 with MCC950 inhibited this caspase-1 activation (Fig. 2c). The transfection of Rac2 GTPase or activated mutant forms of Rac2 (including Q61E mimicking the CNF1 modification or Q61L and G12V) were sufficient to activate caspase-1, in contrast to the inactive mutant Rac2<sup>T17N</sup> (Fig. 2d). Interestingly, the strength of caspase-1 activation observed using the activated forms of Rac2 GTPase was correlated with the amount of Rho GTPases that were bound to GST–Pak–RBD (Fig. 2e). These data indicate that NLRP3 senses the activation level of the Rho GTPase Rac2 proportionally to the strength of activation rather than by detecting the structural modification made by the toxin as it would be predicted for a classical PRR.

The correlation between caspase-1 activation and the amount of Rac2 bound to GST–Pak–RBD suggested a potential role of Pak kinases in CNF1-triggered NLRP3 inflammasome activation. We therefore knocked-down Pak1 and/or Pak2 in BMDMs by transfecting siRNA (Pak3 is predominantly expressed in the brain<sup>25,26</sup>). We observed a major decrease in caspase-1 cleavage in cells treated with *Pak1* siRNA but a moderate impact when using siRNA targeting *Pak2*, indicating that Pak1 has a main role (Fig. 3a). However, we could not exclude the possibility that the total inhibition of

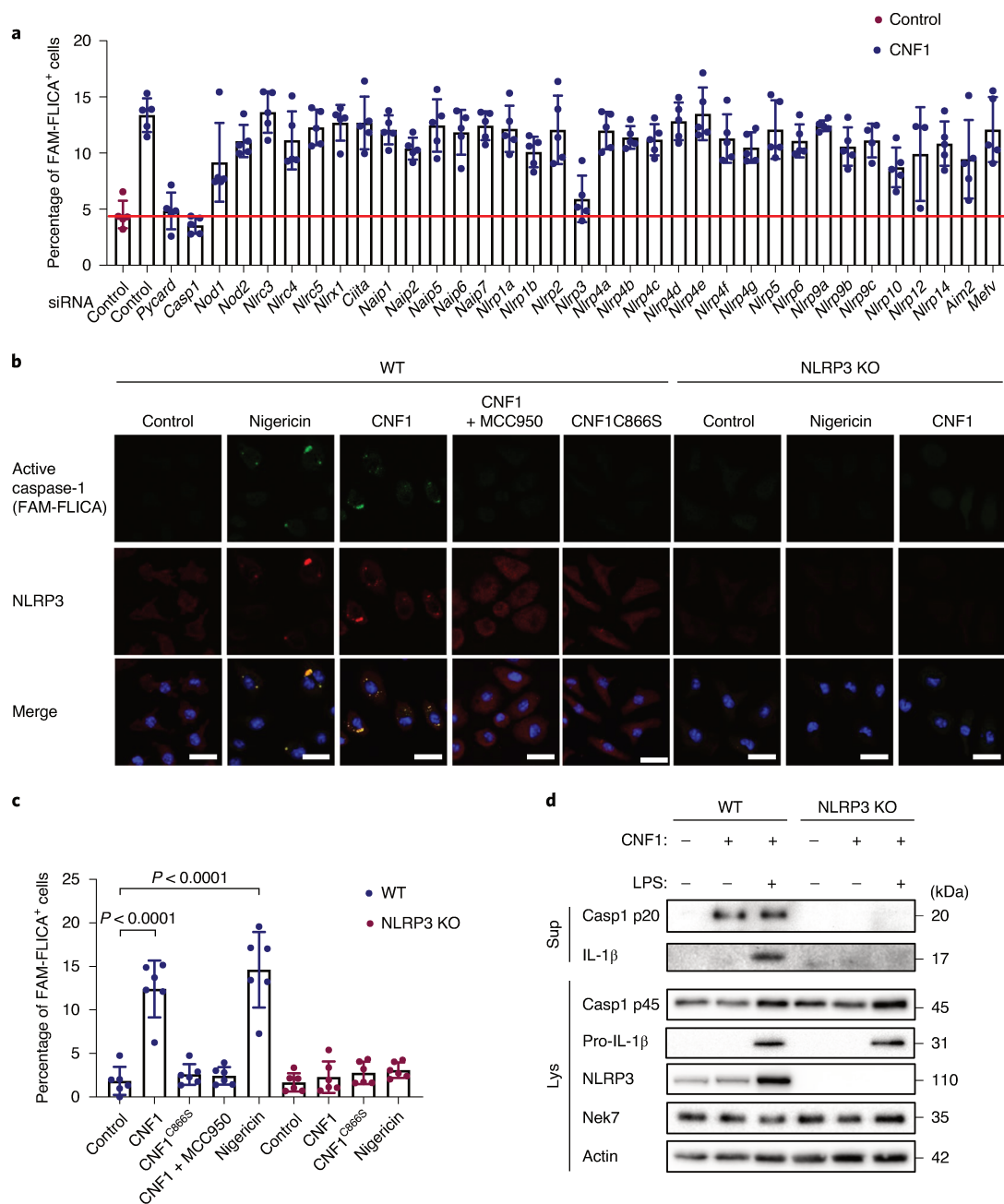


**Fig. 1 | CNF1-triggered caspase-1 activation and IL-1 $\beta$  maturation requires NLRP3.** **a**, BMDMs isolated from BALB/c mice were transfected with the indicated siRNA for 72 h before treatment for 6 h with CNF1 (500 ng ml<sup>-1</sup>). Active caspase-1 was detected using the FAM-FLICA probe. Cells harbouring FAM-FLICA dots were counted as positive using Fiji. The red horizontal line indicates the mean percentage of FAM-FLICA<sup>+</sup> cells in the untreated control. Each dot represents 200 cells.  $n = 1,800$  cells. Data are mean  $\pm$  s.e.m. **b, c**, BMDMs extracted from WT or NLRP3-knockout C57BL/6J mice were or were not pretreated for 45 min with MCC950 (1  $\mu$ M) before treatment for 6 h with CNF1 (500 ng ml<sup>-1</sup>), or the CNF1 catalytic inactive mutant CNF1<sup>C866S</sup> (500 ng ml<sup>-1</sup>) or nigericin (5  $\mu$ M). **b**, Cells were analysed using immunofluorescence and confocal imaging. Active caspase-1 (FAM-FLICA) is shown in green, NLRP3 in red and nuclei in blue. Scale bars, 20  $\mu$ m. **c**, Quantification of FAM-FLICA<sup>+</sup> cells in WT (blue) or NLRP3-knockout BMDMs (red). Each dot represents 100 cells.  $n = 600$  cells. Data are mean  $\pm$  s.e.m. Statistical analyses were performed using two-tailed unpaired Student's *t*-tests. **d**, WT or NLRP3-knockout BMDMs were treated with CNF1 (500 ng ml<sup>-1</sup>) and/or LPS (100 ng ml<sup>-1</sup>) for 8 h before the supernatants (Sup) and cell lysates (Lys) were collected and analysed using immunoblotting. Experiments were repeated at least three times, and representative data are shown.

caspase-1 cleavage observed with the *Pak1* siRNA treatment might be due to a limit in the detection level of cleaved caspase-1, or to *Pak1* siRNA that may affect *Pak2*, suggesting that there is a partial *Pak1/2* redundancy. The treatment with *Pak1* inhibitors (IPA-3 or FRAX597) was sufficient to block the CNF1-triggered IL-1 $\beta$  maturation that was observed in macrophages treated with LPS,

and was also sufficient to block caspase-1 activation (Fig. 3b,c). The inhibition of the caspase-1 cleavage after IPA-3 treatment was similarly observed in macrophages treated with DNT (Extended Data Fig. 4d). Interestingly, IPA-3 was shown to inhibit the binding of activated forms of Rac and Cdc42 to *Pak1*, thereby inhibiting the autophosphorylation of Thr423, whereas the FRAX597



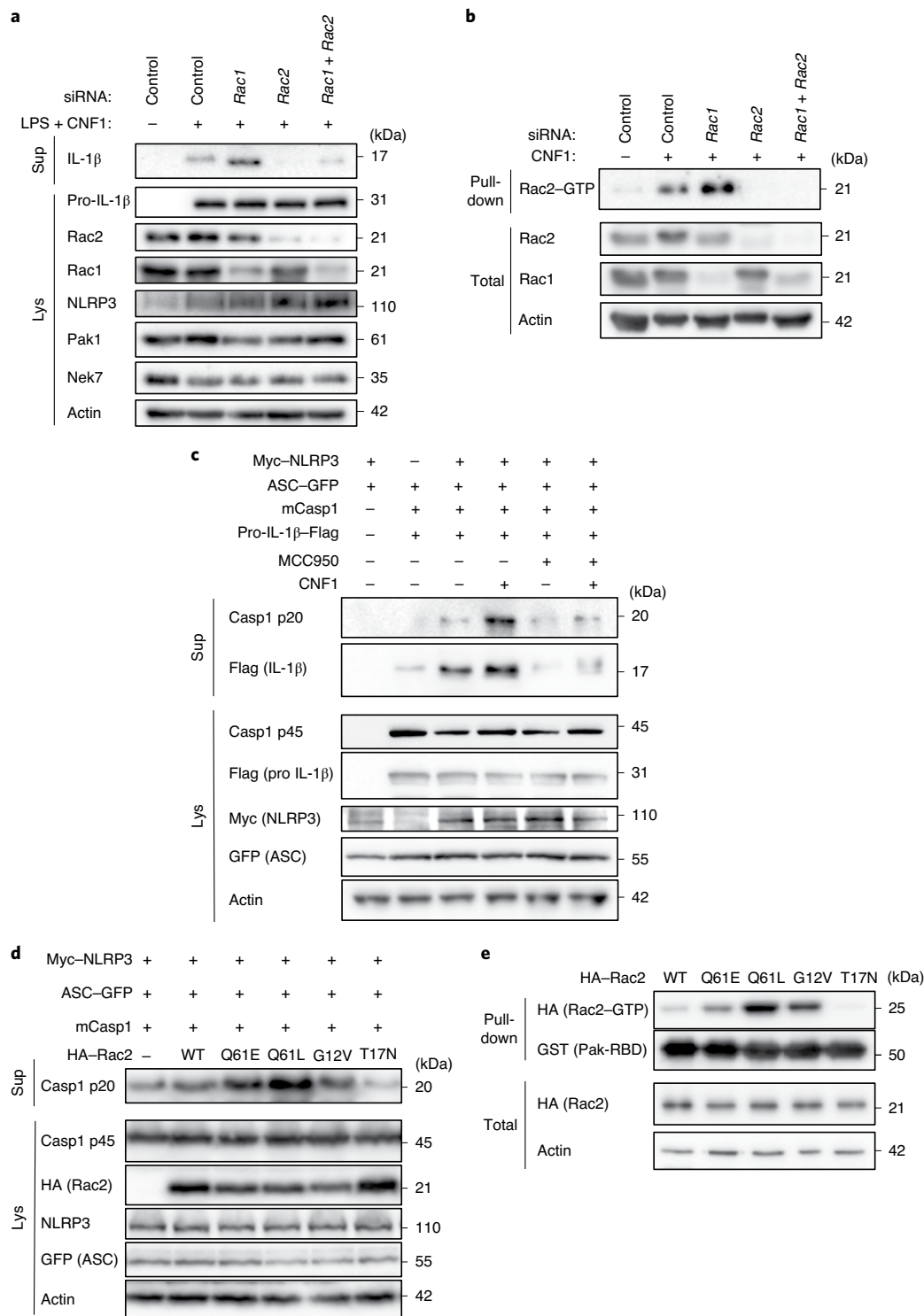


**Fig. 2 | Rac2 activation triggers NLRP3 inflammasome activation. a**, BMDMs extracted from BALB/c mice were transfected with siRNA targeting the indicated isoform of Rac GTPase for 72 h and treated with CNF1 (500 ng ml<sup>-1</sup>) and LPS (100 ng ml<sup>-1</sup>) for 8 h. Supernatants and cell lysates were analysed using immunoblotting. **b**, Immortalized BMDMs (iBMDMs) were transfected with the indicated siRNA for 72 h before being treated or not treated with CNF1 (500 ng ml<sup>-1</sup>) for 6 h before analysis using a GST-Pak-RBD pull-down assay. The Rac2 associated with the GST-Pak-RBD beads is indicated as Rac2-GTP. **c,d**, HEK293T cells were transfected for 16 h with plasmids encoding NLRP3 inflammasome components: Myc-NLRP3, green fluorescent protein (GFP)-tagged ASC, mouse caspase-1 (mCasp1) and pro-IL-1 $\beta$ -Flag as indicated, before analysing caspase-1 cleavage or pro-IL-1 $\beta$  maturation using immunoblotting. **c**, Cells were pretreated or not with 1  $\mu$ M MCC950 for 45 min before treatment for 6 h with CNF1 (500 ng ml<sup>-1</sup>). **d**, Cells were transfected with the following haemagglutinin (HA)-tagged mutants of Rac2: the constitutively active mutant mimicking CNF1-induced deamidation Rac2<sup>Q61E</sup> (Q61E), the constitutively active mutants Rac2<sup>Q61L</sup> (Q61L) or Rac2<sup>G12V</sup> (G12V), or the dominant negative mutant Rac2<sup>T17N</sup> (T17N). Supernatants and cell lysates were analysed using immunoblotting. **e**, HEK293T cells were transfected for 16 h with HA-tagged active mutants Rac2<sup>Q61E</sup>, Rac2<sup>Q61L</sup> or Rac2<sup>G12V</sup>, or the dominant negative mutant Rac2<sup>T17N</sup> before analysis using a GST-Pak-RBD pull-down assay. HA-Rac2 associated with the GST-Pak-RBD beads is indicated as Rac2-GTP. Experiments were repeated at least three times, and representative data are shown.

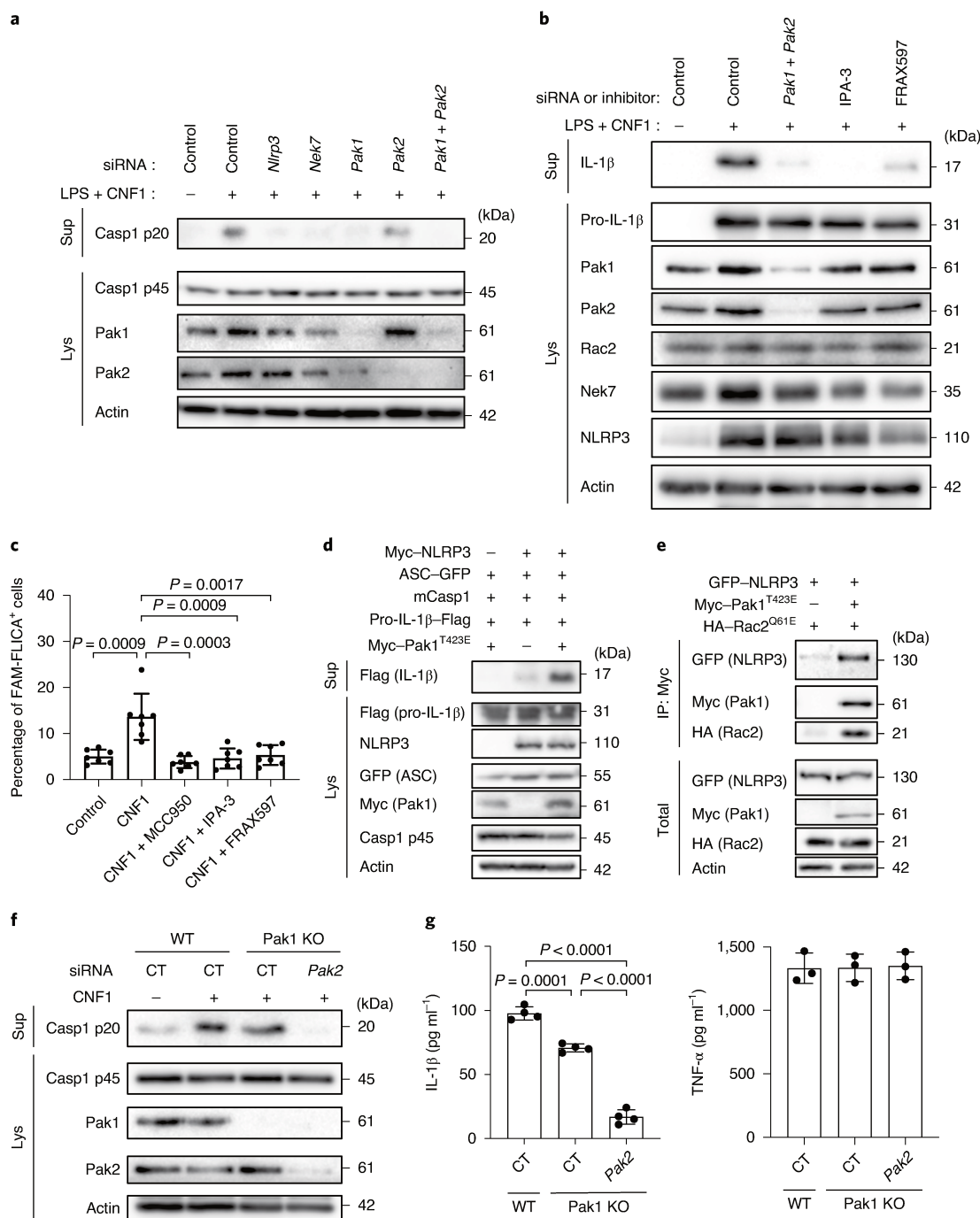


**Fig. 3 | Rac2-NLRP3 signalling is dependent on Pak1 kinase.** **a**, BMDMs isolated from BALB/c mice were transfected for 72 h with siRNA targeting *Nlrp3*, *Nek7*, *Pak1* or *Pak2* as indicated; non-targeting siRNA was used as a control. Cells were treated with CNF1 (500 ng ml<sup>-1</sup>) and LPS (100 ng ml<sup>-1</sup>) for 8 h, as indicated. Supernatants and cell lysates were analysed using immunoblotting. **b**, BMDMs isolated from BALB/c mice were transfected with *Pak1*- and *Pak2*-targeting siRNA or with non-targeting siRNA for 72 h, and treated with 5 μM IPA-3, 1 μM FRAX597 or vehicle for 45 min before treatment with CNF1 (500 ng ml<sup>-1</sup>) and LPS (100 ng ml<sup>-1</sup>) for 8 h. Supernatants and cell lysates were analysed using immunoblotting. **c**, BMDMs isolated from BALB/c mice were treated with vehicle (control), or treated either with 1 μM MCC950, 5 μM IPA-3 or 1 μM FRAX597 for 45 min before treatment with CNF1 (500 ng ml<sup>-1</sup>) for 6 h. Active caspase-1 was stained with FAM-FLICA, analysed using microscopy and FAM-FLICA<sup>+</sup> cells were counted. Each dot represents 100 cells. *n* = 800 cells. Data are mean ± s.e.m. Statistical analyses were performed using two-tailed unpaired Student's *t*-tests. **d**, HEK293T cells were transfected as indicated with plasmids encoding components of the NLRP3 inflammasome (Myc-NLRP3, ASC-GFP, mouse caspase-1) and pro-IL-1β-Flag together with Myc-Pak1<sup>T423E</sup> and pro-IL-1β-Flag cleavage was analysed using immunoblotting. **e**, HEK293T cells were transfected with plasmids encoding GFP-NLRP3, Myc-Pak1<sup>T423E</sup> and HA-Rac2<sup>Q61E</sup>. Cell lysates were processed for anti-Myc immunoprecipitation (IP). **f**, BMDMs isolated from WT or Pak1-knockout C57BL/6J mice were transfected 72 h with non-targeting or *Pak2*-targeting siRNA before treatment with CNF1 (500 ng ml<sup>-1</sup>) for 8 h. Supernatants and cell lysates were analysed using immunoblotting. CT, control. **g**, BMDMs isolated from WT or Pak1-knockout C57BL/6J mice were transfected for 72 h with non-targeting or *Pak2*-targeting siRNA before treatment with CNF1 (500 ng ml<sup>-1</sup>) and LPS (100 ng ml<sup>-1</sup>) for 8 h. Supernatants were analysed using enzyme-linked immunosorbent assay (ELISA) for IL-1β (*n* = 4 biologically independent samples) and TNF-α (*n* = 3 biologically independent samples). Data are mean ± s.e.m. Statistical analyses were performed using two-tailed unpaired Student's *t*-tests. Experiments were repeated at least three times, and representative data are shown.

is an ATP-competitive inhibitor<sup>27</sup>. In the inflammasome reconstitution system in HEK293T, we expressed the activated form of Pak1 (T423E) together with caspase-1, ASC and pro-IL-1 $\beta$ , and we observed no IL-1 $\beta$  maturation. By contrast, when NLRP3 was transfected together with ASC and caspase-1, the expression of the activated form of Pak1 was sufficient to trigger maturation of IL-1 $\beta$  (Fig. 3d). Furthermore, phosphorylated forms of Pak colocalized in dot-like structures with NLRP3 and active caspase-1 (Supplementary Fig. 2). We next investigated whether Rac2, Pak1 and NLRP3 proteins formed a complex. We found NLRP3 interacting with activated Rac2 when activated Pak1 was expressed (Fig. 3e). We next investigated whether Pak1 was involved in the nigericin-triggered activation of the NLRP3 inflammasome and observed that IPA-3 treatment was sufficient to inhibit both caspase-1 cleavage and the release of LDH (Extended Data Fig. 5a,b). Furthermore, siRNA targeting of *Pak1* was found to decrease nigericin-triggered caspase-1 maturation (Extended Data Fig. 5c).

To genetically prove the involvement of Pak1 in NLRP3 inflammasome activation, we used Pak1-knockout mice. We observed a reduction in caspase-1 cleavage triggered by CNF1 in Pak1-knockout macrophages and a reduction in IL-1 $\beta$  secretion (Fig. 3f,g). By contrast, the secretion of TNF- $\alpha$  was unaffected (Fig. 3g). Both caspase-1 cleavage and IL-1 $\beta$  secretion triggered by CNF1 were substantially reduced when the Pak1-knockout macrophages were treated with the *Pak2* siRNA, suggesting that there is a partial compensation in Pak1-knockout macrophages (Fig. 3f,g).

**Pak1 phosphorylates NLRP3 and triggers inflammasome activation.** To further investigate whether NLRP3 is a substrate for the Pak1 serine–threonine kinase, we set-up an in vitro kinase assay. When both Pak1 and NLRP3 proteins were incubated with ATP- $\gamma$ -<sup>32</sup>P, we observed a band at the size of NLRP3, indicating that NLRP3 is directly phosphorylated by Pak1 in vitro (Fig. 4a). The in vitro kinase assay was then used to identify the phosphorylated sites of NLRP3 by analysing the band corresponding to NLRP3 using mass spectrometry. The analysis revealed that Pak1 phosphorylates NLRP3 at three independent positions that correspond to Ser 163, Ser 198 and Thr 659 in the human NLRP3 (Extended Data Fig. 6a,c and Supplementary Table 1). Interestingly, the Ser 163 and Ser 198 residues were previously reported to be phosphorylated, and Ser 198 was reported to be important for NLRP3 priming<sup>28</sup>. NLRP3 Thr 659 was not reported to be phosphorylated and, interestingly, the identified peptide appears to be conserved between humans and mice (Extended Data Fig. 6d). Reinforcing the potential conservation of the Pak–NLRP3 axis, CNF1-triggered caspase-1 activation was observed in primary human macrophages and was inhibited by treatment with NLRP3 inhibitor or Pak1 inhibitor (Extended Data Fig. 7a,b). In the inflammasome reconstitution system, we next expressed the activated Pak1<sup>T423E</sup> and compared the effect of the expression of NLRP3 WT with the triple-mutant NLRP3<sup>S163A S198A T659A</sup> or single mutants NLRP3<sup>S163A</sup>, NLRP3<sup>S198A</sup> and

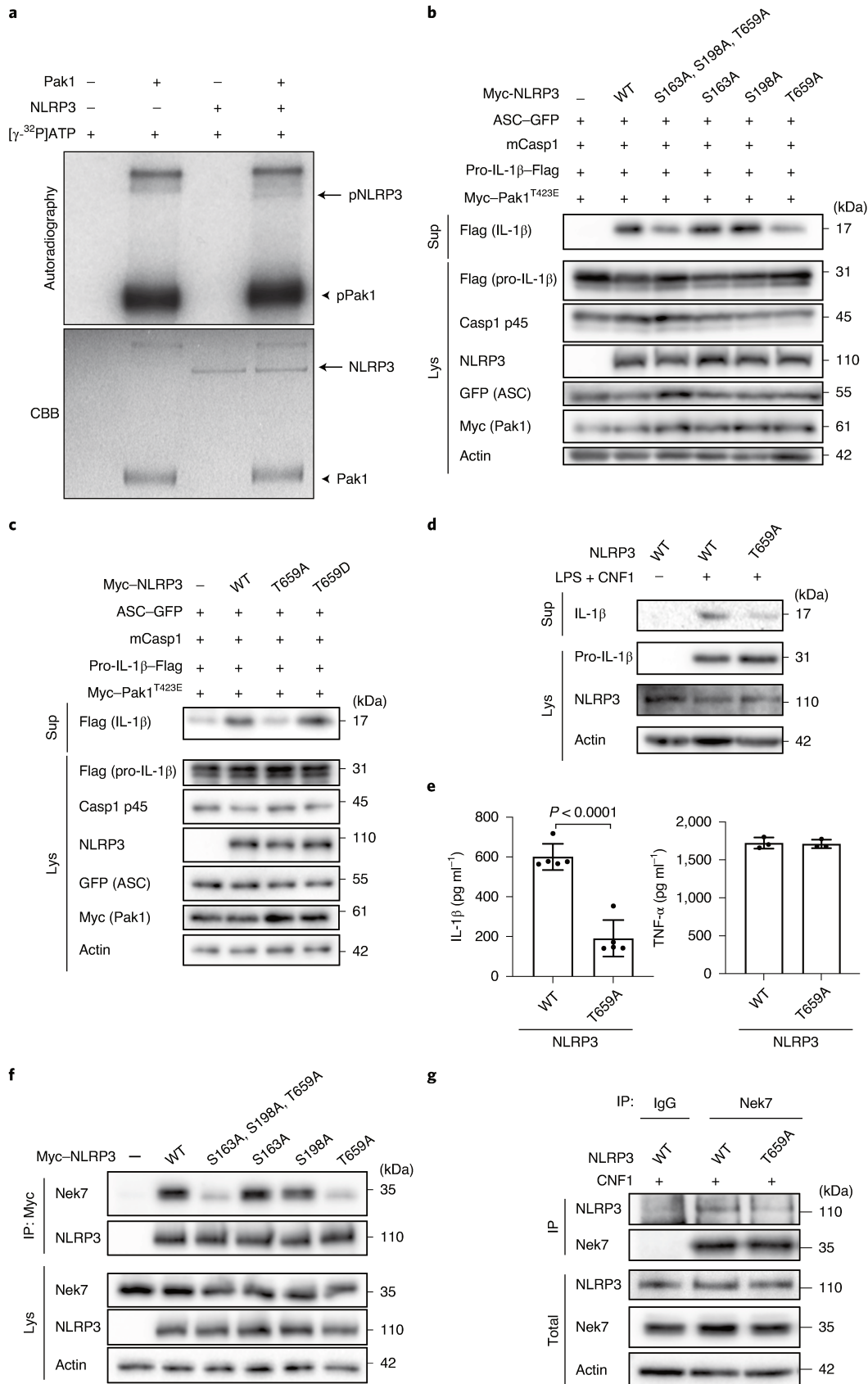
NLRP3<sup>T659A</sup> in which the phosphorylated residues were replaced with alanine residues, which are not sensitive to phosphorylation. The results show that the triple-mutant NLRP3<sup>S163A S198A T659A</sup> and the single mutant NLRP3<sup>T659A</sup> is impaired in IL-1 $\beta$  maturation triggered by the activated Pak1<sup>T423E</sup>, indicating that the NLRP3 Thr 659 residue has an important role in Pak1-triggered NLRP3 inflammasome activation (Fig. 4b). Furthermore, we generated a T659D phosphomimetic NLRP3 mutant and observed that, compared with NLRP3<sup>T659A</sup>, the NLRP3<sup>T659D</sup> mutant had an increased ability to trigger pro-IL-1 $\beta$  maturation (Fig. 4c). Importantly, similar results were obtained when the Rho-GTPase-activating virulence factor SopE was transfected to activate the pathway, highlighting the involvement of this NLRP3 post-translational regulation for the sensing of other virulence factors activating Rho GTPases (Extended Data Fig. 8a). We next stably reconstituted immortalized macrophages knocked-out for NLRP3 with plasmids encoding either NLRP3 or NLRP3<sup>T659A</sup>. Confirming our results, we observed impaired CNF1-triggered IL-1 $\beta$  maturation/secretion in macrophages expressing NLRP3<sup>T659A</sup> compared with macrophages expressing WT NLRP3 (Fig. 4d,e). By contrast, TNF- $\alpha$  was similarly secreted by macrophages expressing either NLRP3 or NLRP3<sup>T659A</sup> (Fig. 4e). After treatment with the DNT toxin, we also observed an impairment in CNF1-triggered IL-1 $\beta$  maturation in macrophages expressing the NLRP3<sup>T659A</sup> mutant compared with macrophages expressing WT NLRP3 (Extended Data Fig. 8b). Reinforcing the importance of this NLRP3 phosphorylation site in the inflammasome activation process, nigericin-triggered IL-1 $\beta$  maturation and secretion were reduced in macrophages expressing the NLRP3<sup>T659A</sup> compared with the macrophages expressing NLRP3, whereas TNF- $\alpha$  secretion was unaffected (Extended Data Fig. 9). Taken together, these results show that phosphorylation of NLRP3 at Thr 659 has a functional role, and that Pak1 is a regulator of the NLRP3 inflammasome. Structural analysis of the NLRP3–Nek7 interaction revealed a putative interaction domain at the level of the Thr 659 of NLRP3 (ref. <sup>29</sup>). Using co-immunoprecipitation experiments, we tested whether the NLRP3<sup>S163A S198A T659A</sup> triple mutant or NLRP3<sup>S163A</sup>, NLRP3<sup>S198A</sup> and NLRP3<sup>T659A</sup> single mutants affected the interaction with endogenous Nek7. The interaction between NLRP3 and Nek7 was impaired in the NLRP3<sup>S163A S198A T659A</sup> triple mutant and in the NLRP3<sup>T659A</sup> mutant, indicating that Thr 659 is a critical site for NLRP3–Nek7 interaction and suggesting that the phosphorylation of NLRP3 at Thr 659 is important for the NLRP3–Nek7 interaction (Fig. 4f). This observation was confirmed using anti-Nek7 immunoprecipitation in macrophages in which we found a decrease in NLRP3<sup>T659A</sup> binding to Nek7 compared with WT NLRP3 (Fig. 4g).

**Clearance of CNF1-expressing *E. coli* during bacteraemia requires the Pak–NLRP3 signalling axis.** We next addressed the relevance of the CNF1-triggered Pak–NLRP3 signalling axis during infection. We observed an increase in caspase-1 maturation when macrophages were infected with CNF1-expressing *E. coli* compared

**Fig. 4 | Pak1 phosphorylates NLRP3 to promote inflammasome activation.** **a**, In vitro [ $\gamma$ -<sup>32</sup>P]ATP kinase assay using human recombinant NLRP3 (arrows) and human recombinant Pak1 (arrowheads) analysed using autoradiography and Coomassie brilliant blue (CBB) staining. **b**, HEK293T cells were transfected with plasmids encoding components of the NLRP3 inflammasome (ASC–GFP, mouse caspase-1), pro-IL-1 $\beta$ –Flag, Myc–Pak1<sup>T423E</sup>, with Myc–NLRP3, Myc–NLRP3<sup>S163A</sup>, Myc–NLRP3<sup>S198A</sup>, Myc–NLRP3<sup>T659A</sup> or Myc–NLRP3<sup>S163A S198A T659A</sup>, and IL-1 $\beta$  maturation was analysed using immunoblotting. **c**, HEK293T cells were transfected with plasmids encoding components of the NLRP3 inflammasome (ASC–GFP, mouse caspase-1) and Myc–Pak1<sup>T423E</sup>, with Myc–NLRP3, Myc–NLRP3<sup>T659A</sup> or Myc–NLRP3<sup>T659D</sup>, and IL-1 $\beta$  maturation was analysed using immunoblotting. **d,e**, NLRP3-knockout iBMDMs that were reconstituted with either NLRP3 or NLRP3<sup>T659A</sup> were treated with vehicle or LPS (100 ng ml<sup>-1</sup>) and CNF1 (500 ng ml<sup>-1</sup>) for 8 h. **d**, Supernatants and cell lysates were analysed using immunoblotting. **e**, Supernatants were analysed using ELISA for IL-1 $\beta$  ( $n = 4$  biologically independent samples) and TNF- $\alpha$  ( $n = 3$  biologically independent samples). Data are mean  $\pm$  s.e.m. Statistical analyses were performed using two-tailed unpaired Student's *t*-tests. **f**, HEK293T cells were transfected with plasmids encoding Myc–NLRP3, Myc–NLRP3<sup>S163A</sup>, Myc–NLRP3<sup>S198A</sup>, Myc–NLRP3<sup>T659A</sup> or Myc–NLRP3<sup>S163A S198A T659A</sup>. Cell lysates were processed for anti-Myc immunoprecipitation and endogenous Nek7 was revealed using anti-Nek7 antibodies. **g**, NLRP3-knockout iBMDMs that were reconstituted with either NLRP3 or NLRP3<sup>T659A</sup> were treated with CNF1 (500 ng ml<sup>-1</sup>) for 6 h. Cell lysates were analysed using immunoprecipitation with anti-Nek7 antibodies or isotopic IgG. Experiments were repeated at least three times, and representative data are shown.

with the isogenic *E. coli* CNF1-knockout strain, and treatment with NLRP3 or Pak1 inhibitors decreased the caspase-1 cleavage triggered by the *E. coli* expressing CNF1 (Fig. 5a). Furthermore, IL-1 $\beta$  secretion triggered by the CNF1-expressing *E. coli* was reduced when

bacteria were added to NLRP3-knockout macrophages (Fig. 5b). Furthermore, the secretion of IL-1 $\beta$  triggered by CNF1-expressing *E. coli* in macrophages complemented with the NLRP3<sup>T659A</sup> mutant was decreased compared with control macrophages expressing



NLRP3 (Fig. 5c). TNF- $\alpha$  secretion measured during infection with CNF1-expressing *E. coli* was not affected in macrophages that were isolated from NLRP3-knockout mice or macrophages expressing the NLRP3<sup>T659A</sup> mutant (Fig. 5b,c). We previously demonstrated that the CNF1 toxin expressed by *E. coli* triggered both an immune response in vivo and bacterial clearance during bacteraemia<sup>11</sup>. To investigate the role of Pak1 during CNF1-expressing *E. coli* bacteraemia, we used the Pak1 inhibitor AZ13711265, which blocks CNF1-triggered IL-1 $\beta$  maturation (Supplementary Fig. 3) and is associated with good in vivo pharmacokinetic properties<sup>27</sup>. We monitored the bacterial burden during bacteraemia in control mice or mice injected with AZ13711265. Mice bacteraemia was measured for each mouse at 4 h, 24 h and 48 h after infection (Fig. 5d). The bacterial clearance of CNF1-expressing *E. coli* was observed; no bacteria were detectable at 48 h in all of the control animals (Fig. 5d). We measured a statistically significant higher bacterial load at 48 h and 77% of the animals were found to be positive for bacteraemia in the mice that were injected with the Pak1 inhibitor, indicating that in vivo the inhibition of Pak1 is sufficient to inhibit the CNF1-expressing *E. coli* clearance (Fig. 5d). We next used an NLRP3 inhibitor, MCC950, which has been shown to be efficient in vivo<sup>30</sup>. We monitored bacteraemia in mice injected with MCC950 compared with the controls. The bacterial clearance of CNF1-expressing *E. coli* in mice injected with the NLRP3 inhibitor was significantly higher at 48 h, and 70% of the animals were found to be positive for bacteraemia (Fig. 5d). Consistent with our model, we observed no significant effect of both AZ13711265 and MCC950 towards the bacterial clearance when we infected mice with the isogenic *E. coli* CNF1-knockout strain (Extended Data Fig. 10a). To genetically prove this point, we infected WT mice, NLRP3-knockout mice or Pak1-knockout mice, and compared the CNF1-expressing *E. coli* burden. Consistent with the results obtained with the NLRP3 and Pak1 inhibitors, we did not detect any bacteria in the blood of infected WT mice at 48 h, whereas we measured a mean of  $1.5 \times 10^4$  and  $2.5 \times 10^2$  bacteria per mouse in the blood of NLRP3-knockout and Pak1-knockout mice, respectively (Fig. 5e,f). The smaller effect observed in Pak1-knockout mice compared with NLRP3-knockout mice could be explained by the redundancy observed between Pak1 and Pak2 at the cellular level. The difference in the clearance of CNF1-expressing *E. coli* measured at 48 h between WT and NLRP3-knockout mice was still observable at later time points and was not observed when mice were infected with the isogenic *E. coli* CNF1-knockout strain, indicating the specificity of the CNF1 response towards the NLRP3 pathway in vivo (Extended Data Fig. 10b,c). Furthermore, we measured a similar trend in the clearance of the CNF1-expressing *E. coli* strain in WT and GSDMD-knockout mice (Extended Data Fig. 10d). We next monitored the bacterial burden in mice that were infected with CNF1-expressing *E. coli* and treated with AZ13711265, MCC950 or both. We observed no differences in the bacterial clearance between the three groups (Fig. 5d). NLRP3-knockout mice that were injected with vehicle or with AZ13711265 demonstrated no differences in bacterial clearance, suggesting that Pak1 and NLRP3 act within the

same signalling pathway during bacteraemia (Fig. 5g). Together, these results unravel the critical role of Pak1 and NLRP3 in the clearance of CNF1-expressing bacteria and their importance in the innate immune response during bacteraemia.

## Discussion

Our results shed light on a regulatory mechanism for NLRP3 after the activation of Rac2 by the bacterial toxin CNF1. The level of NLRP3 inflammasome activation is correlated with the strength of the interaction between activated Rac2 and Pak1-RBD, indicating that the innate immune system can adapt its response to the level of Rac2 activity. This seems to be an elegant strategy to deliver a commensurate response to the level of CNF1 toxin activity. Notably, the phosphorylated peptide containing Thr 659 of human NLRP3 isolated by mass spectrometry is highly conserved between species, and the Pak–NLRP3 axis is conserved in human macrophages and is involved in the nigericin-triggered NLRP3 inflammasome activation. Complementary studies will be necessary to determine the precise molecular mechanism in other species or in other contexts as well as to determine whether the phosphorylation of NLRP3 at Thr 659 is a consensus site used by other kinases. Nevertheless, our results show that phosphorylation of NLRP3 at Thr 659 is important for NLRP3 inflammasome activation and suggest that it is implicated in NLRP3-related inflammatory disorders or susceptibility to infection.

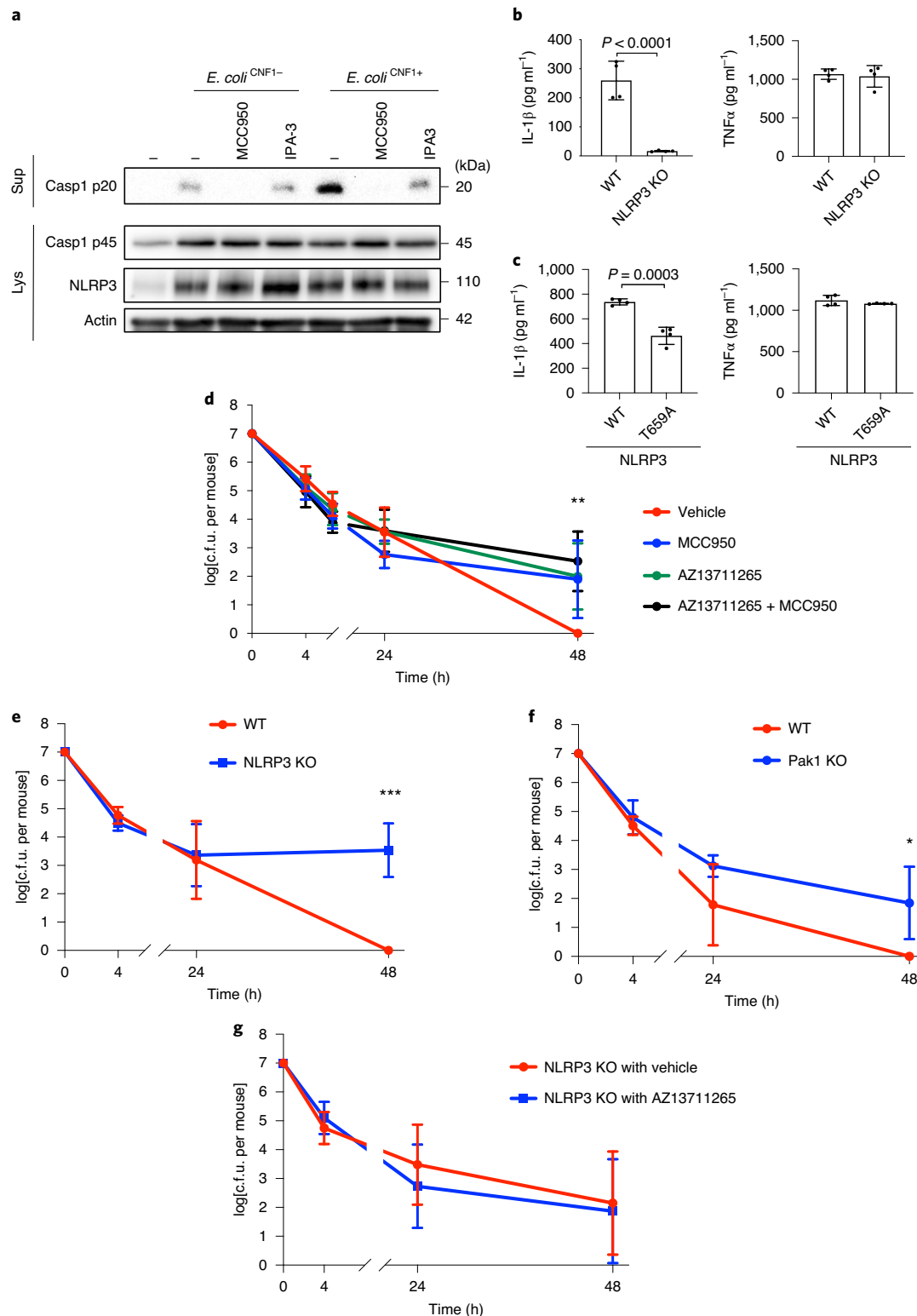
Our results suggest that there is redundancy between Pak1 and Pak2, as shown by a partial compensation by Pak2 in Pak1-knockout macrophages and mice. Further studies are required to clarify the importance of each of the group-1 Pak proteins in the activation of the NLRP3 inflammasome. Unfortunately, the Pak2-knockout mutations in mice are embryonically lethal (at embryonic day 8.0) and these studies would require the generation of conditional transgenic mice<sup>31</sup>.

We unravelled a CNF1-triggered secretion of IL-1 $\beta$  that is not linked to an increase in cell death and is independent of GSDMD. Studies of NLRP3 inflammasome canonical triggers have demonstrated different IL-1 $\beta$  secretion scenarios. In the conventional scenario, caspase-1 cleaves the inflammasome-related cytokines and GSDMD to generate active N-GSDMD<sup>32,33</sup>. N-GSDMD relocates in the plasma membrane to form pores, enabling IL-1 $\beta$  secretion<sup>32,33</sup>. GSDMD pores are associated with pyroptosis in the case of classical inflammasome activation or are controlled during inflammasome hyperactivation, leading to secretion without pyroptosis<sup>34–36</sup>. The CNF1-triggered IL-1 $\beta$  secretion seems to fall into another category, independent of both GSDMD cleavage and cell death, that may share similarities with the unconventional IL-1 $\beta$  secretion<sup>37</sup>. This unconventional secretion relies on the affinity of IL-1 $\beta$  to the plasma membrane ruffles that are characteristic of the CNF1-triggered Rac GTPase activation. The mechanism explaining how CNF1 triggered caspase-1 activation without GSDMD cleavage remains to be elucidated and may be unique to toxins activating Rho GTPases. One hypothesis is that the activation of Rac2, in parallel to the

**Fig. 5 | Pak1 and NLRP3 control the burden of CNF1-expressing *E. coli* during bacteraemia.** **a**, BMDMs isolated from C57BL/6 mice were pretreated for 45 min with 1  $\mu$ M MCC950 or 5  $\mu$ M IPA-3 and were infected or not (multiplicity of infection (m.o.i.) = 5) with either *E. coli*<sup>CNF1+</sup> or isogenic CNF1-deleted mutant *E. coli*<sup>CNF1-</sup>. Supernatants and cell lysates were analysed using immunoblotting. **b,c**, BMDMs isolated from C57BL/6 or C57BL/6 NLRP3-knockout mice (**b**) or iBMDMs expressing NLRP3 or NLRP3<sup>T659A</sup> (**c**) were infected (m.o.i. = 5) with *E. coli*<sup>CNF1+</sup>. The supernatants were analysed using ELISA.  $n = 4$  biologically independent samples per group. Data are mean  $\pm$  s.e.m. Statistical analyses were performed using two-tailed unpaired Student's *t*-tests. **d–g**, Mice were intravenously infected with  $10^7$  colony-forming units (c.f.u.) of *E. coli*<sup>CNF1+</sup>, before collecting peripheral blood at 4 h, 24 h and 48 h for the measurement of bacteraemia. **d**, C57BL/6J mice were injected intraperitoneally with vehicle, or with 50 mg kg<sup>-1</sup> MCC950 ( $n = 10$  mice), 10 mg kg<sup>-1</sup> AZ13711265 ( $n = 10$  mice) or both once a day ( $n = 9$  mice).  $^{**}P < 0.01$  (each individual inhibitor-treated group compared with the group injected with vehicle). **e**, WT ( $n = 7$  mice) or NLRP3-knockout C57BL/6J mice ( $n = 6$  mice) were analysed.  $^{***}P < 0.001$ . **f**, WT ( $n = 4$  mice) or Pak1-knockout C57BL/6J mice were analysed ( $n = 4$  mice).  $^{*}P < 0.05$ . **g**, NLRP3-knockout C57BL/6J mice were injected intraperitoneally with 10 mg kg<sup>-1</sup> AZ13711265 ( $n = 7$  mice) or vehicle ( $n = 9$  mice) once each day. Experiments were repeated at least two times, and representative data are shown. Data are the geometric mean  $\pm$  95% confidence interval. Statistical analyses were performed using two-tailed nonparametric Mann-Whitney *U*-tests.  $^{*}P < 0.05$ ,  $^{**}P < 0.01$ ,  $^{***}P < 0.001$ .

Pak1–NLRP3 pathway activation, inhibits the cleavage of GSDMD. Similar to *Toxoplasma gondii*, the NF- $\kappa$ B activation triggered by Rac2 might be another mechanism explaining the IL-1 $\beta$  secretion independent of cell death and GSDMD<sup>38</sup>. Rac2 signalling may also regulate a potassium channel explaining the inhibition by KCl of the CNF1-triggered IL-1 $\beta$  secretion. Favouring this hypothesis, Rac GTPases have been found to modulate Kir2.1, a Kir-family potassium channel<sup>39</sup>.

Our study shows that NLRP3 is a major sensor of toxins that activate Rho GTPases, whereas previous research has shown the sensing of Rho-GTPase-inactivating toxins by Pyrin<sup>12</sup>. These studies highlight that the mammalian innate immune system has evolved strategies that share similarities with the effector-triggered immunity to detect abnormal activation of Rho GTPases<sup>3,40,41</sup>. Interestingly, both inactivation of RhoA and activation of Rac2 by bacterial toxins are monitored by Pyrin and NLRP3, respectively. More precisely,



here we show that Rac GTPases that activate bacterial factors are sensed by NLRP3 independently of the type of modification made. Similarly, bacterial factors that inactivate RhoA activate Pyrin independently of the type of modifications<sup>12,42,43</sup>. These results suggest that the host guarding of Rho GTPase signalling integrity relies on two sensors that monitor the abnormal Rho GTPase cycling rather than toxin-triggered post-translational modifications of host proteins or virulence factor enzymatic activities. Interestingly, both Pyrin and NLRP3 require regulation by the serine–threonine kinases PKN1/2 and Pak1/2, respectively. The fact that two different inflammasomes have been evolutionarily selected to detect bacterial toxins that modify Rho GTPases highlights the importance of Rho GTPases in innate immunity.

Further studies are necessary to determine the *in vivo* conservation of the Pak–NLRP3 axis and whether the sensing of other Rho–GTPase-activating virulence factors by the NLRP3 inflammasome impacts the bacterial burden during infection. Similarly, we expect that further studies will determine the importance of other inflammasomes in detecting bacterial virulence factors that are endowed with enzymatic activities.

Our results reveal the importance of Pak1 and NLRP3 in controlling the bacterial burden during bacteraemia in mice. Even though further studies will be required to determine the role of the Pak–NLRP3 signalling axis in patients with bacteraemia, our results showing an increase in bacterial burden in MCC950-treated mice suggest that caution will be necessary for the use of NLRP3 inhibitors in the clinical setting. This is consistent with clinical data showing that there is an increased risk of infections associated with IL-1 signalling inhibition<sup>44,45</sup>. One option would be to consider combining inflammasome inhibitors with antibiotherapies or with an enhanced surveillance for a potential for bacteraemia risk.

## Methods

**Ethics statement.** This study was carried out in strict accordance with the guidelines of the Council of the European Union (Directive 86/609/EEC) regarding the protection of animals used for experimental and other scientific purposes. The protocol was approved by the Institutional Animal Care and Use Committee on the Ethics of Animal Experiments of Nice, France (APAFIS#18322-20181218099427035 v2 and APAFIS#24906-2020031614223228 v2).

**Bacterial strains and toxins.** The *E. coli* UTI89 clinical isolate was originally obtained from a patient with cystitis<sup>46</sup> and the isogenic UTI89 CNF1<sup>+</sup> (*E. coli*<sup>CNF1+</sup>) or UTI89 CNF1<sup>-</sup> (*E. coli*<sup>CNF1-</sup>) streptomycin-resistant strain generation and culture conditions were previously described<sup>1</sup>. For the infections, a 1/100 dilution of an overnight culture was inoculated and grown up to an optical density at 600 nm of 1.2 using a Luria–Bertani (LB) medium supplemented with streptomycin (200 µg ml<sup>-1</sup>). Bacteria were collected by centrifugation and washed twice in PBS before dilution in PBS to obtain the desired bacterial concentrations for the mouse infection experiments. Recombinant WT CNF1 and its catalytically inactive form (CNF1<sup>C865S</sup>) were produced and purified as previously reported<sup>47,48</sup>. The recombinant DNT toxin was purified from pQEDNTwt using the same protocol<sup>49</sup>. The recombinant proteins were passed through a polymyxin B column (Affinity Detoxi-Gel, Pierce). The removal of endotoxin was verified using a colorimetric limulus amoebocyte lysate (LAL) assay (LAL QCL-1000, Cambrex). Each stock of the CNF1 preparation (2 mg ml<sup>-1</sup>) was shown to contain less than 0.5 endotoxin units per ml. Plasmid expressing the virulence factor pCMV-SopE-HA was previously reported<sup>22</sup> and SopE expression was stabilized by adding MG132 (10 µM) to the cells to block its proteasomal degradation as previously described<sup>50</sup>. Plasmids expressing the PRK5-Myc-DNT were obtained by PCR amplification of pQEDNTwt, and pCMV-HA-YopE was obtained by PCR amplification and subcloning from pACY184-YopE-GSK (gift from I. Brodsky). All of the plasmids were verified by sequencing (Eurofins).

**Cell culture, transfection and inhibitors.** HEK293T cells were obtained from ATCC (CRL-3216) and maintained according to the ATCC instructions. BMDMs were extracted from the femurs of BALB/c, C57BL/6J, C57BL/6J knockout or C57BL/6J knockout mice (aged 6–10 weeks) as indicated in the legends and were cultured in RPMI GlutaMax medium (Life Technologies) supplemented with 100 ng ml<sup>-1</sup> M-CSF (premium grade, Miltenyi Biotec), 10% heat-inactivated FBS (Biowest) and 50 µg ml<sup>-1</sup> gentamycin (Life Technologies) at 37 °C in an atmosphere containing 5% CO<sub>2</sub>. The cells were seeded at a concentration of 10<sup>6</sup> cells per well in a six-well plate. After 6 d of differentiation, BMDMs were used for

experiments. HEK293T cells were transfected with plasmids using Lipofectamine 2000 (Life Technologies) according to the manufacturer's instructions. siRNAs were transfected in BMDMs for 72 h using Lipofectamine RNAiMAX Reagent (Thermo Fisher Scientific) according to the manufacturer's instructions. Cells were transfected as indicated in the figure legends with siRNAs (Dharmacon) targeting *Nlrp3* (L-053455-00), *Rac1* (L-041170-00), *Rac2* (L-041171-01), *Nek7* (J-063266-09), *Pak1* (L-048101-00), *Pak2* (L-040615-00) or non-targeting control siRNA (D-001810-10). For the siRNA screen, the BMDMs were transfected with siRNA (Dharmacon) targeting *Nod1* (L-055182-00), *Nod2* (L-052735-00), *Nlr3* (L-052823-01), *Nlr4* (L-055000-00), *Nlr5* (L-067620-01), *Nlr1* (L-057712-01), *Ciita* (L-043166-02), *Naip1* (L-047682-00), *Naip2* (L-044151-01), *Naip5* (L-044142-01), *Naip6* (L-044145-01), *Naip7* (L-065757-00), *Nlrp1a* (L-066229-00), *Nlrp1b* (L-161107-01), *Nlrp2* (L-053528-01), *Nlrp3* (L-053455-01), *Nlrp4a* (L-052395-01), *Nlrp4b* (L-058181-01), *Nlrp4c* (L-049416-01), *Nlrp4d* (L-067051-01), *Nlrp4e* (L-068064-01), *Nlrp4f* (L-052668-01), *Nlrp4g* (L-066364-01), *Nlrp5* (L-045315-01), *Nlrp6* (L-066157-01), *Nlrp9a* (L-058269-01), *Nlrp9b* (L-066417-01), *Nlrp9c* (L-057344-01), *Nlrp10* (L-056559-01), *Nlrp12* (L-060234-01), *Nlrp14* (L-066093-01), *Pycard* (L-051439-01), *Mefv* (L-048693-01) and *Aim2* (L-044968-01). BMDMs were pretreated with the following inhibitors for 45 min: 1 µM CP-456773 or MCC950 (Sigma-Aldrich), 5 µM IPA-3 (Tocris), 1 µM FRAX597 (Tocris) or the indicated concentration of AZ13711265 (AGV Discovery) in 2% FBS containing RPMI followed by the addition of CNF1 500 ng ml<sup>-1</sup> and/or ultrapure LPS 100 ng ml<sup>-1</sup> (Invivogen) as indicated in the figure legends. Cells treated with nigericin 5 µM (Invivogen) or ATP 5 mM (Invivogen) for 30 min were used as positive control for NLRP3 inflammasome activation. For K<sup>+</sup>-efflux-preventing experiments, BMDMs were treated with 10 mM, 20 mM or 40 mM KCl. Primary macrophages were infected with *E. coli*<sup>CNF1+</sup> or the isogenic *E. coli*<sup>CNF1-</sup> (m.o.i. = 5) for 16 h. Immortalized NLRP3-knockout BMDMs were stably complemented with pINDUCER21 plasmids encoding human NLRP3 WT or NLRP3<sup>T659A</sup> under a doxycycline-inducible promoter as previously described<sup>51</sup>. NLRP3 expression was induced by adding 2 µg ml<sup>-1</sup> doxycycline for 16 h (Takara Bio). All of the cell lines were authenticated using PCR assays with species-specific primers. Mycoplasma testing was negative.

**Mouse model of infection.** Female C57BL/6J mice (aged 7 weeks; Charles River Laboratory) were injected intraperitoneally with MCC950 (Sigma-Aldrich) at 50 mg kg<sup>-1</sup> every 24 h or AZ13711265 (AGV Discovery) at 10 mg kg<sup>-1</sup> every 24 h or both. NLRP3-knockout mice were provided by V. Petrilli and were described previously<sup>52</sup>. The Pak1-knockout, GSDMD-knockout and ASC–citricine-knockin mice used in this study were reported previously<sup>17,32,53</sup>. Female NLRP3-knockout or Pak1-knockout and female congenic WT C57BL/6J littermate mice were injected intravenously with 10<sup>7</sup> colony-forming units of *E. coli* and the determination of bacteraemia was monitored as previously described<sup>1</sup>. Mice were housed with their littermates and kept under a regular 12 h–12 h light–dark cycle at room temperature (20–25 °C) and a relative humidity of 50–70%. Food and water were available *ad libitum*. Experiments were performed under pathogen-free conditions with randomly chosen animals (same sex, matched by age and body weight). Investigators were blinded for *in vivo* experiments. Sample size was determined on the basis of our previous research<sup>1</sup> and using G\*Power software.

**Reconstituted NLRP3 inflammasome in HEK293T cells.** HEK293T cells were transfected with plasmids encoding the NLRP3 inflammasome components as previously described<sup>11,28</sup>. HEK293T cells were transfected with plasmids encoding Myc–NLRP3 or NLRP3 mutants, ASC–GFP, mpro-caspase1 and pro-IL-1β–Flag. Where indicated in the legend, cells were cotransfected with HA–Rac2, the constitutively active mutant of Rac2 mimicking CNF1-induced deamidation Rac2<sup>Q61E</sup>, Rac2<sup>Q61L</sup>, Rac2<sup>G12V</sup> or Rac2<sup>T17N</sup>, a dominant negative mutant of Rac2 for 16 h. The monitoring of caspase-1 or IL-1β cleavage was performed using supernatant immunoblotting.

**Immunoprecipitation.** HEK293T cells were transfected with plasmids encoding Myc–NLRP3, Myc–NLRP3<sup>S163A/S198A/T659A</sup>, Myc–NLRP3<sup>S163A</sup> and Myc–NLRP3<sup>T659A</sup>, GFP–NLRP3, Myc–Pak1<sup>T423E</sup> and HA–Rac2<sup>Q61E</sup>, or NLRP3 expression was induced by adding 2 µg ml<sup>-1</sup> doxycycline for 16 h to iBMDMs stably expressing NLRP3 or NLRP3<sup>T659A</sup>. Cells were lysed and processed for immunoprecipitation using 2 µg of anti-Myc or 3 µg of anti-Nek7 antibodies according to previously described conditions<sup>54</sup>. The expression of NLRP3 and endogenous levels of Nek7 were monitored in the cell lysate as well as in the immunoprecipitated fraction.

**LDH release.** The supernatant of stimulated macrophages was collected and centrifuged at 300g for 5 min to remove cellular debris. LDH measurement was performed using the LDH Cytotoxicity Assay Kit (Thermo Fisher Scientific) according to the manufacturer's instructions, in samples diluted 1:5 in PBS. Data were plotted as the percentage of LDH release considering a Triton X-100 treated well as 100%.

**Cell permeabilization kinetics.** BMDMs were plated and stimulated in a 96-well plate in medium containing propidium iodide (0.1 µg ml<sup>-1</sup>) and data were acquired with a ×10 objective using the InCyte Zoom system v.6.2.9200.0

(Essen BioScience) under a CO<sub>2</sub>- and temperature-controlled environment. Each condition was run in quadruplicate. The number of fluorescent objects was counted using Incucyte Zoom (Essen BioScience).

**In vitro kinase assay.** Recombinant purified Pak1 (500 ng) was incubated with 1 µg of recombinant human NLRP3 protein (Abcam, ab165022), and with 50 µM ATP and 4 µCi of [<sup>32</sup>P]ATP in kinase buffer (50 mM HEPES pH 7.3, 50 mM NaCl, 0.05% Triton X-100, 10 mM β-glycerophosphate, 5 mM NaF, 10 mM MgCl<sub>2</sub> and 0.2 mM MnCl<sub>2</sub>) at 30°C for 30 min in a final volume of 39 µl. The reaction was stopped by adding 15 µl of LDS (Thermo Fisher Scientific) and 6 µl of dithiothreitol 500 mM. Samples were analysed by electrophoresis using Bolt 4–12% Bis-Tris Plus gels (Thermo Fisher Scientific) followed by Coomassie blue staining and autoradiography.

**Immunofluorescence staining, antibodies and ELISA assays.** Caspase-1 activation was detected using the fluorescent probe FAM-FLICA (ImmunoChemistry Technologies) after 6 h of treatment, according to the manufacturer's instructions. After labelling, cells were fixed in 4% paraformaldehyde for 15 min, PFA was neutralized with 50 mM NH<sub>4</sub>Cl for 15 min, cells were permeabilized with 0.5% Triton X-100 for 5 min and blocked with 2% TBS-BSA. Cells were incubated with mouse anti-NLRP3 (clone Cryo-2, Adipogen) and/or rabbit anti-ASC (AG-25B-0006, Adipogen) or rabbit anti-phosphorylated-Pak (ab40795, Abcam) antibodies for 1 h followed by incubation with the secondary antibodies TexasRed anti-mouse IgG (TI-2000, Vector Laboratories) or Cy5 anti-mouse IgG (715-175-151, Jackson ImmunoResearch) and/or TexasRed anti-rabbit IgG (711-075-152, Jackson ImmunoResearch) and/or phalloidin Alexa Fluor 647 (ab176759, Abcam) and Hoechst 33342 (H1399, Thermo Fisher Scientific) for 30 min. Cells were imaged using a Nikon A1R confocal microscope. The following antibodies were used in this study: rabbit anti-IL-1β (GTx74034, Genetex), mouse anti-caspase-1 (clone Casper-1, Adipogen), mouse anti-Rac (clone 102/Rac1, BD Biosciences), goat anti-Rac2 (ab2244, Abcam), mouse anti-NLRP3 (clone Cryo-2, Adipogen), rabbit anti-Nek7 (ab133514, Abcam), rabbit anti-Pak1 (2602, CST), rabbit anti-Pak2 (2608, CST), rabbit monoclonal anti-GSDMD (ab209845), mouse anti-β-actin (AC-74, Sigma-Aldrich), mouse anti-Myc (9E10, Roche), mouse anti-HA (16B12, Covance), mouse anti-Flag (clone M2, Sigma-Aldrich), mouse anti-GFP (clone 7.1, 13.1, Roche). Cytokine secretion was determined by ELISA using the mouse Quantikine ELISA kits for mouse IL-6, IL-18, TNF-α and IL-1β (R&D Systems) according to the manufacturer's instructions.

**Flow cytometry analysis.** BMDMs isolated from C57BL/6J mice constitutively expressing ASC-citrine fusion protein (R26-CAG-ASC-citrine) were treated with LPS (100 ng ml<sup>-1</sup>) for 16 h before 6 h of treatment with vehicle or CNF1 (500 ng ml<sup>-1</sup>) or 30 min with nigericin (5 µM). Cells were collected and analysed by flow cytometry using a BD FACSCanto II cytometer (BD Biosciences). Cytometry data were analysed using FlowJo v.10.6.2. Doublets were excluded using a side scatter (SSC)-A (area) and SSC-H (height) plot; cells with a high expression of ASC-citrine were gated and then analysed for ASC-citrine signal area (ASC-citrine-A) and ASC-citrine signal height (ASC-citrine-H). Cells with ASC specks were defined with a higher ASC-H:ASC-A ratio.

**Statistical analyses.** Statistical analyses were performed using GraphPad Prism v.8.2.1. Comparisons of the bacterial load of mice were performed using nonparametric Mann-Whitney *U*-tests. Statistical analyses of FAM-FLICA<sup>+</sup> cells, cytokine secretion and LDH release were performed using unpaired two-tailed Student's *t*-tests.

**Reporting Summary.** Further information on research design is available in the Nature Research Reporting Summary linked to this article.

## Data availability

All data supporting the findings of this study are available within the Article and its Supplementary Information or from the corresponding author on reasonable request. Source data are provided with this paper.

Received: 21 August 2019; Accepted: 13 November 2020;

Published online: 11 January 2021

## References

- Martin, G. S., Mannino, D. M., Eaton, S. & Moss, M. The epidemiology of sepsis in the United States from 1979 through 2000. *N. Engl. J. Med.* **348**, 1546–1554 (2003).
- Vance, R. E., Isberg, R. R. & Portnoy, D. A. Patterns of pathogenesis: discrimination of pathogenic and nonpathogenic microbes by the innate immune system. *Cell Host Microbe* **6**, 10–21 (2009).
- Stuart, L. M., Paquette, N. & Boyer, L. Effector-triggered versus pattern-triggered immunity: how animals sense pathogens. *Nat. Rev. Immunol.* **13**, 199–206 (2013).
- Flatau, G. et al. Toxin-induced activation of the G protein p21 Rho by deamidation of glutamine. *Nature* **387**, 729–733 (1997).
- Schmidt, G. et al. Gln63 of Rho is deamidated by *Escherichia coli* cytotoxic necrotizing factor-1. *Nature* **387**, 725–729 (1997).
- Aktories, K. & Barbieri, J. Bacterial cytotoxins: targeting eukaryotic switches. *Nat. Rev. Microbiol.* **3**, 397–410 (2005).
- Galán, J. E. Common themes in the design and function of bacterial effectors. *Cell Host Microbe* **5**, 571–579 (2009).
- Bruno, V. M. et al. *Salmonella* Typhimurium type III secretion effectors stimulate innate immune responses in cultured epithelial cells. *PLoS Pathog.* **5**, e1000538 (2009).
- Munro, P. et al. Activation and proteasomal degradation of Rho GTPases by cytotoxic necrotizing factor-1 elicit a controlled inflammatory response. *J. Biol. Chem.* **279**, 35849–35857 (2004).
- Boquet, P. & Lemichez, E. Bacterial virulence factors targeting Rho GTPases: parasitism or symbiosis? *Trends Cell Biol.* **13**, 238–246 (2003).
- Diabate, M. et al. *Escherichia coli* α-hemolysin counteracts the anti-virulence innate immune response triggered by the Rho GTPase activating toxin CNF1 during bacteremia. *PLoS Pathog.* **11**, e1004732 (2015).
- Xu, H. et al. Innate immune sensing of bacterial modifications of Rho GTPases by the pyrin inflammasome. *Nature* **513**, 237–241 (2014).
- Gros Lambert, M. & Py, B. F. Spotlight on the NLRP3 inflammasome pathway. *J. Inflamm. Res.* **11**, 359–374 (2018).
- Yang, Y., Wang, H., Kouadir, M., Song, H. & Shi, F. Recent advances in the mechanisms of NLRP3 inflammasome activation and its inhibitors. *Cell Death Dis.* **10**, 128 (2019).
- Gao, W., Yang, J., Liu, W., Wang, Y. & Shao, F. Site-specific phosphorylation and microtubule dynamics control pyrin inflammasome activation. *Proc. Natl Acad. Sci. USA* **113**, E4857–E4866 (2016).
- Park, Y. H., Wood, G., Kastner, D. L. & Chae, J. J. Pyrin inflammasome activation and RhoA signaling in the autoinflammatory diseases FMF and HIDS. *Nat. Immunol.* **17**, 914–921 (2016).
- Zheng, T. C. et al. A fluorescent reporter mouse for inflammasome assembly demonstrates an important role for cell-bound and free ASC specks during in vivo infection. *Cell Rep.* **16**, 571–582 (2016).
- Sester, D. P. et al. Assessment of inflammasome formation by flow cytometry. *Curr. Protoc. Immunol.* **114**, 14.40.1–14.40.29 (2016).
- Lamkanfi, M. & Dixit, V. M. In retrospect: the inflammasome turns 15. *Nature* **548**, 534–535 (2017).
- He, Y., Hara, H. & Núñez, G. Mechanism and regulation of NLRP3 inflammasome activation. *Trends Biochem. Sci.* **41**, 1012–1021 (2016).
- Shi, H., Murray, A. & Beutler, B. Reconstruction of the mouse inflammasome system in HEK293T cells. *Bio. Protoc.* **6**, e1986 (2016).
- Keestra, A. M. et al. Manipulation of small Rho GTPases is a pathogen-induced process detected by NOD1. *Nature* **496**, 233–237 (2013).
- Doye, A. et al. CNF1 exploits the ubiquitin-proteasome machinery to restrict Rho GTPase activation for bacterial host cell invasion. *Cell* **111**, 553–564 (2002).
- Boyer, L. et al. Pathogen-derived effectors trigger protective immunity via activation of the Rac2 enzyme and the IMD or Rip kinase signaling pathway. *Immunity* **35**, 536–549 (2011).
- Manser, E., Leung, T., Salihuddin, H., Zhao, Z. S. & Lim, L. A brain serine/threonine protein kinase activated by Cdc42 and Rac1. *Nature* **367**, 40–46 (1994).
- Wells, C. M. & Jones, G. E. The emerging importance of group II PAKs. *Biochem. J.* **425**, 465–473 (2010).
- Semenova, G. & Chernoff, J. Targeting PAK1. *Biochem. Soc. Trans.* **45**, 79–88 (2017).
- Song, N. et al. NLRP3 phosphorylation is an essential priming event for inflammasome activation. *Mol. Cell* **68**, 185–197 (2017).
- Sharif, H. et al. Structural mechanism for NEK7-licensed activation of NLRP3 inflammasome. *Nature* **570**, 338–343 (2019).
- Coll, R. C. et al. A small-molecule inhibitor of the NLRP3 inflammasome for the treatment of inflammatory diseases. *Nat. Med.* **21**, 248–255 (2015).
- Kelly, M. L. & Chernoff, J. Mouse models of PAK function. *Cell Logist.* **2**, 84–88 (2012).
- Shi, J. et al. Cleavage of GSDMD by inflammatory caspases determines pyroptotic cell death. *Nature* **526**, 660–665 (2015).
- He, W. T. et al. Gasdermin D is an executor of pyroptosis and required for interleukin-1β secretion. *Cell Res.* **25**, 1285–1298 (2015).
- Broz, P., Pelegrín, P. & Shao, F. The gasdermins, a protein family executing cell death and inflammation. *Nat. Rev. Immunol.* **20**, 143–157 (2020).
- Rühl, S. et al. ESCRT-dependent membrane repair negatively regulates pyroptosis downstream of GSDMD activation. *Science* **362**, 956–960 (2018).
- Evavold, C. L. et al. The pore-forming protein gasdermin D regulates interleukin-1 secretion from living macrophages. *Immunity* **48**, 35–44 (2018).
- Monteleone, M. et al. Interleukin-1β maturation triggers its relocation to the plasma membrane for gasdermin-D-dependent and -independent secretion. *Cell Rep.* **24**, 1425–1433 (2018).



38. Pandori, W. J. et al. *Toxoplasma gondii* activates a Syk-CARD9-NF- $\kappa$ B signaling axis and gasdermin D-independent release of IL-1 $\beta$  during infection of primary human monocytes. *PLoS Pathog.* **15**, e1007923 (2019).
39. Muessel, M. J., Harry, G. J., Armstrong, D. L. & Storey, N. M. SDF-1 $\alpha$  and LPA modulate microglia potassium channels through rho GTPases to regulate cell morphology. *Glia* **61**, 1620–1628 (2013).
40. Jones, J. D. & Dangl, J. L. The plant immune system. *Nature* **444**, 323–329 (2006).
41. Lopes Fischer, N., Naseer, N., Shin, S. & Brodsky, I. E. Effector-triggered immunity and pathogen sensing in metazoans. *Nat. Microbiol.* **5**, 14–26 (2020).
42. Aubert, D. F. et al. A *Burkholderia* type VI effector deamidates Rho GTPases to activate the pyrin inflammasome and trigger inflammation. *Cell Host Microbe* **19**, 664–674 (2016).
43. Medici, N. P., Rashid, M. & Bliska, J. B. Characterization of pyrin dephosphorylation and inflammasome activation in macrophages as triggered by the yersinia effectors YopE and YopT. *Infect. Immun.* **87**, e00822-18 (2019).
44. Cabral, V. P., Andrade, C. A., Passos, S. R., Martins, M. F. & Hökerberg, Y. H. Severe infection in patients with rheumatoid arthritis taking anakinra, rituximab, or abatacept: a systematic review of observational studies. *Rev. Bras. Reumatol. Engl. Ed.* **56**, 543–550 (2016).
45. Ridker, P. M. et al. Antiinflammatory therapy with canakinumab for atherosclerotic disease. *N. Engl. J. Med.* **377**, 1119–1131 (2017).
46. Mulvey, M. A., Schilling, J. D. & Hultgren, S. J. Establishment of a persistent *Escherichia coli* reservoir during the acute phase of a bladder infection. *Infect. Immun.* **69**, 4572–4579 (2001).
47. Buetow, L., Flatau, G., Chiu, K., Boquet, P. & Ghosh, P. Structure of the Rho-activating domain of *Escherichia coli* cytotoxic necrotizing factor 1. *Nat. Struct. Biol.* **8**, 584–588 (2001).
48. Doye, A., Boyer, L., Mettouchi, A. & Lemichez, E. Ubiquitin-mediated proteasomal degradation of Rho proteins by the CNF1 toxin. *Methods Enzymol.* **406**, 447–456 (2006).
49. Matsuzawa, T., Kashimoto, T., Katahira, J. & Horiguchi, Y. Identification of a receptor-binding domain of *Bordetella* dermonecrotic toxin. *Infect. Immun.* **70**, 3427–3432 (2002).
50. Kubori, T. & Galán, J. E. Temporal regulation of salmonella virulence effector function by proteasome-dependent protein degradation. *Cell* **115**, 333–342 (2003).
51. Lagrange, B. et al. Human caspase-4 detects tetra-acylated LPS and cytosolic *Francisella* and functions differently from murine caspase-11. *Nat. Commun.* **9**, 242 (2018).
52. Martinon, F., Pétrilli, V., Mayor, A., Tardivel, A. & Tschopp, J. Gout-associated uric acid crystals activate the NALP3 inflammasome. *Nature* **440**, 237–241 (2006).
53. McDaniel, A. S. et al. *Pak1* regulates multiple c-Kit mediated Ras-MAPK gain-in-function phenotypes in *Nf1*<sup>+/-</sup> mast cells. *Blood* **112**, 4646–4654 (2008).
54. Stutz, A. et al. NLRP3 inflammasome assembly is regulated by phosphorylation of the pyrin domain. *J. Exp. Med.* **214**, 1725–1736 (2017).

## Acknowledgements

We thank P. Auburger, A. Baumler, I. Brodsky, J. Chernoff, D. Golenbock, T. Henry, M. Keestra-Gounder, E. Lemichez, E. Manser, E. Meunier, V. Petrilli, D. Pisani, J.-E. Ricci, G. Robert, P.-M. Roger, L. Stuart, P. Vandenabeele, S. Ivanov and L. Yvan-Charvet for sharing materials or discussions; A.-S. Dufour, E. Garcia, M. Irondelle and J. Murdaca for technical assistance; members of the Innate Sensors Community (InnaSCO) for sharing tools; A. Cuttriss and staff at the Office of International Scientific Visibility of Université Côte d'Azur for professional language editing; staff at the Etablissement Français du Sang of Marseille for providing human blood from human healthy donors; and staff at the C3M facilities (animal, genomic, cytometry and imaging) and the Harvard Taplin mass spectrometry core. The mouse strain used for this research project, B6.129S2-Pak1tm1Cher/Mmnc (RRID, MMRRRC\_031838-UNC) was obtained from the Mutant Mouse Resource and Research Center (MMRRC) at University of North Carolina at Chapel Hill, an NIH-funded strain repository, and was donated to the MMRRRC by J. Chernoff, Fox Chase Cancer Center. This work was supported by grants from the ANR (ANR-17-CE15-0001), Investments for the Future programs LABEX SIGNALIFE ANR-11-LABX-0028-01, IDEX UCA<sup>EDU</sup> ANR-15-IDEX-01, ARC (RAC15014AAA), Université Côte d'Azur, Infectiopole sud and REDPIT. B.F.P. is supported by ERC (ERC-2013-CoG\_616986). A.M. is supported by a fellowship from FRM; C.T. by a fellowship from Ville de Nice; and O.D. by a fellowship from INSERM and Université Côte d'Azur.

## Author contributions

O.D. and A.D. designed, performed and analysed most of the experiments with input from C.T., C.L., A.J., A.G., A.M., P.C., A.R. and S.M.; J.C. and R.R. provided advice on the mice infection model. E.V., R.R.G., D.C., B.F.P., A.R., P.H.V.S. and M.L. provided tools and advice on NLRP3 inflammasome regulation. P.M. generated NLRP3 mutants and, with G.M. and O.D., performed and analysed most of the in vivo experiments. O.V. performed virulence factor and toxin subcloning, protein purifications, the in vitro kinase assay and analysed the mass spectrometry results. L.B. conceived the project, designed experiments and wrote the manuscript.

## Competing interests

The authors declare no competing interests.

## Additional information

**Extended data** is available for this paper at <https://doi.org/10.1038/s41564-020-00832-5>.

**Supplementary information** is available for this paper at <https://doi.org/10.1038/s41564-020-00832-5>.

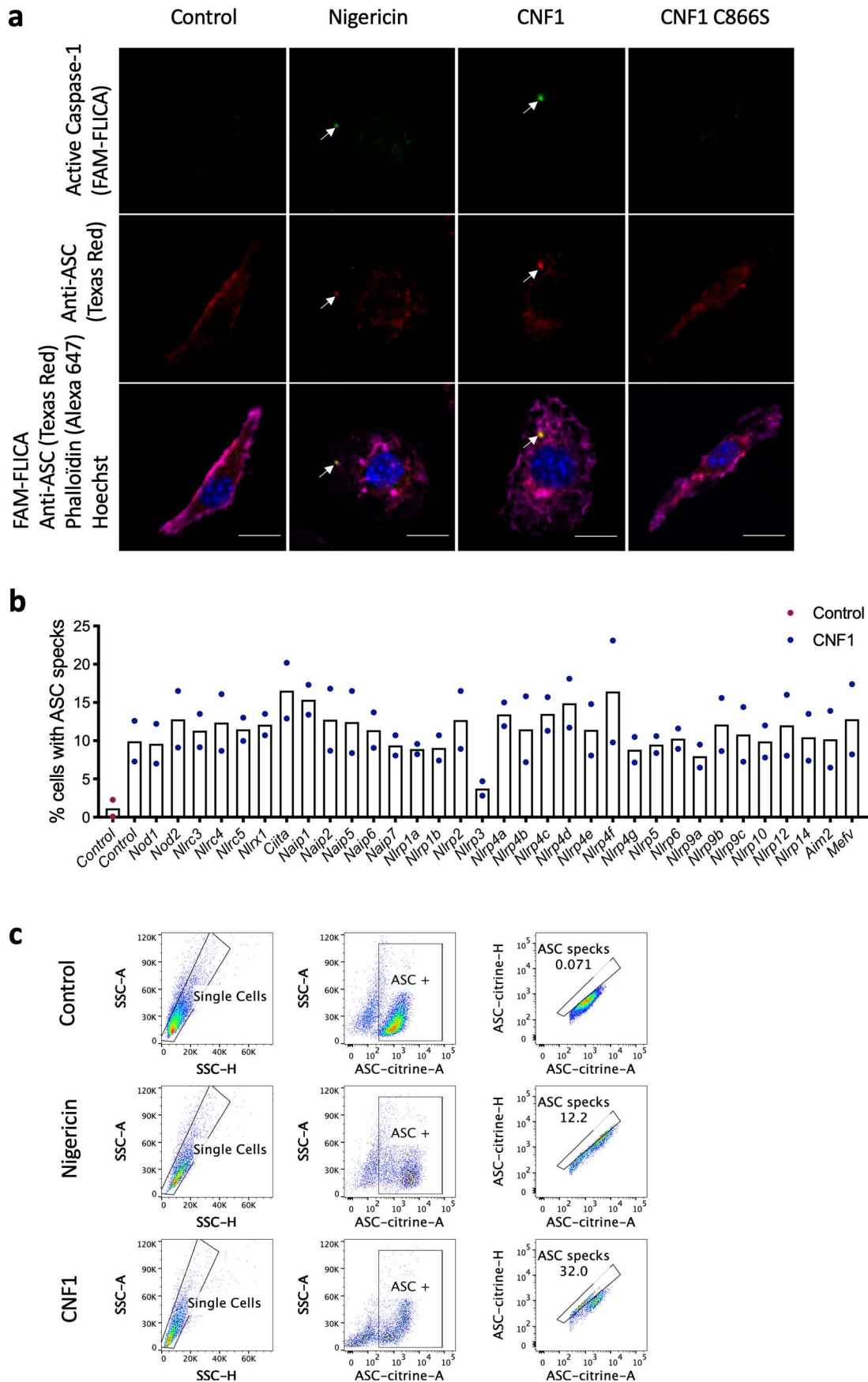
**Correspondence and requests for materials** should be addressed to L.B.

**Peer review information** *Nature Microbiology* thanks Igor Brodsky, Gad Frankel and the other, anonymous, reviewer(s) for their contribution to the peer review of this work.

**Reprints and permissions information** is available at [www.nature.com/reprints](http://www.nature.com/reprints).

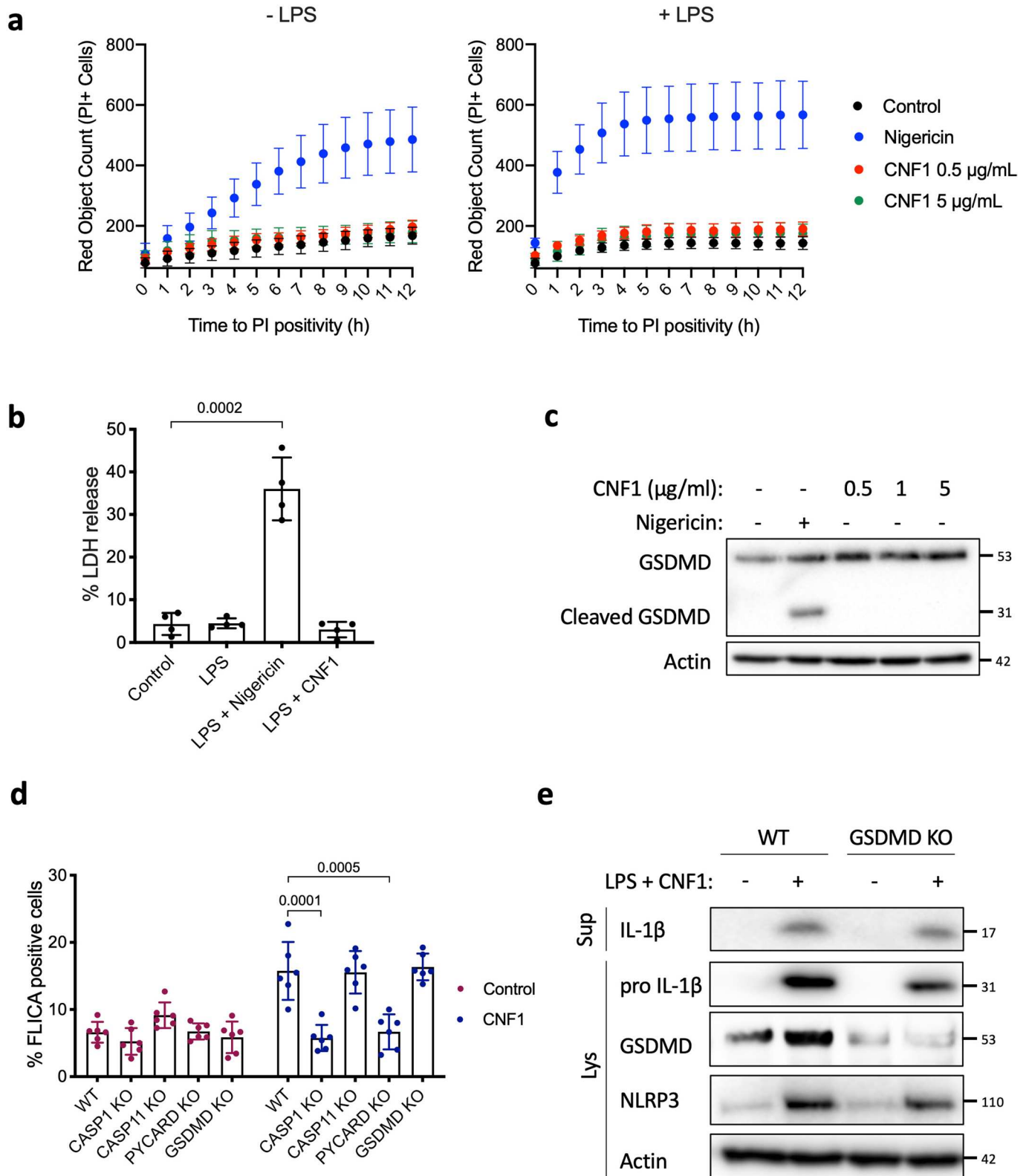
**Publisher's note** Springer Nature remains neutral with regard to jurisdictional claims in published maps and institutional affiliations.

© The Author(s), under exclusive licence to Springer Nature Limited 2021



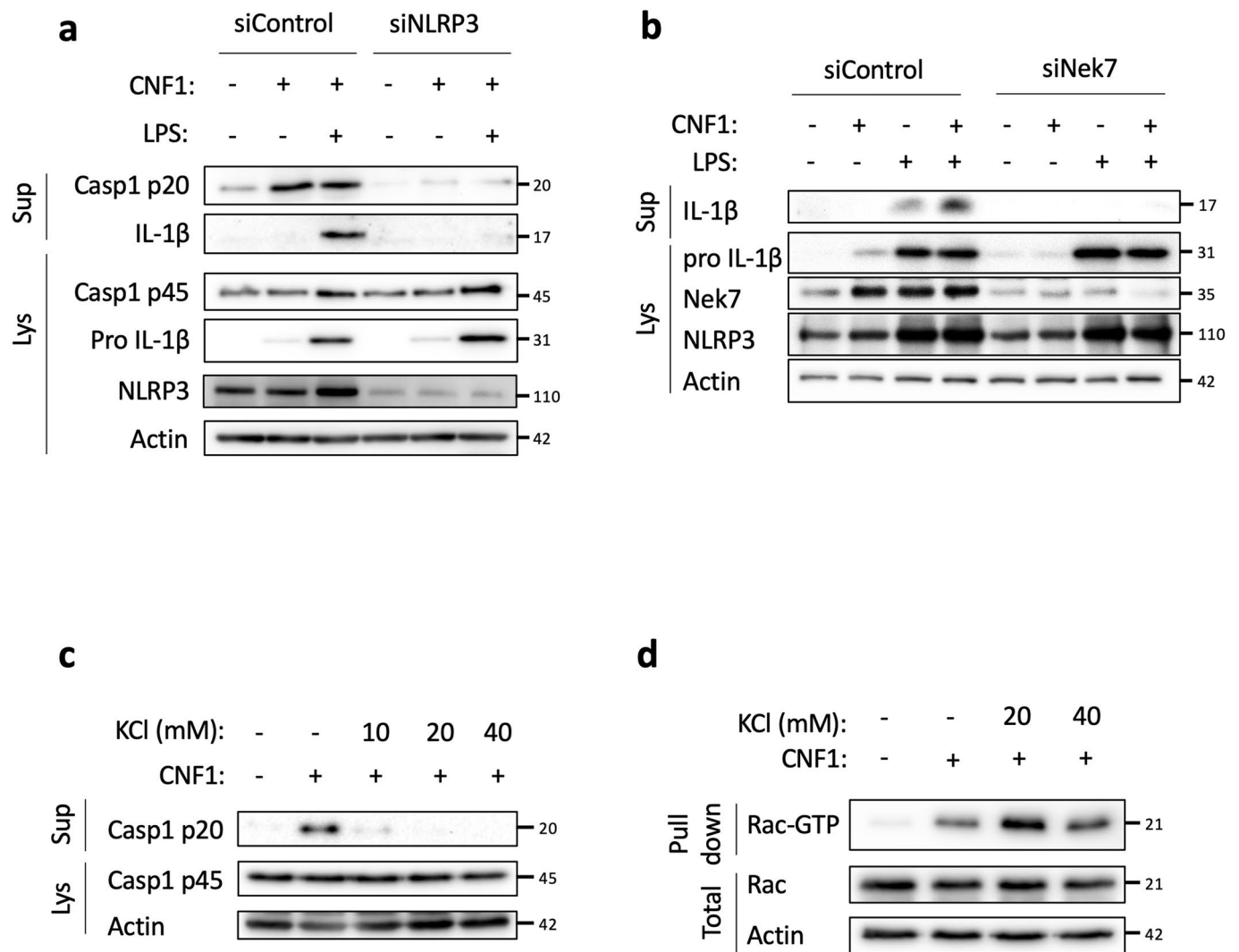
Extended Data Fig. 1 | See next page for caption.

**Extended Data Fig. 1 | CNF1 triggers Caspase-1 activation and ASC specks formation.** **a**, BMDMs isolated from BALB/c mice were either treated with vehicle (control) or CNF1 (500 ng ml<sup>-1</sup>), inactive catalytic mutant CNF1 C866S (500 ng/mL) for 6 h, or Nigericin (5 μM) for 30 min. Active Caspase-1 was revealed with FAM-FLICA (green), ASC was stained using an anti-ASC antibody (Texas Red), nuclei and actin filament were stained with Hoechst and phalloidin-Alexa 647 respectively. Cells were analyzed by confocal microscopy. Arrows indicates FAM-FLICA dots that colocalize with the ASC staining. Scale bar: 10 μm. **b**, BMDM isolated from C57BL/6 J mice constitutively expressing ASC-citrine fusion protein (R26-CAG-ASC-citrine) were transfected with the indicated siRNA for 72 h prior to 6 h of CNF1 treatment (500 ng/mL) or treated with vehicle (control). Percent of cells with ASC specks. Data are expressed as the mean ± SEM. Each dot represents 10<sup>5</sup> cells (n = 2 biologically independent samples). **c**, BMDM isolated from C57BL/6 J mice constitutively expressing ASC-citrine fusion protein (R26-CAG-ASC-citrine) were treated 6 h with CNF1 (500 ng/mL) or Nigericin (5 μM) for 30 min or vehicle (control). Cells were analyzed for ASC speck formation by flow cytometry as indicated, doublets were excluded using SSC-A and SSC-H plot, cells with a high expression of ASC-citrine were gated and then analyzed for ASC-citrine area (ASC-citrine-A) and ASC-citrine height (ASC-citrine-H). Cells with ASC specks are defined with a higher ASC-H:ASC-A ratio. Experiments were repeated at least three times, and representative data are shown.

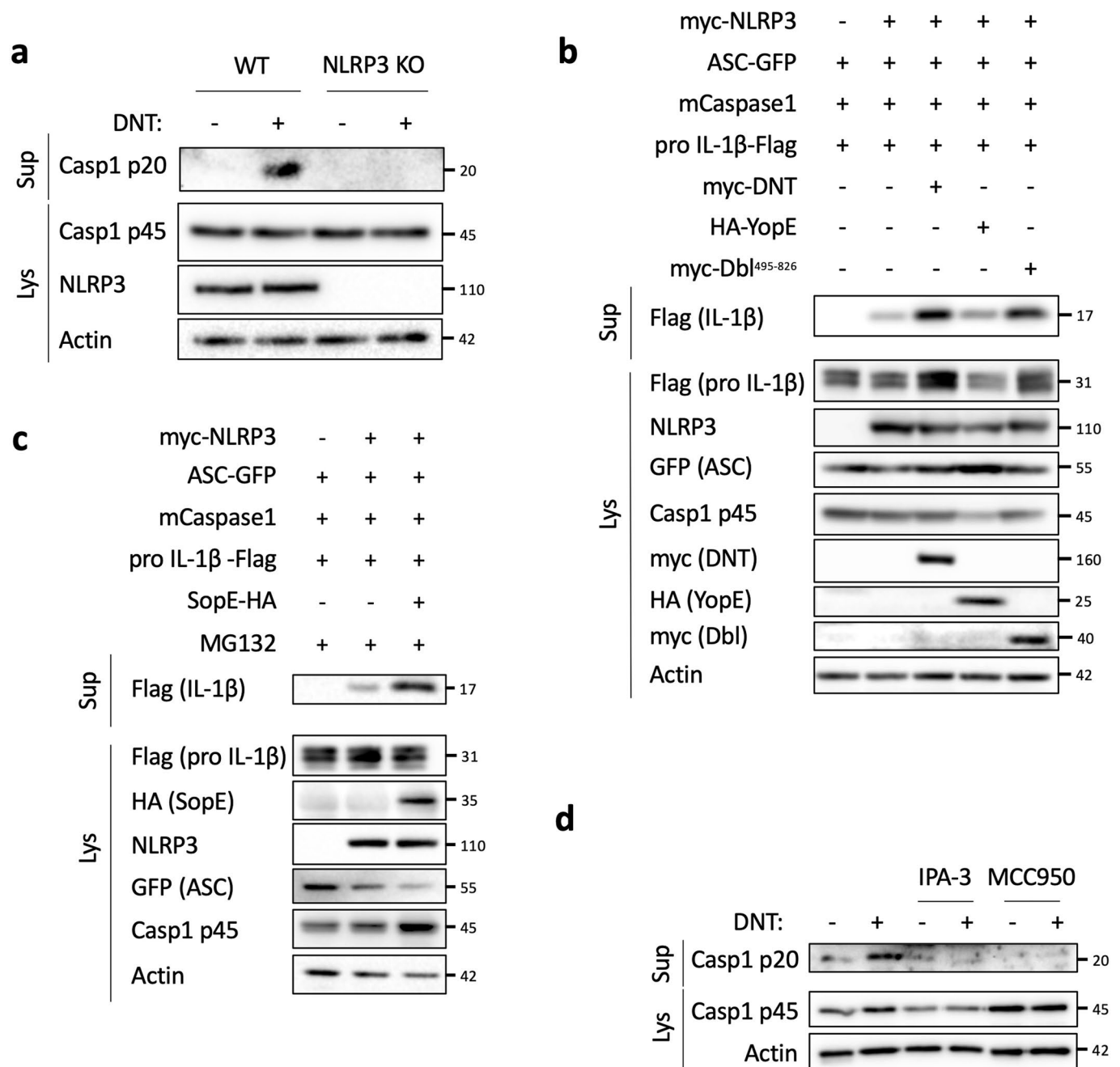


Extended Data Fig. 2 | See next page for caption.

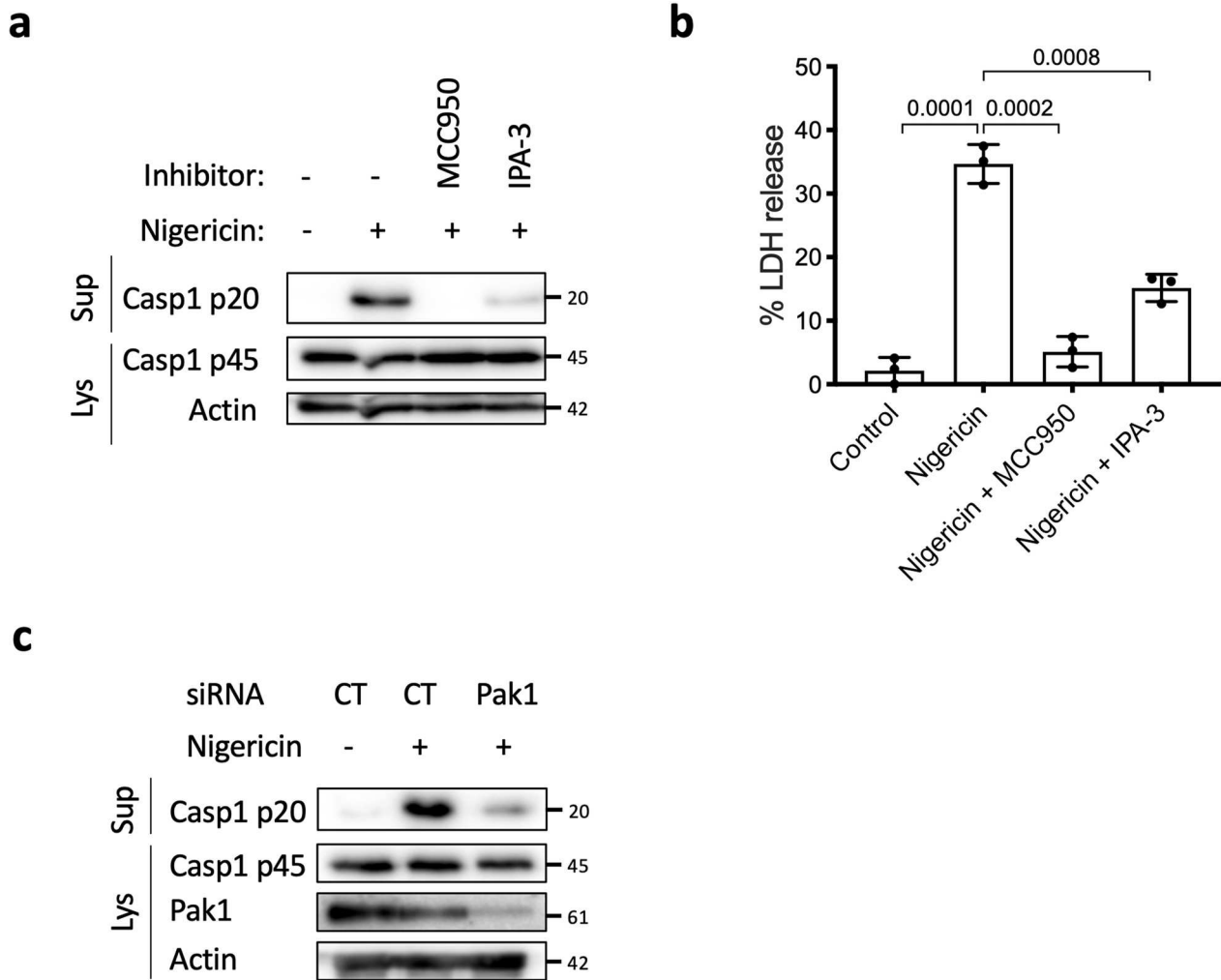
**Extended Data Fig. 2 | NLRP3 inflammasome activation by CNF1 does not induce pyroptosis.** **a**, BMDMs isolated from C57BL/6 J mice were treated with vehicle (control), Nigericin (5  $\mu$ M) or CNF1 (500 ng/mL or 5  $\mu$ g/mL) with or without LPS (100 ng/mL). Propidium iodide (PI) uptake was monitored over time (red object count) by real time imaging. Data are expressed as mean  $\pm$  SD.  $10^4$  cells were analyzed for each replicate (n = 4 independent wells). **b**, BMDMs isolated from C57BL/6 J mice were treated with vehicle (control, n = 6 independent experiments), LPS (100 ng/mL, n = 4 independent experiments), LPS and CNF1 (500 ng/mL, n = 6 independent experiments) or LPS and Nigericin (5  $\mu$ M, n = 4 independent experiments), and LDH release was assessed. Data are expressed as the mean  $\pm$  SEM. Statistical analyses were performed using a two-tailed nonparametric Mann Whitney test. **c**, BMDMs isolated from C57BL/6 J mice were treated either with Nigericin (5  $\mu$ M) for 30 min or CNF1 (0.5, 1 or 5  $\mu$ g/mL) for 8 h and GSDMD cleavage in cell lysates is shown. **d**, BMDMs isolated from C57BL/6 J wild-type or CASP1, CASP11, PYCARD (coding for ASC) or GSDMD knock-out mice were untreated or treated with CNF1 (500 ng/mL) for 6 h and were analyzed for Caspase-1 activation using the FAM-FLICA probe. Data are expressed as the mean  $\pm$  SEM. Statistical analyses were performed using a two-tailed unpaired Student's t-test. Each dot represents 100 cells (n = 700 cells). **e**, BMDMs isolated from wild-type or GSDMD knock-out mice were treated with CNF1 (500 ng/mL) and LPS (100 ng/mL) for 8 h as indicated. Supernatants and cell lysates were analyzed by immunoblot. The numbers on the side of the immunoblots indicate molecular weight (kDa). Experiments were repeated at least three times, and representative data are shown.



**Extended Data Fig. 3 | CNF1-triggered inflammasome activation depends on NLRP3, Nek7 and K<sup>+</sup> efflux. a,b**, BMDMs isolated from C57BL/6J mice were transfected with siRNA-targeting NLRP3 (**a**), siRNA-targeting Nek7 (**b**), or control non-targeting siRNA for 72 h before treatment with CNF1 (500 ng/mL) and/or LPS (100 ng/mL) for 8 h. Supernatants and cell lysates were analyzed by immunoblot. **c,d**, BMDMs isolated from C57BL/6J mice (**c**) or iBMDMs (**d**) were treated with the indicated KCl concentration and CNF1 (500 ng/mL) for 8 h. **c**, Supernatants and cell lysates were analyzed by immunoblot, or (**d**) cell lysates were analyzed using a GST-Pak-RBD pull-down assay. The Rac associated with the GST-Pak-RBD beads is indicated as Rac-GTP. The numbers on the side of the immunoblots indicate molecular weight (kDa). Experiments were repeated at least three times, and representative data are shown.

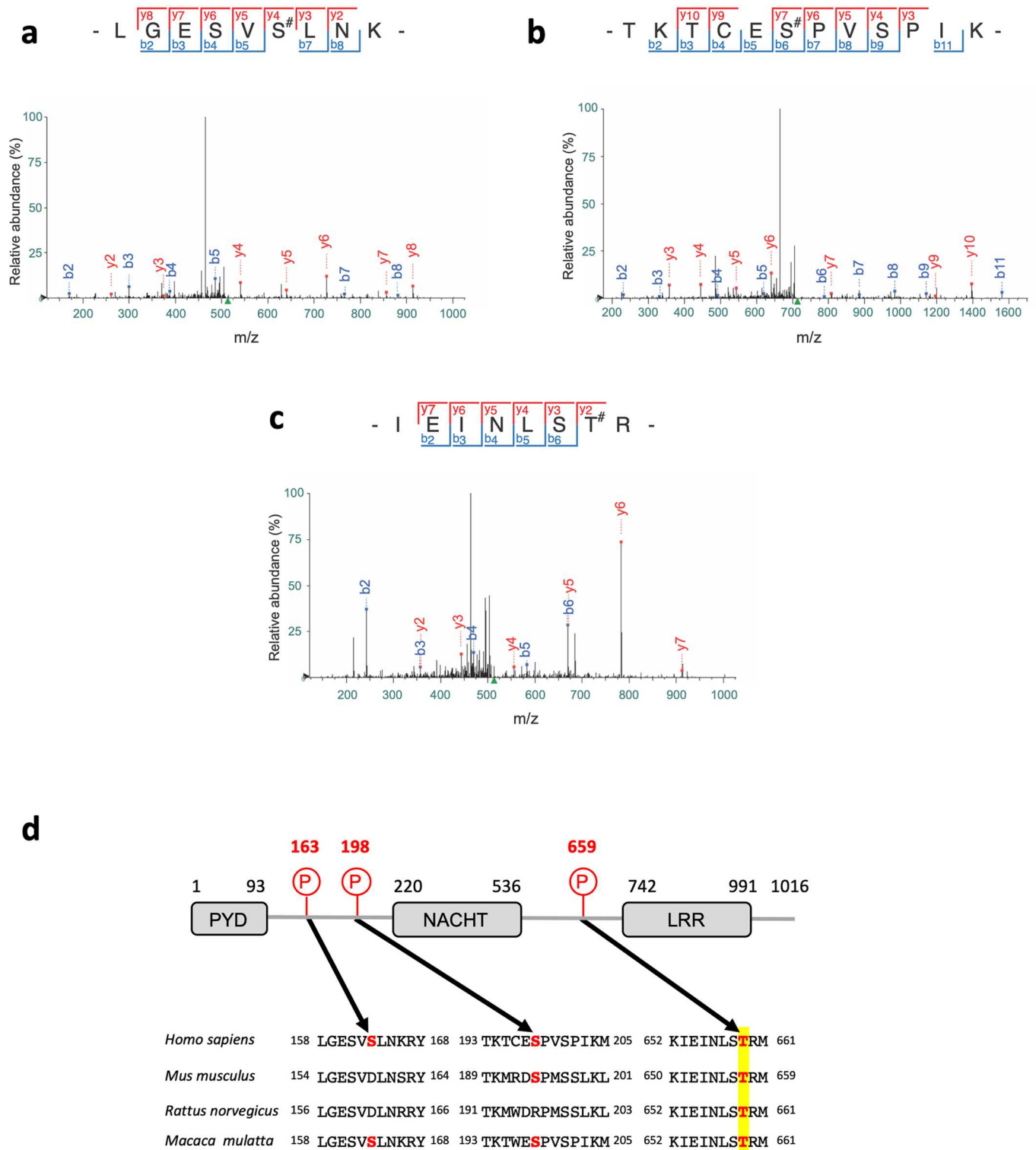


**Extended Data Fig. 4 | Toxins mediated Rho GTPases activation but not inhibition trigger the NLRP3 inflammasome. a**, BMDMs isolated from wild-type or NLRP3 knock out C57BL/6J mice were treated with DNT (1  $\mu$ g/mL) for 8 h. Supernatants and cell lysates were analyzed by immunoblot. **b-c**, HEK293T cells were transfected as indicated with plasmids encoding NLRP3 inflammasome components (myc-NLRP3, ASC-GFP, mCaspase-1) and pro-IL-1 $\beta$ -Flag together with **(b)** myc-DNT, HA-YopE or myc-DbI<sup>495-826</sup> or **(c)** transfected with SopE-HA and treated with MG132 to block SopE degradation (10  $\mu$ M). Supernatants and cell lysates were analyzed by immunoblot. **d**, BMDMs isolated from C57BL/6J mice were treated with IPA-3 (5  $\mu$ M) or MCC950 (1  $\mu$ M) for 45 min prior to 8 h of DNT treatment (1  $\mu$ g/mL). Supernatants and cell lysates were analyzed by immunoblot. The numbers on the side of the immunoblots indicate molecular weight (kDa). Experiments were repeated at least three times, and representative data are shown.



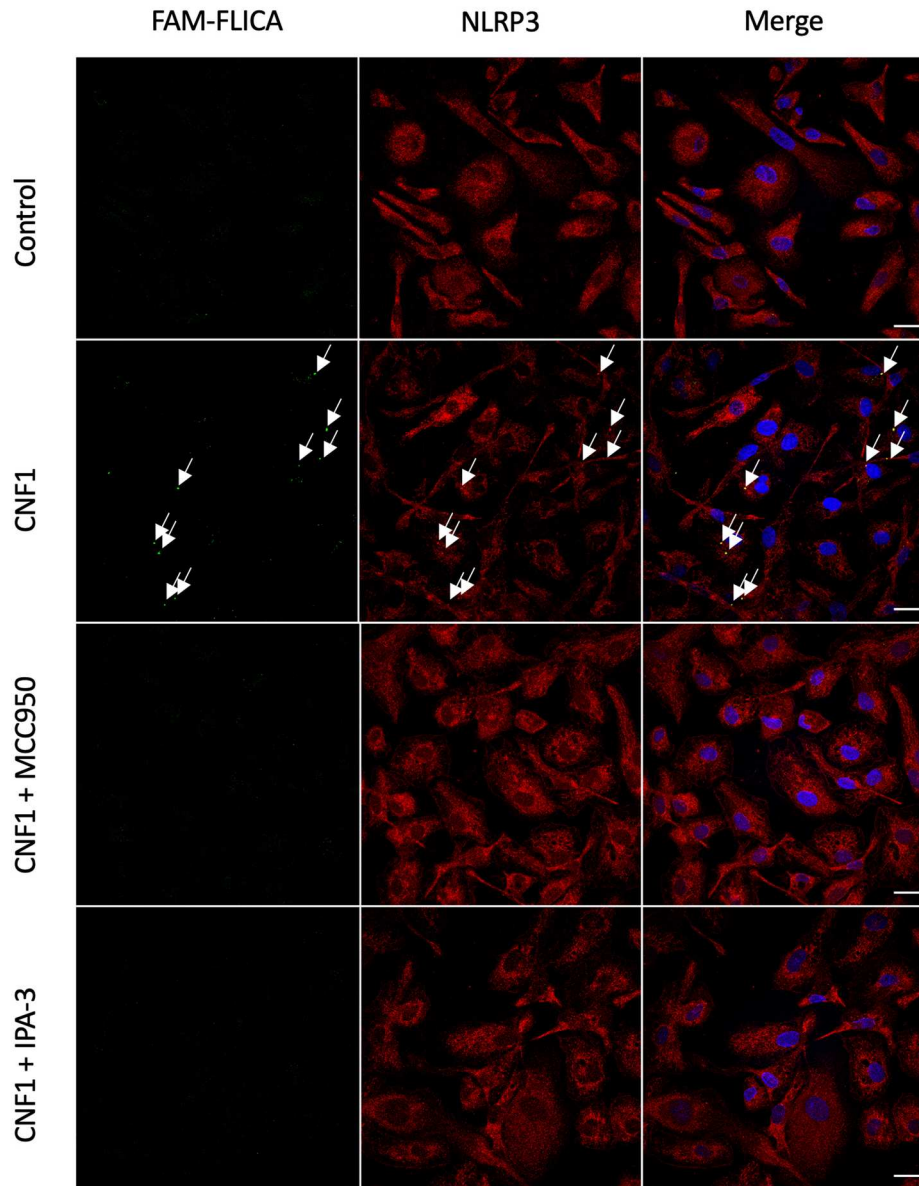
**Extended Data Fig. 5 | Inhibition of Pak1 diminishes NLRP3 activation by Nigericin.** **a,b**, BMDMs isolated from C57BL/6 J mice were treated with MCC950 (1  $\mu$ M) or IPA-3 (5  $\mu$ M) for 45 min prior to Nigericin (5  $\mu$ M) treatment for 30 min. Supernatants and cell lysates were analyzed by **(a)** immunoblot and **(b)** supernatants were analyzed for LDH release ( $n=3$  biologically independent experiments). Statistical analyses were performed using a two-tailed nonparametric Mann Whitney test.  $n=3$  biologically independent samples were analyzed. **c**, BMDMs isolated from C57BL/6 J mice were treated for 72 h with non-targeting (CT) or Pak1-targeting siRNA before treatment with Nigericin (5  $\mu$ M) for 30 min. Supernatants and cell lysates were analyzed by immunoblot. The numbers on the side of the immunoblots indicate molecular weight (kDa). Experiments were repeated at least three times, and representative data are shown. Data are expressed as the mean  $\pm$  SEM.



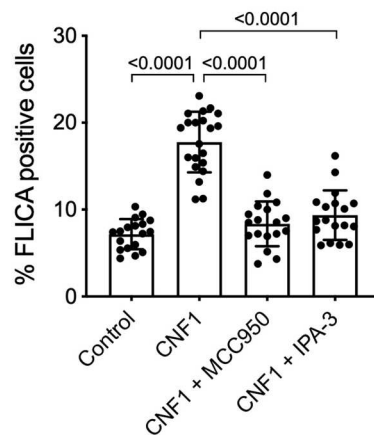


**Extended Data Fig. 6 | Mass spectrometry analysis of Pak1 triggered NLRP3 phosphorylation. a-c.** Fragmentation spectra of human NLRP3 peptides showing phosphorylation of Ser-163, Ser-198 and Thr-659. **d.** Representation of NLRP3 domain structure and sequence alignment of NLRP3 ortholog peptides surrounding phosphorylated residues identified by mass spectrometry. The phosphorylated residues are in bold red.

**a**

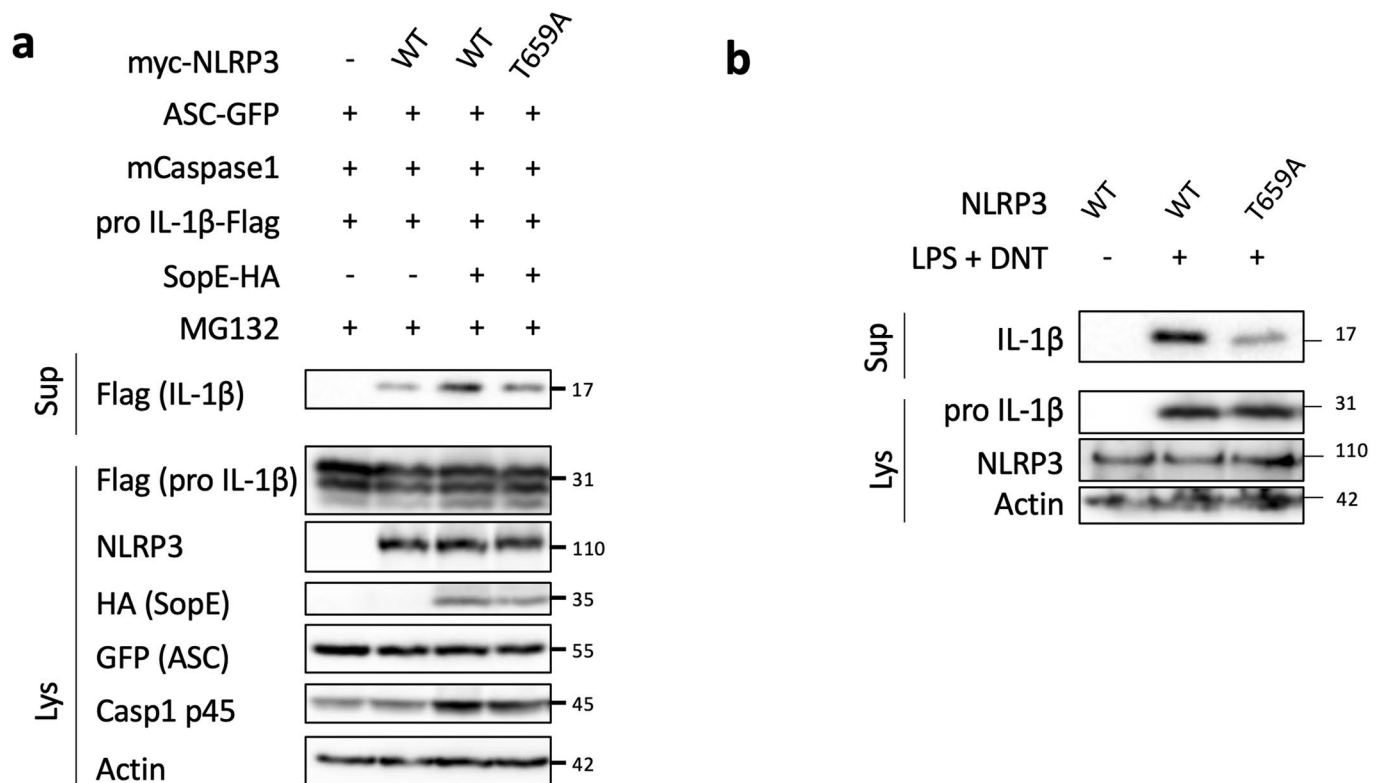


**b**



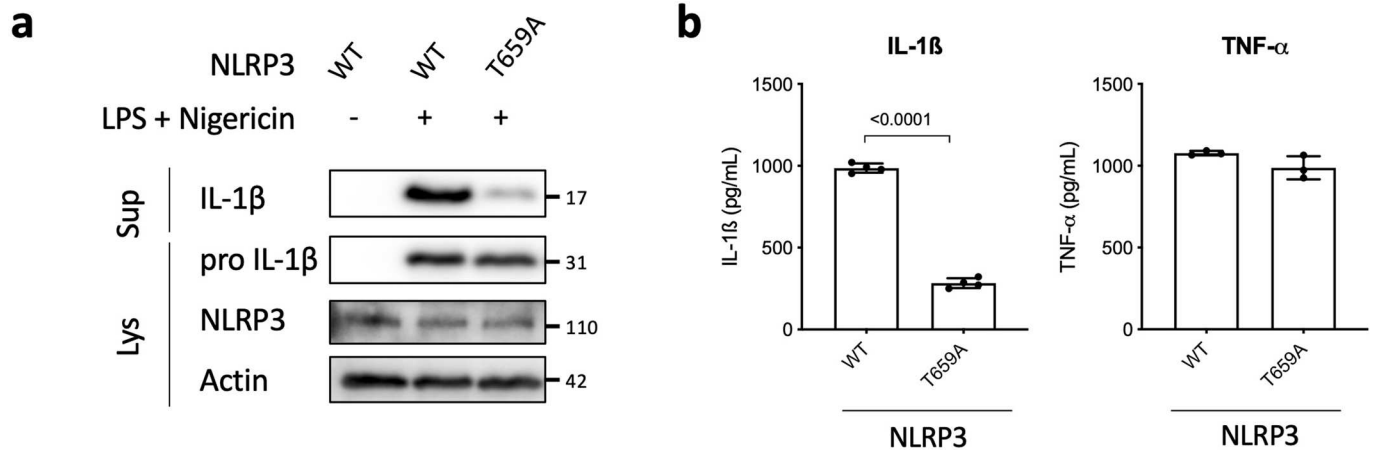
Extended Data Fig. 7 | See next page for caption.

**Extended Data Fig. 7 | Conservation of the Pak-NLRP3 axis in Human monocyte-derived macrophages. a-b,** Human monocyte-derived macrophages (hMDMs) were pretreated with vehicle, MCC950 (1  $\mu$ M) or IPA-3 (5  $\mu$ M) for 45 min before CNF1 (500 ng/mL) treatment for 6 h. Active Caspase-1 was stained with FAM-FLICA (green), NLRP3 (red) and nuclei (blue) were stained for immunofluorescence and confocal microscopy imaging. Arrows indicates FAM-FLICA dots that colocalize with NLRP3. Scale bar: 20  $\mu$ m. **b,** quantification of FAM-FLICA positive cells. Data are expressed as the mean  $\pm$  SEM. Statistical analyses were performed using a two-tailed unpaired Student's t-test. Each dot represents 100 cells (n = 1800 cells). Experiments were repeated at least three times, and representative data are shown.

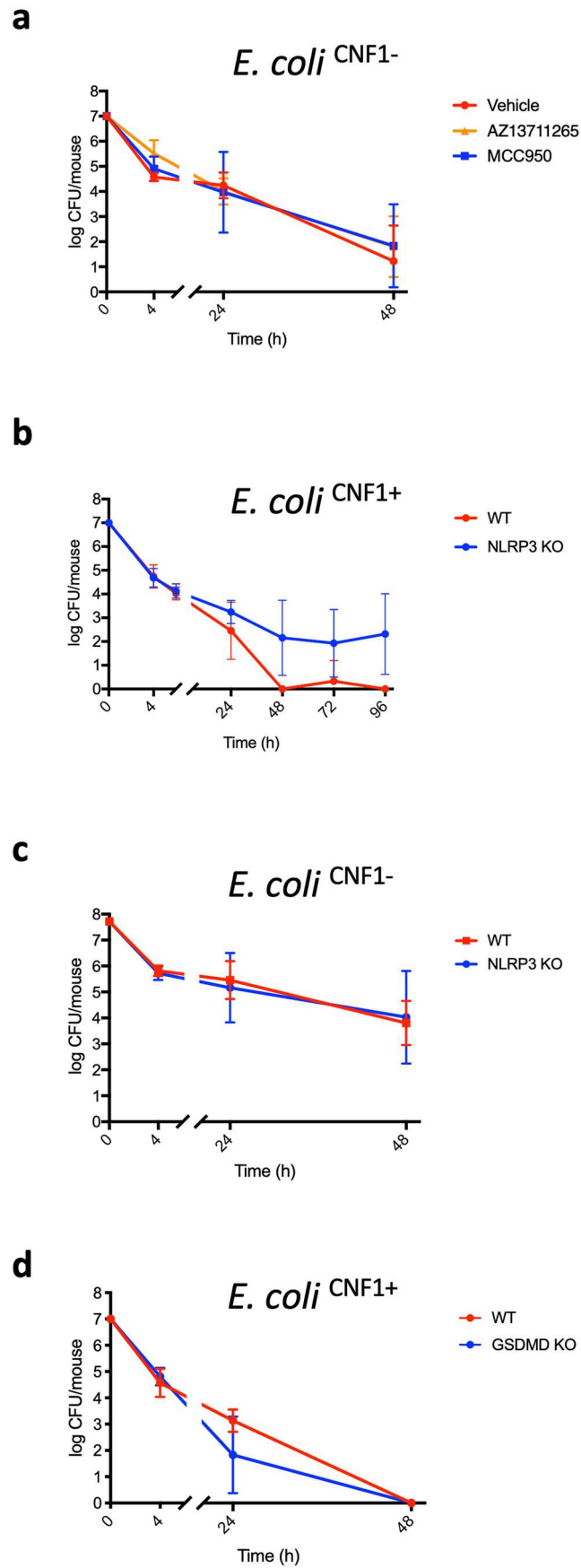


**Extended Data Fig. 8 | The NLRP3 T659A mutant inhibit the IL-1 $\beta$  maturation triggered by SopE and DNT.** **a**, HEK293T cells were transfected with plasmids encoding NLRP3 inflammasome components (ASC-GFP, mCaspase-1) and pro-IL-1 $\beta$ -Flag and either myc-NLRP3 (WT) or myc-NLRP3 T659A together with SopE-HA and treated with MG132 (10  $\mu$ M) to block SopE degradation. Supernatants and cell lysates were analyzed by immunoblot.

**b**, NLRP3 knock-out iBMDMs reconstituted either with NLRP3 or NLRP3 T659A were treated with vehicle or LPS (100 ng/mL) and DNT (1  $\mu$ g/mL) for 8 h. The numbers on the side of the immunoblots indicate molecular weight (kDa). Experiments were repeated at least three times, and representative data are shown.



**Extended Data Fig. 9 | Macrophages expressing the NLRP3 T659A mutant have an impaired Nigericin- triggered IL-1 $\beta$  maturation. a-b,** iBMDMs stably expressing either NLRP3 or NLRP3 T659A were treated with Nigericin (5  $\mu$ M) for 30 min. Supernatants and cell lysates were analyzed by immunoblot and by ELISA for IL-1 $\beta$  ( $n = 4$  biologically independent samples) and TNF- $\alpha$  ( $n = 3$  biologically independent samples). Data are expressed as the mean  $\pm$  SEM. Statistical analyses were performed using a two-tailed unpaired Student's t-test. The numbers on the side of the immunoblots indicate molecular weight (kDa). Experiments were repeated at least three times, and representative data are shown.



Extended Data Fig. 10 | See next page for caption.

**Extended Data Fig. 10 | *E. coli*<sup>CNF1-</sup> clearing is not affected by Pak1 or NLRP3 inhibition and *E. coli*<sup>CNF1+</sup> clearing does not rely on GSDMD. a-d**, Wild-type or knock-out mice were infected intravenously with isogenic CNF1-deleted *E. coli* (*E. coli*<sup>CNF1-</sup>) or CNF1 expressing *E. coli* (*E. coli*<sup>CNF1+</sup>). **a**, Wild-type mice were injected intraperitoneally with 10 mg/kg AZ13711265 or 50 mg/kg MCC950 or vehicle once a day and were infected intravenously with isogenic CNF1-deleted *E. coli* (*E. coli*<sup>CNF1-</sup>) prior to the collection of peripheral blood at 4 h, 24 h and 48 h for measurement of bacteraemia (n = 5 mice per group). **b**, Wild-type or NLRP3 knock-out C57BL/6 J mice were infected intravenously with CNF1 expressing *E. coli* (*E. coli*<sup>CNF1+</sup>) prior to the collection of peripheral blood at 4 h, 24 h, 48 h, 72 h and 96 h for measurement of bacteraemia (n = 6 per group). **c**, Wild-type (n = 6 mice) or NLRP3 knock-out C57BL/6 J mice (n = 4 mice) were infected intravenously with isogenic CNF1-deleted *E. coli* (*E. coli*<sup>CNF1-</sup>) prior to the collection of peripheral blood at 4 h, 24 h and 48 h for measurement of bacteraemia (n = 6 per group). **d**, Wild-type (n = 6 mice) or GSDMD knock-out C57BL/6 J mice (n = 6 mice) were infected intravenously with *E. coli*<sup>CNF1+</sup> prior to the collection of peripheral blood at 4 h, 24 h and 48 h for measurement of bacteraemia. Experiments were repeated two times and representative data are shown. Data are expressed as the geometric mean  $\pm$  95 CI.







# Participation aux Congrès et présentations

1<sup>st</sup> International Caparica Congress on Leishmaniasis – Capuchos, Caparica, Portugal en 2018 –  
Présentation d'un Poster : “Innovative screening method for drugs against visceral  
Leishmaniasis”

1<sup>st</sup> International Caparica Congress on Leishmaniasis – Capuchos, Caparica, Portugal en 2018 –  
Présentation Orale “Shotgun” de 5 minutes : “Innovative screening method for drugs against  
visceral Leishmaniasis” – Prix de la meilleure communication Shotgun *ex-aequo*

31<sup>st</sup> European Congress of Clinical Microbiology & Infectious Diseases – 2021 Online –  
Présentation d'un e-poster avec présentation orale : “Development of enhanced sensitivity  
tools to monitor *Leishmania* infection”

Journées de l'Ecole Doctorale de Nice 2021 (JEDNs 2021) – Présentation Orale de 10 minutes  
– Prix de la meilleure communication orale en Microbiologie



# Innovative screening method for drugs against visceral Leishmaniasis

<sup>1st</sup> International Caparica Congress on Leishmaniasis – Capuchos, Caparica, Portugal en 2018

Alissa Majoor<sup>1\*</sup>, Christelle Pomares<sup>2</sup>, Maeva Gesson<sup>1</sup>, Laurent Boyer<sup>1</sup>, Pierre Marty<sup>2</sup>, Grégory Michel<sup>1</sup>

<sup>1</sup> Université Côte d'Azur, C3M Inserm, U1065, 06204, Nice Cedex3, France. <sup>2</sup> Service de Parasitologie- Mycologie, Centre Hospitalier Universitaire de Nice, 06202, Nice Cedex 3, France \*Presenting author

## **Abstract**

Leishmaniasis is a tropical neglected disease caused by an intracellular protozoan carried by female phlebotomine sandflies. Each year this disease causes 20 000 to 30 000 deaths worldwide. It is characterized by several forms : cutaneous, muco-cutaneous and visceral leishmaniasis. The latter can be due to *Leishmania infantum*, and is fatal without treatment. Currently only few treatments are available, but they are expensive, toxic, as well as presenting high risks of relapse. This leads to the urgency to develop new treatments against *L.infantum*. In collaboration with the Institut de Chimie de Nice, the laboratory decided to screen plants coming from perfumery waste for innovative active compounds. This has already led to the identification of CA-TM-0015, a fraction with leishmanicidal activity.

During my internship, I screened sub-fractions of CA-TM-0015 as well as purified molecules for their cytotoxicity on primary murine macrophages. I determined their activity on the promastigote form of *L. infantum* using a bioluminescent parasite model expressing firefly luciferase. Next I determined their activity on the amastigote form using the same bioluminescence technique, as well as another technique of microscopy visualisation using GFP parasites. I have identified a molecule, identified as « molecule 8 » due to confidentiality reasons, which has no cytotoxicity on our murine macrophages. It has no effect on promastigotes, but has an effect on amastigotes following luciferase and GFP essays. These kind of compounds could be promoting the elimination of *Leishmania* amastigotes by stimulating host immunity, and thus present an interest for many intracellular pathogens.

# Innovative screening method for drugs against visceral Leishmaniasis

Alissa Majoor<sup>1</sup>, Aurélie Schwing<sup>1,2,3</sup>, Maéva Gesson<sup>1,4</sup>, Christelle Pomares<sup>1,2</sup>, Pierre Marty<sup>1,2</sup>, Thomas Michel<sup>5</sup>, Laurent Boyer<sup>1</sup>, Grégory Michel<sup>1</sup>

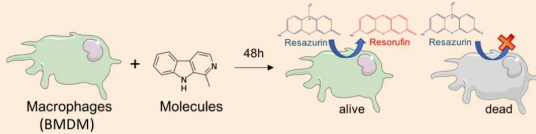
1. UCA, INSERM, U1065, C3M, Microbial virulence and inflammatory signaling in disease, Nice, France ; 2. Centre Hospitalier Universitaire de Nice, Laboratoire de Parasitologie-Mycologie, Nice, France ; 3. Université de la Méditerranée, Marseille, France ; 4. INSERM, U1065, C3M, Imaging facility ; 5. CNRS, UMR7272, ICN, Nice, France.

## Introduction

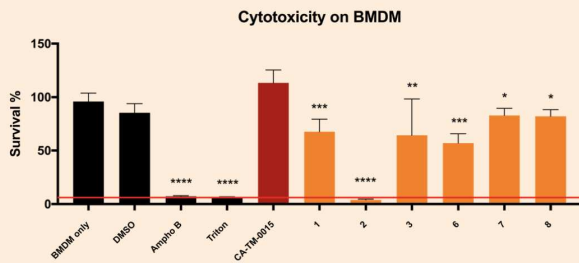
Visceral leishmaniasis is a disease caused by *Leishmania* parasites, transmitted by female sandflies to hosts such as dogs and humans. It is fatal without treatment. Current treatment involving Amphotericin B presents several issues, including its cost, the need for hospitalization due to side effects, and the emerging resistance to this molecule. In this work, we use *L.infantum* parasites expressing Luciferase or GFP to screen plant extracts (like CA-TM-0015) for new molecules that could promote activation of the innate immune system in order to avoid resistance.

## Results

### 1. Cytotoxicity assay

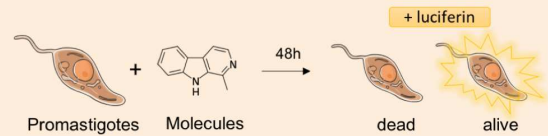


Cytotoxicity of the molecules used at 100 µg/ml was assessed on primary murine macrophages (BMDM) using Alamar Blue test, then measuring fluorescence after 48h of incubation.

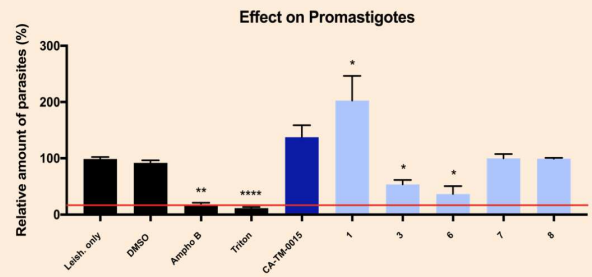


This test showed the cytotoxicity of amphotericin B on macrophages, and that 5 out of 6 tested molecules are less cytotoxic than amphotericin B.

### 2. Activity on Promastigotes by luciferase assay

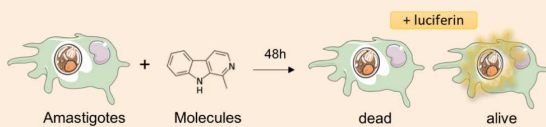


The effect of the molecules used at 100 µg/ml was assessed on promastigotes expressing luciferase after 48h of incubation by using the luciferin substrate, then measuring emitted bioluminescence from live parasites.

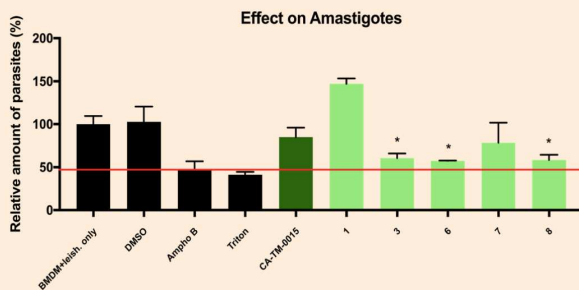


This test showed that 2 molecules out of 5 have a leishmanicidal activity on *L.infantum* promastigotes.

### 3. Activity on Amastigotes by luciferase assay

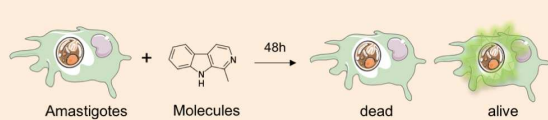


The effect of the molecules used at 100 µg/ml was assessed on amastigotes expressing luciferase after 48h of incubation by using the luciferin substrate, then measuring emitted bioluminescence from live parasites.

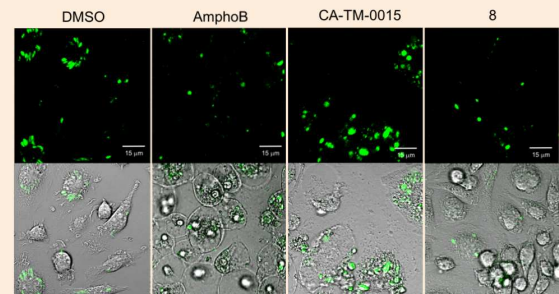


This test showed that 3 molecules out of 5 have a leishmanicidal activity on *L.infantum* amastigotes. Molecule 8 shows activity only on the amastigote form, which could suggest it activates the innate immune system, promotes activation of macrophages and thus leads to parasite clearance.

### 4. Activity on Amastigotes assessed by microscopy



The effect of the molecules used at 100 µg/ml was assessed on amastigotes expressing GFP after 48h of incubation through confocal microscopy imaging.



Microscopy imaging confirms a reduction in number of parasites when cells are infected with *L.infantum* parasites, then treated with molecule 8, which supports the choice of this molecule as a potential new anti-leishmania treatment

## Conclusion

Through an innovative screening method identifying potential immune-stimulating compounds, we highlighted a new candidate molecule as anti-leishmania treatment with reduced cytotoxicity in comparison with Amphotericin B. Further studies now focus on understanding the underlying pathways. In the future, immunostimulating molecules could be used to treat a broad range of intracellular pathogens.

# Leishmaniasis 2018

## Excellent Shotgun Communication Award

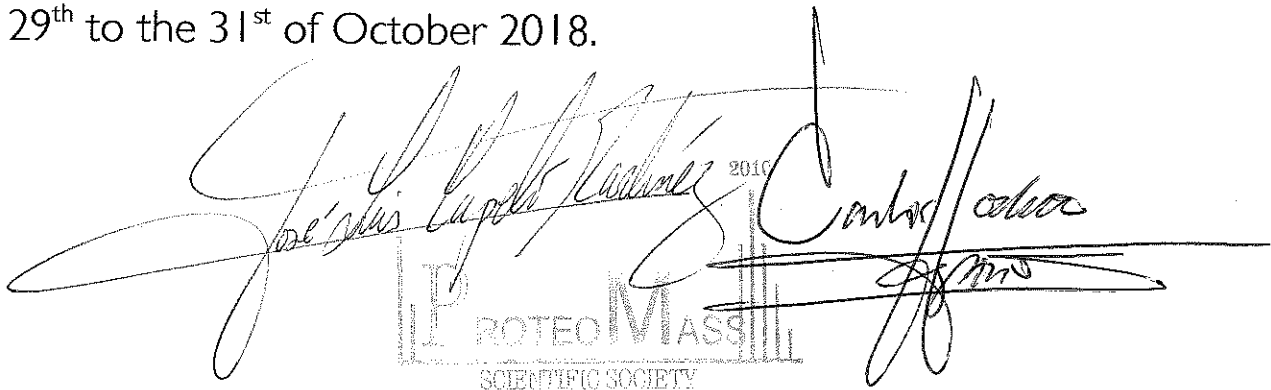
Sponsored by PROTEOMASS Scientific Society

Having been chosen by the Shotgun Award Selection Committee, for  
the shotgun presentation entitled:

“Innovative screening method for drugs against visceral Leishmaniasis”

**ALISSA MAJOOR**

Has been awarded (Ex aequo) The Excellent Shotgun (5 minutes)  
Communication Award Presented in the *1<sup>st</sup> International Caparica  
Congress on Leishmaniasis* held in Capuchos, Caparica – Portugal, the  
29<sup>th</sup> to the 31<sup>st</sup> of October 2018.



The image shows two handwritten signatures in black ink. The signature on the left is 'José Luis Capelo' and the one on the right is 'Carlos Lodeiro'. Below the signatures is a logo for 'PROTEOMASS SCIENTIFIC SOCIETY' which includes a stylized 'P' and 'M' and the year '2010'.

-----  
José Luis Capelo, PhD, FRSC & Carlos Lodeiro, PhD, FRSC

For the Selection Committee, October 2018

# Development of enhanced sensitivity tools to monitor *Leishmania infantum* infection

31<sup>st</sup> European Congress of Clinical Microbiology & Infectious Diseases – 2021 Online

Alissa Majoor<sup>1\*</sup>, Christelle Pomares<sup>2</sup>, Laurent Boyer<sup>1</sup>, Pierre Marty<sup>2</sup>, Grégory Michel<sup>1</sup>

<sup>1</sup>Université Côte d'Azur, C3M Inserm, U1065, Nice Cedex3, France. <sup>2</sup>Service de Parasitologie-Mycologie, Centre Hospitalier Universitaire de Nice, 06202, Nice Cedex 3 France. \*Presenting author

## **Abstract**

Leishmaniasis is a neglected tropical disease caused by an intracellular protozoan transmitted by female phlebotomine sandflies. Each year this disease causes 20 000 to 30 000 deaths worldwide. *Leishmania infantum* is responsible for a visceral form of leishmaniasis which is fatal without treatment, and today only few treatments are available presenting issues of toxicity, high risks of relapse and emerging resistance. Therefore, development of new treatments is necessary, and requires models allowing to monitor *leishmania* survival. Due to important autofluorescence in mice, it is commonly accepted that bioluminescent detection is most sensitive *in vivo* whereas fluorescence visualization is a key tool to monitor *Leishmania* infection *in vitro*. Tools to monitor *L.infantum* infection are often found to be either bioluminescent or fluorescent, requiring multiple cultures and different constructs for *in vivo* and *in vitro* imaging, which can cause a bias in subsequent results and applications. Therefore, we aimed to develop a stable construction which allows parasites to emit both enhanced bioluminescence and fluorescence, through the integration in the 18S RNA region of a modified firefly luciferase and of the monomeric red fluorescent protein mCherry. Microscopy analysis showed that mCherry-expressing parasites can be observed both in their extracellular promastigote and intracellular amastigote form. These results have been corroborated by Flow Cytometry, showing that mCherry is a reliable fluorescent marker of live parasites. Moreover, both forms expressed important levels of bioluminescence. Currently, weekly follow-up of bioluminescence emission on live infected mice is ongoing to assess localization of infection in the liver and spleen. Developing new tools to monitor Neglected Tropical diseases is a key point in the research for alternative treatments against leishmaniasis. Insertion of both bioluminescent and fluorescent constructs allows for easier culture follow-up as well as reliable comparison between *in vivo* and *in vitro* experimentation. These double transformed constructs will be used as a model to rapidly screen for novel molecules. Moreover, the developed constructions allow for insertion in parasites of the genus *Leishmania* without restriction of sub-genus. Experimentation on transformed *L.major* will furthermore increase reliability of subsequent screening by allowing the identification of molecules active against visceral or cutaneous leishmaniasis.

# Development of enhanced sensitivity tools to monitor *Leishmania* infections

Alissa Majoor<sup>1\*</sup>, Pierre Marty<sup>1,2</sup>, Alexandre Perrone<sup>1</sup>, Laurent Boyer<sup>1</sup>, Christelle Pomares<sup>1,2</sup>, Grégory Michel<sup>1</sup>

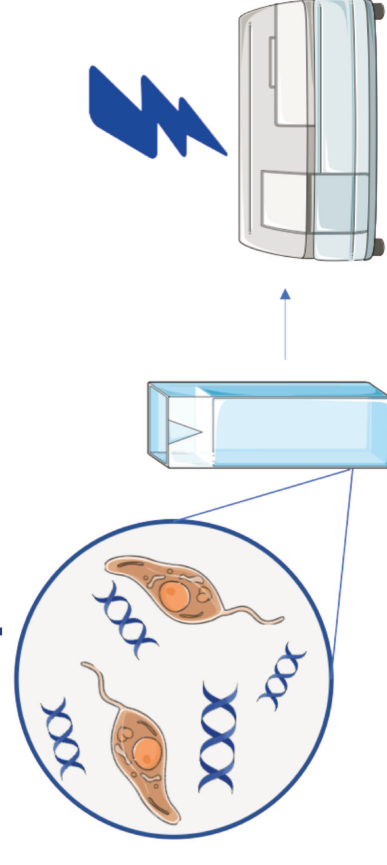
<sup>1</sup>Université Côte d'Azur, C3M Inserm, U1065, Nice Cedex 3, France ; <sup>2</sup>Service de Parasitologie-Mycologie, Centre Hospitalier Universitaire de Nice, 06202, Nice Cedex 3 France ; \*Alissa.MAJOOR@univ-cotedazur.fr

## Introduction

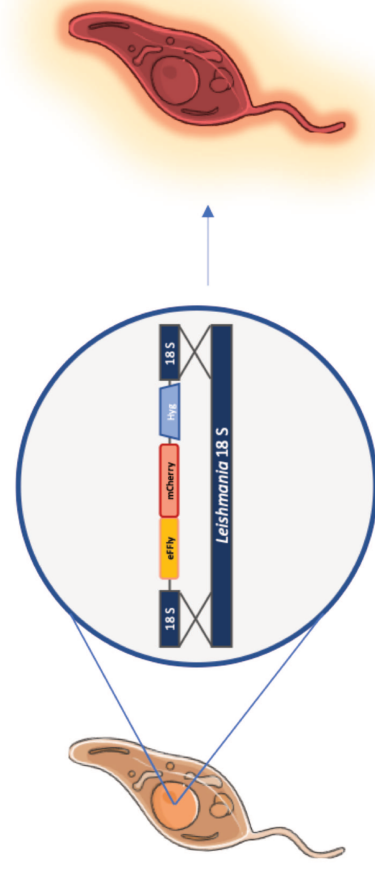
Leishmaniasis is a neglected tropical disease causing 20 000 to 30 000 deaths per year. Different forms of the disease exist, showing gradual severity : a cutaneous form conferred by *L. major*, a mucocutaneous form, and a visceral form conferred by *L. infantum*, which is fatal when left untreated. Today only few treatments are available, and they are toxic, lead to relapses and face emerging resistance. **Therefore, development of new treatments is necessary, and requires models allowing to monitor *Leishmania* survival.** We propose the creation of eFFly-mCherry strains expressing enhanced bioluminescence coupled to red fluorescence to facilitate screening of new compounds against *Leishmania*, and to avoid necessity and bias of multiple cultures for *in vivo* and *in vitro* detection.

## Methods

### 1. Electroporation



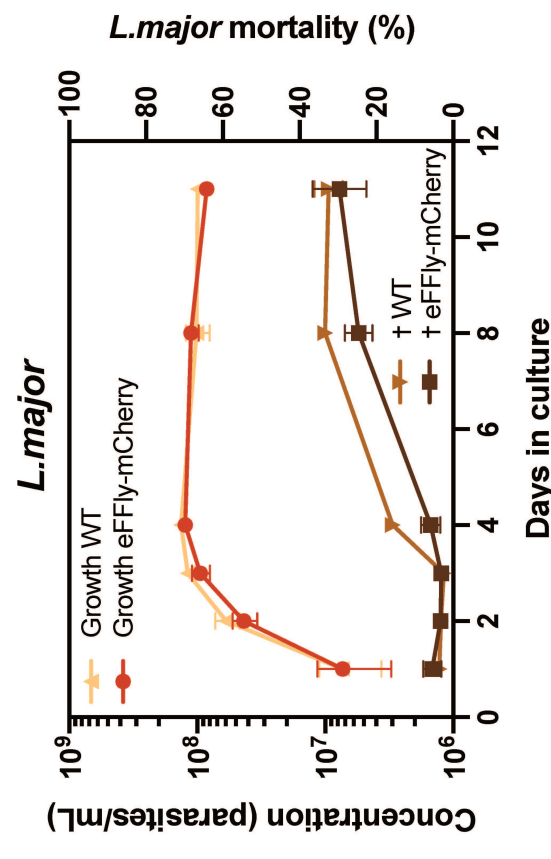
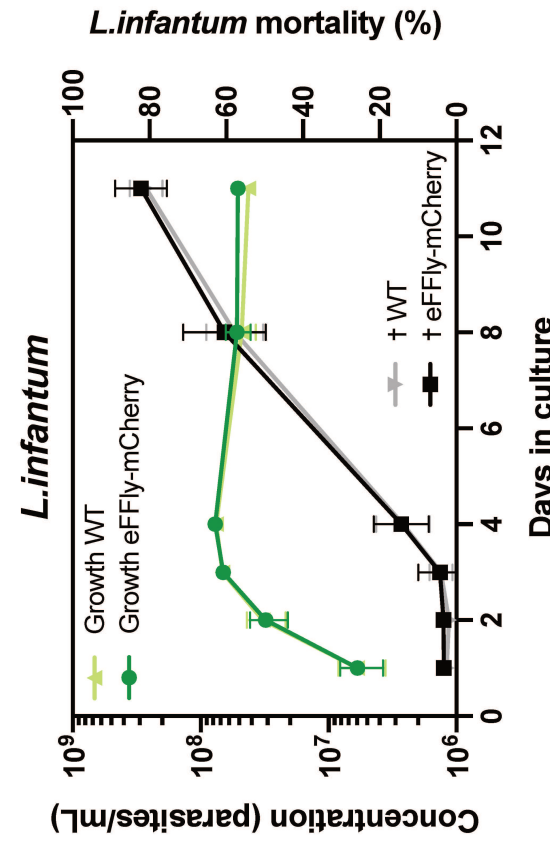
### 2. Homologous recombination



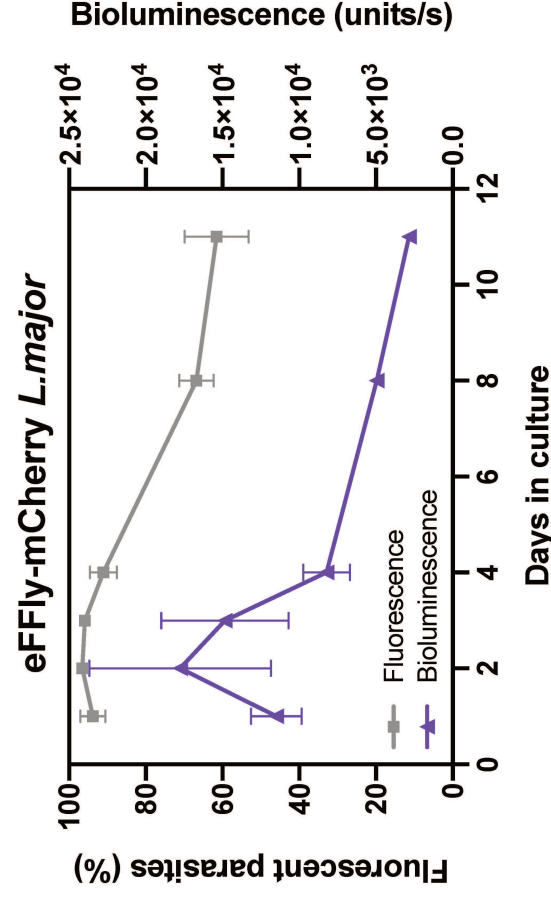
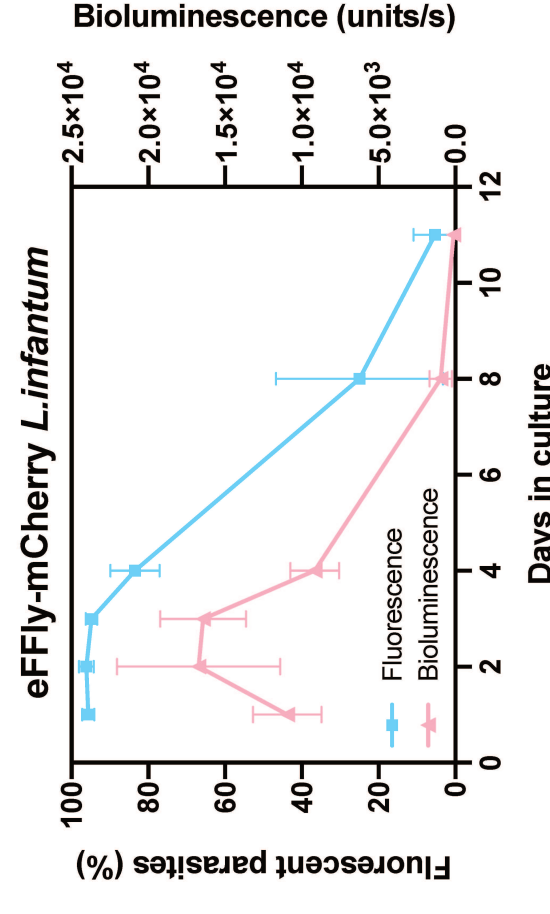
pLEXSY-hygro2.1 was purchased from JenaBioSciences (Catalog number: EGE-272)  
pCDH-EF1a-eFFly-mCherry was a gift from Irnelma Jeremias (Addgene plasmid # 104833; RRID: Addgene\_104833)

## Results

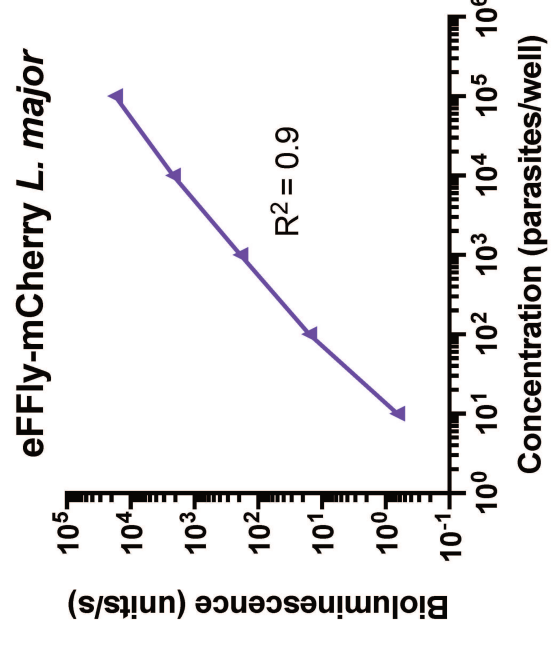
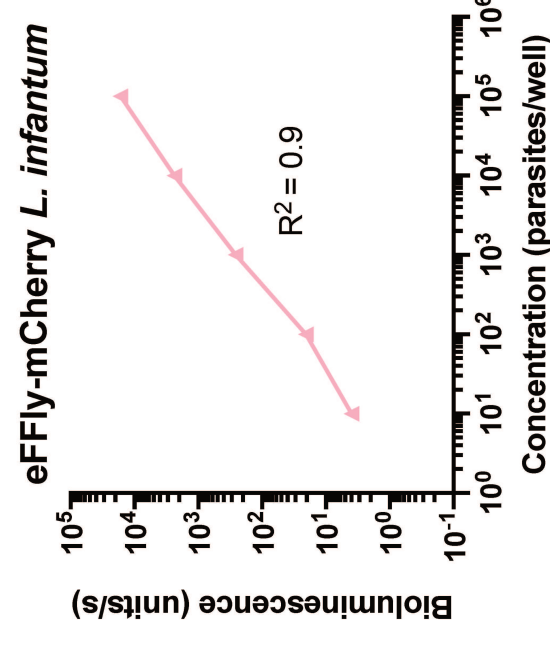
### 1. Growth and mortality of *Leishmania* by flow cytometry



### 2. Fluorescence and bioluminescence emission of promastigotes

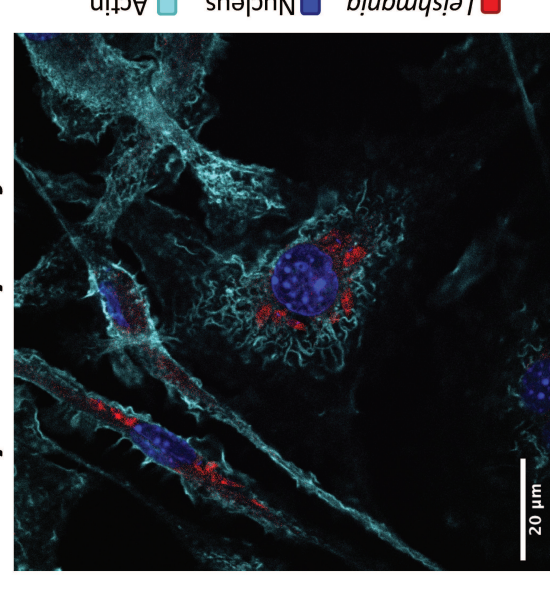


### 3. Bioluminescence emission related to parasite concentration

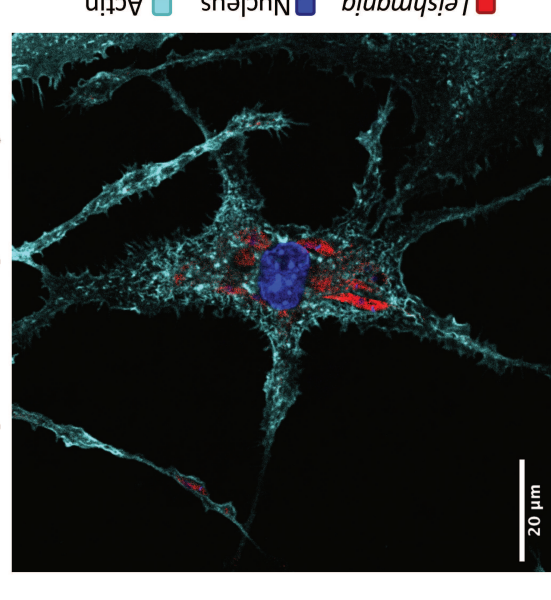


### 4. Infected primary murine macrophages by microscopy

eFFly-mCherry *L. infantum*



eFFly-mCherry *L. major*



Intracellular *Leishmania* were visible 24h post-infection, confirming eFFly-mCherry did not alter parasite entry.

Luciferin tests showed a strong correlation between the two variables, presenting eFFly-mCherry as a good reporter strain.

Bioluminescence (multi-reader) and fluorescence (cytometry) decreased 4 days post dilution, in stationary phase.

eFFly-mCherry strains showed no difference in growth/mortality, suggesting transformation did not alterate their development.

## Conclusion

Leishmaniasis are neglected tropical diseases with limited access to treatments. Current treatments present multiple drawbacks, leading to the urgent need of new alternatives, which implies to set up new tools to perform efficient and fast screenings of drug libraries. The eFFly-mCherry reporter strains are a tool for rapid screening of anti-leishmanial compounds, and the possibility to use *L. major* and *L. infantum* presents an opportunity to rapidly screen for broad-spectrum anti-leishmanial compounds.

## Aknowledgments





# Identification of immuno-stimulating compounds in the fight against Leishmaniasis

Journées de l'École Doctorale de Nice 2021 (JEDNs 2021)

Alissa Majoor<sup>1</sup>, Christelle Pomares<sup>2</sup>, Pierre Marty<sup>2</sup>, Laurent Boyer<sup>1</sup>, Grégory Michel<sup>1</sup>

<sup>1</sup>Université Côte d'Azur, C3M Inserm, U1065, Nice Cedex3, France, <sup>1</sup>Service de Parasitologie-Mycologie, Centre Hospitalier Universitaire de Nice, 06202, Nice Cedex 3 France

## **Abstract**

Leishmaniasis is a Neglected Tropical Disease, accounting for one million cases and leading to 20 to 50 000 deaths a year. There are 3 main forms of the disease showing gradual severity : cutaneous, muco-cutaneous, and visceral leishmaniasis. The most severe form is visceral leishmaniasis which is fatal without treatment. *Leishmania infantum* (*L.infantum*), my study model, is transmitted as an extracellular promastigote form by the bite of female phlebotomine sandflies, and targets host macrophages where it transforms into an amastigote form and replicates for the disease to spread and colonize the spleen and liver, conferring visceral leishmaniasis. Treatments exist, but they present important limitations, including high pricing, invasive administration, needed hospitalization due to the toxicity of treatments and increased apparition of resistance. Thus my thesis aims to identify alternative treatments based on natural molecules extracted from plants. In order to identify such compounds, I have generated a reporter strain of *L.infantum* expressing Firefly luciferase, and the red fluorescent protein mCherry (eFFly-mCherry). During my thesis, I have identified a molecule that is active on the intracellular amastigote form of the parasite, with reduced toxicity compared to current treatment Amphotericin B. Further studies showed the compound could modulate cytokines in both non infected and infected conditions. The effect of this molecule on classical pathways involved in the destruction of intracellular pathogens is currently under investigation. The identified compound seems to act as an immunostimulator, promoting macrophage activity for the destruction of intracellular parasites. We are currently testing the leishmanicidal effect of around twenty other structural derivatives of the identified molecule, in order to identify active chemical structures, and hopefully to identify a compound with increased efficiency. *In vivo* experiments are ongoing, and aim to verify the innocuity of the molecule, and the best administration route in mice. Finally, we will also test its leishmanicidal activity in a model of murine visceral leishmaniasis.

# BEST ORAL PRESENTATION

JEDNs 2021

100 €

*Is attributed to :*

Alissa Majoor

May 25<sup>th</sup> 2021







# Identification de composés immuno-stimulateurs anti-microbiens de nouvelle génération

La Leishmaniose est une maladie tropicale négligée que l'on retrouve dans plus de 98 pays à travers le monde. On compte par an jusqu'à 1 000 000 de nouveaux cas, menant à près de 30 000 morts. Chez l'homme, il existe plusieurs formes de la maladie, allant d'une forme cutanée pouvant guérir spontanément, à la forme viscérale la plus grave.

La leishmaniose viscérale est conférée par plusieurs espèces de leishmanies, dont *L. infantum* dans le pourtour du bassin Méditerranéen. Ce parasite dimorphique envahit les macrophages de ses hôtes notamment l'humain et le chien où il est responsable de la maladie. En l'absence de traitement, la leishmaniose viscérale est mortelle et les traitements existants aujourd'hui sont toxiques, coûteux, et font face à l'apparition croissante de résistances.

Trouver de nouveaux traitements est donc aujourd'hui une priorité, et ce projet de thèse vise à identifier des alternatives naturelles aux molécules anti-*Leishmania*. En prenant une approche écologique, nous récupérons des déchets de la parfumerie et des plantes issues de la biodiversité locale et nous en testons les extraits sur les parasites afin d'identifier des composés immunostimulateurs, qui permettraient de favoriser une élimination du parasite par l'hôte. Afin de pouvoir suivre l'évolution au cours du temps d'une infection *in vitro* et/ou *in vivo*, nous avons également cherché à créer de nouveaux outils pour visualiser la présence du parasite *Leishmania* en développant de nouvelles souches rapportrices fluorescentes et bioluminescentes.

Au cours de ma thèse, nous avons identifié une plante dont l'extrait favorise l'élimination de la forme amastigote intracellulaire retrouvée dans les macrophages hôtes. A l'aide de nos collaborateurs à l'Institut de Chimie de Nice (ICN), nous avons réalisé un fractionnement bioguidé et obtenu des sous-fractions de cette plante ainsi que des molécules pures capables d'éliminer le parasite *Leishmania infantum*.

Une seule molécule, dont le nom est soumis à confidentialité pour des raisons de dépôt de brevet, a montré un effet sur le parasite intracellulaire, sans montrer de toxicité. Cette dernière module la sécrétion de cytokines de la cellule hôte. Actuellement, l'étude de 20 dérivés structuraux de cette molécule est en cours. Des études préliminaires chez la souris ont permis de montrer que la prise de cette molécule par voie orale, de façon préventive, pouvait diminuer la charge parasitaire dans l'animal.

Nous avons en parallèle développé la construction de nouvelles souches rapportrices de *Leishmania* exprimant la luciférase teLuc, le fluorophore rouge mRuby ou rouge lointain mMaroon1, et des souches exprimant fluorescence et bioluminescence, eFly-mCherry. Cette dernière construction a été intégrée dans 3 espèces différentes de leishmanies : *L. infantum*, responsable de leishmaniose viscérale, *L. major* responsable de leishmaniose cutanée, et *L. tarentolae* qui est une souche non pathogène pour l'homme.

**Mots clef : *Leishmania*, immunostimulation, souche rapportrice**